Comfort and Energy Optimizing Control of Thermal Systems

Thybo (Deng), Honglian

Publication date:
2010

Document Version
Accepted author manuscript, peer reviewed version

Comfort and Energy Optimizing Control of Thermal Systems

Ph.D. Thesis

Honglian Deng

Danfoss A/S
DK-6430 Nordborg, Denmark.

Ph.D. thesis

ISBN: 978-87-92328-46-5
May 2010

Preface and Acknowledgments

The work presented in this thesis has been carried out under the Industrial Ph.D. programme supported by the Danish Ministry of Science, Technology and Innovation. The thesis is submitted in partial fulfilment of the requirements for the degree of Doctor of Philosophy in Control Engineering at Automation and Control, Department of Electronic Systems, Aalborg University, Denmark. The work has been carried out at the Central R&D department, Refrigeration and Air Conditioning Division and Technical Business Development department, Heating Division, Danfoss A/S and at the section of Automation and Control, Aalborg University in the period July 2006 to March 2010 under supervision of Research Engineer Lars Finn Sloth Larsen, Professor Jakob Stoustrup, Associate Professor Henrik Rasmussen, Professor Bjarne Wilkens Olesen and Peter Weitzmann.

I am heartily thankful to my colleague and supervisor Lars Finn Sloth Larsen, for his patience, support and inspiration. His guidance throughout the project has taught me a lot especially how a great research engineer works. Without him, the work can not be so enjoyable. I would like to express my gratitude to professor Jakob Stoustrup, an outstanding professor in mathematics and control theory, and associate professor Henrik Rasmussen, who has lifetime experience in control theory and its applications for sharing their profound knowledge. Moreover, I would like to thank professor Bjarne Wilkens Olesen , Peter Weitzmann, for their support and help during the project period. Thanks also to Hardy Jepsen, who has initiated this project and given me a good time working with him. Finally, I want to acknowledge the financial support from the Danish Ministry of Science, Technology and Innovation and Danfoss A/S.

May 2010, Nordborg, Denmark
Honglian Deng

Summary

The subject for this Ph.D thesis is comfort and energy optimizing control of thermal systems in a domestic house. Examples of thermal systems could be air conditioning systems, floor heating systems, electrical heaters etc. The work in this thesis consists of a first part treating control of air conditioning systems and a second part treating control of heating systems. The first part of the thesis regarding control of air conditioning systems focuses on deriving a low complexity and general applicable method for optimal control of systems with binary inputs that have cost related to the switching. The proposed method is a gradient based approach, minimizing a cost function by weighing the control error and the switching of the input. Hereby the optimal switching period and duty cycle can be found. The proposed method is of low complexity and can be easily applied on various industrial systems, such as an air conditioning system. The method does not require special tuning or knowledge of specific system parameters, which makes it ideal for industrial implementation. The method relies only on information of the controlled variable. The method method showed to work well on a typical thermal system without delay and complex poles. For systems with dominating delays, can the problems however be overcome by use of an observer. The proposed method has been applied on a test refrigeration system, placed at Aalborg University. Here it was proven that by using the optimizing switch control method, it was possible to drive the system close to the optimal period and duty cycle, and hereby the proposed method outperformed the traditional relay control.

The second part of the thesis regarding control of heating systems focuses on modeling and control of a water-based floor heating system and control of systems with multiple heat sources. A finite difference model of a water-based floor heated house was developed for simulation and prototyping of the proposed control algorithms. A novel cascaded control approach for water-based floor heating systems has been proposed. The inner loop of the cascaded controller contains the subfloor temperature estimation and control, and the outer loop controls a room temperature. In the outer loop a feed forward scheme for disturbance rejection was further implemented. The inner control loop is based on a novel approach for energy based control of the subfloor temperature. The proposed approach showed significantly improvement of the floor heating system dynamic response time with respect to a change in the room temperature. The feed for-

ward disturbance rejection uses an inverse model of the floor and the wall to derive the compensation model for the outdoor temperature variations. The proposed water-based floor heated room control approach is applied on a domestic house located in Sønderborg, Denmark. Here it has been shown that the subfloor temperature can be estimated and controlled with good performance, hereby high water inlet temperature can be used directly to achieve a much improved response time. The feed forward approach for disturbance rejection has been shown to give good improvements. Perfect disturbance rejection is however difficult to obtain as the accuracy of the floor and the wall model identification is limited in a real domestic application as not all incoming disturbances can be measured. A model predictive control (MPC) of a multiple heat source system is proposed. The MPC is based on a setup that includes the various dynamics of the heat sources as well as the different cost of using. By formulating a cost function that penalizes the discomfort in terms of a control error and the cost of using for the different heat sources, an optimal control sequence that optimizes the comfort and economic requirement can be computed. The thesis is presented as a collection of papers accompanied by an overall introduction to comfort and energy optimizing control of thermal systems. An introduction, a summary of work and a conclusion is made separately for the two parts, control of air conditioning systems and control of heating systems.

Sammenfatning

Emnet for denne Ph.D. afhandling er komfort og energi optimerende regulering af termiske systemer i private huse. Eksempler på termiske systemer kan fx være luftkonditioneringsanlæg, gulvvarmeanlæg, elektriske radiatorer osv. Afhandlingen er opdelt i to dele, den første del omhandler regulering af luftkonditioneringsanlæg og den anden del omhandler regulering af varmesystemer. Den første del af afhandlingen der omhandler regulering af luftkonditioneringsanlæg fokusere på udledning af en enkel og generelt anvendelig metode til optimal regulering af systemer med binære input, hvor det er forbundet med kost at lave et skift i inputtet. Den fremsatte metode er en gradientbaseret fremgangsmåde, hvorved en kost funktion, der vægter reguleringsfejlen og skift i inputtene, minimeres. Metoden er baseret på en antagelse om af at systemets output følger en første ordens limit cycle. Herved kan den optimale switch periode og duty cycle findes. Den fremsatte metode er enkel og kan nemt anvendes på forskellige industrielle anlæg, som eksempelvis luftkonditioneringsanlæg. For at udnytte metoden kræves ingen speciel tuning eller viden om specifikke systemparametre, hvilket gør metoden ideel for industriel anvendelse. Metoden baserer sig kun på information om den regulerede variabel. Metoden virker på systemer uden tidsforsinkelser og komplekse poler. For systemer med betydelige tidsforsinkelser kan problemerne dog afhjælpes ved brug af en observer. Metoden er blevet afprøvet på et testkøleanlæg på Aalborg universitet. Her blev det vist at det med den fremsatte optimerende reguleringsmetode er muligt at drive systemet tæt til den optimale switch periode og duty cycle. Det var med metoden muligt at levere en bedre performance end med en traditionel relæregulering.

Den anden del af afhandlingen, der omhandler regulering af varmesystemer, fokusere på modellering og regulering af vandbåren gulvvarme anlæg, samt på regulering af anlæg med multiple varmekilder. En finite difference model af et hus, opvarmet med vandbåren gulvvarme, er blevet opstillet til simulering og prototype test af nye reguleringsalgoritmer. Ny metode kaskade baseret regulerings metode til vandbåren gulvvarme er blevet fremsat. Den indre sløjfe i kaskade reguleringen indeholder en gulvtemperaturestimering samt en temperaturregulering og den ydre sløjfe varetager rum temperaturen reguleringen. I den ydre sløjfe er der ydermere implementeret en feed forward til kompensering af forstyrrelser. Den indre sløjfe er baseret på en ny energi baseret reguleringsmetode af gulv temperaturen. Den fremsatte metoden forbedrer den dynamiske

reaktionstid af rum temperaturen betydeligt. Den feed forward forstyrrelseskompensatoren gør brug af en invers model af gulvet og væggen til beregning af bidraget til styresignalet ved en ændring i udendørs temperaturen. Den fremsatte metode reguleringsmetode til vandbåren gulvvarme er blevet testet i et privat beboelseshus i Sønderborg, Danmark. Forsøgene har vist at gulv temperaturen kan estimeres og reguleres tilstrækkeligt nøjagtigt, således at en højre fremløbstemperatur af vandet til gulvvarmen kan anvendes hvorved systemets reaktionstid kan øges betragteligt. Feed forward kompenseringen af forstyrrelser har at vist sig at give en ganske god forbedring. Det er dog i praksis svært at opnå en nøjagtig forstyrrelses model idet ikke alle forstyrrelserne måles. En model prædiktiv regulering (MPC) af et system med multiple varme kilder er blevet fremsat. Den fremsatte MPC reguleringen medtager varmekildernes forskellige dynamik samt driftskost. Ved at opstille en kost funktion. som vægter indeklima i form af reguleringsfejlen samt driftsomkostningerne, kan en optimal sekvens af styre signal beregnes som optimere indeklimaet og driftsomkostningerne. Afhandlingen består af en samling af videnskabelige artikler samt en introduktion til komfort og energi optimerende regulering af termiske systemer. For hver af de to dele af afhandlingen, regulering af luftkonditioneringsanlæg samt regulering af varmeanlæg, er der lavet en introduktion, sammenfatning af arbejdet samt en konklusion

Contents

Chapter 1

Introduction to comfort and energy optimizing control

1.1 Background and motivations

This project was proposed by Danfoss A/S. Danfoss is a global Group which plays a leading role within research, development, production, sales and service of mechanical and electronic components and solutions for a large range of sectors. Danfoss has approximately 31000 employees and an annual turnover of 27.127 mill. DKK. [1]. Danfoss′ activities are divided into three main business areas, Refrigeration and Air Conditioning (RA), Heating and Motion Controls. The RA division develops, produces and sells products and services worldwide within the area of refrigeration and air conditioning. The strategy emphasizes that more intelligence should be put into the products, with the overall objective of achieving higher energy efficiency and thereby offer more value for the customers. Optimizing control of refrigeration and air conditioning systems is one step in this direction. The heating division is a world leading supplier of a range of components and services for heating and water including floor heating systems, thermostatic valves, ventilation systems etc. The focus of the division is on total comfort system, where control of the subsystems is an important area. The first part of this thesis focuses on control of air conditioning systems.The second part of the thesis focuses on control of floor heating system and multiple heat source systems. Both parts are in the area of building control with respect to indoor comfort and energy efficiency.

Indoor climate has become an important issue for comfort and health reasons. Research of indoor comfort has been carried out extensively, for example, [1] introduces PMV (Predicted Mean Vote) and PPD (Predicted Percentage of Dissatisfied) for comfort evaluation, where the author suggests that the comfort is a function of temperature,

[1] Annual report Danfoss A/S, 2008

humidity, air velocity etc, and [2] studies the relation of acceptability between clean air and polluted air under different air temperature and humidity. These studies point out that air temperature, humidity, and air quality (The air quality here refers to pollution, odd etc.) are important aspects of indoor climate and that they have influence on each other. The conclusion is that these aspects have to be maintained together to provide a good indoor climate.

Different equipments can be installed as subsystems in the same house, e.g. floor heating, electrical heater, air cooling system (The air cooling system here refers to a device installed in a house which includes an refrigeration cycle. Typically such a system is called an air conditioning system. In this thesis, the air conditioning system only has the function of cooling the air.), ventilation system etc. to regulate the temperature and air quality. With the current control strategy, these control variables are regulated independently disregarding strong cross couplings. This often results in a poor indoor comfort and loss of energy efficiency. The problem is that some of these subsystems have no knowledge of the existence of the other subsystems. For instance, a floor heating system and an electrical heater are installed in the same room. The floor heating system with slow dynamics provides warm floor surface, and the electrical heater with fast dynamics is aimed at rejecting the fast disturbances. When the room temperature is lower than the reference, both heating subsystems are active. The floor heating system first needs to transmit the heat through the large heat capacity of concrete subfloor. This results in slow dynamics of the room temperature especially due to the large amount of energy stored in the subfloor. The electrical heater emits heat directly to the air of the room, hence a much faster room temperature reaction can be observed. When the reference is reached, both of the subsystems switch off, but a large amount of heat stored in the subfloor is released until the floor is not warmer than the air in the room. Therefore a significant temperature overshoot is resulted. This is obviously uncomfortable and waste of energy and vice versa with temperature undershoot. The main problem today is that all of these subsystems in the same house have their own controllers and they work independently without the knowledge of each others existence.

An overall control of the climate system is essential to handle these subsystems as one combined control objective to provide a good indoor climate and high energy efficiency. Another requirement for such an overall control is that it should have a flexible structure to cope with a range of different subsystems that are installed and updated throughout the life cycle of the house without reconfiguration of the whole climate control system. The idea is to divide the control into different levels so that an overall climate comfort and a flexible structure can be achieved.

The focus of this PhD project is mainly on: control of air conditioning systems, control of floor heating system and control of multiple heat source systems. Control of the air conditioning systems is focused on the challenges arising from the ON/OFF switching property typically found in such systems. The floor heating system considered in this thesis is water-based, characterized by slow dynamics for which the control strategy is also with ON/OFF nature. Common for these two control systems is that they are both

ON/OFF switching.

1.2 Vision of a total climate control system

As stated in the previous section, it is essential to apply an overall intelligent climate control system to handle the different subsystems e.g. floor heating systems, electrical heaters, air cooling systems, and ventilation etc. to achieve a good temperature, air quality and high energy efficiency. A proposed control architecture of the climate system is depicted in Fig. 1.1.

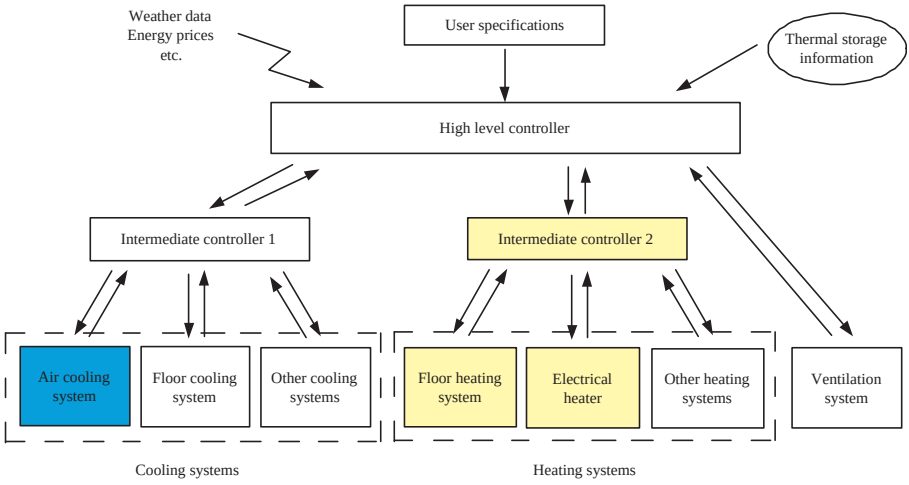

Figure 1.1: Control architecture of a total climate system. The focus of Part I is highlighted in blue. The focus of Part II is highlighted in yellow.

As depicted in Fig. 1.1, there are three hierarchies in the control architecture - the top layer which is the High Level Controller, the intermediate layer which is composed of two intermediate controllers and the low layer where the local controllers are placed in the different subsystems. These subsystems can be divided into three groups: the cooling systems, the heating systems and the ventilation system. Due to that the air quality is controlled by only one subsystem - the ventilation system. Therefore the intermediate layer is not necessary.

The high level controller receives the user set-points, thermal storage information, weather data and prices for different types of energy. Based on these information, the high level controller plans for the future - makes decision to activate either the cooling or the heating systems, and sends the necessary information to the intermediate controllers including set-points, weather information, feed forward disturbance on the room temperature from the ventilation system etc.

The main function of the intermediate controllers is to cooperate the subsystems characterized by different dynamics, energy price etc. to achieve the control goal. It also communicates with the high level controller. The information received from the high level controller includes the temperature set-points, weather data, energy prices, feed forward disturbance on the room temperature caused by the ventilation system etc. The intermediate controllers also send back some information to the high level controller for example the room temperature necessary to make the control strategy.

The low level subsystems classified in the following three groups - the cooling systems, the heating systems and the ventilation system have their own controllers, which have no information from the other local controllers and only communicate with the corresponding intermediate controllers.

An objective of this control architecture design is to encapsulate the specific properties and functionality of the individual lower level controllers to enable a more generic interface towards the intermediate controllers. This makes it possible to extend the system with new lower level controllers without a redesign of the higher levels. The challenge in this is to describe the generic properties, such as dynamic range and saturations using a generic protocol that suits all lower level controllers. By doing this, specific implementation details of the lower level controller - such as an improved valve principle is transparent for the upper level controllers. This is an important commercial aspect that enables a modular improvement and upgrade of the installed systems without needing to release of a full products hierarchy for each minor improvement or addition in the lower level. The intermediate controllers benefit from this functional encapsulation, by being able to model the lower level controllers with a uniform and simple model expressing properties that are closely related to the control objectives and limitations, without a need for handling specific properties.

The thermal storage refers to a large amount of thermal capacity which can be used to store ′heating′ or ′cooling ′ energy when it is cheap to produce, for instance a big well insulated water tank which in the winter season can be heated up with a heat pump during the day when the energy is cheap to produce with a heat pump, and release the energy to the room in the evening, while in the summer season, the water can be cooled down during the night with an air conditioning system when the energy is cheap to produce and used to cool the room in the day time. Also the building materials can contribute to such storage effects. A few new building materials implements phase changing properties to increase the storage effect and thereby decrease temperature variations in the building[2].

An example of climate control during an autumn day demonstrates how the whole system works. First the high level controller receives the weather data, energy prices etc at a certain time of a day for example 6 o'clock in the morning. Based on the weather information, the decision whether to run the heating or the cooling systems has to be made for a period e.g. next 12 hours. Assume that the decision is to run the heating systems in this specific way: the intermediate controller 2 receives the activation information along with the room temperature set-point, weather data, energy prices for electrical

[2]http://www2.basf.us/corporate/080204_micronal.htm

heating and water heating and the feed forward disturbance information caused by the ventilation. Then the subsystems, in this example water-based floor heating system and electrical heater, receive the necessary information and run. This way of controlling the climate system avoids energy waste caused by activating the heating and cooling systems at the same time or alternating with short interval.

The advantage of the control architecture is that it provides a good climate comfort, energy efficiency, and flexibility in exchanging, adding or removing subsystems without reconfiguring the whole climate control system. However, in this thesis the main focus is on control of two subsystems: air cooling systems, floor heating systems and the Intermediate Controller 2 as emphasized in Fig. 1.1. The remaining control architecture is left for future work. The readers who are insterested in control architecture design are referred to [3] [4] [5].

1.3 Objectives

The two main focus areas in the thesis are control of air-conditioning and heating systems and they are as follows.

Control of air conditioning systems
Most of the residential air conditioning systems have been operated with relay controls of the compressor switch based on the room temperature. This is not optimal for the components wear and energy efficiency. The objective in thesis Part I is to derive a low complexity optimizing switch control method to regulate this type of systems where both switching cost - due to wear of the components - and energy efficiency are important factors.

Control of heating systems
Most of the water-based floor heating systems are controlled with relay controls of water circuit circulation valves based on the room temperature which results in unsatisfying performance. [6] indicates that the performance can be improved with a more sophisticated control based on the emitted power directly. The objective here is to develop a energy based control method to improve performance of floor heating systems.

To overcome the discomfort caused by the slow reaction of a typical floor heating system, it is often complimented by a faster reacting heat source, such as an electric heater. This is studied in this case. Control of multiple heat source systems illustrates the challenges of the intermediate control layer which manages both a floor heating system and an electrical heater respecting the different dynamics, different energy price and system limitations. Here the main objective is to benefit from the comfort of the floor heating control, and at the same time allow the fast heating system to compensate for the rapidly occurring disturbances. An inherit challenge in the set-up is the obvious inability of fast heat source to remove heat to reject disturbances.

1.4 Contributions and publications

The contributions of this thesis fall in two parts concerning respectively ON/OFF switched air conditioning systems and the heating systems.

The main contribution in the area of switching control is a low complexity method optimizing the switching period and duty cycle to balance cost related to switching with a perceived comfort, expressed as a temperature variation. The method is based on the gradient of the cost function which does not require special tuning or knowledge of specific system parameters. The method relies only the information of the controlled variable (if the system is without delay), or the estimated delay-free output (if the system is delay dominant).

The air conditioning related publications are

- *Optimizing switch control: applications to air conditioning systems. Submitted May 2010 for journal publication*
  This paper is a synthesis of the work carried out in control of air conditioning systems in thesis Part I. A novel method of optimizing switch control is presented thoroughly and experimental validation is also included.

- *Control of systems with costs related to switching: applications to air-condition systems. Proceedings of Multi-conference on Systems and Control, 2009.*
  In this paper the switching control problem is considered. First a cost function is defined and analyzed, and based on that two methods of switching control are proposed - a half period method and a full period method.

- *A new method for control of systems with costs related to switching: applications to air-conditioning systems. Proceedings of European Control conference, 2009.*
  This paper continues the work in the paper above . Further study of the full period method is carried out and the conclusion is that the improved full period method drives the system towards the optimal solution.

- *Control of delay dominant systems with costs related to switching. Proceedings of Multi-conference on Systems and Control, 2010.*
  In this paper, the method developed above is extended to include delay dominant systems by introducing an observer. Experimental results are given and a comparison with a benchmark relay control is presented. The conclusion is that the optimizing switch control method works well with the delay dominant system and outperforms the relay control.

The main contribution in the area of heating system control:

- Modeling of a water based floor heating system. A finite difference model of a water-based floor heating system is made, which is three dimensional model where both the temperature drop along the water pipe and around the pipe radius

direction is taken into account. Comparing with existing models, the proposed model predicts the outlet water temperature more accurate. The work is published in [7].

- Subfloor temperature control of a water based floor heating system. An energy based subfloor temperature control method is proposed where only the required amount of energy is applied to the floor. Thereby overshoot in the subfloor temperature can be avoided and the dynamic response is increased. A new approach to approximate the subfloor temperature using the water temperature is further applied in the subfloor temperature control. The work is published in [8].

- Control challenge analysis in relation to house construction types. Different combination of the wall and floor type in a house poses different challenge in control. Systematic analysis points out the control challenges. The work is published in [7].

- Feed-forward disturbance rejection method to control the room air temperature in a house with a water based floor heating system. The method uses a wall model and a floor model to compensate for slow dynamic disturbance e.g. the outdoor temperature variation effect on the indoor temperature. The work is published in [9].

- A controller for multiple actuator systems characterized by different dynamics, energy prices etc. Model predictive control method was proposed to solve the problem where the different prices of using different heating systems can be reflected with the weight factors on the inputs in the objective function.

The related publications are:

- *Control of a water-based floor heating system, Proceedings of Multi-conference on Systems and Control, 2007.*
  This paper proposes a control scheme with increased dynamic performance for water-based floor heating systems. A novel approach for temperature control of large thermal capacity systems is introduced and validated with experimental results.

- *Disturbance rejection of a water-based floor heating system, UKACC Control Conference, 2006.*
  This paper describes a feed-forward disturbance rejection method for a water-based floor heating system. The method is tested both with simulations and experiments. The result shows that the outdoor temperature variation can be compensated well with the proposed method.

- *Control challenge for domestic heating systems, Proceedings of European Control conference, 2007.*

In this paper, control challenges of different house construction types are analyzed. Modeling of different types of floor heating systems and wall constructions are presented. The models are analyzed by simulation.

- *Control of a system with a large thermal capacity, patent, publication No.: WO/2007/090405, 2007.*
  The invention provides a method and a system for controlling floor heating or climate regulating systems with long time constants. According to the invention, a flow of a fluid is provided through the floor or through a similar medium with large thermal inertia. An induced heat is determined by adding up a plurality of differences between an inlet temperature of the fluid when it enters the medium and an outlet temperature of the fluid when it leaves the medium. The temperatures are sampled with a fixed sampling time and within a fixed period of time, and a corresponding change in temperature of the medium over the fixed period of time is determined. In the future, the temperature of that medium is controlled by use of a ratio between the induced heat and the change in temperature.

- *Method and system for controlling the climate in a house, patent, publication No.: WO/2007/090400, 2009.*
  The invention provides a method for controlling the climate of an environment, e.g. a house, which exchanges thermal energy with an ambient space. Energy is supplied to the environment e.g. by radiators, floor heating, electrical heating fans etc. According to the method, a numerically expressed comfort criteria, and a numerically expressed weight of importance of compliance with the comfort criterion are defined. Subsequently, a supply of a specific amount of energy is considered, and with respect to that amount, a numerical expression of a degree of compliance with the comfort criterion, and a numerical expression of costs related to the supply of that amount of energy are provided.

- *A model prediction controlled energy system, patent, publication No.: WO/2009/039849, 2009.*
  The invention provides a method of controlling a release of thermal energy in a building. The method comprises steps of defining a control criterion for the building, defining a set of climate variables which influence the release of thermal energy in the building, and defining for each climate variable, a climate signification index which defines the importance of that climate variable for the release of thermal energy in the building. Furthermore, the method comprises a step of receiving a set of predicted future climate variables, and subsequently a step of combining the climate signification indices and the predicted future climate variables to provide control instructions for release of an amount of thermal energy in the building to satisfy the control criterion. The invention further provides a comfort control system.

1.5 Thesis outline

The thesis is presented as a collection of papers and is divided into four parts:

- Part I that treats control of air conditioning systems.
- Part II that deals with control of heating systems.
- Part III that presents the conclusions for the whole thesis.
- Part IV that includes the published papers and a report, that document the work in details.

Both Part I and Part II treat systems with switching input nature and building comfort control. The outlines of these two parts are similar. Both Part I and Part II include a motivation, review of the previous work within the area, summary of the work and conclusions. The related papers and reports are provided as appendices. The thesis is organized as follows:

Chapter 1: Introduction to comfort and energy optimizing control
A general introduction to comfort and energy optimizing control including a control system architecture highlighting the objectives of the different subsystems and the overall control structure are described. Project background and motivations are also explained. The main focus in this thesis is on control of air cooling systems and heating systems.

Part I: Control of air conditioning systems
The focus in Part I is on solving a generalized ON/OFF switching control problem exemplified by an air conditioning system. The following three chapters are included.

Chapter 2: Introduction to control of air conditioning system
In this chapter, motivations of investigating switching controlled air conditioning systems are first presented. After that the principle of an air conditioning system is explained with a simple static model. A test system for validating the method is briefly introduced, and the previous work related to switching controlled air conditioning system is reviewed.

Chapter 3: Summary of work
This chapter briefly presents the work that has been carried out to solve a general ON/OFF switching problem. The intention here is to give readers an overview of the method without going into details. Details about the applied methods are elaborated in appendices.

Chapter 4: Conclusions, perspectives and future work

Conclusions regarding the optimizing switch control method are drawn based on the work carried out in Chapter 3. Applications of the developed method on other systems are briefly introduced. Recommendations on future work with both academic and industrial aspects are given.

Part II: Control of domestic heating systems
This part describes control of heating systems especially on the water-based floor heating system with a large thermal mass. Implementation of an intermediate level controller is demonstrated with an example of multiple heat source system control.

Chapter 5: Introduction to control of heating systems
In this chapter, motivations of investigating on control of heating systems are first presented. After that the a general introduction on floor heating systems including construction types and pipe tubing styles are explained. A test system for validating the developed methods is described and at last previous work related to modeling and control of floor heating systems and multiple heat source systems is reviewed.

Chapter 6: Summary of work
This chapter briefly presents the work that has been carried out to solve the control problems of a water-based floor heating system, which is characterized by slow dynamics, due to large thermal mass. Intermediate Controller 2 in Fig. 1.1 is described as an example of controlling a multiple heat source system.

Chapter 7: Conclusions, perspectives and future work
Conclusions regarding the modeling and control of floor heating systems and MPC control of multiple heat source system are drawn based on the work carried out in Chapter 6. Applications of the developed subfloor temperature control method on other systems are briefly introduced. Recommendations on future work including both academic and industrial aspects are given.

Part III: Conclusions, perspectives and future work
The overall conclusions, perspectives and future work of the thesis are given in this part.

Chapter 8: Conclusions, perspectives and future work
The conclusions, perspectives and future work for both thesis Part I and thesis Part II are presented.

Part IV: Appendices

- A: Optimizing switch control: applications to air conditioning systems. (Journal paper)
- B: Control of systems with costs related to switching: applications to air-condition

systems. (Conference paper)

- C: A new method for control of systems with costs related to switching: applications to air-conditioning systems. (Conference paper)
- D: Control of delay dominant systems with costs related to switching. (Conference paper)
- E: Control of a water-based floor heating system. (Conference paper)
- F: Disturbance rejection of a water-based floor heating system. (Conference paper)
- G: Control Challenges in Domestic Heating Systems. (Conference paper)
- H: Model predictive control of domestic heating systems. (technical report)

Part I

CONTROL OF AIR CONDITIONING SYSTEMS

Chapter 2

Introduction to control of air conditioning systems

2.1 Motivations and objectives

Switching compressors ON/OFF is the most commonly used control strategy in air conditioning and refrigeration applications. In this thesis, the term /switching system/ is used for such a system with binary inputs. The control of such a system will be called /switching control/. For many years, these systems have been operated using relay controller with a temperature bound. This is mainly because the relay control is easy to implement. The relay control is usually applied by specifying the temperature set-point and temperature bounds, but it is unable to achieve optimality with varying operating conditions. There are also other ways of tuning the relay controller to work optimally under a certain nominal condition, however the disadvantage is that it performs suboptimal under non-nominal conditions. An optimizing control approach is one of the options to improve the system performance.

Lots of air conditioning and refrigeration systems operate with a fixed speed compressor due to the relatively high price of a variable speed drive. Though variable speed compressors have been applied to some of the systems, even in these cases, switching control is still important. When the cooling demand is lower than what the compressor provides running at the minimum speed, a switching control strategy has to be applied. Even variable speed compressors implements a lower speed limit to maintain sufficient lubrication [10][11].

Switching controlled systems, typically produce a limit cycle in steady state[12][13], where the amplitude of the limit cycle reduces the control performance. The high switching frequency contributes to an increased component wear. Hence an objective of the control scheme is to implement an optimal trade off between output deviation from the reference, system wear and low system performance.

In this part of the thesis, an air conditioning system is used as a case study to address the challenges of switching controlled systems. Here the amplitude of the limit cycle influences the thermal comfort and the cost of the switching can be expressed in terms of compressor wear and reduced energy efficiency during the starting and stopping transients. However, the addressed challenges exists in many systems exhibiting switching feature. The example includes condensing boilers, gas boilers, oil boilers and heat pumps etc.

The objective in Part I is to develop a low complexity, optimizing switch control method for switching systems. The advantage of the proposed method is that no special tuning or knowledge of specific system parameter is required for applying the method. Low complexity is important to penetrate markets for low cost industrial products where the installers have only little control expertise, so a simple commissioning process is required.

In the following section, an introduction of an air conditioning system is given to help the readers to get an overview on how an air conditioning system works including the theory of the vapour compression cycle, modeling of the air conditioning system, modeling of the room and the problems when a compressor runs at low speed. The test system for carrying out experiments is described in Section 2.3. Previous work regarding the switching control is reviewed in Section 2.4. At last the contributions and publications are listed in Section 2.5.

2.2 Air conditioning systems

The objective of an air conditioning system is to remove heat from a room and transfer it to the outdoor ambient in order to maintain a comfortable indoor temperature. An air conditioning system can be seen as an air conditioning unit and a house as shown in Fig. 2.1. The air conditioning unit highlighted in the ellipse is a typical so-called split unit which includes an outdoor unit and an indoor unit. The outdoor unit is as the name indicates usually placed outdoors and contains a compressor and a condenser. The indoor unit refers to an evaporator and an expansion valve, which is usually connected to a supply air duct. The outdoor and the indoor units are connected with the refrigeration pipes. The house is usually constructed with an supply air duct, which is connected to the evaporator. The warm air is cooled when passing by the evaporator and releases heat to the evaporator. After that the cooled air is sent to the rooms through the air inlets. The air sent to the evaporator could be exhaust air from the house, fresh outdoor air or a mixture of both. A thermostat is usually installed in the house to keep track of the indoor air temperature for the air conditioning control.

In the following, the vapour compression cycle process, modeling of the air conditioning unit, modeling of the room and the problem with system running at low compressor speed will be briefly presented.

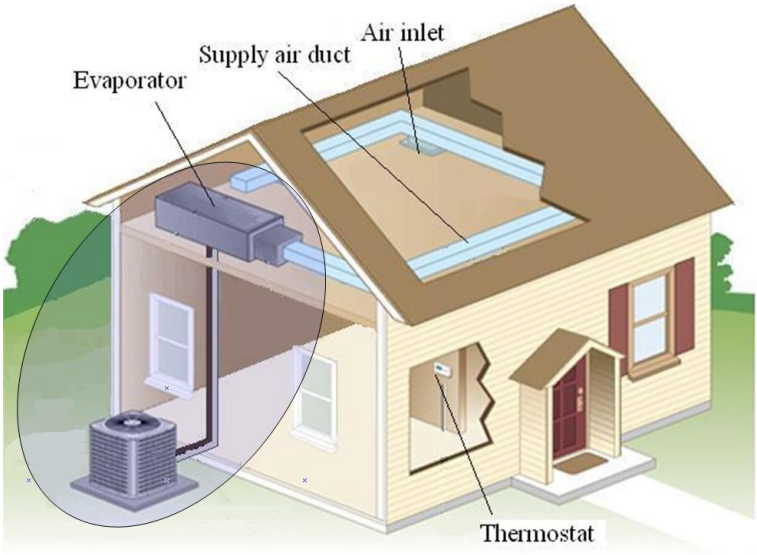

Figure 2.1: An air conditioning system including an air conditioning unit and a house.

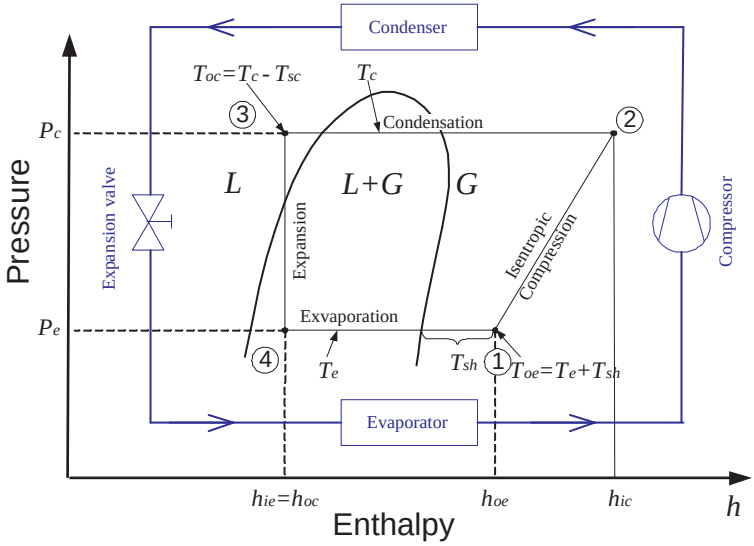

Figure 2.2: The vapour compression cycle in $log(p) - h$ diagram (in black) and layout of the refrigeration system (in blue). The numbers indicate the state points in the cycle.

2.2.1 The vapour compression cycle process

An air conditioning unit in fact contains a refrigeration system which is usually a vapour compression cycle. The vapour compression cycle $log(p) - h$ diagram is shown in Fig. 2.2. The diagram is specific for a given refrigerant and gives a general view of the process cycle and the phase changes that take place. The specific enthalpy[1] at the different state points of the refrigeration cycle is denoted by the subindexes i and o for 'inlet' and 'outlet' plus e and c for evaporator and condenser, i.e. h_{oe} is the specific enthalpy at the outlet of the evaporator. The vapour compression cycle consists of four connected sub-processes namely a compression, a condensation, an expansion and an evaporation, which are realized by four main components: a compressor, a condenser, an expansion valve and an evaporator, and as shown in Fig. 2.2.

From State 1 to 2, the gas phase refrigerant is compressed from low pressure low temperature to high pressure high temperature.

From State 2 to 3, the gas condenses to liquid by releasing heat to the surroundings through the condenser. At the last part of the condenser, the refrigerant temperature is pulled down below the condensing temperature T_c creating a so-called sub-cooling T_{sc}. This sub-cooling ensures that all of the refrigerant is fully condensed when it passes on to the expansion valve (state 3 to 4). This is important because even a small fraction of gas bubbles in the liquid refrigerant would lower the mass flow through the valve dramatically, causing a major drop in the cooling capacity ($\dot{Q}_e$).

From State 3 to 4, the expansion valve separates the high pressure side from the low pressure side. When the refrigerant passes the valve, it is therefore exposed to a large pressure drop causing some of the refrigerant to evaporate. This can be seen as the process moves from the liquid phase (L) in state point 3 to the two-phase region ($L + G$) in state point 4.

From State 4 to 1, refrigerant evaporation takes place by absorbing heat from the indoor air passing by the evaporator due to the low evaporator temperature T_e. At the outlet of the evaporator, all of the refrigerant has evaporated and the temperature has increased slightly above the evaporation temperature. This small temperature increase is called the superheat T_{sh}, which is important to maintain in order to ensure that all of the liquid has evaporated, so that no liquid gets into the compressor. Liquid in the compressor can be fatal as it may result in a break down of the compressor. The superheat is maintained by the opening degree of the expansion valve.

[1] Specific enthalpy is a refrigerant specific property that only depends on the state of the refrigerant, i.e. pressure, temperature and quality. The specific enthalpy is defined as: $h \equiv u + Pv$, where u is the specific internal energy, P is the pressure and v is the specific volume. The enthalpy of a refrigerant can be interpreted as the quantity of energy supplied to the refrigerant to bring it from a certain initial reference state to its current state.

2.2.2 Static model of a refrigeration system

To help the readers understand the working principle of a refrigeration cycle, and how the compressor speed is related to the cooling capacity, static modeling of a simple refrigeration system is introduced in this section. For each of the components, the condenser, the evaporator and the compressor, a static model will be derived. These models are all tied together by the flow of the refrigerant between them. By assuming a steady state flow and neglecting losses in the piping, the state of the refrigerant at the outlet of one component equals the state of the inlet at the next. By applying this, a static model of the entire system can be constructed by combining the individual component models.

The modeling procedure has been divided into parts according to the main components of the plant.

2.2.2.1 The condenser

A condenser is a heat exchanger, in which condensation takes place and the heat is transferred to the ambient. To increase the heat transfer coefficient from the condenser to the air, a fan is usually installed at the condenser. There are different ways of applying condenser fan control in the existing systems, for example, constant fan speed, adjusting the fan speed to keep the condensation pressure constant, fan speed as a function of the compressor speed etc. For all types of fan control, the fan is switched off when the compressor stops. In this project the fan speed is controlled locally, and we do not have access to it. In the modeling here, the condensation pressure is kept constant by regulating the fan speed, which is typical in air conditioning applications. The power released by condensation process to the surroundings is defined as,

$$\dot{Q}_c = \dot{m}_{ref} \cdot (h_{ic} - h_{oc}) \tag{2.1}$$

$\dot{m}_{ref}$ is the mass flow of the refrigerant. The power can also be expressed as heat exchange through the condenser,

$$\dot{Q}_c = k \cdot (T_c - T_{amb}) \tag{2.2}$$

k is a function of the fan speed which is dependent on the outdoor temperature T_{amb}. Due to the constant condensation pressure, T_c is constant.

2.2.2.2 The evaporator

The evaporator is a heat exchanger, in which the refrigerant absorbs heat from the indoor air and evaporates. Similar to the condenser, a fan is usually installed to improve heat transfer efficiency. The fan speed is usually a function of the compressor speed. For fixed speed compressors, the fan speed is constant, which means that the heat transfer coefficient is constant. The super heat is controlled by the expansion valve locally, and we do not have access to it.

The cooling capacity[2] $\dot{Q}_e$ from the refrigerant side can be calculated as

$$\dot{Q}_e = \dot{m}_{ref} \cdot (h_{oe} - h_{ie}) \tag{2.3}$$

which is the same as the power that is removed from the room by the evaporator,

$$\dot{Q}_e = \dot{m}_{air} \cdot c_{p,air} \cdot (T_{air,in} - T_{air,out}) \tag{2.4}$$

$\dot{m}_{air}$ is the air mass flow passing the evaporator and $c_{p,air}$ is the specific air heat capacity. $T_{air,in}$ and $T_{air,out}$ are the air temperature before and after passing the evaporator.

2.2.2.3 The compressor

The compressor maintains the flow of the refrigerant in the system,

$$\dot{m}_{ref} = N_c \cdot V_d \cdot \eta_{vol} \cdot \rho_{oe} \tag{2.5}$$

where $\dot{m}_{ref}$ is the refrigerant mass flow, N_c is the compressor speed, V_d is the volumetric displacement, η_{vol} is the volumetric efficiency and ρ_{oe} is the density of the refrigerant at the compressor inlet (as defined in [14]).

The required work for compression $\dot{W}_c$ can be expressed as

$$\dot{W}_c = \dot{m}_{ref} \cdot (h_{is} - h_{oe}) + \dot{Q}_{loss} \tag{2.6}$$

where $\dot{Q}_{loss} = f_q \cdot \dot{W}_c$ is the heat loss during the non-adiabatic compression process. f_q is defined as the heat fraction of the applied compressor work that is transmitted to the surroundings.

Coefficient of Performance (COP) is an important measure of the performance of a refrigeration and an air conditioning system, which is defined as,

$$COP = \frac{\dot{Q}_e}{\dot{W}_c} \tag{2.7}$$

The higher COP, the better performance of the system.

In this project, the air conditioning system is regarded as a whole unit. The compressor switch is the only external control access to the air conditioning system. All the other components are controlled by their local controllers. In this part of the project, the cooling of the room is controlled by switching the compressor and thereby the air conditioning unit ON/OFF.

[2] In this work, cooling capacity is defined as the heat flow from the hot side to the refrigerant when the refrigeration system is turned on.

2.2.3 The room model

As shown in Fig. 2.1, the warm air is cooled down by transferring heat to the refrigerant in the evaporator. Then the cooled air is sent to the supply air ducts and released to the different rooms in the house through air inlets. The warm air passing by the evaporator typically comes from the exhaust duct, or a mixture of the exhaust and outdoor air. To make the modeling easier here, the air is assumed to be circulated internally, meaning that the exhaust air from the room is cooled by the evaporator and then sent back to the rooms again, with no outdoor air added. The chosen way of air supply to the evaporator only have effect on the cooling capacity, and will not affect the control method developed later on.

To simplify the problem, it is also assumed that there is only one room in the house. This is not typical in family houses but it helps us to focus on the main problem of switching control.

A lumped model of the air in the room is presented below,

$$\begin{aligned} \dot{T}_{room} &= \frac{\dot{Q}_{load} - \dot{Q}_e}{M_{air} \cdot C_{p,air}} \\ \dot{Q}_{load} &= \frac{(T_{amb} - T_{room})}{R_{a2r}} \end{aligned} \tag{2.8}$$

T_{room} is the room air temperature, and T_{amb} is the ambient temperature. $\dot{Q}_{load}$ is the heat load from the ambient to the house. $\dot{Q}_e$ is the heat removed by the air conditioning system from the room air. R_{a2r} is the heat transfer coefficient of the ambient to the room. M_{air} is the mass of the air in the house which is adjusted to compensate the ignored capacity of wall floor, furniture etc.

The parameters that will be used later in the thesis are, $C_{p,air} = 1005 J/kg^\circ C$, $M_{air} = 226kg$, $R_{a2r} = 0.022^\circ C/W$, $\dot{Q}_e \in \{0, 300W\}$.

2.2.4 Problems related to switching frequency.

2.2.4.1 Problems when the compressor runs at low speed

Usually an air conditioning unit includes a scroll or piston compressor which can be a fixed or a variable speed compressor. Common for these compressors is that they all have centrifugal oil injection system, where the lubrication begins with the bearings by the oil from an oil tank, and after that the oil is injected into the compression room to seal and transfer heat with refrigerant, and the rest returns to the oil tank [15]. A scroll compressor with such a centrifugal oil injection system is shown in Fig. 2.3. With this type of oil injection system, the lubrication will only be sufficient when the speed of the compressor is high enough. Another problem when the compressor running with low speed is that, the gas phase refrigerant has to be sealed in the compression room for longer time, which causes a significant leakage. This is especially a problem for a

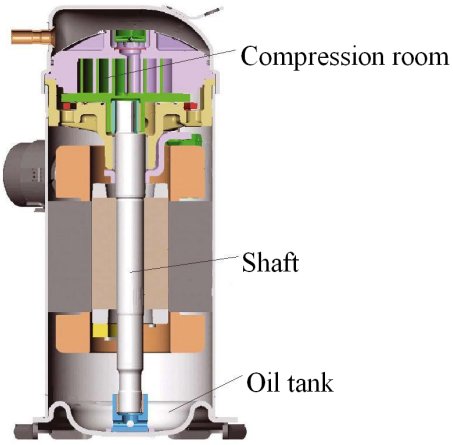

Figure 2.3: A scroll compressor profile.

variable speed compressor, as the speed can not go down to zero. Therefore a minimal speed v_{min} is implemented to provide sufficient lubrications and a reasonable sealing. This means that the variable speed compressor has to switch ON/OFF if the cooling load is smaller than the load the air conditioning system provides running with minimal speed.

2.2.4.2 Low system energy performance related to switching frequency

System energy efficiency COP defined by (2.7) varies with the switching frequency. During the startup/stop process, the COP is lower than when the system runs in steady state. There are three main reasons for this: (1) the evaporator has to be filled in when the system starts. There is only a little liquid left in the evaporator after the last stop. Therefore this has to be filled to a certain level before the system reaches the designed COP. (2) compressor operates at a low efficiency when the system starts. This is mainly caused by a poor lubrication and poor sealing, where a large amount of the work is converted to friction heat instead of compressing the refrigerant. (3)liquid refrigerant flows out of the evaporator to the suction line and evaporates there when the system stops. Most of the liquid refrigerant evaporated in the suction line after the refrigeration system is switched off, absorbs heat from the ambient, and will therefore not contribute to cooling the room air down.

2.3 Test system description

A refrigeration test plant in Aalborg University is chosen to verify the developed control method. A picture of the refrigeration plant (More information can be found at the refrigeration laboratory home page [3]) is shown in Fig. 2.4.

The refrigeration system is a very flexible test system suitable for experiments with a variety of different control schemes. The heat load on the system is maintained by an electrical water heater with an adjustable power supply for the heat element. The compressor, the evaporator fan and the condenser fan are equipped with variable speed drives so that the rotational speed can be adjusted continuously. The system is further more equipped with an electronic expansion valve that enables a continuous variable opening degree. The system is moreover equipped with temperature and pressure sensors on each side of the components in the refrigeration cycle. Mass flow meters measures the mass flow of respectively refrigerant in the refrigeration cycle and water on the secondary side of the evaporator. Temperature sensors measures the inlet and outlet temperature of the secondary media on respectively the evaporator and the condenser. The applied power to the condenser fan, the heater and the compressor is measured. Finally the entire test system is located in a climate controlled room, so that the ambient temperature can be regulated. The system is connected to the internet, which means that it is possible to conduct experiments for researchers not geographically located at the university. More details of the test system can be found in [16].

The refrigeration test plant emulates an air conditioned room, where the water tank can be considered as the room, and the refrigeration system works as the air conditioning unit. The layout of the refrigeration plant is depicted in Fig. 2.5. The heater in the water tank simulates the heating load of the room.

2.3.1 Modeling of the test system

Similar to air conditioning systems, the refrigeration plant can also be seen as two parts: the refrigeration system and the water tank. The refrigeration system modeling has been presented in Subsection 2.2.2. The water tank is similar to the house in Subsection 2.2.3.

The modeling of the water tank is described below,

$$\begin{aligned} \dot{T}_{water} &= \frac{\dot{Q}_{load} - \dot{Q}_e}{c_{p,water} \cdot m_{water}} \\ \dot{Q}_e &= c_{p,water} \cdot \dot{m}_{water}(T_{w,out} - T_{w,in}) \end{aligned} \tag{2.9}$$

$\dot{T}_{water}$ is the average tank water temperature, which is the state that we aim to control.
$\dot{Q}_e$ is the cooling capacity from the refrigeration system.
$\dot{Q}_{load}$ is the heating load from the electrical water heater. The disturbance from the ambient to the water tank is ignored due to good insulation of the tank.

[3] http://www.control.aau.dk/koelelab/index.php?actionParam=0

Figure 2.4: The refrigeration test plant in Aalborg University

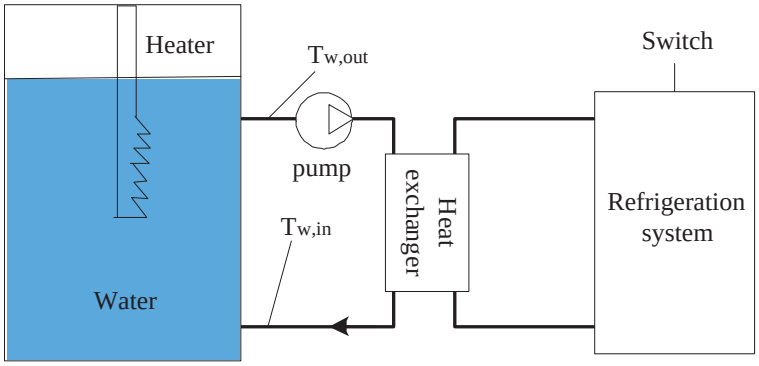

Figure 2.5: Layout of the refrigeration test plant in Aalborg University

$c_{p,water}$ and m_{water} are the specific heat capacity and mass of water in the tank.
$T_{w,in}$ and $T_{w,out}$ are the water temperature coming into and out of the tank, which is corresponding to the water temperature after and before passing the evaporator.
$\dot{m}_{water}$ is the water mass flow passing by the evaporator.

The electrical water heater in the tank simulates the heat load to the house in Subsection 2.2.3. The house is exposed to the heating disturbance from both outdoor and indoor environment in form of solar radiation, heat penetration through walls, human and electronic appliance heat generation etc., and all of these heat loads are simulated by the electrical water heater. The water tank is so well insulated, that the heat loss to the ambient can be ignored which makes it similar to a well insulated house. The water capacity is much higher than the air capacity, but it can be regarded as a house with thick brick indoor wall, or with some furniture with a large heat capacity. The changing of water mass in the water tank can be considered as modeling of houses with different size.

A mixer is installed to keep the water in the tank well mixed so that the water temperature can be considered uniform and therefore the water coming out of the tank $T_{w,out}$ can be approximated as the water temperature inside the tank. The reason to use this approximation is that measuring the average temperature of the tank water is not easy with a non-uniform temperature profile. By experiment it is found out that there is a delay from the time when the refrigeration system removes heat from the water until $T_{w,out}$ reacts, and it is modeled as

$$T_{w,out} \quad = \quad T_{water(t-\theta)} \tag{2.10}$$

where θ is the delay. The delay could be caused by the imperfect mixed water in the tank and the slow water circulation with the pump etc.

In the experiments conducted for the PhD project, XPC toolbox for SIMULINK has been used for the data acquisition and the control interface.

2.4 State of the art

Control of air conditioning and refrigeration systems have gained considerably interests recently especially on energy efficiency, e.g. [17][18] point out that a system level optimizing control of a refrigeration system with variable speed compressors, variable speed fans, and variable speed pumps can save significant amount of energy, [19] shows that by applying optimal set-points for the different components, an overall energy consumption can be reduced etc. All these studies have important impact on the energy efficiency of the air conditioning and refrigeration systems, however, there are also other important aspects that are worth of working on, for instance, switching control of air conditioning and refrigeration system. The reason that switching control of air conditioning and refrigeration systems is important is that unsatisfying temperature variation, components wear and low system energy performance during start and stop transient phases are often

resulted for switching systems. Much literature can be found regarding switching control of air conditioning and refrigeration systems. For instance [20] [21] [22] [23] [24] focus mainly on desynchronization of the multiple compressors in refrigeration systems with multiple display cases to improve the energy efficiency and reduce the components wear of the compressors; [25], [26] attempt to solve compressor switching problem for a refrigeration or an air conditioning system where only one compressor exits. This type of switching systems is one subcategory of the hybrid switching systems.

Hybrid switching systems can be divided into several classes according to the nature of the controlled systems. One class is the systems that have discrete states where the states contain different continuous dynamics. An example of such a system is car gear shifting system. Control of this type of hybrid systems have been widely studied, see [27] [28] [29] [30] and the references therein. Switching between different controllers to compensate system nonlinearities is another type of hybrid switching systems. One of the examples is sliding mode control [31]. The third type is the systems with ON/OFF switched actuators, for instance [32] [33] [34] consider systems with Pneumatic ON/OFF valves. There are also other type of hybrid switching systems, however they are not mentioned here since they are not the focus of the thesis. Optimal control of hybrid systems is one of the most challenging and important class of problems for switching systems as mentioned in [35] [36] [37], since for an optimal control problem of a switched system, both an optimal continuous input and an optimal switching sequence have to be determined and the system dynamics may vary significantly before and after every switch. However, in thesis Part I, the focus is on optimal control of hybrid switching systems with ON/OFF switched actuators. This type of systems typically have very limited computational power to implement the advanced methods. A significant control challenge is designing low complex control schemes. The contributions attempt to solve control problems for a subcategory of switching systems - systems with ON/OFF switched actuators are reviewed in this section. The previous work is classified in two groups.

Advanced methods

Sliding mode control is one common type of switching control, which has been applied widely to aerospace and robot applications where a high levels of instrumentation allow measurement of the full state vector. In situations where the state vector is unable to be fully measured, observers are required and robustness problems can ensue if they are not correctly designed and implemented [38].

[39] proposes a framework for modeling and controlling systems described by interdependent physical laws, logic rules, and operating constraints, denoted as Mixed Logical Dynamical (MLD) systems. These are described by linear dynamic equations subject to linear inequalities involving real and integer variables. The resulting optimization procedures can then be solved online through MIQP (Mixed Integer Quadratic Programming). However using the MPC approach straight forward adding cost[4] to a

[4]In this part of the thesis, switching cost is defined as the system wear, system low energy performance

switch leads to rather suboptimal solutions. This is due to that the cost function has to include discrete inputs and the method are limited to use finite prediction horizon. The problem with finite horizon optimization for system with discrete inputs is that the controller will push the discrete value changes as late as possible to reduce the cost for the current time instant, which in the end results in suboptimal limit cycles. If special care is not taken using finite horizon methods on systems with discrete inputs, it can lead to rather poor performance. Another problem with this method is that the computational load is high. An extension of the method to avoid high online computational load is explicit MPC, which reduces the on-line computational demand. An overview of the developments in control of hybrid systems focusing on MPC can be found in [40]. However the computational load is still too high for the domestic air conditioning system.

To avoid the finite prediction horizon problem from the moving horizon methods, [41] suggests a method to deal with this kind of switching problems based on steady state limit cycle. The author first calculated the optimal limit cycle trajectory, and then proposed two ways to bring the systems to the optimal trajectory. One of them is to employing MPC to track the optimal trajectory, and the other is a variant of time-optimal control, which drives the state to the optimal trajectory along the fastest way which means that it uses fewest limit cycle. For different reference and disturbances, the procedure of finding the optimal trajectory and bring the system to the optimal trajectory requires high computational power. Although some of it can be implemented as look-up table, the computational load is still too high for a domestic air conditioning unit. Besides the method is designed for a specific application, redesigning of the method is necessary for another system.

Some other researchers have worked on a different way of formulating the hybrid switching problems: transcribe an optimal control problem into an equivalent problem parameterized by the switching instants and then obtain the values of the derivatives to get the optimal solution, e.g. [21] [42]. The progress of this way of formulating the problem is surveyed in [43]. In [21], the ON/OFF inputs are formulated in terms of time instants of occurrence of events, instead of as binary values in each sampling time. The author first defined a cost function of the accumulated output deviation from the reference for the prediction horizon. The prediction horizon is a number of switching periods assumed to be required for obtaining a stable operational pattern. From the control horizon to the end of the prediction horizon, the author forces the system to repeat the last switching patter from the control horizon which avoids the compressors' synchronization problem. A non-linear programming (Sequential Quadratic Programming) is used to solve the problem. Since all the switching decision variables are of real types, the associated optimization problem can be solved more efficient. The author reached their goals: desynchronization and lower computational demand compared with the MLD+MPC solution. The same method has also been successfully applied in batch processes in [44] [45]. The switching cost was not considered in the two examples, but

due to start and stop transients caused by switches.

it can be easily included by modifying the cost function to add a switching cost term. The computational load is still too high for a domestic air conditioning system.

[25] has explained the problem of operating a variable speed compressor air conditioning system, which is when the heat load is lower than the capacity of the air conditioning system, operating at the minimum compressor speed, the system has to run ON/OFF. In the paper, the system has the compressor speed and the expansion valve opening degree as inputs. Operating with a reference lower than half of the minimum compressor speed, the compressor is switched off, and operating between half and the minimum speed, the compressor operates at the minimum speed. The authors propose to use a continuous control for the air conditioning system, controlling the superheat and the room temperature, but include the low speed ON/OFF switching error as a disturbance. A dynamic compensator implementing an observer structure is added to compensate the difference between the applied and the required compressor speed. The approach succeed in avoiding an excessive compressor speed transient and provide better indoor temperature regulation, but in fact it introduces more ON/OFF switches. This did not address the challenge with frequent compressor switching - components' wear.

[46] proposes hybrid fuzzy control method for high-speed ON/OFF valve in pneumatic systems, where the high-speed ON/OFF valves are controlled by the PWM [5] signal from the control unit. The author tried to control the pressure in a chamber, which vibrates rapidly, by modifying the PWM signals. The results were good for the authors problem, but the method is mainly applicable for pneumatic systems. There is no such rapid output change characteristics in ON/OFF switching AC systems, and at the same time, the switching cost is not taken into account.

An ON/OFF switching control scheme is introduced in [47], where the author claims that the method produce suboptimal solutions near the optimal. First the author set up a cost function which accumulates the energy input and the output deviation from the reference during a period (which is the time period where the load is predicted and the optimization is only focused on this time period), and then a finial state offset limit, at last a numerical search to find the time that the system should start up ahead of the load changes and the opening time of the system, that together minimize the cost function. The results look good based on the assumption that the load profile is known a priori, which is not always easy to predict in reality. The switching cost is not included in the cost function, but a simple reformulation of their cost function could include the switching cost. However the problem is that the computational power required for the numerical calculation is pretty high, which makes it impossible to apply the algorithm to mass produced domestic air conditioning systems.

Classical methods

Very few studies have focused on low complexity methods solving switching control problems. Classical methods that attempts to solve binary input problems are PWM and relay control with output bounds.

[5] PWM is the abbreviation of pulse width modulation

PWM control is typically used where no cost is associated with a switch. The switching frequency is therefore typically chosen much higher than the dominating time constant of the system, such that the control input can be regarded as continuous.

A pulse modulation adaptive controller is introduced in [48], where the improved PWM incorporates with conventional feedback control strategy to reduce the component wear caused by switching and at the same time maintain the output. The overall control system includes a conventional controller and a PWM controller, where the conventional feedback controller gets the output feedback and calculates a continuous control signal which is received by the improved PWM controller; the PWM controller converts the continuous signal to a digital value (0 or 1) suitable for input to the plant. The main idea is to implement both pulse width and pulse frequency modulation on PWM. The pulse width (ON time) is calculated according to the continuous input from the conventional controller and some constraints of shortest ON/OFF time. The cycle period is calculated based on the pulse width and the system time constant. The experimental results show that the method works well. However the disadvantage of the method is that the system can not be switched totally ON or OFF since it has been designed to have a minimum ON and minimum OFF time; the solution is not optimal on the output performance and switching frequency.

A standard relay control with fixed bounds on the output can also be applied. Setting the output bounds to the maximal limit for the process, ensures a minimal switching frequency, however at the expense of large output variations. Finding the optimal tradeoff between switching frequency and output variations, by setting the bounds in a relay controller is difficult. Furthermore, as it will be shown, the optimal bounds varies with the operating conditions.

[26] describes how disturbances can cause unnecessary switches for relay controllers, resulting in a faster wear-out of the components. To overcome the problem, the authors propose an extended version of a relay controller with an adaptive filter, where the filter is equipped with an adaption mechanism to tune the filter parameters to preserve the oscillation parameters facing the system dynamics change, hereby the switches caused by disturbances can be reduced. However the approach still faces the problem of traditional relays - losing optimality under non-nominal conditions.

[49] presents a simple method which is a combination of ON/OFF valves with a temporized virtual PID controller. The ON/OFF valve opening time is determined by the virtual PID. The virtual PID is a function of the error in the system output, and the output from the PID varies according to this error. The opening time is then determined by this error. The total switching period is then calculated based on the opening time. The method works fine for the problem, but again, switching cost is not considered.

In this part of the thesis, the objective is to develop a low complexity, optimizing switch control method for SISO (single input single output) switching systems that have costs associated with the switching.

2.5 Contributions and publications

The main contribution in the area of switching control is a low complexity method optimizing the switching period and the duty cycle to balance cost related to switching with a perceived comfort, expressed as a temperature variation. The method is based on the gradient of the cost function which does not require special tuning or knowledge of specific system parameters. The method relies only the information of the controlled variable (if the system is without delay), or the estimated delay-free output (if the system is delay dominant).

The air conditioning related publications are

- *Optimizing switch control: applications to air conditioning systems. Submitted May 2010 for journal publication.*
  This paper is a synthesis of the work carried out in control of air conditioning systems in thesis Part I. A novel method of optimizing switch control is presented thoroughly and experimental validation is also included.

- *Control of systems with costs related to switching: applications to air-condition systems. Proceedings of Multi-conference on Systems and Control, 2009.*
  In this paper the switching control problem is considered. First a cost function is defined and analyzed, and based on that two methods of switching control are proposed - a half period method and a full period method.

- *A new method for control of systems with costs related to switching: applications to air-conditioning systems. Proceedings of European Control conference, 2009.*
  This paper continues the work in the paper above. Further study of the full period method is carried out and the conclusion is that the improved full period method drives the system towards the optimal solution.

- *Control of delay dominant systems with costs related to switching. Proceedings of Multi-conference on Systems and Control, 2010.*
  In this paper, the method developed above is extended to include delay dominant systems by introducing an observer. Experimental results are given and a comparison with a benchmark relay control is presented. The conclusion is that the optimizing switch control method works well with the delay dominant system and outperforms the relay control.

These papers are attached as appendices in Part III.

2.6 Outline of the thesis Part I

The rest of thesis part Part I is organized as follows:

Chapter 3 summary of work: This chapter presents a brief description of the work that was carried out in developing the optimizing switch control method. The main goal is to give a comprehensive formulation of the problem and method derivation as well as some validation of the method.

Chapter 4 conclusions, perspectives and future work: conclusions on the optimizing switch control method are given. Applications of the developed method on some other systems are briefly explained. Future work with both academic and industrial aspects is suggested.

Chapter 3

Summary of work

This chapter summarizes the contributions regarding control of air conditioning systems in the PhD project. The chapter is organized in the following way. First a cost function is introduced and analyzed in Section 3.1, where the properties of the cost function including convexity is studied. Based on the cost function, a novel low complexity switching control method is derived in Section 3.2. Simulation results of the developed method is presented in Section 3.3. Extension of the method with an observer to work with delay dominant systems is treated in Section 3.4. At last results of experimental validation of the proposed method and comparison with benchmark controls are given in Section 3.5. The work is based on Appendix A, B, C and D.

3.1 Cost function study

In this section a cost function suitable for developing the optimizing switch control method is defined. Having defined this cost function, an analysis of the properties with regards to various system dynamics is carried out.

3.1.1 Cost function definition

An open loop stable system with a binary input, which is controlled by a relay controller, will typically converge to a first order limit cycle. Given such a system and a cost function, where making a switch is associated with a cost; it will be assumed that the optimal steady state output trajectory follows a first order limit cycle. This is an assumption also made in [12]. The goal is to seek an optimizing switch control driving the output towards a stable limit cycle, meaning that the output is not converging to a fix-point. A standard summation of the squared control error does therefore not tend to a constant value and is thereby not a good measure of the performance. The system performance is consequently evaluated as the *average* squared control error over one switch period.

For a first order limit cycle two switches are done in each cycle period. The total switch cost for one period therefore accounts to $2R$, where R is the cost of making one switch. The total average cost over one cycle period (T) can then be defined as follows

$$J = \frac{\int_{t_0}^{t_0+T} (y(t) - y_{\text{ref}})^T Q(y(t) - y_{\text{ref}})dt + 2R}{T} \tag{3.1}$$

where t is the time, $y(t)$ is the measured output, y_{ref} is the output reference, Q is the cost associated with having a certain control error, and t_0 is the initial time for the cycle period. The control error and number of switches will then be balanced by the two weight factors Q and R. In the following, one assumption is made that the cost R accounts for as well the costs of component wear as the efficiency loss at start/stops. This cost function represents the performance of the system over one cycle period, which will be used in the remainder of this chapter.

3.1.2 Cost function analysis

Having defined the cost function, the next step is to study convexity and its dependence of system order. In the following an analysis of convexity is based on first order (SISO) system, i.e.

$$\begin{aligned} \dot{x} &= ax + bu + d \\ y &= cx, \end{aligned} \tag{3.2}$$

where $u \in \{\underline{u}, \overline{u}\}$ is the binary valued input and d is the term related to disturbance.

A first order limit cycle consists of an ON period and an OFF period as indicated in Fig. 3.1. The output error accumulation can be divided into two parts: error from the ON period $t \in [t_0, t_0 + \alpha T]$, and error from the OFF period $t \in [t_0 + \alpha T, t_0 + T]$, where α denotes the duty cycle which is the fraction of the cycle period the input is ON ($0 \leq \alpha \leq 1$). The cost function (3.1) can therefore be written as

$$J = \frac{Q(\int_{t_0}^{t_0+\alpha T} (y_1(t) - y_{ref})^2 dt + \int_{t_0+\alpha T}^{t_0+T} (y_2(t) - y_{ref})^2 dt) + 2R}{T} \tag{3.3}$$

y_1 and y_2 refer to the output in respectively the ON and OFF period as indicated in Fig. 3.1.

In the following a further assumption is that the system given by (3.2) is stable, ($a \leq 0$), and $c = 1$. Further-more the convention that in a ON period $u = \overline{u}$ and the OFF periods $u = \underline{u}$ will be used. For the ON period, the explicit solution of (3.2) is given by (3.4), where $y_{1,\text{init}}$ is the initial value at the beginning of the ON period. For the OFF period, the explicit solution of (3.2) can be written as (3.5) where $y_{1,\text{end}}$ refers

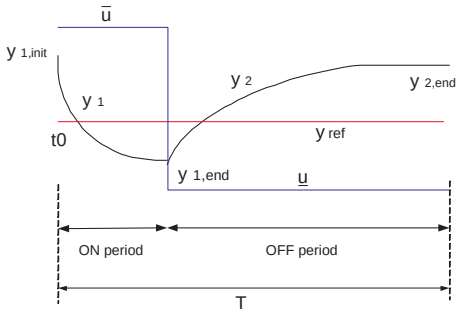

Figure 3.1: One cycle period

to the initial value at the end of the ON period / beginning of the OFF period.

$$y_1(t) = \frac{b \cdot \overline{u} + d}{-a} + \left(x_{1,\text{init}} + \frac{b \cdot \overline{u} + d}{a} \right) \cdot e^{at} \tag{3.4}$$

$$y_2(t) = \frac{b \cdot \underline{u} + d}{-a} + \left(x_{1,\text{end}} + \frac{b \cdot \underline{u} + d}{a} \right) \cdot e^{a(t-\alpha T)} \tag{3.5}$$

By operating at steady limit cycles, the system output will be periodical. This means that the output at the end of one period equals the output at the beginning of the period, $y_{1,\text{init}} = y_{2,\text{end}}$. Applying this condition together with the continuous condition $y_{1,\text{end}} = y_{2,\text{init}}$ at $t = \alpha T$, to (3.4) and (3.5), the following can be derived,

$$y_{1,\text{init}} = \frac{\frac{b \cdot \underline{u} + d}{-a} + \frac{b \cdot \overline{u} - b \cdot \underline{u}}{-a} e^{a \cdot (1-\alpha) T} + \frac{b \cdot \overline{u} + d}{a} e^{a \cdot T}}{1 - e^{a \cdot T}} \tag{3.6}$$

$$y_{1,\text{end}} = \frac{\frac{b \cdot \overline{u} + d}{-a} + \frac{b \cdot \underline{u} + d}{a} \cdot e^{a \cdot T} + \frac{b \cdot \overline{u} - b \cdot \underline{u}}{a} \cdot e^{a \cdot \alpha T}}{1 - e^{a \cdot T}} \tag{3.7}$$

$y_{1,\text{init}}$ and $y_{1,\text{end}}$ can be obtained by applying $t = 0$ and $t = \alpha T$ to (3.4). $y_{2,\text{init}}$ and $y_{2,\text{end}}$ can be obtained by applying $t = \alpha T$ and $t = T$ to (3.5).

In this set of equations $y_{1,\text{init}}$ and $y_{1,\text{end}}$ are functions of α and T, hence the cost according to (3.3) can be computed as a function of α and T. Even so it is not easy to prove directly that the cost function (3.3) is mathematically convex. The alternative is simply to calculate the cost within a reasonable range of $\alpha \in [0, 1]$ and $T > 0$ and investigate the existence of an unique optimum by inspection.

For the computations the parameters corresponding to the first order room model 2.8

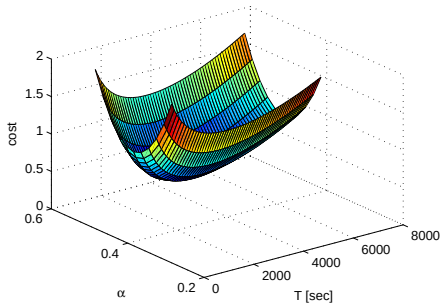

Figure 3.2: The computed cost, for a first order system following a steady first order limit cycle, as function of the cycle period T and the duty cycle α. $T_{amb} = 25.97°C$.

in Subsection 2.2.3 will be used. Rewriting the model in the form of (3.2) gives

$$\begin{aligned} a &= -1/(R_{a2r})/(C_{p,air} \cdot M_{air}) = -2.00 \times 10^{-4} \quad s^{-1} \\ b &= -1/C_{p,air} \cdot M_{air} = -4.40 \times 10^{-6} \quad °C/J \\ c &= 1 \\ d &= 1/R_{a2r}/(C_{p,air} \cdot M_{air}) \cdot T_{amb} = 2 \times 10^{-4} \cdot T_{amb} \quad °C/s \\ u &\in \{\underline{u}, \overline{u}\} \\ \underline{u} &= 0W \\ \overline{u} &= \dot{Q}_e = 300W \end{aligned} \tag{3.8}$$

In Fig. 3.2 the computed cost is plotted as a function of α and T. It clearly appears from the figure that the cost function for this system indeed is convex. We will in the following assume that the cost function only has one minimum.

3.2 Novel approach for optimizing switch control

In the previous section, it has been shown by inspection that the cost function for a stable first order system without non-minimum phase behavior has one minimum only. In the following a novel approach for optimizing switch control based on this will be derived.

Consider the cost function (3.1). As the cost J is a continuous and smooth function of T, the minimum can be found among cycle periods T where $\frac{dJ}{dT} = 0$. Differentiating (3.1) gives:

$$\frac{dJ}{dT} = \frac{Q(y(t0+T) - y_{ref})^2}{T} - \frac{Q\int_{t0}^{t0+T}(y(t) - y_{ref})^2 dt + 2R}{T^2} \tag{3.9}$$

A cycle period for a first order limit cycle includes two switches and hence two half periods: T_{old} which is the previous half cycle period and T_{new} which is the current half cycle period (either OFF or ON periods). By inserting T_{old} and T_{new} in (3.9) and setting equal to zero we get (note that $\frac{dJ}{dT} = \frac{dJ}{dT_{new}}$ as $T = T_{old} + T_{new}$):

$$\begin{aligned}(y(t_0 + T_{old} + T_{new}) - y_{ref})^2(T_{old} + T_{new}) = \\ \int_{t_0}^{t_0+T_{old}} (y(t) - y_{ref})^2 dt + \int_{t_0+T_{old}}^{t_0+T_{old}+T_{new}} (y(t) - y_{ref})^2 dt + 2\frac{R}{Q}\end{aligned} \tag{3.10}$$

To keep the notation short, the left and right side of (3.10) are defined as follows:

$$\begin{aligned} ls(T_{new}) &= (y(t_0 + T_{old} + T_{new}) - y_{ref})^2(T_{old} + T_{new}) \\ rs(T_{new}) &= \int_{t_0}^{t_0+T_{old}} (y(t) - y_{ref})^2 dt \\ &+ \int_{t_0+T_{old}}^{t_0+T_{old}+T_{new}} (y(t) - y_{ref})^2 dt + 2\frac{R}{Q} \end{aligned} \tag{3.11}$$

Assuming the system follows the optimal steady limit cycle, then the following holds for T_{new} being in the neighborhood of T^*_{new} (optimal half period) :

$$ls(T_{new}) = rs(T_{new}) \Leftrightarrow \frac{dJ}{dT} = \frac{dJ}{dT_{new}} = 0 \Leftrightarrow T_{new} = T^*_{new} \tag{3.12}$$

Thus the idea is to use T_{new} as the adaptation variable for finding the switch time for the current half period and use a switching criterion, i.e. when $ls(T_{new}) = rs(T_{new}) \Leftrightarrow \frac{dJ}{dT_{new}} = 0$ at the time $t_0 + T_{old} + T_{new}$ the input will be switched. However to ensure that the switch in fact is done at a minimum cost, the second derivative should be positive $\frac{d^2J}{dT^2_{new}} > 0$.

$$\frac{d^2J}{dT^2_{new}}|_{T=T_{old}+T_{new}} = \frac{2\left(Q(y(t_0 + T) - y_{ref})\frac{dy(t_0+T)}{dT_{new}} - \frac{dJ}{dT_{new}}\right)}{T} \tag{3.13}$$

As $\frac{dJ}{dT_{new}} = 0$ when doing a switch (according to the switching criteria (3.12)), $\frac{d^2J}{dT^2_{new}} > 0$ requires that $(y - y_{ref})\frac{dy}{dT_{new}} > 0$. Note that y, $y(t_0 + T_{old} + T_{new})$, $y(t_0 + T)$, $y(T_{new})$ all represent the current measured output. Given an open loop SISO stable system with monotonic step response and no non-minimum phase behaviors, such that the output $y(t)$ monotonically increases/decreases depending on the direction of the input. Further assume, that the optimal switch time at the earliest will be after the output $y(t)$ has crossed the reference, thereby $(y - y_{ref})\frac{dy(T)}{dT_{new}} > 0$. This ensures $\frac{d^2J}{dT^2_{new}} > 0$ for all values of T_{new} (being it in an ON as well as an OFF period) where $\frac{dJ}{dT_{new}} = 0$. Consequently there can be no maxima or saddle points with the convex

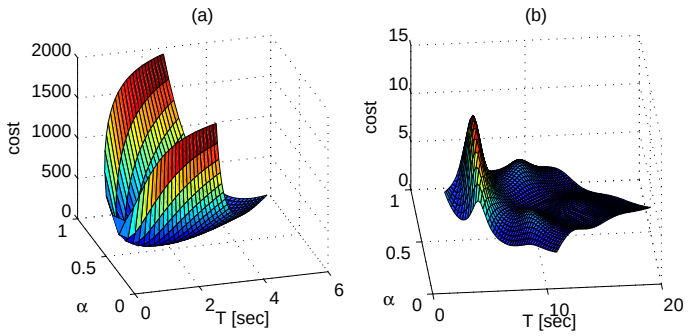

Figure 3.3: Cost J as function of the period T and duty cycle α plotted for second order system $\frac{1}{(s-p_1)(s-p_2)}$ with: (a) poles $p_1 = -1, p_2 = -2$. $Q = 1, R = 50$. (b) poles $p_1 = -0.25 + 1.39i, p_2 = -0.25 - 1.39i, Q = 1, R = 5$.

domain $T > 0$, hence as J is continuous and smooth, there can be one minimum only.

The following conjecture is stated,
The cost function (3.3) has one minimum only (a global minimum) given an open loop SISO stable system with monotonic step response and no non-minimum phase behavior.

To illustrate the conjecture by examples, Fig. 3.3a depicts a cost function for a SISO second order system with monotonic step response and no no-minimum phase behavior. In this case the cost function is clearly convex. Fig. 3.3b depicts the result for a stable SISO second order system with complex poles, which is clearly not convex. The maxima of the cost function, seen in Fig. 3.3b, appears when the switching period corresponds to the harmonic frequencies of the system.

The optimizing switch control can be implemented in the following way, that at each time instance $t = t_0 + T_{old} + T_{new}$ it should be decided whether a switch should be

made or not based on following criteria.

Switch the control input

if

$$\left((y(T_{new}) - y_{ref})\frac{dy(t)}{dt} > 0\right) \wedge (ls(T_{new}) \geq rs(T_{new})) \wedge (|y(T_{new}) - y(t_0)| \leq \Delta y) \tag{3.14a}$$

or

$$\left((y(T_{new}) - y_{ref})\frac{dy(t)}{dt} > 0\right) \wedge ((y(T_{new}) - y(t_0) > \Delta y) \wedge (y > y_{ref})) \tag{3.14b}$$

or

$$\left((y(T_{new}) - y_{ref})\frac{dy(t)}{dt} > 0\right) \wedge ((y(t_0) - y(T_{new}) > \Delta y) \wedge (y < y_{ref})) \tag{3.14c}$$

where Δy is adjustment parameter setting the maximal correction step. The last half cycle period T_{old} has been decided earlier, hence it should only be decided whether to do the switch for the current half cycle period T_{new} at the current time instance or not. The algorithm only strives at optimizing time for the current half cycle period T_{new}, based on the integrated error over the time elapsed of the total cycle period.

In the following, a discrete version of the optimizing switch control algorithm based on (3.15) is applied, which is,

$$\begin{aligned} lsd &= (y_{N_{t_0}+N_{T_{old}}+N_{T_{new}}} - y_{ref})^2 (N_{T_{old}} + N_{T_{new}}) \cdot T_{samp} \\ rsd &= \sum_{N_{t_0}}^{N_{t_0}+N_{T_{old}}} (y_{N_{T_{new}}} - y_{ref})^2 \cdot T_{samp} \\ &+ \sum_{N_{t_0}+N_{T_{new}}}^{N_{t0}+N_{T_{old}}+N_{T_{new}}} (y_{N_{T_{new}}} - y_{ref})^2 \cdot T_{samp} + \frac{2R}{Q} \end{aligned} \tag{3.15}$$

where lsd, rsd are the discrete version of ls, rs. The integration term in (3.11) is expressed as a sum of the values, which is easy to implement in experiments. The sampling time is T_{samp}. N_{t_0} refers to the number of samples at the starting time of the total cycle period; $N_{T_{new}}, N_{T_{old}}$ represents the current half cycle period and the previous half cycle period respectively in samples.

According to the conjecture, the cost function (3.1) for a system fulfilling the requirements has one minimum only. Fig. 3.4 shows how periods update take place on a contour plot of the cost defined by (3.3) for the first order system (3.2). In the example, at a certain time, the $T_{old} = T_{ON} = 950sec$, then $T_{new} = T_{OFF}$ found according to the

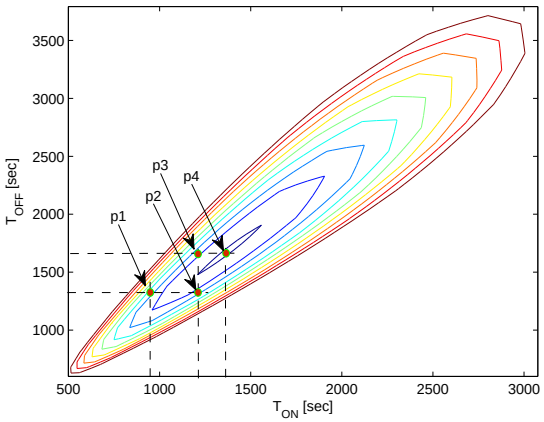

Figure 3.4: Illustration of the periods update on a contour plot of the cost defined by (3.1) with a certain load. T_{ON} is the ON period and T_{OFF} is the OFF period.

T_{old} is $T_{OFF} = 1350sec$. Then update $T_{old} = T_{OFF} = 1350sec$, then $T_{new} = T_{ON}$ found based on the T_{old} is $T_{ON} = 1230sec$. Repeating the above procedures, at last the optimal solution $T_{ON} = 1374sec$, $T_{OFF} = 1685sec$ is reached in this example.

The optimizing switch control algorithm deduced above optimizes the current half periods according to the previous period, i.e. T_{new} is optimized according to T_{old}. If the correction of the half periods is sufficiently small, the performance cost can be arbitrarily close to the steady limit cycle performance cost depicted in Fig. 3.4. Hence if the maximal correction step is chosen sufficiently small the optimizing switch control will iteratively step towards the global minimum as indicated in Fig. 3.4.

3.3 Simulation results

In this part, several simulations will be conducted to test the developed optimizing switch control method. The simulations are based on the simplified first order room model (2.8) in Subsection 2.2.3 where the air conditioning system is not modeled in detail, but represented by constant ON/OFF heat removal form the room model.

Throughout Part I of the thesis a definition of load (in percentage) is used. This is defined as a percentage of maximal capacity. For example load 85% means that the system has a load corresponding to 85% of $\dot{Q}_e$ where $\dot{Q}_e = 300W$ when the system is ON. The reference for the simulations is set to be $23°C$.

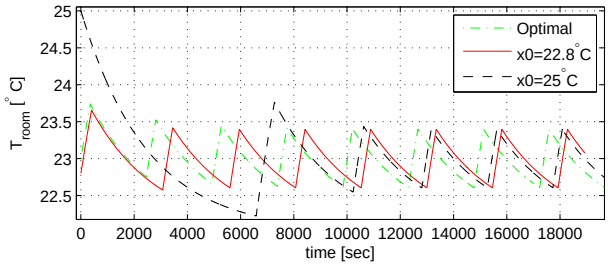

Figure 3.5: Comparison of outputs with the optimal solution. 'Optimal': the optimal solution. $x_0 = 22.8°C$: optimizing switch control method with initial state $22.8°C$. $x_0 = 25°C$: optimizing switch control method with initial state $25°C$. The results in this figure are all from load 85%. Q/R=2/500.

3.3.1 Convergence

Simulations of the optimizing switch control method with different initial conditions but the same load sequences are conducted, and they show that if the initial conditions are not so far away from the reference e.g. in this example with load 85%, from initial condition $20 - 25°C$, the results converge close to the optimal solution independent of the initial conditions. The reason that the results do not converge to the optimal solution when initial condition is far from the reference is that the right side of (3.10), rs keeps integrating, which becomes large with this initial condition, but the left side of (3.10), ls will not be able to catch up rs due to the first order system behavior. The result would converge for an integration system due to that the time constant is infinite. Under the condition that the initial conditions are far from the reference, the system should be kept on until the indoor air temperature gets down close to the reference and then change to the optimizing switch controller.

As an example, the output of the results $T_{room}$with initial conditions $x_0 = 22.8°C$ and $x_0 = 25°C$ are shown in Fig. 3.5, where both outputs converge to a result very close to the optimal solution. The optimal solution in Fig. 3.5 is achieved by applying a pulse input with the optimal duty cycle and cycle period calculated directly from the cost function J, to the system given by (3.2). The period, duty cycle and cost from the optimal solution and the optimizing switch control method with two initial conditions are presented in Table 3.1, where the initial conditions are not too far away from the reference.

Notice in Table 3.1, that the duty cycles are 85.69% which is different from the load. According to the definition of the load, if the system runs with the duty cycle equals to the load, the average will be maintained at the reference. Therefore the results with the optimal duty cycle actually do not maintain the average output at the reference. The reason why the duty cycle is different from the load is explained in Subsection 3.3.4.

	period	duty cycle	cost
opt.	4919	85.69%	0.31115
$x_0 = 22.8°C$	4925	85.69%	0.31117
$x_0 = 25°C$	4925	85.69%	0.31117

Table 3.1: Comparison of the results from different initial conditions with the optimal solution. The load is 85%, and Q/R=2/500.

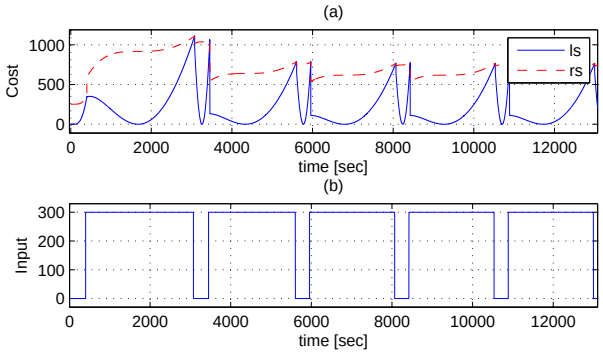

Figure 3.6: lsd, rsd from the simulations with initial state $x_0 = 22.8°C$, and load 85%

To demonstrate the optimizing switch method functionality, the left and the right side of (3.10) and the input switches are plotted in Fig. 3.6. The figure shows that during each half of the cycle period, the right side (rsd) of the equation is accumulating, and is re-initialized at each switch; the left side (lsd) of equation after a switch first decreases, and later increases again. This is due to that the half cycle period T_{new} is initialized to 0 at each switch, and the output moves from one limit towards the reference, crosses the reference and at last move towards the other output limit on the other side of the reference. The switches only take place when the left (lsd) and the right side (rsd) equal.

Simulations are made to study whether the optimizing switch control algorithm drives the output towards the optimal solution under different Q/R ratios and different loads. The results are shown in Fig. 3.7. It can be seen that the optimizing switch control method indeed converges close to the optimal solution with different Q/R under different loads.

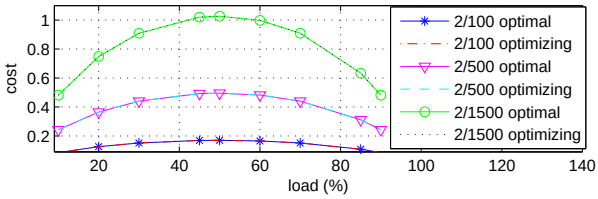

Figure 3.7: Simulation results of the optimizing switch control method with different Q/R ratio compared with the optimal solution. The initial state $x_0 = 22.8°C$

3.3.2 Comparison with a benchmark relay controller

It has been shown that the optimizing switch control method drives the system towards the optimal limit cycle independent of the working conditions. Since the output of the system (as shown in Fig. 3.5) seems to be very similar to a traditional relay control result, the following question arises: What is the difference between the proposed method and a traditional relay control method when applied to the considered system? A comparison between the two controllers is made based on simulations below.

Simulation with a relay controller applied to the switching system is carried out first. The relay controller is tuned at 50% load, such that the best possible relay bounds on the temperature can be found, i.e which gives the same cost as the optimal solution. The tuning results are shown in Fig. 3.8. The corresponding output deviation at 50% load is $0.5°C$ (relay input limits equal the reference $\pm 0.5°C$). Applying the tuned relay controller on system (3.2) under different loads, yields the results shown in Fig. 3.8, where the cost, period, duty cycle deviation from the optimal solution under different loads are plotted. Obviously the relay controller tuned at 50% load produces results very close to the optimum at this load. Away from 50% load, the results are deviating from the optimal solution, for example at 90% load, the performance cost defined by (3.1) for the relay controller is 20% higher than the optimal solution.

A controller with the proposed optimizing switch control method is applied to the system under the same loads, and the results are plotted in Fig. 3.8 too. It can be seen that the proposed optimizing switch control method attains close to the optimal solution as stated previously.

3.3.3 Performance during load change

A simulation test of the optimizing switch control method with load change has been performed, and the result can be seen in Fig. 3.9. The load at the beginning is 70% corresponding to $T_{amb} = 27.62°C$, and at sample 30000 it is reduced to 10% corresponding to $T_{amb} = 23.66°C$. The result shows that the optimizing switch control method works under load change as long as the load is below 100% corresponding to $T_{amb} = 29.6°C$.

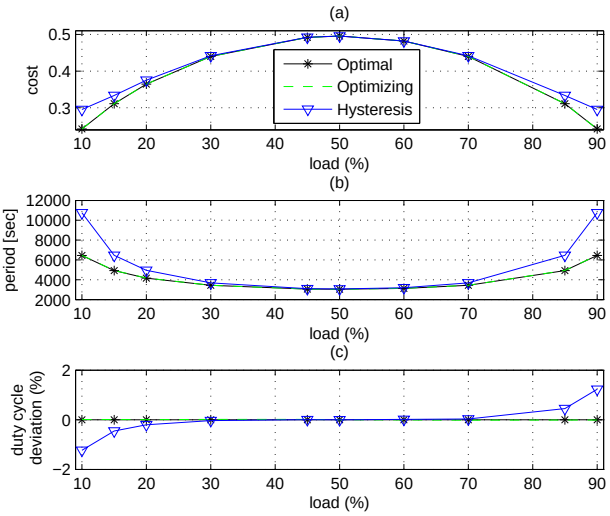

Figure 3.8: Comparison of solutions from the different methods. 'Optimal': the optimal solution. 'Optimizing': the developed optimizing switch control method. 'Hysteresis': hysteresis control. The initial state is $x_0 = 22.8^{\circ}C$.

From sample 30000 to 80000, the average output is higher than the reference, which demonstrates the difference between the optimizing switch controller and the relay controller. When the load is higher than 100%, the switching system saturates. The system stays ON, resulting in a infinitely long period. In this case, the optimizing control has similar problem as the windup in e.g. PID control approach. Therefore special care similar to anti-windup measures has to be taken to solve this problem. However, this will not be discussed in details due to that the main focus of the work is to develop an optimizing switching control method.

3.3.4 Notes regarding the load and duty cycle

It is worth mentioning that the optimal duty cycle and load might be different for the first order switching system. This can be seen in Subsection 3.3.1. The closer the load to 1 (or 0), the larger difference is between the optimal duty cycle and the load. The reason is that, the half cycle period error accumulation (either ON or OFF period) has a smaller gradient in the end of longer half cycle period than the short half cycle period, which means that prolonging the longer half cycle period will not result in much output deviation, but a much longer period and much smaller cost, therefore the optimal duty cycle is different from the load as long as the load is not 50%.

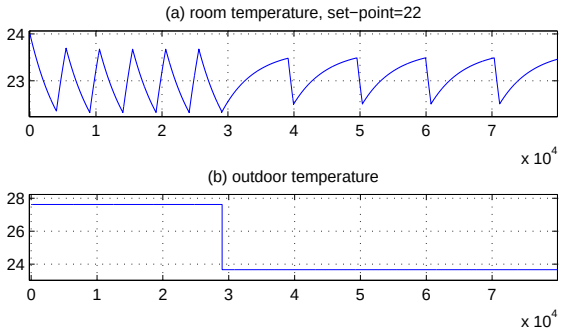

Figure 3.9: The optimizing switch control method performance during load change. The disturbance $T_{amb} = 27.62^{\circ}C$ and $T_{amb} = 23.66^{\circ}C$ is corresponding to load=70% and 10%. Penalty ratio Q/R=2/1500.

For example, the optimal solution for a 90% load with Q/R=2/500 yields $T^* = 6447s$ and $\alpha^* = 90.91\%$, where T^* and α^* denote the optimal period and the optimal duty cycle. It is clear that the optimal duty cycle is different from the load (remember that the load is defined as a percentage. It means that if the system removes $load \times (\overline{u} - \underline{u})$ amount of power, the room temperature will be controlled at the reference.). The optimal cost is 0.242. For comparison purpose, the smallest cost for duty cycle 90% was found by fixing the duty cycle to 90% and then running the system with different periods. The smallest cost was found to be 0.249, which is obtained with a period $T = 6082s$. The optimal solution actually results in a longer period ((6447-6082)/6082=6%) but at the same time achieves smaller cost.

Two further studies were carried out to demonstrate the effect of the load and Q/R ratio on the differences between the load and duty cycle.

The first investigation concerned the influence of the load and was carried out by calculating the optimal solution under different loads. The results are presented in Table 3.2 which show that if the load α is not equal to 50%, the optimal duty cycle and the load are always different. The closer the load to 1 (or 0), the larger difference is between the optimal duty cycle and the load. The reason is as explained at the beginning of this subsection.

The second investigation concerned the impact of the choice of the Q/R ration on the obtained solution. It was carried out by evaluating the obtained optimal solutions with different Q and R but under the same load condition. The results are presented in Table 3.2 which shows that the value of the difference depends also on the ratio of Q/R ratio. With increase of R, the difference becomes bigger because the penalty of switching is increasing, therefore, the long half cycle period will be prolonged even longer. For 50% load, the error accumulation in both the ON and the OFF period has the same gradient

Q/R	results from	load							
		90%		60%		50%		10%	
		period (S)	duty cycle	period (S)	duty cycle	period (S)	duty cycle	period (S)	duty cycle
2/500	opt.	6447	90.91%	3125	60.12%	3037	50.00%	6447	9.09%
	cont.	6460	90.89%	3130	60.16%	3042	50.00%	6460	9.10%
2/2500	opt.	13947	93.12%	5421	60.48 %	5257	50.00%	13947	6.88%
	cont.	13955	93.11%	5427	60.48 %	5262	50.00%	13956	6.89%

Table 3.2: The solutions for different load and different penalty ratio. 'opt.' refers to the optimal solutions calculated from the cost function. 'cont.' refers to the solutions from the optimizing switch controller.

over the corresponding period, therefore, the optimal duty cycle is the same as the load. (More details can be found in [50]). A note here is that when the system is under load α, the optimal periods are the same as under load $1 - \alpha$.

Until now an optimizing switch control method has been developed, which controls stable first order systems towards the optimal limit cycle, has low complexity, and outperforms relay controllers in simulation tests. An exciting step is to experiment the optimizing switch control method with a real plant. However, the problem is that in the real world, systems can very seldom be modeled as first order systems, which the optimizing switch control method is designed based on. Under some operating conditions, some of these plants can be modeled as high order linear systems. In many applications, these high order linear systems can be approximated as a first order system with a delay. Therefore extension of the method to system with delays is necessary in order apply it to applications.

3.4 Systems with delays

The reason why extending the optimizing switch control method to work with systems with delay is important has been explained. Applying the optimizing switch method directly to a first order system with a delay leads to suboptimal solution because the information that is fed back to the controller is 'old'. The optimal solution for a first order switching system is independent of whether the system has a delay or not, meaning that if the delay-free output is fed back to the controller, the system should perform exactly the same as for the systems without delay under no disturbances. The question is how the delay-free output information can be achieved.

Extensive research has been carried out on controlling systems with delays, see the survey [51]. One traditional method is based on the Smith Predictor [52]. Due to the problem that Smith Predictor does not work with unstable systems as for example systems with an integrator, [53], [54], [55] have proposed modified Smith Predictor methods. A common prerequisite for successful employment of Smith Predictor (both the

original as well as the modified ones) is the accurate knowledge of the model and delay. For most industrial cases this knowledge is not easily available.

Another approach is based on the idea of representing the delay with a Pade approximation, see e.g.[56]. A systematical approach of designing observer based on Pade approximation is introduced in [57], which will be explained briefly here.

3.4.1 Observer based on Pade approximation

The proposed observer design approach in [57] is to first partition the delay θ into p non-overlapping delays as (3.16), then introduce Pade approximation (3.17) to each partition of the delay and formulate a state space model of the Pade approximated delay together with the system model (3.2). This approach facilitates using well-established design techniques to construct an observer that provides the delay-free output.

$$e^{-\theta s} = (e^{-\frac{\theta}{p}s})^p \tag{3.16}$$

$$e^{-\frac{\theta}{p}s} \approx \frac{1 - \frac{\theta}{2p}s}{1 + \frac{\theta}{2p}s} \tag{3.17}$$

3.4.2 Novel approach of designing observer for systems with delay

Our proposal of designing observer for delay systems can be explained in the following steps:
(1) Discretize the system including delay with a large sampling time $\frac{\theta}{m}$, so that the delay can be partitioned into m partitions, and each of the delay partition can be modeled as one sampling time delay, and therefor the whole systems becomes a discrete LTI system.
(2) Design an observer for this discrete time system - find the gain L_d.
(3) Check whether the observer is stable if the discrete observer gain is directly applied into the continuous (or system with a much faster sampling time) system. If it is stable, then the observer is found, otherwise, increase m, repeat the above procedure. It is preferred to have a minimal m because it ensures that the observer has a minimal number of states.

In continuous time, the delay in the observer is divided into m number of delays $e^{\frac{\theta}{m}s}$, and the corresponding terms in gain L_d to compensate each term of $e^{\theta s}$. The observer stability can be checked in this way: find the observer transfer function from the error (between the measured and estimated output) to the estimated output, and check the stability based on e.g. a Nyquist diagram. Such an observer stability Nyquist diagram is shown in Fig. 3.10, where the observer gains are designed based on different sampling times. From the figure, it can be seen that the observer stability increases with decrease of the sampling time.

The proposed observer design approach is systematical, and comparing with the observer based on Pade approximation, the advantage is, that the observer stability is

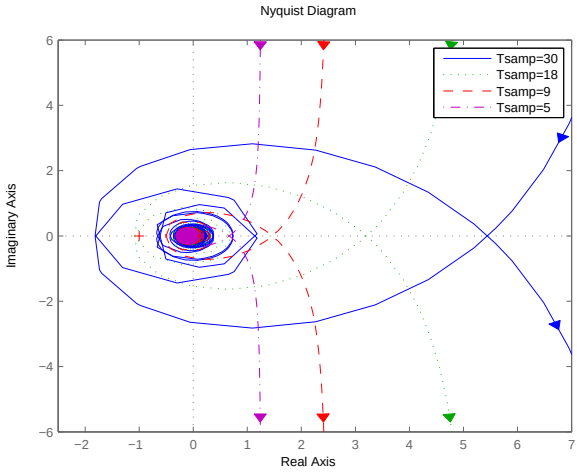

Figure 3.10: Nyquist diagram of the continuous observer transfer function. The observer gain is designed in discrete time based on different sampling time. Stability is obtained for sufficiently small sampling times only.

ensured. However, in the experiments the observer based on Pade approximation $p = 1$ is stable. No further study regarding this new approach of designing observers for systems with delays will be discussed in this chapter, due to that the focus of the chapter is the optimizing switch control method.

3.5 Experiments with a refrigeration plant

In this section, the optimizing switch method developed in Section 3.2 is tested with the refrigeration system described in Section 2.3. As presented previously in (2.10), the refrigeration system is characterized with a delay θ. Hence an observer is required in order to apply the optimizing switch control method. The observer is shown in Subsection 3.5.1. The experimental results from the optimizing switch control method including the observer, and comparison with a benchmark relay controller are presented in Subsection 3.5.2.

3.5.1 The observer

The observer applied together with the optimizing switch control method is based on Pade approximation as described in Subsection 3.4.1 with $p = 1$. The model of the refrigeration plant used for the observer is (2.9). Due to the difference between the input

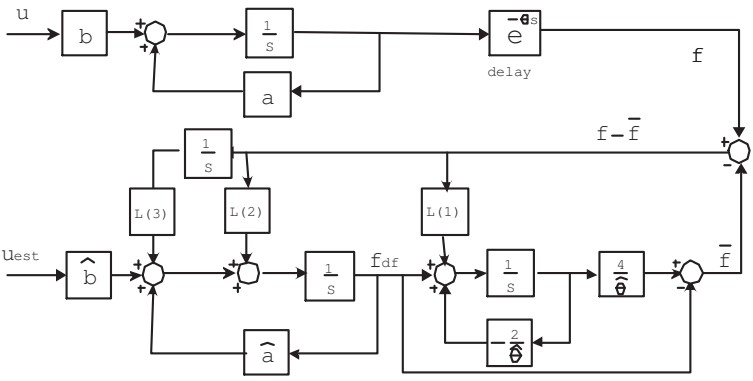

Figure 3.11: Pade PI observer, where the delay is based on Pade approximation. $L = [L_{(1)}, L_{(2)}, L_{(3)}] = [1.23 \times 10^{1}, 6.75 \times 10^{-2}\, 1.25 \times 10^{-4}]$. θ is the delay time. u is the actual input energy to the system. u_{est} is the input to the observer which is estimation of u. f is the measured output. $\overline{f}$ is the estimated output. f_{df} is the delay-free output.

energy to the refrigeration plant and the estimation of the input to the observer, an offset appears on the estimated delay-free output. To remove the offset, an extra integration term is introduced, which eventually becomes a proportional and integral (PI) observer. Design of such a PI observer can be found in [58], and the procedure will not be repeated here. The resulting observer is shown as in Fig. 3.11, which is referred as Pade PI observer in this chapter. The following observer gains are applied in experiments.

$L = [1.23 \times 10^{1}, 6.75 \times 10^{-2}, 1.25 \times 10^{-4}]$.

3.5.2 Experimental results

Experiments with the test plant described in Section 2.3 are conducted to validate the optimizing switch control method. Tow groups of experiments are conducted to answer the following questions: (1) Does the optimizing switch control method drive the system towards the optimal solution? (2) Does the optimizing switch control method outperform the relay control method? For the experiments, the test plant water tank set-pint temperature is $22°C$.

3.5.2.1 Optimizing switch control method vs. optimal solutions

In this part, experiments have been conducted to investigate whether the developed optimizing switch control method with observer designed in Subsection 3.5.1 drives the refrigeration plant towards the optimal solution defined by (3.3).

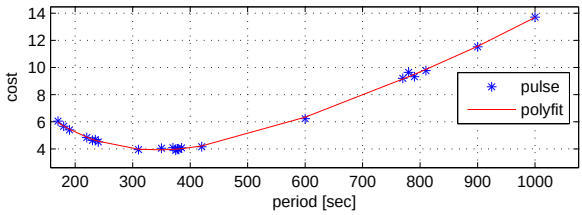

Figure 3.12: Cost vs. periods. $Q = 20$, $R = 500$. Heating load $1000W$. 'pulse' refers to the cost results from the pulse input experiments. 'polyfit' is the polynomial fit of the discrete test points of the pulse experimental results.

The first question is what is the optimal solution for the refrigeration plant. The optimal solution for the refrigeration plant is different from the calculated optimal solution based on the model (2.9), because the model (2.9) (integration and delay) is a crude approximation of a high order system. The only way to achieve the optimal solution for the test system is to run pulse experiments with different periods and duty cycles until it reaches the stable limit cycle, then calculate the cost using (3.3) to find the period and duty cycle combination corresponding to the smallest cost. Due to that the refrigeration plant is very close to an integration system, the duty cycle and the load are very close to each other, which can be calculated directly by the heating to cooling ratio, while for a first order system, the optimal duty cycle will be different from the load when the load is different from 50%.

The above procedure of finding the real optimal solutions is illustrated by Fig. 3.12. where the penalty is $Q = 20$, $R = 500$ and heating load is $1000W$. A polynomial fit of the test points has minimal cost at around $350s$. The benefit of the polynomial fit is that with discrete test points, a continuous expression of the cost as a function of the period can be achieved.

To investigate the ability of the optimizing switch control method to achieve the optimal solution at different penalty ratios, another two optimal solutions for the real penalty $Q = 2$, $R = 500$ and $Q = 80$, $R = 500$ are also demonstrated with pulse experiments. The resulting three optimal solutions at three different Q (R is kept at 500 for all the experiments) are shown in Fig. 3.13. For comparison, the optimizing switch control resulting costs at different Q/R ratio and heating disturbance $1000W$ are also plotted Fig. 3.13.

Fig. 3.13 demonstrates that the solutions from the optimizing switch control (legend 'optimizing') are very close to the optimal solution (legend 'real'). The error defined by (3.18) at the three $Q = 2, 20, 80$ are $2.30\%, 4.85\%, 3.00\%$. These results prove that - the optimizing switch controller achieves results very close to the optimal solutions.

$$error = \frac{|cost_{optimizing} - cost_{real}|}{cost_{real}} \tag{3.18}$$

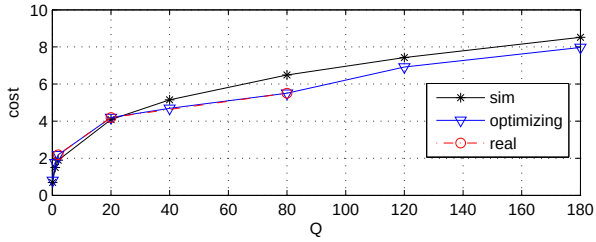

Figure 3.13: Comparison of optimizing switch controller and real optimal solution at heating load $1000W$. R is kept at 500. 'sim' is the optimal solution for the model (2.9). 'optimizing' is the optimal solutions by applying the optimizing switch control on the refrigeration system. 'real' is the optimal solution from the pulse experiments with the refrigeration system.

3.5.2.2 Comparison with the benchmark relay controller

In Subsection 3.3.2, simulation results from the optimizing switch control and relay controller for a first order system have been compared, and they show that the optimizing switch control method outperforms the relay control when the systems are not at the nominal working condition for the relay.

Several experiments have been carried out to investigate the performance of the optimizing switch control method and the relay controller with and without observers at different heating loads.
(1) Optimizing switch control method. Run the optimizing switch control method including the Pade PI observer at different heating loads with parameter $Q = 2, R = 500$. The observer gains are $L = [1.23 \times 10^{1}, 6.75 \times 10^{-2}, 1.25 \times 10^{-4}]$.
(2) Standard relay controller. Tune the relay controller at about 50% corresponding to about $1500W$ heating load, which reaches results very close to the optimizing switch control. The resulting relay band is $0.36°C$, which means that the refrigeration system switches on when $T_{w,out}$ is higher than $22 + 0.36°C$ and switches off when $T_{w,out}$ is lower than $22 - 0.36°C$. Then run the experiments with this relay controller at different heating loads.
(3) Relay controller with observer. An improvement for the relay controller could be to include the Pade PI observer. Apply the Pade PI observer and feed the non-delayed information to the relay controller. Repeat the procedure of tuning the standard relay controller. The resulting relay band is $1°C$. which means that the refrigeration system switches on when $T_{w,out}$ is higher than $22 + 1°C$ and switches off when $T_{w,out}$ is lower than $22 - 1°C$. Then run the experiments with this controller at different heating loads.

The results from the above three experiments are shown in Fig. 3.14, where it can be seen that close to the nominal condition 50% load, the relay controller with and without an observer produces fine results, but when the heating load moves away from 50%, for example at heating load $500W$, the standard controller cost deviation from

the optimizing switch controller is very large, while the relay controller including the observer improves the result, but still the cost is much larger than the optimizing switch control result.

The temperature outputs from these three controllers at heating load $500W$ are plotted in Fig. 3.15. It can be easily seen that when the system reaches a stable limit cycle, the standard relay control output has an offset, which results in an increased cost. The reason for this offset is that during the delay time, the heating power $\dot{Q}_{load}$ to raise the temperature (when refrigeration system is switched OFF) and the heating power minus the cooling power $\dot{Q}_e - \dot{Q}_{load}$ (when refrigeration system is switched ON) to remove heat is different. The offset in the standard relay is removed by applying the Pade PI observer to the relay controller and it performs better than the standard relay controller. The difference in the controlled temperature between the relay controller plus the observer and the optimizing switch controller including the observer is not that obvious. However the difference in performance cost defined by (3.1) between the two controllers can easily be seen with the switching cost in Fig. 3.14, where the switching cost for the optimizing switch method including the observer is smaller than the relay controller with the observer. From these results it can be concluded that the optimizing switch controller outperforms the traditional relay and relay with Pade PI observer.

Despite that the optimizing switch controller performs well during stable limit cycles, the result from the optimizing switch controller converges much slower to the stable limit cycle, and consequently a much larger temperature variation at the beginning is resulted. This is caused by the initial states of the observer - mainly due to the Pade approximation state and the accumulation of this output deviation from the reference in the controller. In relay controllers, the effect of of the estimated output deviation from the reference is not so obvious because the relay controllers do not make control decision based on the previous input. The problem can be solved by a better assignment of the initial states in the observer. However this is not further presented due to that it is not the main focus of this work.

From all the experimental results in this section it can be concluded that the optimizing switch controller drive the plant towards to the optimal solution and outperforms the traditional relay and relay with Pade PI observer.

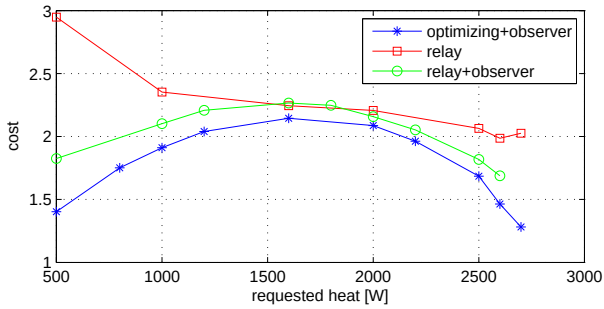

Figure 3.14: Comparison: optimizing switch controller with Pade PI observer, standard relay controller and relay controller with observer. The relay controller is tuned under 50% load

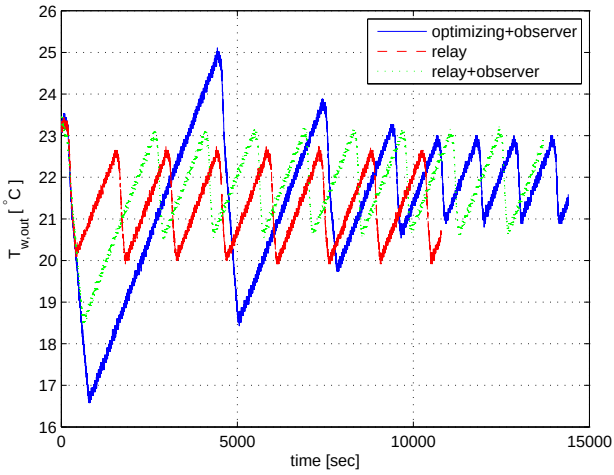

Figure 3.15: Comparison: the temperature output from the optimizing switch controller with Pade PI observer, standard relay controller and relay controller with observer at heating load $500W$.

Chapter 4

Conclusions, perspectives and future work : control of air conditioning systems

4.1 Conclusions

In thesis Part I, control of switching systems was considered. The work was presented in a collection of papers enclosed in Part IV. The main focus was on deriving a low complexity and low cost optimizing switch control scheme for mass produced systems such as residential air conditioning units. The proposed method was designed for SISO stable systems with monotonic step response and no non-minimum phase behavior under binary input conditions.

Firstly a cost function optimizing the switch period and duty cycle was formulated and proven to be convex for stable first order systems. Secondly a control method based on the gradient of the cost function was proposed. Thirdly, the control method was extended to incorporate first and high order systems with or without delays. Finally the method was validated by experimental results.

The following conclusions can be extracted from thesis Part I.

- For stable first order systems, the optimizing switch control method achieves results close to the optimal solutions. For first order systems with delays and a class of SISO stable high order systems with monotonic step response and no non-minimum phase behavior, the method controls the systems towards the optimal solutions when the included observer retrieves the delay-free output.

- The low complexity method does not require special tuning or knowledge of specific system parameters which makes it ideal for industrial implementation. The

method relies only on the information of the controlled variable (if the system is without delay), or the estimated delay-free output (if the system is delay dominant).

- The method avoids the fundamental problem of finite horizon prediction methods.
- To give an idea of the improvement of the optimizing switch control method, the results of a traditional relay tuned at nominal condition was compared to the optimizing switch control method results. The results of both simulation and experiments showed that the optimizing switch control method outperforms the traditional relay.

The optimizing switch control method achieves better results than the relay method for first order or high order switching systems. Compared with the standard relay method, the optimizing switch control method required only a little more computational power, for example an extra state for integration term etc. This means that systems with high costs related to switching frequency, i.e. components wear, low performance, can achieve much better results if the optimizing switch control method is applied instead of a relay. In systems containing delay, both the relay and the optimizing switch control method benefits from the delay-free information, which can be achieved by introducing an observer.

However the method is limited to stable first order (including delay) or SISO stable high order systems with monotonic step response and no non-minimum phase behavior, in both cases with binary inputs.

The proposed method is empirically inspired, and it is not claimed that it holds in all generality. It is tested on a specific test system with good results. The authors, however, are convinced that the optimizing switch control method can be applied to a wide class of systems, including many arising from a variety of industrial areas.

4.2 Perspectives

A low complexity optimizing switch control method has been developed based on an switching controlled air conditioning system. In addition to the air conditioning system, many other industrial systems exhibit switching features, where the proposed optimizing switch control method might be able to solve the control problems. These systems often have low energy efficiency and/or components wear during start/stop transients. To be able to apply the optimizing switch control method, the systems have to SISO stable high order systems with monotonic step response and no non-minimum phase behavior. Several industrial examples of such nature are given below.

Heat pumps. A heat pump is usually installed to provide heating, which can be delivered in form of hot water or air. Depending on the heat uptake, the heat pump can often be classified as air or geothermal heat pump. However, this will not affect the application of the optimizing switch control method in heat pump systems. The

heat pump is indeed a refrigeration system which utilizes the heat released from the condensation process.

Where the air heat pump is very similar to a typical residential air conditioning system, the water based heat pump is similar to the test system in Aalborg University. Both heat pump types include a switching cost related to component wear and low energy efficiency during start and stop transient. The internal media circulation can be considered as a first order system, and disturbance is the heat loss to the outdoor ambient. When the heating load is low, the systems have to be switching controlled. Therefore the optimizing switch control method can be applied to heat pump systems when the heating load is low.

Condensing boilers. A condensing boiler is very energy efficient due to cooling of the exhaust gas and the latent heat of water vapour in exhaust gases. The return water temperature is recommended to be below $60°C$. However, the gas burning must be kept above a specified minimum to avoid excessive pollution and degraded efficiency. There are different control strategies applied to these systems. However when the heat load is low, switching control has to be applied.

An example is that the boiler provides hot water to heating systems. This is similar to the heat pump example. The system can be modeled as a first order system and the disturbance is the heat loss to the indoor air. The system has a switching cost related to low energy efficiency and thermal stress of the components. Therefore the optimizing switch control method can be applied.

District heating plants. Similar to the above examples, some district heating plants may also need switching controlled operation. There is usually a internal water circulation which deliveries heat to nearby houses and buildings through heat exchangers. The internal water system can also be seen as a first order system. Here is also a switching cost related to low energy efficiency during startup phase. Therefore the optimizing switch control method can be applied to some district heating plants. Typically for this type of systems computational power is not a major problem, the method avoids the problem with finite prediction horizon approaches, and therefore might provide better performance.

The examples given here are only confined to energy systems, however the author believes that the switching controlled system problems also exist in other type of systems, and for some of them, the problem can be solved by the optimizing switch control method.

4.3 Future work

In this section, some suggestions for future work and research are stated concerning two aspects - academic and industrial.

4.3.1 Academic aspect

Robustness property of the method is not addressed in the thesis, therefore a rigorous proof of robustness issues would be interesting for future research.

The method is designed for SISO systems, however there exist many switching systems with multiple inputs. Extending the method to cooperate with systems with several inputs is an important direction for the future work too.

The method takes only the output variation and a switching cost in deciding the control action. Another term that is interesting to be included in the control is the energy consumption which is important to a lot of applications. This requires modification in the cost function and therefore the corresponding optimizing switch control algorithm.

The study in this part of the thesis has been focusing on switching systems with a binary input. It would be very interesting to extend the method to systems that can run continuously in the range of $[\overline{u} \quad u_{max}]$ where u_{max} is the maximum of the input and have to run switching control between $\underline{u}$ and $\overline{u}$ when the required input is lower than $\overline{u}$. In this case, a high level controller is proposed, which switches between the continuous controller when the input is $u \subset [\overline{u} \quad u_{max}]$ and switching controller when the required input is between $\underline{u}$ and $\overline{u}$.

Another direction is of course to merge continuous and discrete inputs. Many systems have both and then it really becomes difficult. One trick, however, is to make an alternate design of discrete and continuous designs.

4.3.2 Industrial aspect

A controller needs to implement a user adjustable balance between the comfort and economic issues. This can then be translated into a Q/R ratio for the cost function. Reasonable Q/R ratios might depend on the construction type and size of the house and on personal preference of the inhabitants.

Part II

CONTROL OF DOMESTIC HEATING SYSTEMS

Chapter 5

Introduction to control of heating systems

5.1 Motivations and objectives

Application of control algorithms in floor heating systems, especially in water-based floor heating systems is an area that is relatively unknown within the community of control engineering, only a few publications can be found. Traditionally most of the development of floor heating system control algorithms has been carried out by specialists within the building and architectural area. Lack of dynamic mathematical models has made it difficult for a non-building specialist to contribute to the development of the control algorithms.

Among floor heating systems, the water-based floor heating system with a heavy concrete construction is the one that poses the most challenges to the design of the control algorithms. This is because the water pipes are cast in a thick concrete layer with a large heat capacity. For water-based floor heating systems, the inlet water temperature of the heating pipes is strictly limited due to the discomfort of having a very hot floor and the temperature limitations of the floor material. For these reasons, the indoor air temperature exhibits very slow dynamics. The room temperature control of such a system becomes hard, especially when fast disturbances are present.

To overcome the problem with fast disturbances, a fast heating system is often installed to compensate the slow dynamics of the floor heating system. However with the current control strategy, the heating systems are regulated independently, disregarding the strong cross couplings. This often results in a inferior indoor comfort and a poor energy efficiency. The main problem is that these subsystems typically have no knowledge of each other. An example could be a floor heating system with a large heat capacity installed in the same room with an electrical heater.When the room temperature is lower than the reference, both heating subsystems (heat source) are active. The floor heating

system first needs to transmit the heat through the large heat capacity of concrete subfloor, resulting in a slow dynamic. The electrical heater emits heat directly to the air of the room, hence a much faster room temperature reaction can be observed. When the reference is reached, both heating systems switch off, but large amount of heat stored in the subfloor is released until the floor and the air in the room reach the same temperature, hence resulting in a significant temperature overshoot. This is obviously uncomfortable and waste of energy. The main problem today is that all of these heating systems in the same house have their own controllers and they work independently without the knowledge of each others existence.

The main objective of Part II of the thesis is to investigate control in domestic heating systems such that the indoor comfort with respect to temperature and energy efficiency are optimized. This is divided into following two ares.

Control of a water-based floor heating system applied for heavy construction.
Most of water-based floor heating systems are controlled with relay controls of the water circuit circuit inlet/outlet valve based on the room temperature which results in unsatisfying performance. The study in [6] indicates that the performance can be improved with a more sophisticated control based on the emitted power directly. The objective of this part of the thesis is to develop an energy based control method for floor heating system that improves the comfort with respect to temperature and energy efficiency. The focus is on the heavy construction water-based floor heating systems with a spiral pipe layout.

Control of multiple heat source system.
To overcome the discomfort caused by the slow reaction of a typical floor heating system, it is often complimented by a faster reacting heat source. An example could be an electric heater. The two heat sources are characterized with different dynamics and economic cost of using. The water-based floor heating system is slow dynamic and cheap to use, while the electrical heater is fast dynamic in heating the room air but much more expensive due to that the electricity price is much higher than the water heating energy price in some of the area in Denmark. Hence the objective is to benefit from the comfort of the floor heating control, and at the same time allow the fast heating system to compensate for the fast occurring disturbances and taking the economic cost of energy into consideration such that both comfort and economic cost are optimized. Control of systems with multiple heating source systems illustrates the challenges of the intermediate control layer. An inherit challenge in the set-up is the obvious inability of fast heat source to remove heat to reject disturbances.

The chapter is organized as follows. First an introduction of floor heating system with respect to classification and challenges is given in Section 5.2. Then the test system used for experiments is described in Section 5.3. After that, the previous work in the area of modeling and control of floor heating systems is reviewed in Section 5.4. At last

contribution and publication in the control of the heating systems is listed in Section 5.5 and the rest of the thesis Part II is briefly introduced in Section 5.6.

5.2 Floor heating systems

During the last two decades, radiant floor heating applications have increased significantly. In Germany, Austria and Denmark, 30% to 50% of new residential buildings have floor heating. In Korea, about 90% of all residential buildings are heated by floor heating systems, as stated in [59][60]. The reason why floor heating systems are preferred over the air convective heating systems is mainly due to the increased comfort of having a warm floor. Furthermore a uniform temperature distribution in the heated room is achieved due to the large heat transmitting surface. In the following firstly a classification of floor heating system will be given, secondly control challenges of the floor heating systems and of multiple heat source systems will briefly be described.

5.2.1 Classification of floor heating systems

5.2.1.1 Electrical vs. hydronic floor heating

Floor heating systems can be divided into two groups - electrical and hydronic (water-based) floor heating systems. For a hydronic floor heating system the hot water supply can be provided by an oil burner, an electrical boiler, a heat pump or district heating[1]. The cost of using different heating sources to provide heating is different. Usually using electricity as heating energy directly is the most expensive choice, while district heating is typically cheapest, but is limited to houses in proximity of a district heating plant. For example, in Sønderborg area in Denmark, the price for electrical heating is about $190DKK/GJ$, while the district water heating costs $95DKK/GJ$ plus fixed yearly fee per square meter. Therefore in Denmark, most of heating systems in new houses close to city areas are water-based. Electrical floor heating systems which are much more expensive to use are therefore mainly used for retrofit in buildings.

5.2.1.2 Floor construction type

Two different construction types are typically used namely a heavy and a light construction type.

The heavy floor construction type refers to systems where water pipes (water-based) or an electrical heating mat is cast into a concrete layer. The heat is first distributed to the concrete layer and then to the surface floor and room. A typical water based heavy construction floor heating system is shown in Fig. 5.1(a). Here the metal grid supporting

[1]District heating is a system for distributing heat generated in a centralized location for residential and commercial heating requirements such as space heating and water heating. More information can be found on: $http://en.wikipedia.org/wiki/District\_heating$

the floor heating pipes is placed on a thick insulation layer, and the pipes are cast into a concrete layer of typical 10 cm, weighing 240kg/m2. A moisture barrier layer with a sound damping material integrated is placed on top of the concrete subfloor. The surface floor can be tiles, linoleum, carpet or wooden floor.

The light floor construction type is depicted in Fig. 5.1(b). Here the main difference from the heavy construction is the water pipes placed on a metal heat distribution plate exactly below the surface floor with a thin layer in between to remove sound. This type of floor construction is typically used in connection with wooden floors, since tiles, linoleum and carpet requires a plywood plate or similar load bearing material between the heat distribution plate and the actual surface floor.

The two construction types are very different seen from a control point of view. The heavy construction reacts slow to changes in the room temperature. The time constant of the heavy construction floor is typically between 2-6 hours depending on the surface floor. The light floor construction on the other hand, has a time constant around 30 minutes, again depending on the thermal resistance of the surface floor. Therefore the heavy construction type typically poses the most control challenges.

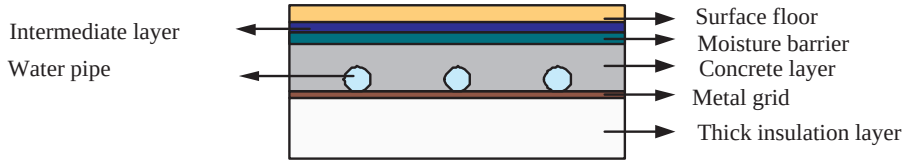

(a) Heavy construction

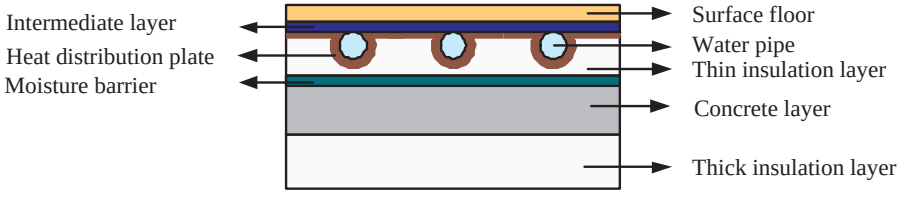

(b) Light construction

Figure 5.1: Floor construction types.

5.2.1.3 Tubing style

The tubing style of a water-based floor heating system is usually laid out either in a spiral or a serpentine style as shown in Fig. 5.2(a) and 5.2(b). The serpentine layout produces a large temperature variation across the floor surface due to the drop of water temperature along the pipe. Close to the inlet, the floor is warmer, but close to the outlet, the floor will be colder. The spiral layout provides a more uniform temperature

distribution across the floor surface, because the water temperature in pipes located next to each other is 'warm' and 'cold'. Therefore the spiral layout style is recommended as the best option, and here in this thesis, only the spiral pipe layout is considered.

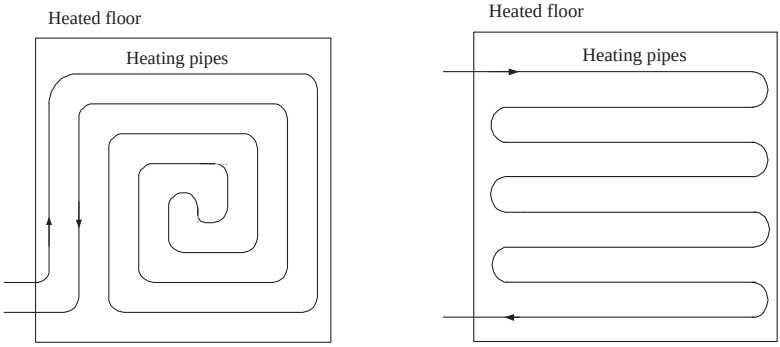

(a) Spiral tubing style (b) Serpentine tubing style

Figure 5.2: Floor heating tubing styles.

5.2.2 Control challenges for heavy floor constructions

In heavy floor constructions, the thick concrete subfloor will be heated up to a temperature higher than the room air in order to transfer heat through the surface floor to the room air. The surface floor material, which can be wood, tiles etc. has very different thermal resistances. The thermal resistance of a wooden floor is much higher than that of a tile floor, hence the temperature of the concrete subfloor layer should be higher with a wooden surface floor than with a tile floor. Due to the large thermal capacity of the concrete layer, the room temperature exhibits very slow dynamic and that the concrete layer stores a large amount of energy, which causes problem when the room is heated warm enough but the floor continues to emit heat to the room.

For water-based floor heating systems, to ensure that the surface floor material is not destroyed and to maintain an acceptable indoor comfort, the water inlet temperature is limited. For instance, some installers suggest the water inlet temperature for a heavy construction floor to be max. $42°C$, and for light construction to be $29°C$. However these suggestions are often very conservative because the concrete temperature is not measured by the controller. The limited inlet temperature contributes to the slow dynamics of the room temperature especially when heating up the room. A high supply temperature from district heating requires a temperature blending circuit to be installed. This is controlled to the maximum allowed inlet temperature for the floor heating system.

The international standards [61][62] recommends a maximum floor heating surface temperature to be $29°C$ in the occupied zone for rooms with sedentary and/or standing

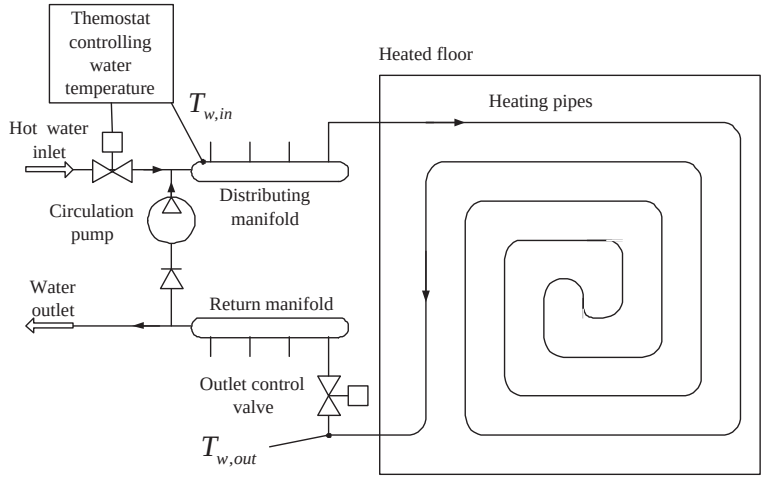

Figure 5.3: Schematic view of a water-based floor heating system

occupants wearing normal shoes. European standards state that it is acceptable to use $35°C$ as the design floor temperature outside the occupied zone[60]. These standards have also affected the decision for the relative low inlet water temperature limitations.

5.2.3 Multiple heat source systems

As stated previously, the floor heating heating system exhibits slow dynamics due to the large thermal capacity of the subfloor. To compensate the slow dynamics of the floor heating system, a fast heating system can be installed, here assumed to be an electrical heating system (refers to an electrical radiator in this section). Control of such a multiple heat source system is investigated and a MPC controller is designed.

5.3 Test system description

A family house in Sønderborg, Denmark was used to validate the model and test the developed control algorithms. The house has two storages, where the ground floor is equipped with a water-based heavy floor construction heating system. There are four rooms in the ground floor, each of them having one heating circuit. The water-based floor heating system is in the following divided into two parts: a water circuit and the heated floor + the room.

5.3.1 The water circuit

The water circuit of the floor heating system in the test house is depicted in Fig. 5.3, where only one of the floor pipe circuit is shown. The pipe is cast into the concrete subfloor. The water circuit supplies warm water to the four rooms by mixing the return water from the heated floors with a supply of hot water. The redundant amount of cold water in the water circuit is released at the outlet of the return manifold, see Fig. 5.3. Each of the floor heating circuit includes an ON/OFF valve at the circuit outlet.

The water inlet temperature to the distributing manifold and thereby to the rooms is controlled by a thermostatic valve that adjusts the amount of hot water mixed in the water circuit as shown in Fig. 5.3. The inlet water temperature $T_{w,in}$ of the floor circuits is measured at the distributing manifold, and the outlet temperature $T_{w,out}$ is measured just before the outlet valve.

5.3.2 The floor, the room and the wall

The heated floor can be divided into a surface floor and a subfloor. The subfloor is made of concrete with heating pipes cast in. By supplying warm water to the heating pipes the subfloor is heated. The heat from the sub-floor is transmitted to the room through the surface floor. The wooden surface floor is placed on the top of the concrete subfloor.

The room thermostat transmits the actual temperature together with a user defined set-point to a central controller that controls the room temperature by switching the circuit outlet control valve ON/OFF.

There are both inner walls and outer walls in the room where the validation was carried out. The outer walls toward the colder ambient are where the main heat loss is taking place. Heat is also transferred between the rooms through inner walls and door openings. In the following the heat interchange between rooms is neglected and seen as a part of the disturbances to the room. In the experiments, the temperature is kept at similar levels in all rooms to avoid a large heat interchange. The heat loss through the ceiling is neglected because of the heated upstairs rooms.

One room of the house has been used as an example for the investigation on control of the floor heating system. The room size is $length \times width \times high = 4m \times 4m \times 3m$ and the pipe is approximately $4m$ per m^2. The surface floor is Junckers [2] ask nordic wooden floor. The pipe is standard PEX pipe. The room has two outside walls which are built with two brick layers with an air gap in between as insulation. The parameters of the above components are listed in Table 5.1. The experimental work in Part II is based on this room in the test house.

[2]The product information can be found on www.junckers.dk

The wooden floor thickness	$20.5mm$
The concrete subfloor thickness	$100mm$
The pipe inner diameter	$20mm$
The pipe outer diameter	$25mm$
The wall brick layer	$120mm$
The wall air gap	$80mm$

Table 5.1: Parameters of the room in the test house

5.4 State of the art

In this part of the thesis, the main focus is on control of a water-based floor heating system and control of a multiple heat source system. Modeling of the floor heating system is also an important part of the work since it can be used to test the control algorithms. Review of previous work is divided in: modeling of floor heating systems, control of floor heating systems and control of multiple heat source systems

5.4.1 Modeling of floor heating systems

Modeling of floor heating systems, especially water-based heavy construction floor heating systems can be a challenge. The reason is that the floor includes a large thermal capacity and the temperature distribution in such a floor system is not uniform. The floor temperature decreases horizontally along the water pipe, and vertically with distance to the pipe. Much literature can be found about modeling such a floor heating system. Some of them assume lumped floor temperature, resulting in a one dimensional dynamical model. Some use finite difference method, to make two or three dimensional models.

[63] introduces a two-dimensional model for a water-based floor heating system with serpentine tubing style. The water pipe is considered as a whole piece in stead of being divided up into several small sections. Based on this, the floor can be seen as one long concrete block around one straight pipe. The two dimension refers to the horizontal direction and the vertical direction perpendicular to the pipe. The floor temperature along the pipe is assumed constant. The author studied half of the block around the pipe based on symmetrical condition, and formulated a PDE (Partial Differential Equation). With some assumptions, an explicit solution is derived. The water temperature gradient in the pipe is modeled but based on the assumption of uniform concrete temperature along the pipe. The model is made for a building energy simulation software, and the authors aim is to use the model to calculate the heat transfer within the building construction assemblies. The model can predict the water outlet temperature, but it is inaccurate due to the assumption of uniform concrete temperature along the water pipe.

To calculate the heat loss and heat supply to the room through the floor, [64] develops

a two-dimensional finite control volume model of a water-based floor heating system with serpentine tubing style. This work takes ground heat loss and interaction between floor heating system and the room into account. The floor temperature variation along the pipe direction is not considered. The author divides the pipe into several pieces and assumes that the water temperature in all the pipe sections are same, which is the average of the inlet and outlet water temperature. With this assumption, all the blocks with one pipe piece and the concrete around it can be seen as duplicates of each other and no heat transfers to the adjacent block. Therefore the whole floor model can be easily made by modeling of only one of block and then duplicate it. Since in every block the temperature distribution is symmetrical over the vertical line cross the pipe center. Therefore the author can calculate for the whole floor by modeling only half of a block. The energy from the pipe to the concrete floor equals to the energy added to the pipe by the flow. The water in the pipe is considered as an average of the inlet and outlet temperature of the pipe, which is corresponding to that the floor temperature along the pipe is uniform. Several assumptions in this paper, e.g. the floor is symmetrical around the pipes for this layout, the floor temperature does not change along the pipe, make the outlet water temperature calculation inaccurate which is important for our case.

An improved two-dimensional model is presented in [65] for a serpentine tubing style floor. The pipe is divided into several sections according to the number of the tube turns. The two dimension is on the vertical surface perpendicular to the pipe. The floor temperature gradient along the pipe direction is ignored inside each section. The water temperature in different pipe sections are linear interpolated between the inlet and outlet water temperature. However, the prediction of the water outlet temperature is not accurate due to the ignored temperature gradient along the pipe in each section.

An accurate estimate of the water outlet temperature is essential in the proposed control algorithm, where the outlet temperature contributes to a sub-floor temperature estimate.

5.4.2 Control of floor heating systems

Control of floor heating systems is a hard task due to the large time constants introduced by the large heat capacity of the floor and the low water inlet temperature which limits the rate of heating [66]. In some of the work, this large thermal capacity has been treated as a delay. Example of treating thermal systems with delay are [67] where a fuzzy prediction algorithm is implemented to estimate the delay free information in the control of the system, [6] where a delay is used in the prediction model for the control. More references on control of delay systems are given in survey paper [68]. However, in reality, the large thermal capacity in the floor heating system is more close to a long system time constant instead of a delay. Therefore in this thesis, the floor heating system with a large thermal capacity is considered as a system with a long time constant.

The existing methods for controlling floor heated houses can be categorized into two groups: classical methods and advanced methods.

Classical methods

Intermittent control is an open loop control method for floor heating systems especially in Korea. With such a control scheme, a valve installed at the inlet or outlet of the water circuit regulates the circuit following a pre-defined table. The table includes weather conditions, how many times of valve opening, when to open the water circuit valve, and the duration of each opening. For instance, in a specific day with outdoor temperature between 0 to -5$^{\circ}C$, the water circuit valve opens 2 times, 05-07 am, 16-20 pm [69]. The specification of the control is based on past operating experiences. To improve the comfort, an additional water temperature adjustment algorithm is applied to regulate the inlet water temperature based on the outdoor air temperature.

[69] introduces a predictive control strategy to improve the intermittent operation performance. Here the valve opening time is calculated instead of reading it from a table. In this method, hour by hour outdoor temperature information is used to predict the valve opening time each hour, which is the total energy demand divided by the heating energy produced by a boiler each hour. The energy demand is estimated with the building simulation model. This method improves the indoor temperature performance, but due to the open loop operation, the system can not handle disturbances. A closed loop control therefore has to be applied in order to improve the indoor comfort and the energy savings.

To compensate the lack of the room temperature feedback, [70] suggests a control algorithm, which uses the indoor temperature as one of the parameters in making control decision. The idea is to apply the heat demand determined based on the ambient temperature with heating energy pulses by operation of the floor water pipe circulation pump. The circulation pump operates with a period of 2 hours, with a duty cycle that is decided based on the heat demand and the current available heating power. Here the current available heating power is calculated as heating power transfer from the water to the room air when the circulation pump is on. However compared with the open loop method presented by [69], the improvement with respect to disturbances using the proposed control method in [70] is limited. This is because the assumption that the water in the pipe has the temperature as the water at the inlet is inaccurate, and the heat power delivered from the water to the room is estimated as the heat transfer from water to air without taking the floor dynamics into consideration.

To overcome the problem caused by the ignored floor heat capacity in the methods above, [71] proposes a new method. The idea is to check sequentially for the high and low limits of air and floor temperatures over a predefined switching interval, that is the first interval uses the air temperature for ON/OFF control of the circulation valve, and the next interval uses the floor temperature for ON/OFF control of the circulation valve. The author also suggested to include this in the intermittent method. The improvement of the method comparing with the methods mentioned above is that the floor temperature has been taken into consideration for control input decision. [72] also points out that it would be beneficial to control both the temperature of the subfloor and the room temperature.

Installation of a temperature sensor in subfloor has been proven not practical due to a distributed temperature profile in the thick layer of the concrete floor. Besides, service of the sensor is not easy because it is below the top floor and such a sensor also increase the cost of the floor heating system.

Today most of the water-based floor heated houses are controlled with room thermostats in European countries where typically a relay controller with temperature bounds is implemented. If the room temperature is higher than the upper temperature limit, the water circuits for this room will be closed, and if the room temperature is lower than the lower temperature limit, the circuit is open. The controlled room temperature variations are large due to the large thermal capacity of the concrete subfloor and the low inlet water temperature.

In [6] both ON/OFF switched and PI controllers are implemented with an electrical floor heating with large thermal capacity. The power emitted to the floor heating system is controlled directly. The results show that both controllers produce larger temperature variation compared with a more advanced controller e.g. GPC (general predictive method).

Some advanced methods of controlling heating systems also exists.

Advanced methods

[66] introduces adaptive control for domestic floor heating systems, where the control input is the inlet water temperature and the output is the indoor air temperature. The indoor air temperature is modeled as a linear function of the inlet water temperature, the ambient temperature and wind disturbance. The indoor air temperature model parameters are updated with recursive least-squares algorithm, and the control input is calculated to optimize a predefined performance index employing the updated estimation of the process parameters. The controller produces a rather oscillatory output for the supply water temperature due to the oversimplified model, where the large thermal capacity is not taken with special care. Another problem with the proposed method is that, it is not easy to expand the method to work with systems including multiple circuits. The reason is that using inlet water temperature as control input, each circuit has to equipped with a mixing valve, which results in a high cost.

GPC is applied to a high thermal mass electrical floor heating system by [6]. The room temperature used for the prediction is modeled as a function of the input with a delay and disturbances. The control input is the power emitted by electrical panels to the floor where the power is directly controlled. The results are superior than ON/OFF and PI controllers. This points to benefits of a more sophisticated control when the emitted power can be controlled directly, which is not trivial for water-based floor heating systems.

To be able to control the room temperature precisely, it is important to be able to control the temperature of the subfloor with large thermal capacity, as pointed out by [70] and [71]. One of the technology to solve this problem is to employ an observer.

However, to implement an observer successfully, it is necessary to have the subfloor information e.g. the thermal capacity. The challenge is that in different houses the thickness of the subfloor concrete layer and room size are not the same, therefore the capacity of the subfloor is not easy to achieve. This has posed challenges on an accurate control of the room temperature in a floor heated house.

In thesis Part II, methods utilizing the ON/OFF switches of the water circuit valve to drive the floor heating system to a specific state to estimate the concrete subfloor heat capacity and the subfloor temperature are proposed. Following that a cascade control of a floor heating system is introduced.

5.4.3 Control of multiple heat source systems

As described in Subsection 5.2.3, multiple heat sources are implemented to get a better comfort. These different heat sources are characterized with different dynamics in heating the room and different cost of using. Some methods that attempt to control this type of systems are reviewed below.

[73] considered a similar problem in power plants where multiple power plant units with different dynamics and different cost of using them exist. MPC is proposed to solve the problem. The objective of the controller is to coordinate a portfolio consisting of multiple actuators in an effort to perform reference tracking and disturbance rejection in an economically optimal way. The performance function is chosen as a mixture of the output deviation from the reference, the expenses of using the different power plant units and the cost on input rate change. In the work, the authors assume that the reference for each power plant unit (that each power plant unit should produce) is a fixed portion of the total reference and the sum of them is the total reference. The simulation results show a significant improvement of the MPC control performance to the current distributed PI controller structure in terms of the overall cost and ability to minimize deviation from the reference. However the overall performance can be even improved if the portion of each power plants unit is determined dynamically based on their price of using and dynamic characteristics.

The problem of how to distribute the total load to different actuators optimally was studied in [74]. A large scale power plant system with three types of actuators and each type includes a number of the same subsystems is used as example. The authors formulated a function including earning of running each actuator, cost of the production change with each actuator and availability, extra actuation power to overcome possible faults in the system and mixing of the different actuators. The objective is to maximize the total earning with different combination of actuators at different production loads. The approach is first to use the method in [74] to find the optimal actuator configuration and then apply the scheme in [73]. Following that the optimal control problem of a large scale power plant can be solved. Although the methods work fine for the power plant system, there are challenges implementing them in the multiple heat source system. The reference in such a domestic heating system is temperature, which can not be distributed

to the different heaters directly as for the power plant power production. Besides, the configuration of actuators can be a challenge in defining the cost for the heating power change of each actuators due to that dynamics of the heaters varies with different houses constructions. Therefore the actuator configuration has to be done with each houses, which is far too expensive for a low cost domestic heating controller.

[75] defined an objective function similar to the one in [74]. The difference is that the dynamics of the power plant units and the changing price of the produced power are included. The problem now is formulated as a dynamic optimization problem, where the control input decision is which power plant units should be activated and how much fuel should be applied. The optimization problem is solved in details in [76]. This solves the problem in one step in stead of first configuring the actuators using [74] and then using the method in [73]. Application of the method in [75] to the multiple floor heat source systems is not straightforward. The reason is that in the objective function in [75], the output (overall power production) is considered as sum of the outputs from the different subsystems, which is different for temperature output in the multiple heat source systems.

In thesis Part II, MPC is employed to control a multiple heat source system, where the input to the different heat sources is power. The water based floor heating system is controlled by ON/OFF valve. The control is divided into 2 layers, where the higher layer is a MPC controller, which takes the floor heating system and other heating sources as heat sources, and the heat sources for example, a floor heating system has a local controller to provide the demanded power from the MPC controller.

5.5 Contributions and publications

The main contribution in thesis Part II in control of heating systems :

- Modeling of a water based floor heating system. A finite difference model of a water-based floor heating system is made, which is three dimensional model where both the temperature drop along the water pipe and around the pipe radius direction is taken into account. Comparing with existing models, the proposed model predicts the outlet water temperature more accurate. The work is published in [7].

- Subfloor temperature control of a water based floor heating system. An energy based subfloor temperature control method is proposed where only the required amount of energy is applied to the floor. Thereby overshoot in the subfloor temperature can be avoided and the dynamic response is increased. A new approach to approximate the subfloor temperature using the water temperature is further applied in the subfloor temperature control. The work is published in [8].

- Control challenge analysis in relation to house construction types. Different combination of the wall and floor type in a house poses different challenge in control.

Systematic analysis points out the control challenges. The work is published in [7].

- Feed-forward disturbance rejection method to control the room air temperature in a house with a water based floor heating system. The method uses a wall model and a floor model to compensate for slow dynamic disturbance e.g. the outdoor temperature variation effect on the indoor temperature. The work is published in [9].

- A controller for multiple actuator systems characterized by different dynamics, energy prices etc. Model predictive control method was proposed to solve the problem where the different prices of using different heating systems can be reflected with the weight factors on the inputs in the objective function.

The related publications are:

- *Control of a water-based floor heating system, Proceedings of Multi-conference on Systems and Control, 2007.*
  This paper proposes a control scheme with increased dynamic performance for water-based floor heating systems. A novel approach for temperature control of large thermal capacity systems is introduced and validated with experimental results.

- *Disturbance rejection of a water-based floor heating system, UKACC Control Conference, 2006.*
  This paper describes a feed-forward disturbance rejection method for a water-based floor heating system. The method is tested both with simulations and experiments. The result shows that the outdoor temperature variation can be compensated well with the proposed method.

- *Control challenge for domestic heating systems, Proceedings of European Control conference, 2007.*
  In this paper, control challenges of different house construction types are analyzed. Modeling of different types of floor heating systems and wall constructions are presented. The models are analyzed by simulation.

- *Control of a system with a large thermal capacity, patent, publication No.: WO/2007/090405 , 2007.*
  The invention provides a method and a system for controlling floor heating or climate regulating systems with long time constants. According to the invention, a flow of a fluid is provided through the floor or through a similar medium with large thermal inertia. An induced heat is determined by adding up a plurality of differences between an inlet temperature of the fluid when it enters the medium and an outlet temperature of the fluid when it leaves the medium. The temperatures are sampled with a fixed sampling time and within a fixed period of time,

and a corresponding change in temperature of the medium over the fixed period of time is determined. In the future, the temperature of that medium is controlled by use of a ratio between the induced heat and the change in temperature.

- *Method and system for controlling the climate in a house, patent, publication No.: WO/2007/090400, 2009.*
  The invention provides a method for controlling the climate of an environment, e.g. a house, which exchanges thermal energy with an ambient space. Energy is supplied to the environment e.g. by radiators, floor heating, electrical heating fans etc. According to the method, a numerically expressed comfort criteria, and a numerically expressed weight of importance of compliance with the comfort criterion are defined. Subsequently, a supply of a specific amount of energy is considered, and with respect to that amount, a numerical expression of a degree of compliance with the comfort criterion, and a numerical expression of costs related to the supply of that amount of energy are provided.

- *A model prediction controlled energy system, patent, publication No.: WO/2009/039849, 2009.*
  The invention provides a method of controlling a release of thermal energy in a building. The method comprises steps of defining a control criterion for the building, defining a set of climate variables which influence the release of thermal energy in the building, and defining for each climate variable, a climate signification index which defines the importance of that climate variable for the release of thermal energy in the building. Furthermore, the method comprises a step of receiving a set of predicted future climate variables, and subsequently a step of combining the climate signification indices and the predicted future climate variables to provide control instructions for release of an amount of thermal energy in the building to satisfy the control criterion. The invention further provides a comfort control system.

5.6 Outline of thesis Part II

The rest of Part II is organized as follows:

Chapter 6 summary of work. This chapter presents a brief description of the work that was carried out in the areas; modeling of floor heating systems, control of floor heating systems and control of multiple heat source systems. The goal is to give a comprehensive explanation of the control challenge and the proposed methods.

Chapter 7 conclusions, perspectives and future work. Conclusions on the modeling and control of floor heating system and multiple heat source systems are given. Applications of the developed method on some other systems are briefly explained. Future work including both academic and industrial aspects is suggested.

Chapter 6

Summary of work

This chapter summarizes the contributions made in Part II of the thesis. The chapter is organized in sections describing modeling of a floor heated house, control of a floor heated house and control of multiple heat source systems. The work in this section was originally presented in the papers found in Appendix E, G, F and technical report H.

6.1 Modeling of a floor heated house

In this section the test house as described in Section 5.3 is modeled, where the focus is on one room of the test house. The work was originally presented in the paper found in Appendix E. Comparing with the existing models, the advantage of this model is that the outlet water temperature is predicted more accurately. This is important for the subfloor temperature control.

The house is equipped with a heavy construction water-based floor heating system with a spiral piping. A wooden surface floor is placed on top of the concrete subfloor. The wall of the house is built with two layer of bricks and an air gap in-between as insulation. The modeling is divided into two parts - the floor and the room + the wall.

6.1.1 Floor model

For a heavy floor construction, the subfloor temperature can not be lumped because of the relatively thick concrete layer, the low heat transfer from the concrete to the room, and the low heat conduction in the concrete. Hence a distributed temperature model has to be used [77] for the concrete subfloor.

The concrete floor can be seen as a long concrete block around the water pipe. To simplify the model, the concrete subfloor is divided in to a number of volumes with a uniform temperature in each of them. As the temperature gradient changes in a radial direction from the heating pipes into the concrete, the subfloor is divided into $n + 1$

cylindric volumes with identical thicknesses L (see Fig. 6.1(a)). To make the modeling easier, the pipe is assumed to be placed in the middle of the concrete layer. In reality the pipe is placed on the bottom of the concrete subfloor as in Fig. 5.1(a). This leads to a small error which is insignificant comparing to the modeling inaccuracy of the heat loss from the floor to the group. The 'top concrete layer' (number $n+1$) is not cylindric but considered to have a uniform temperature T_{top}.

When the heat is transmitted from the water to the concrete, the water and the concrete temperature drops along the pipe. This can be modeled by dividing the concrete subfloor into m slices along the pipe, as depicted in Fig. 6.1(b). Here the transversal heat conduction between slices is neglected. Furthermore the 'top concrete layer' in all of the slices are assumed to be one big lumped mass with uniform temperature.

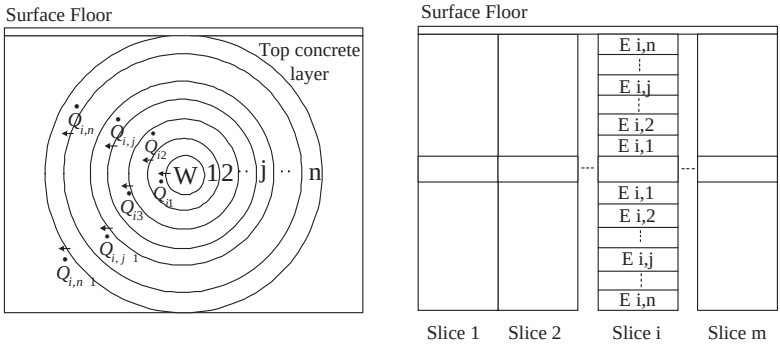

(a) Layers around water pipe (b) Slices along water pipe

Figure 6.1: Finite difference of the floor.

All in all this results in a two dimensional model as depicted in Fig. 6.1(a) and 6.1(b). The notation $E_{i,j}$ is used for the element located at j^{th} layer in i^{th} slice. In the same way, $T_{i,j}$ is the temperature of the cylindrical concrete element (i,j) and $\dot{Q}_{i,j}$ is heat flow from the cylindrical element $(i,j-1)$ to (i,j). $\dot{Q}_{i,1}$ is the heat flow from water pipe slice i to concrete layer $(i,1)$. $T_{w,in,i}$ is the water inlet temperature of the i^{th} pipe slice. $T_{w,out,i}$ is the water outlet temperature of the i^{th} pipe slice. The mean temperature of the water in a slice is approximated by the inlet water temperature of the slice.

The heat flow $\dot{Q}_{i,j}$ can be written as,

$$\dot{Q}_{i,j} = \begin{cases} \frac{(T_{w,in,i}-T_{i,j})}{Rw2c} & i=1,2\cdots m, j=1, \\ \frac{(T_{i,j-1}-T_{i,j})\cdot K\cdot A_{i,j}}{L} & i=1,2\cdots m, j=2,3\cdots n, \\ \frac{(T_{i,j-1}-T_{top})\cdot K\cdot A_{i,j}}{L} & i=1,2\cdots m, j=n+1, \end{cases} \tag{6.1}$$

where $R_{w2c}$is the thermal resistance from water to the concrete, $A_{i,j}$ is the surface area

between element $(i, j-1)$ and (i, j) and, K is heat conductivity of concrete. The total heat transmitted from water is given by $\dot{Q}_w = \sum_{i=1}^{m} \dot{Q}_{i,1}$

The temperature $T_{i,j}$ can be determined as:

$$\frac{dT_{i,j}}{dt} = \frac{\dot{Q}_{i,j} - \dot{Q}_{i,j+1}}{C_{p,con} \cdot m_{i,j}} \quad \text{where } i = 1, 2 \cdots m,\ j = 1, 2 \cdots n \tag{6.2}$$

where $C_{p,con}$ is the specific heat capacity of concrete and m_{ij} is the mass of the element (i, j).

The top concrete layer is considered as a whole piece and the temperature of this layer is assumed to be uniform. Hence it can be computed as,

$$\frac{dT_{top}}{dt} = \frac{\sum_{i=1}^{m} \dot{Q}_{i,n+1} - \dot{Q}_f}{C_{p,con} \cdot m_{top}} \tag{6.3}$$

where the $\dot{Q}_f$ is the heat flow from subfloor to the room through the wood surface floor, which can be calculated as

$$\dot{Q}_f = \frac{(T_{top} - T_{room})}{R_{c2a}} \tag{6.4}$$

R_{c2a} is the thermal resistance between the top concrete layer and the room air and T_{room} is the lumped room air temperature. The wooden surface floor is considered a thermal resistance because the heat capacity of the surface floor is much smaller than that of the concrete subfloor.

The temperature of the water out of slice i is

$$\frac{dT_{w,out,i}}{dt} = T_{w,in,i} - \frac{\dot{Q}_{i,1}}{C_{p,water} \cdot \dot{m}_{water}} \quad \text{where } i = 1, 2 \cdots m, \tag{6.5}$$

where $C_{p,water}$ is specific heat capacity of water, $\dot{m}_{water}$ is water mass flow in the water pipe and the inlet temperature of water to the i^{th} slice $T_{w,in,i}$ is given by,

$$T_{w,in,i} = \begin{cases} T_{w,out,i-1} & i = 2, 3 \cdots m \\ T_{w,in} & i = 1 \end{cases} \tag{6.6}$$

$T_{w,in}$ is the water inlet temperature to the floor and $T_{w,out} = T_{w,out,m}$ is the water outlet temperature from the floor.

6.1.2 Room and wall model

The room temperature T_{room} can be computed as

$$\frac{dT_{room}}{dt} = \frac{\dot{Q}_f - \dot{Q}_d}{C_{p,air} m_{air}}, \tag{6.7}$$

with the assumption of a uniform temperature distribution in the room (i.e.perfect mixing of the air). $C_{p,air}$ is the specific heat capacity of air and, m_{air} is the mass of the air in the room.

The main disturbance $\dot{Q}_d$ is the climate disturbances, i.e. day to day temperature change, sun radiation etc. Among these disturbances the outdoor temperature variations is the one that causes the largest heat loss to the ambient. This will be considered in the modeling in this work.

The room in the house has two outside walls and two insides walls. The heat loss through the inside walls to other rooms are so little that it can be neglected because the other rooms are kept at around the set-point temperature of the test room. The outside wall of the test house is built with two layers of bricks with an air insulation layer in between as depicted in Fig. 6.2. On the two outside walls, there are two small windows. However in the modeling, the windows are not modeled but taken into consideration by modifying the thermal resistance of the walls. The heat loss through the wall $\dot{Q}_d$ is the

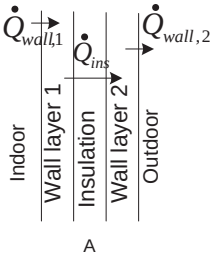

Figure 6.2: wall construction

heat transferring from indoor air to Wall layer 1. By assuming that each layer of the walls is lumped, the following model can be derived:

$$\dot{Q}_d = \dot{Q}_{wall,1}, \tag{6.8}$$

$$\dot{Q}_{wall,1} = \frac{(T_{room} - T_{wall,1})}{R_{a2w}}, \tag{6.9}$$

where R_{a2w} is the thermal resistance from indoor air to Wall layer 1. The temperature of the Wall layer 1 can be calculated as,

$$\frac{dT_{wall,1}}{dt} = \frac{\dot{Q}_d - \dot{Q}_{ins}}{C_{p,wall,1} \cdot m_{wall,1}}, \tag{6.10}$$

where $C_{p,wall,1}$ is the specific heat capacity of wall layer 1, $m_{wall,1}$ is the mass of the Wall layer 1. The heat transmission through insulation layer is,

$$\dot{Q}_{ins} = \frac{(T_{wall,1} - T_{wall,2})}{R_{ins}} \tag{6.11}$$

where R_{ins} is the thermal resistance of the insulation layer. The temperature of Wall layer 2 is,

$$\frac{dT_{wall,2}}{dt} = \frac{\dot{Q}_{ins} - \dot{Q}_{wall,2}}{C_{p,wall,2} \cdot m_{wall,2}}, \tag{6.12}$$

$C_{pw,2}$ is the specific heat capacity of Wall layer 2. The heat loss from Wall layer 2 to ambient environment is,

$$\dot{Q}_{wall,2} = \frac{(T_{wall,2} - T_{ambient})}{R_{w2a}}, \tag{6.13}$$

where R_{w2a} is the thermal resistance from Wall layer 2 to the ambient environment, $T_{ambient}$ is the ambient air temperature. Connecting the floor and the room + the wall models gives the total room model of the test house.

6.1.3 Model validation

The model validation can be divided in two steps: the room and wall model validation and the floor model validation. The room and wall model is simple and easy to validate by comparing the room temperature time constant and steady state energy consumption. Therefore no more details is explained here. The focus is on the floor model validation.

The floor model validation experiment is carried out on the test house. A one hour burst of hot water is led into the floor. Hereafter, the water circuit valve is switched off, and the water circulates through the water circuit in the subfloor without adding heat. The experiment is first done on the test house, hereafter the recorded inlet water temperature data $T_{w,in}$ is feed to the model with the same initial conditions. The result is shown in Fig. 6.3.

It can be seen that the outlet water temperature from the test house and the simulation model are very close to each other. This shows that the model gives a good indication of the temperature propagation in the real floor system.

In Fig. 6.3, there is a little delay between the measured and simulated water output temperature, when starting (where the water inlet temperature increases) and stopping heating (where the water inlet temperature decreases). The reason for the delay is that, for example, when the heating stops, the water in the floor pipe is still warm, which takes a while until the output water temperature decreases. For the simulation model, the outlet water temperature drops immediately when the inlet temperature drops according to the model.

6.1.4 Control challenges from different building construction types

The above modeling of a heavy construction floor heated room is characterized by slow dynamics. Other types of construction of floor and wall might have different challenges. For example, with a light floor construction, the room air is heated up faster because the water pipe is laid down directly below the surface floor. Different ways of constructing

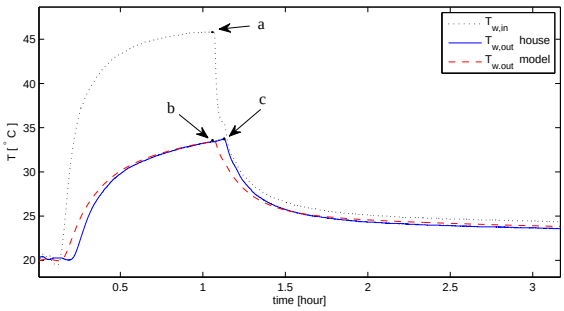

Figure 6.3: Floor model validation with a heat burst from $6 - 68$ minute. $T_{w,in}$ is the water inlet temperature. $T_{w,out}$ is the water outlet temperatures. 'model' refers to the result from the model. 'house' refers to the result from the test house. a is the point where heating stops. b is the point where the simulated water outlet temperature drops. c is the point where the measured water outlet temperature drops.

a wall also affect the control challenge. The insulation layer might be placed inside or outside of the brick wall. More details of control challenges from different construction types can be found in Appendix G.

It was concluded that for heavy wall types (i.e. wall types with a large indoor thermal mass), the wall actually is the most important factor determining the dynamic behavior of the indoor air temperature, whereas for light wall types it is mainly the floor type that determines the dynamics. Furthermore a light inner wall is very sensitive to disturbances, but because of the little thermal mass the temperature can be changed fast. A heavy inner wall will help reducing the disturbance sensitivity, but at the cost of a much slower response time. This means that a light wall in combination with a heavy floor is not recommendable as this brings together the worst of two worlds namely high sensitivity to disturbances and a slow dynamic.

6.2 A novel approach for floor heating control

An overall control strategy of a floor heated house is proposed as shown in Fig. 6.4. The proposed control scheme aims at solving the large time delay issue caused by the large thermal mass of the subfloor by dividing the control strategy into two cascaded controllers. The inner controller implements a subfloor temperature control, enabled by a novel subfloor temperature estimate. The objective of the outer controller is to track the temperature set-point and reject disturbances from the outdoor ambient and the indoor heat dissipation.

The focus of this section is the on concrete subfloor temperature control which is highlighted in grey color. The work is originally presented in the paper found in Ap-

pendix E.

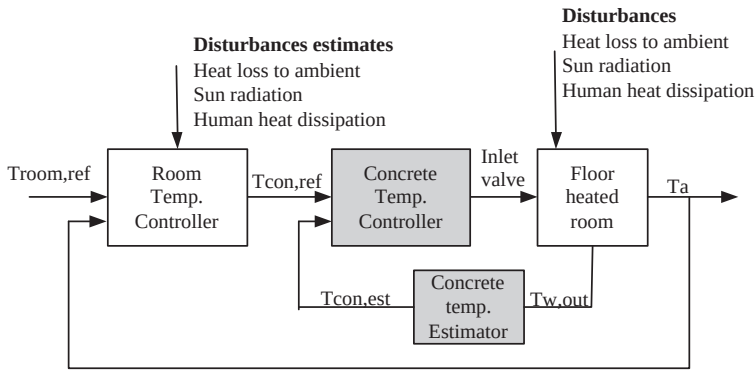

Figure 6.4: A sketch of the proposed control design with an inner loop controlling the concrete temperature and an outer loop controlling the room temperature. The subfloor temperature control part is emphasized in gray color.

The subfloor temperature is not uniform when hot water is added to the floor - the closer to the water pipe, the higher is the concrete temperature. This makes it difficult to regulate the subfloor temperature. However it is important to be able to control the temperature of the subfloor, in order to maintain the subfloor temperature within the required limits (posed by material and comfort) and achieve a better room temperature. In the following a novel approach is proposed to control the subfloor temperature.

6.2.1 Subfloor temperature control

The concrete subfloor temperature control consists of steps
1 Estimate the current subfloor temperature $T_{con,est}$
2 Calculate the required amount of the heat burst Q_{burst} that will bring the subfloor temperature up to the reference
3 Apply the required heat

6.2.1.1 Estimate the subfloor temperature

To install a temperature sensor in the concrete layer to measure the subfloor temperature has proven impractical for a number of reasons. Firstly, a sensor placed in the concrete layer is hard to service and replace, especially with a wooden floor on top. Secondly, the placement of the sensor is very critical. If it is placed close to the water pipes it will react very fast to the heating. If it is placed in the middle between two heat pipes, it will react very late.

The approach proposed here is to use the water temperature to estimate the concrete temperature. After an idle period without heating, the water and the concrete temper-

ature equalize. The measured outlet water temperature after such an idle period, will reflect the warmest place of the concrete, that is closest to the water pipes. With an increased idle period the temperature gradients in the concrete will be smaller and a lower temperature measurement will be obtained. This is illustrated in Fig. 6.3 with the recorded water inlet and outlet temperature. It can be seen that during the first 15 minutes after the heating is stopped, the water outlet temperature drops fast, and after that the outlet water temperature drops slower and slower. Therefore the idle period in this case is chosen to be 20 minutes, which means that the subfloor temperature is the water outlet temperature 20 minutes after the heating is stopped. Recall that after the heating is stopped, the water circulates in the floor without adding any heat.

6.2.1.2 Calculate the heat burst

The heat burst is calculated by

$$Q_{burst} = C_{p,con} m_{con} (T_{con,est} - T_{con,ref}) \tag{6.14}$$

where $T_{con,ref}$ is the reference temperature of the concrete subfloor. $C_{p,con} m_{con}$ is the subfloor heat capacity, which has to be known to calculate Q_{burst}. An experimental based approach is proposed to obtain a "dynamic" heat capacity of the subfloor.

Estimate the subfloor heat capacity.
The main idea is to perform an experiment where a known amount of heat Q_{test} is applied in to the floor and then find the temperature change $T_{con,est,after} - T_{con,est,before}$ before and after applying the heat burst. Q_{test} is applied by (6.17) The heat capacity $C_{p,con} m_{con}$ can then be calculated as

$$C_{p,con} m_{con} = \frac{Q_{test}}{T_{con,est,after} - T_{con,est,before}} \tag{6.15}$$

Fig. 6.5 illustrates such an experiment performed in the test house. From $t = 6 \rightarrow 68\ minute$, heating is applied to the floor and after that the water is circulated in the water pipe without adding any heat. In the initial phase right after applying Q_{test} (from t=68minute) the water outlet temperature dropped fast. After that, the temperature dropped slower and slower until it reached the ambient temperature. The temperature drop after the heating can be divided into 3 phases. Right after the heating stopped, the outlet water temperature dropped very fast due to the temperature gradient in all directions around the pipe. After a short while, the water temperature drop became little bit slower because the temperature gradient went from a radial phase to a transversal phase mainly which is shown in Fig. 6.6, the solid lines with arrow. After a while the water temperature dropped much slower which is because the heat gradient is pretty small in all the directions around the pipe, and the heat loss from the water was mainly the heat transferring from the floor to the indoor air. The concrete subfloor temperature

is assumed to be the same as the water temperature at the end of the second phase. Based on (6.15), a dynamic heat capacity can be obtained

$$C_{p,con}m_{con}(t) = \frac{Q_{test}}{T_{w,out}(t) - T_{w,out,before}} \tag{6.16}$$

where $T_{w,out,before}$ is the estimated concrete temperature before applying the heat burst. The value of this expression is illustrated in Fig. 6.5. The dynamic heat capacity $C_{p,con}m_{con}(t)$ value describes the level of equalization and not the actual heat capacity of the concrete floor.

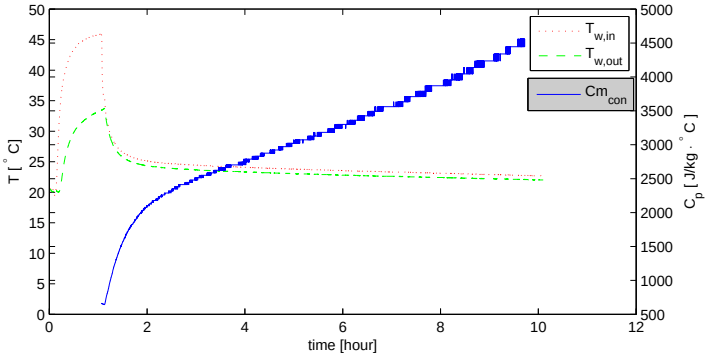

Figure 6.5: A heat burst and the corresponding concrete heat capacity. $T_{w,in}$ is the inlet water temperature. $T_{w,out}$ is the outlet water temperature. Cm_{con} is the estimated concrete heat capacity.

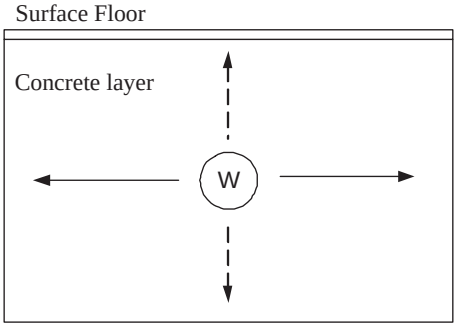

Figure 6.6: Cross section of one floor volume. W is the water pipe

The heat capacity can then be used to calculate the heat burst, that is required to bring the subfloor temperature to the reference expressed by (6.14).

6.2.1.3 Apply the heat burst.

The applied heat burst to the floor heated house Q_{burst} through the water circuit is calculated as

$$Q_{applied} = \int_0^t C_{p,water} \dot{m}_{water} (T_{w,in} - T_{w,out}) dt \tag{6.17}$$

where $\dot{m}_{water}$ is the water mass flow of the test room. When $Q_{applied} = Q_{burst}$, the needed amount of heat is applied and the valve of the water circuit is switched off.

6.2.1.4 Experimental results

An experiment was conducted to test the developed approach for controlling the subfloor temperature. Fig. 6.7 depicts the experimental results.

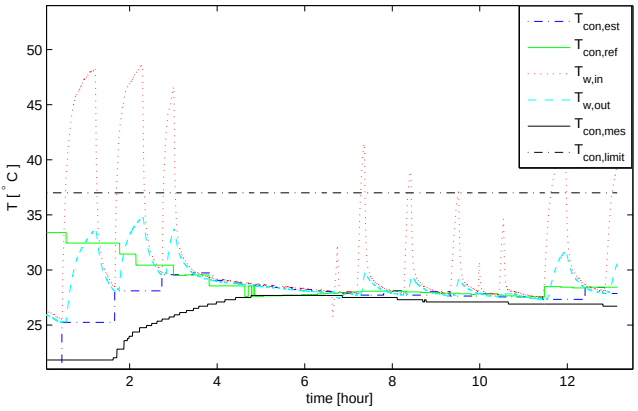

Figure 6.7: Experimental result of concrete temperature control.

$T_{w,out}$ is the water outlet temperature. $T_{con,est}$ is the estimated concrete subfloor temperature obtained by using the proposed method in this section, i.e. by measuring the water outlet temperature a certain period (20 minutes) after a burst. $T_{con,mes}$ is a 'measured' subfloor temperature which is obtained by placing an isolated temperature sensor on the top floor, hereby an approximated temperature of the subfloor layer can be obtained. $T_{con,mes}$ is not used in the control. $T_{con,limit} = 37.5°C$ is the maximal allowed temperature for the wooden surface floor. The test system initial conditions are floor temperature of (23.5 $°C$), an outdoor temperature about $17°C$. The reference to the inner control loop ($T_{con,ref}$) is the output from an outer loop controlling the room temperature, which had a reference $T_{room,ref} = 23.5°C$. The subfloor temperature control is limited such that is only giving the heat burst in steps resulting in a stepwise increase in the temperature of $3°C$.

At the beginning, when the subfloor reference temperature was much higher than the subfloor temperature, therefore larger heat burst was applied and the subfloor temperature increases fast. Later when the reference temperature is lower than the estimated temperature, the heating stops and the subfloor temperature drops until it is lower than reference subfloor temperature and then heating is started again. When no heat is added to the floor, the reference and the estimated temperature are very close to each other. Hereby it is demonstrated that the subfloor temperature control method works well.

From Fig. 6.7 it can furthermore be seen that although the inlet water temperature exceeds the recommended maximum temperature $T_{con,limit} = 37.5°C$ (suggested by [78]) of the concrete subfloor (which is the maximal allowed inlet temperature in the current control schemes) the subfloor temperature never exceeds the limitation $T_{con,limit}$. The estimated subfloor temperature describes, as previously mentioned, the temperature in the warmest place of the concrete. By controlling the estimated concrete temperature to be lower than the limit of the floor, it can therefore be ensured with a good margin that the top layer subfloor temperature never exceeds the temperature limitation. As the test shows it is therefore possible to have a much higher inlet temperature and hence increase the response time considerably, without violating the top floor temperature constraint.

6.2.2 Disturbance rejection in a water-based floor heated house

In previous Subsection 6.2.1, the inner control loop of subfloor temperature for a floor heated house was developed and validated. In this subsection, the disturbance compensation is treated as depicted in Fig. 6.8 via the disturbance rejection block.

There are different kinds of disturbances affecting the room temperature e.g. heat loss to the ambient, sun radiation, human heat dissipation etc. In order to compensate a given disturbance, the heating source must have faster dynamics than the disturbance, unless the disturbance is predicted. The disturbance caused by the ambient temperature through the wall is quite slow, therefore the water based floor heating system can be used to reject it. For the faster disturbances like e.g. sun radiation, a faster heat source like a radiator would be required. In this section, an approach for disturbance rejection of the outdoor temperature variation using the floor heating system is proposed. The work was originally presented in the paper found in Appendix F.

A dynamic feed forward compensation scheme for rejecting the outdoor temperature disturbance is proposed as shown in Fig. 6.8. The key idea is to compensate the concrete temperature reference $T_{con,rec}$ by feeding the outdoor temperature $T_{ambient}$ forward through a transfer function containing a wall model and an inverse model of the concrete floor.

The models are both approximated with first order models. The reason for using such a low order approximation is that the ambient temperature disturbance typically is sinusoidal with a 24 hour period. The modeling problem can therefore be reduced to identifying a transfer function with the same gain and phase-shift as the real system at this particular frequency, hence a first order functions will be sufficient.

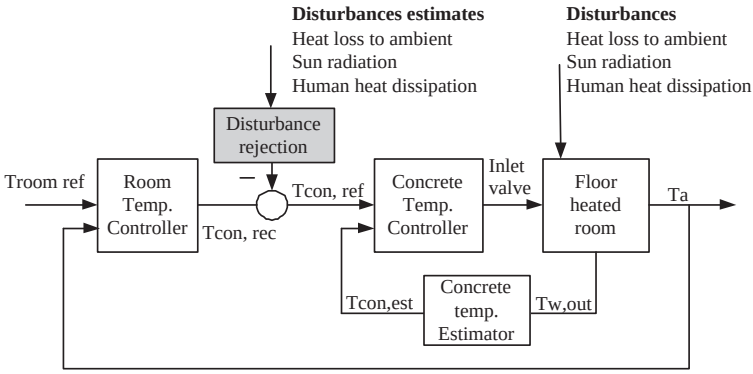

Figure 6.8: A sketch of the proposed control design with an inner loop controlling the concrete temperature and an outer loop controlling the room temperature.

Transfer function of wall.
The wall model $G_d = \frac{T_{room}}{T_{ambient}}$ is obtained through experiments where the indoor temperature is only affected by the ambient temperature through the wall. The first order wall transfer function parameters can be calculated from the gain and the phase shift between the indoor and the ambient temperature at the frequency of 24 hour period corresponding to the period of the ambient temperature disturbance.

Transfer function of the controlled floor.
The model of the controlled floor $G_c = \frac{T_{room}}{T_{con,ref}}$ is obtained similar way as the wall model. The difference is that the room temperature is affected only by the concrete subfloor temperature which is also 24 hour period. Then the first order controlled floor model can be found based on the gain and phase shift between the indoor temperature and subfloor temperature.

The disturbance rejection model can then be expressed as $\frac{G_d}{G_c}$.

6.2.2.1 Experimental results

Experiments to test the dynamic disturbance rejection method was carried out in the test house in May 2006. To avoid the significant disturbance from sunshine, the windows were covered throughout the experiments.

The first experiment was to estimate the model of the wall. The result is shown in Fig. 6.9(a). During the experiment the subfloor was kept around $26°C$ which ensured that the surface floor temperature is close to the room temperature so that no significant heat is transferred from the floor to the room air. The wall transfer function G_d can be calculated based on the indoor and the outdoor temperature. Details can be found in

Appendix F.

The second experiment was to estimate the model of the subfloor with the subfloor temperature controller. The result is depicted in Fig. 6.9(b). The experiment was carried out during several cloudy days when the outdoor temperature variation is small. The subfloor reference temperature $T_{con,ref}$ was applied as a sinusoidal variation which has $25°C$ as the mean value and $2°C$ amplitude. The period is also 24 hour. The subfloor controller follows the reference trajectory, and therefore the room temperature varies. The floor transfer function G_c can then be achieved based on the result in Fig. 6.9(b). The disturbance rejection model $\frac{G_d}{G_c}$ can hereby be obtained.

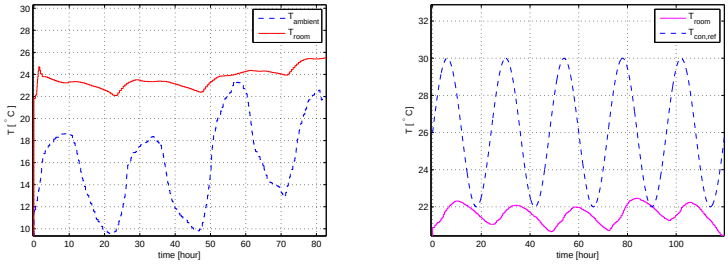

(a) Wall model estimation experiment. (b) Floor model estimation experiments

Figure 6.9: Experiments for estimation of the wall and the floor model. $T_{ambient}$ is the ambient temperature. T_{room} is the indoor room temperature. $T_{con,ref}$ is the reference temperature of the subfloor.

The validation of the disturbance rejection method with $\frac{G_d}{G_c}$ for feed forward of the outdoor temperature was carried out on the test house in May 2006. The result is shown in Fig. 6.10. The room temperature was kept stable while the outdoor temperature changed from 9 to $17.5°C$. However from hour 32 , the indoor temperature increased as a result of sun radiation.

The results presented in Fig. 6.10 shows that the disturbance rejection scheme indeed does reject the outdoor temperature change efficiently, despite the disturbance model is estimated based on the assumption that the disturbances are sinusoidal. The experiments also show that it is not trivial in practice to obtain the wall and concrete transfer function due to unavoidable disturbances as sun radiation, wind etc.

It should be noticed that obtaining the models of the wall and the floor is not trivial in practice. For instance, during the wall model estimation experiment, covering the windows few days to prevent sun radiation is not acceptable for the occupants, and that the occupants also contributes to some unexpected disturbance to the room which results in a inaccurate model. Similar problems exists in the experiments obtaining the floor model. Therefore the method has challenges in implementing in domestic houses.

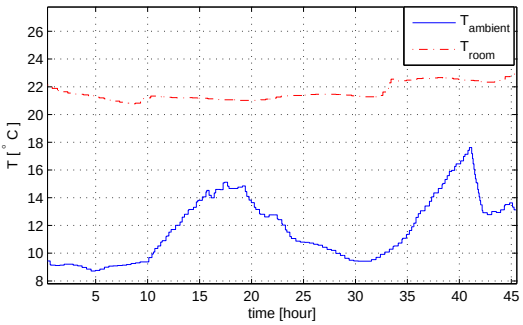

Figure 6.10: Disturbance rejection using a dynamic feed forward scheme.

6.3 Model predictive control for multiple heat source systems

As stated previously, the water-based floor heating system with a heavy concrete construction poses most challenges on the control algorithm design.

Due to the large thermal capacity of the floor, the room temperature control of such a system becomes hard especially when fast disturbances are present.

To overcome the problem with fast disturbances on the room temperature, a faster heating system is often installed to compensate. However with the current control strategy, these systems are regulated independently disregarding strong cross couplings. This often results in a dissatisfying indoor comfort and loss of energy efficiency.

To solve the problems of such a multiple heat source system, MPC is proposed. MPC is used to optimize the future control, based on action predictions of the future plant outputs, based on past and current values and on the proposed optimal future control actions. The control actions are calculated by an optimizer optimizing the cost function where the future tracking error in a prediction horizon is considered as well as constraints. A thorough explanation of MPC method can be found in [79] and [80].

This section presents MPC applied to control a multiple heat source system comprising a water-based floor heating system and an electrical heater. Using MPC, their characteristics i.e. dynamics, price of using different heating sources can be considered. This section is organized as follows, Subsection 6.3.1 introduces a model suitable for MPC internal model. An objective function is defined in Subsection 6.3.2. Simulation results are presented in Subsection 6.3.3. The more detailed study of MPC on multiple heat source systems can be found in Appendix H.

6.3.1 The simplified model

A simplified model of the house with a floor heating system and an electrical heater is used in connection with MPC. In the model, the floor is taken as one lumped mass with a heat input from the water and heat output to the room. Note in this subsection, the floor is defined as a whole piece including the subfloor and the surface. The electrical heater deliveries heat directly to the room air. The room air is assumed perfectly mixed and the walls are also lumped into one mass. The reason for simplifying the model is to limit the computational power for the MPC controller.

The discrete version of the simple model is given

$$\begin{aligned} x_{k+1} &= Ax_k + Bu_k + Ed_k, \\ y_k &= C_z x_k \end{aligned} \tag{6.18}$$

where $x = [T_{con}, T_{room}, T_{wall}]^T$, $u = [\dot{Q}_w, \dot{Q}_{el}]^T$, $y = [T_{con}, T_{room}, T_{wall}]^T$, i.e. $C_z = I$. $T_{con}, T_{room}, T_{wall}$ is the temperature of the subfloor, the room air and the walls. $\dot{Q}_w$ is the energy flow from the water to the floor and $\dot{Q}_{el}$ is the energy flow from electrical heater to the room air.

6.3.2 Objective function

The control objectives are to bring the room temperature close to the reference value r, while fulfilling the soft constraints[1] on the air temperature $T_{room} \in [18, 23.5]$, the wall temperature $T_{wall} \in [5, 30]$, the concrete subfloor temperature $T_{con} \in [5, 29]$ and while using as little money for heating as possible. Note that energy price for electricity and water heating is different. $T_{con}, T_{room}, T_{wall}$ have been constrained softly for two reasons firstly it is not crucial that the temperatures stay within the bounds at all time, secondly it improves feasibility of the optimization problem as it expands the feasible set. The constraints on the room and wall temperatures are based on experience on comfort reasons. The floor temperature constraints are set in this way, the low limit prevents the water from freezing and the high limit avoids destroying the surface floor material.

Here, an objective function penalizes with quadratic norm over a finite horizon the following three terms; (i) the deviation of the room temperature T_{room} from its reference, (ii) the rate of the control input change and (iii) the control input. The control law is then obtained by minimizing the objective function subject to the model and the physical constraints on the manipulated variables. According to the above formulated objectives, the following optimal control problem is considered:

$$\phi = \sum_{k=1}^{N} \frac{1}{2} \|y_k - r_k\|_{Q_z}^2 + \frac{1}{2} \sum_{k=0}^{N-1} \|\triangle u_k\|_S^2 + \frac{1}{2} \|u_k\|_G^2 \tag{6.19}$$

[1] A soft constraint means that the variable is penalized heavily if it crosses the constraint, it however remains feasible in contrast to a hard constrained variable.

in the MPC controller for system (6.18). N is the prediction horizon. Q_z weighs the output deviation from the reference r. S weighs the rate of the control input change and G weighs the control signal. Assignment of the elements in G will be based on energy price of using water heating and electrical heating here.

The objective function represents a balance between comfort and economic cost. By adjusting the ratio between Q_z and G, the comfort and energy expense can be balanced e.g. increasing Q_z results in better output reference tracking by using more electrical heating or fast output rate change and vice versa. The price of getting more comfort is at high energy cost. Implementation of the soft constraints in the MPC controller is documented in details in Appendix H.

6.3.3 Simulation results

Simulations of the MPC controller on a system using a floor heating system and an electrical heating source have been carried out to investigate whether the MPC controller can make the two heating systems cooperate and thereby achieve a better comfort and disturbance rejection. Two scenarios are simulated, a predicted reference change and a predicted ambient temperature change. The reference change could be applied in a house that is empty during day time and occupied in the night. During the day time a low room temperature reference is set to save energy, but in the evening a higher room temperature is required for comfort. The outdoor temperature change scenario simulates when cold air comes, and a large outdoor temperature drop is expected. The simulation results are presented in Fig. 6.11. For the simulations, the house model used for the simulations is the same as the MPC internal model (6.18).

The controller has a sampling time of 0.5 hour, and the prediction horizon $N = 20$; the weight matrices used in the simulations are

$$Q_z = 5000 \begin{bmatrix} 0 & 0 & 0 \\ 0 & 1 & 0 \\ 0 & 0 & 0 \end{bmatrix}, S = 0.1 \begin{bmatrix} 1 & 0 \\ 0 & 1 \end{bmatrix}, G = 0.001 \begin{bmatrix} 0 & 0 \\ 0 & 1 \end{bmatrix}$$

Q_z indicates that there is no penalty on the subfloor and wall temperature deviation from their reference. Matrix S shows that the input change rate is equally penalized for the two heating systems. G indicates that only using of the energy from electrical heater is penalized according to the fact that water district heating is much cheaper than electricity in the test house area.

Hard constraints are applied on the floor heating system input power(working range $0 - 1000w$) and the power of the electrical heater (working range $0 - 500w$).

In Fig. 6.11, at the beginning of the simulation, the electrical heater starts to drive the room temperature to the reference fast instead of only using the floor heating system. However when the room temperature reaches steady state, the electrical heater is switched off. This follows the weight matrix G where using the electrical heating system is penalized. This is seen in period 0-150 hours.

At hour 150, the ambient temperature drops from $0°C$ to $-5°C$ and back to $0°C$ again at hour 350. It can be seen in Fig. 6.11 that when the system is in steady state

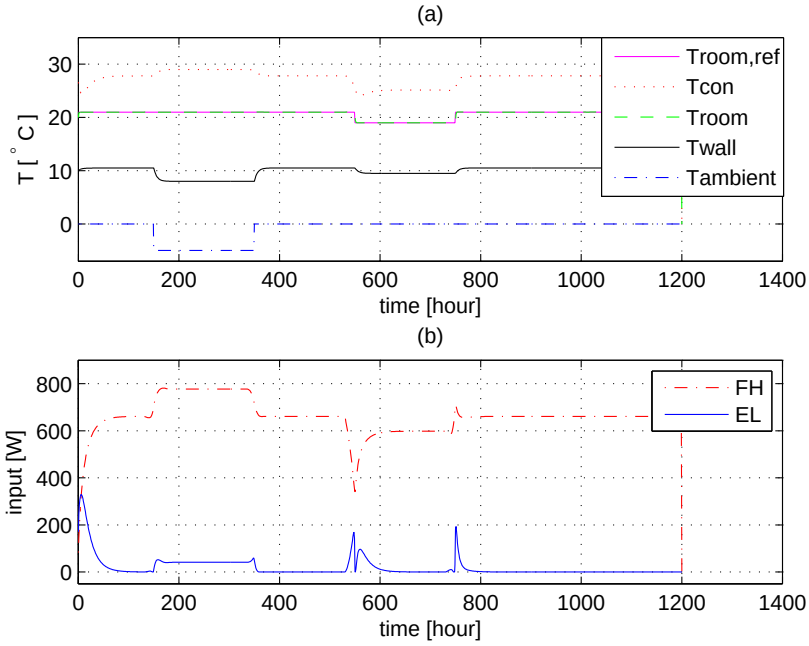

Figure 6.11: MPC simulation results. The ambient temperature drops from $0°C$ to $-15°C$ during hour 150-350. The reference changes from $21°C$ to $19°C$ during hour 550-750. 'FH' refers to the energy delivered by the floor heating system. 'EL' refers to the energy delivered by the electrical heater.

between hour 150 to 350, the electrical heater is activated although the floor heating is not saturated (max. power delivery of the floor heating system is $1000W$, here it deliveries only about $780W$). This is because the floor temperature already reaches the limit ($29°C$), which means that no more heat can be transmitted through the floor. Therefore the electrical heating has to be applied to maintain the room temperature close to the reference.

At hour 550, the room temperature reference is set down from $21°C$ to $19°C$ and back to $21°C$ again at hour 750. It can be seen that both the floor heating and the electrical heater start to react before the time of reference change. For instance the electrical heater starts to heat at hour 530, and the floor heating system decrease the heat delivery at the same time. The amplification of Fig. 6.11 around hour 550 is shown in Fig. 6.12. It might seems strange that the floor heating power drops much lower than the steady state value $600W$ between hour 550-750, and the electrical heating power increases and decreases two times. The reason is that with the prediction of reference decrease at hour 550, to get the room temperature very close to the reference when the

reference happens, the electrical heater has to be activated in advance, and switch off to achieve a fast temperature before hour 550. The floor heating system also decreases at the same time to make the temperature much closer to the reference when the reference change happens. After this, due to the power applied to the floor is too low, the electrical heating power has to be used until the floor heating power again is high enough. After that, during the steady state between hour 550 to 750 the reference can be reached with the floor heating system alone, therefore only the floor heating system is activated. This is corresponding to the weight matrix G. Similar happens at hour 750 when the reference is set back.

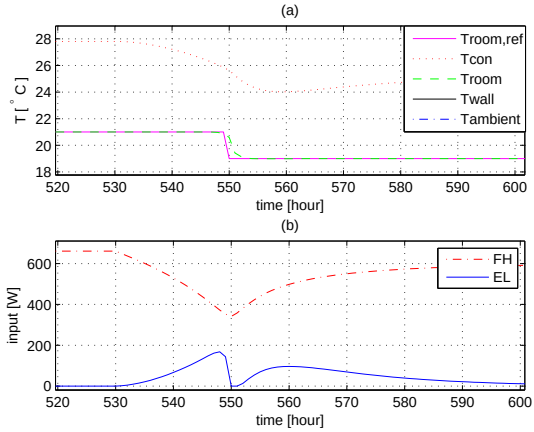

Figure 6.12: Amplification of Fig. 6.11 around hour 550.

It should be noted that the wall temperature shown in Fig. 6.11 is within the constraints but the value is rather low. The reason is that the wall in the model is considered a lumped mass, therefore the wall temperature here is the average wall temperature. In fact, the wall surface towards indoor has higher temperature than the average and on the other hand, the outside layer of the wall has a lower temperature close to the ambient temperature.

From the results it can be seen that MPC can handle control of multiple heat source with very different characteristics assuming well predicted disturbance information. The floor heating system which is cheap in energy price is utilized most. The electrical heater which is expensive to use is only activated when the system reaches saturation, constraints, disturbances that the floor heating system can not reject alone and during reference changes.

Although the MPC scheme shows potential on controlling multiple heat source systems, there are some issues that have to be investigated before implementing the MPC scheme in commercial products. One of the challenge is prediction mismatch for MPC. For instance, when the weather forecast predicted sunshine for a whole day, but in real-

ity the sun disappears for two hours. The MPC controller will not be able to control the room temperature very close to the reference due to the prediction mismatch. A suggestion could be to update the disturbance prediction with the current condition, where the current situation is connected to the original prediction with a smooth curve.

Chapter 7

Conclusions, perspectives and future work: control of domestic heating systems

7.1 Conclusions

In thesis Part II, the topics within modeling, control of a heavy construction floor heating system, and control of a multiple heat source system were considered. The work was presented as a collection of papers and technical reports enclosed in Part IV. The papers described modeling of floor heating systems, development of a temperature control method for a system with a large thermal capacity, control of a room temperature in a floor heated house, and discusses challenge of different house construction types. At last an investigation on control of multiple heat source systems characterized by different dynamics, prices of using etc. was conducted and documented in details in Appendix H.

The following conclusions has been made based on the work presented in Part II.

- A finite difference model of a floor heated house was developed, which was proven to be accurate enough for designing and verifying the control algorithm. The model complexity is relatively high and therefore it is suitable for simulation use, but too complicated for being used in model based control.

- A method for controlling the subfloor temperature was proposed. The advantage of this method is that it makes it possible to do energy based control for floor heating systems. With such a control scheme, the floor heating system dynamic response time with respect to room temperature can be increased, by using higher inlet water temperature. The risk of destroying the surface floor with the high

inlet water temperature can further be eliminated. The method is well suited for temperature control of systems characterized by having a large thermal capacity where strict temperature bounds should be obeyed.

- A feed forward disturbance rejection method was proposed for the floor heated house. Due to the slow dynamic of the floor heating system, this method could only take care of the disturbances with slower dynamics than the floor heating system, such as for example outdoor temperature change with a 24 hour period. For faster disturbances e.g. human dissipation, sun radiation etc., this control method did not perform well, hence a faster heat source should be applied. Perfect disturbance rejection is not easy to obtain as the floor and wall model identification in a real domestic application contains some practical limitations.

- Model predictive control method was applied on a house with a floor heating system and an electrical heater. The two heating systems were characterized by different dynamics and a different energy price. The control method performed well with the well predicted disturbance and reference change etc. A challenge in this setup is defining the disturbance trajectory for sun radiation effects, as it is in reality more an estimate of likelihood than a deterministic entity.

- A control challenge study of different house construction types was conducted. It was concluded that the building style have a strong impact on building dynamics with respect to the room temperature. The combination of different types of wall and floor construction have different influence on room temperature dynamics.

The work has contributed to three patents within control of heating systems. A better insight to the influence of building styles on the control challenge was provided. This can be utilized as an input for controller tuning, and for recommendations of which building designs are appropriate for floor heating systems. The introduction of the subfloor temperature controller, from where the direct heat delivery to the floor was estimated, can be applied i in the floor heating system, which works together with the MPC controller proposed in this work. The top level MPC temperature controller divides the heat delivery request out to a number of different heat sources. The work conducted in thesis Part II is part of the control architecture of the total climate system proposed in Fig. 1.1, which is a first step towards integrated intelligent control of multiple heat source systems.

7.2 Perspectives

A method of controlling temperature of a mass with large thermal capacity has been developed. Although the method was developed based on a floor heating system, it can be applied to other system characterized by large thermal capacity as well. An example of control a bottle cooler is given below.

The control objective of a bottle cooler in a car is to get the bottle cooled down to the desired temperature as fast as possible. This must be done without freezing the outside

layer of the bottle. It is for obvious reasons not feasible to place a temperature sensor in the bottle, so only the temperature of the bottle surface can be measured. This control challenge is much like the concrete floor system focused around controlling a mass with a large heat capacity, where the temperature can only be measured at the actuating point. In both cases a temperature gradient can be observed within the large thermal. The proposed method utilizes the gradient to achieve fast control and obtain a temperature measurement in the off-cycle, where the gradient is close to zero.

The author believes that there are also other systems that have similar properties, where the method can be applied to solve the problems.

7.3 Future work

In this section, some suggestions for future work and research are stated concerning two aspects - academic and industrial.

7.3.1 Academic aspect

MPC was proposed to solve the problem for multiple heat source systems with different dynamics and energy costs. With well predicted disturbance, the method works well, however when prediction mismatch appears, the performance are unsatisfactory. Some ideas have been proposed but not investigated yet, e.g. to update prediction with the current condition, where the current situation is smoothly connected to the original prediction with a curve. Another method to solve this problem could be robust MPC with bounded disturbances.

7.3.2 Industrial aspect

The concrete temperature control method was developed based on one water circuit and the test results show that it performed well. However in most of the domestic houses, there are in some cases more than 10 circuits. The way of estimating concrete temperature by circulating the water without adding heat for a while in each circuit one by one is very time consuming. Therefore an important step is to find a faster way to approximate the temperature of the individual concrete subfloors. An idea could be to simply close the valve of a water circuit for a period corresponding to the period that the subfloor needs to equalize the temperature. After the idle period, the subfloor temperature is more even, and the water temperature inside the pipe (except close to the inlet and outlet) is approximately the same as the subfloor temperature. Then, when the valve is open, the water outlet temperature especially after a short while can be used to approximate the subfloor temperature. As an example, if it takes 5 minutes for the water to run through the water circuit in a floor, then following the procedure above, after the valve is open, the subfloor temperature could be estimated by the average outlet temperature from 2-4 minute. The water outlet temperature during the 1^{st} and the 5^{th} minute does

not represent the subfloor temperature because they are too close to the inlet and outlet. The water outlet temperature after the 5^{th} minute is related to the temperature of the water that was sent to the pipe after the valve was open.

Another interesting direction is to study the possibility to store energy by utilizing the large thermal mass. The advantage of a heavy floor construction house is that this large thermal mass may be used as energy storage. This enables the system to store the energy when it is cheap to use or produce. An example is to combine floor heating system with a solar heater, which can only provide heat in day time. The idea would then be to store the energy in the floor heating system in day time and use it in night time to warm up the room.

Part III

CONCLUSIONS, PERSPECTIVES AND FUTURE WORK

Chapter 8

Conclusions, perspectives and future work

The conclusions, perspectives and future work of the thesis is presented in this chapter. The chapter is divided into two sections corresponding to Part I and Part II: control of air conditioning systems and control of domestic heating systems.

8.1 Control of air conditioning systems

8.1.1 Conclusions

In thesis Part I, control of switching systems was considered. The work was presented in a collection of papers enclosed in Part IV. The main focus was on deriving a low complexity and low cost optimizing switch control scheme for mass produced systems such as residential air conditioning units. The proposed method was designed for SISO stable systems with monotonic step response and no non-minimum phase behavior under binary input conditions.

Firstly a cost function optimizing the switch period and duty cycle was formulated and proven to be convex for stable first order systems. Secondly a control method based on the gradient of the cost function was proposed. Thirdly, the control method was extended to incorporate first and high order systems with or without delays. Finally the method was validated by experimental results.

The following conclusions can be extracted from thesis Part I.

- For stable first order systems, the optimizing switch control method achieves results close to the optimal solutions. For first order systems with delays and a class of SISO stable high order systems with monotonic step response and no non-minimum phase behavior, the method controls the systems towards the optimal

solutions when the included observer retrieves the delay-free output.

- The low complexity method does not require special tuning or knowledge of specific system parameters which makes it ideal for industrial implementation. The method relies only on the information of the controlled variable (if the system is without delay), or the estimated delay-free output (if the system is delay dominant).

- The method avoids the fundamental problem of finite horizon prediction methods.

- To give an idea of the improvement of the optimizing switch control method, the results of a traditional relay tuned at nominal condition was compared to the optimizing switch control method results. The results of both simulation and experiments showed that the optimizing switch control method outperforms the traditional relay.

The optimizing switch control method achieves better results than the relay method for first order or high order switching systems. Compared with the standard relay method, the optimizing switch control method required only a little more computational power, for example an extra state for integration term etc. This means that systems with high costs related to switching frequency, i.e. components wear, low performance, can achieve much better results if the optimizing switch control method is applied instead of a relay. In systems containing delay, both the relay and the optimizing switch control method benefits from the delay-free information, which can be achieved by introducing an observer.

However the method is limited to stable first order (including delay) or SISO stable high order systems with monotonic step response and no non-minimum phase behavior, in both cases with binary inputs.

The proposed method is empirically inspired, and it is not claimed that it holds in all generality. It is tested on a specific test system with good results. The authors, however, are convinced that the optimizing switch control method can be applied to a wide class of systems, including many arising from a variety of industrial areas.

8.1.2 Perspectives

A low complexity optimizing switch control method has been developed based on an switching controlled air conditioning system. In addition to the air conditioning system, many other industrial systems exhibit switching features, where the proposed optimizing switch control method might be able to solve the control problems. These systems often have low energy efficiency and/or components wear during start/stop transients. To be able to apply the optimizing switch control method, the systems have to SISO stable high order systems with monotonic step response and no non-minimum phase behavior. Several industrial examples of such nature are given below.

Heat pumps. A heat pump is usually installed to provide heating, which can be delivered in form of hot water or air. Depending on the heat uptake, the heat pump can often be classified as air or geothermal heat pump. However, this will not affect the application of the optimizing switch control method in heat pump systems. The heat pump is indeed a refrigeration system which utilizes the heat released from the condensation process.

Where the air heat pump is very similar to a typical residential air conditioning system, the water based heat pump is similar to the test system in Aalborg University. Both heat pump types include a switching cost related to component wear and low energy efficiency during start and stop transient. The internal media circulation can be considered as a first order system, and disturbance is the heat loss to the outdoor ambient. When the heating load is low, the systems have to be switching controlled. Therefore the optimizing switch control method can be applied to heat pump systems when the heating load is low.

Condensing boilers. A condensing boiler is very energy efficient due to cooling of the exhaust gas and the latent heat of water vapour in exhaust gases. The return water temperature is recommended to be below $60°C$. However, the gas burning must be kept above a specified minimum to avoid excessive pollution and degraded efficiency. There are different control strategies applied to these systems. However when the heat load is low, switching control has to be applied.

An example is that the boiler provides hot water to heating systems. This is similar to the heat pump example. The system can be modeled as a first order system and the disturbance is the heat loss to the indoor air. The system has a switching cost related to low energy efficiency and thermal stress of the components. Therefore the optimizing switch control method can be applied.

District heating plants. Similar to the above examples, some district heating plants may also need switching controlled operation. There is usually a internal water circulation which deliveries heat to nearby houses and buildings through heat exchangers. The internal water system can also be seen as a first order system. Here is also a switching cost related to low energy efficiency during startup phase. Therefore the optimizing switch control method can be applied to some district heating plants. Typically for this type of systems computational power is not a major problem, the method avoids the problem with finite prediction horizon approaches, and therefore might provide better performance.

The examples given here are only confined to energy systems, however the author believes that the switching controlled system problems also exist in other type of systems, and for some of them, the problem can be solved by the optimizing switch control method.

8.1.3 Future work

In this section, some suggestions for future work and research are stated concerning two aspects - academic and industrial.

8.1.3.1 Academic aspect

Robustness property of the method is not addressed in the thesis, therefore a rigorous proof of robustness issues would be interesting for future research.

The method is designed for SISO systems, however there exist many switching systems with multiple inputs. Extending the method to cooperate with systems with several inputs is an important direction for the future work too.

The method takes only the output variation and a switching cost in deciding the control action. Another term that is interesting to be included in the control is the energy consumption which is important to a lot of applications. This requires modification in the cost function and therefore the corresponding optimizing switch control algorithm.

The study in this part of the thesis has been focusing on switching systems with a binary input. It would be very interesting to extend the method to systems that can run continuously in the range of $[\overline{u} \quad u_{max}]$ where u_{max} is the maximum of the input and have to run switching control between $\underline{u}$ and $\overline{u}$ when the required input is lower than $\overline{u}$. In this case, a high level controller is proposed, which switches between the continuous controller when the input is $u \subset [\overline{u} \quad u_{max}]$ and switching controller when the required input is between $\underline{u}$ and $\overline{u}$.

Another direction is of course to merge continuous and discrete inputs. Many systems have both and then it really becomes difficult. One trick, however, is to make an alternate design of discrete and continuous designs.

8.1.3.2 Industrial aspect

A controller needs to implement a user adjustable balance between the comfort and economic issues. This can then be translated into a Q/R ratio for the cost function. Reasonable Q/R ratios might depend on the construction type and size of the house and on personal preference of the inhabitants.

8.2 Control of domestic heating systems.

8.2.1 Conclusions

In thesis Part II, the topics within modeling, control of a heavy construction floor heating system, and control of a multiple heat source system were considered. The work was presented as a collection of papers and technical reports enclosed in Part IV. The papers described modeling of floor heating systems, development of a temperature control method for a system with a large thermal capacity, control of a room temperature in

a floor heated house, and discusses challenge of different house construction types. At last an investigation on control of multiple heat source systems characterized by different dynamics, prices of using etc. was conducted and documented in details in Appendix H.

The following conclusions has been made based on the work presented in Part II.

- A finite difference model of a floor heated house was developed, which was proven to be accurate enough for designing and verifying the control algorithm. The model complexity is relatively high and therefore it is suitable for simulation use, but too complicated for being used in model based control.

- A method for controlling the subfloor temperature was proposed. The advantage of this method is that it makes it possible to do energy based control for floor heating systems. With such a control scheme, the floor heating system dynamic response time with respect to room temperature can be increased, by using higher inlet water temperature. The risk of destroying the surface floor with the high inlet water temperature can further be eliminated. The method is well suited for temperature control of systems characterized by having a large thermal capacity where strict temperature bounds should be obeyed.

- A feed forward disturbance rejection method was proposed for the floor heated house. Due to the slow dynamic of the floor heating system, this method could only take care of the disturbances with slower dynamics than the floor heating system, such as for example outdoor temperature change with a 24 hour period. For faster disturbances e.g. human dissipation, sun radiation etc., this control method did not perform well, hence a faster heat source should be applied. Perfect disturbance rejection is not easy to obtain as the floor and wall model identification in a real domestic application contains some practical limitations.

- Model predictive control method was applied on a house with a floor heating system and an electrical heater. The two heating systems were characterized by different dynamics and a different energy price. The control method performed well with the well predicted disturbance and reference change etc. A challenge in this setup is defining the disturbance trajectory for sun radiation effects, as it is in reality more an estimate of likelihood than a deterministic entity.

- A control challenge study of different house construction types was conducted. It was concluded that the building style have a strong impact on building dynamics with respect to the room temperature. The combination of different types of wall and floor construction have different influence on room temperature dynamics.

The work has contributed to three patents within control of heating systems. A better insight to the influence of building styles on the control challenge was provided. This can be utilized as an input for controller tuning, and for recommendations of which building

designs are appropriate for floor heating systems. The introduction of the subfloor temperature controller, from where the direct heat delivery to the floor was estimated, can be applied i in the floor heating system, which works together with the MPC controller proposed in this work. The top level MPC temperature controller divides the heat delivery request out to a number of different heat sources. The work conducted in thesis Part II is part of the control architecture of the total climate system proposed in Fig. 1.1, which is a first step towards integrated intelligent control of multiple heat source systems.

8.2.2 Perspectives

A method of controlling temperature of a mass with large thermal capacity has been developed. Although the method was developed based on a floor heating system, it can be applied to other system characterized by large thermal capacity as well. An example of control a bottle cooler is given below.

The control objective of a bottle cooler in a car is to get the bottle cooled down to the desired temperature as fast as possible. This must be done without freezing the outside layer of the bottle. It is for obvious reasons not feasible to place a temperature sensor in the bottle, so only the temperature of the bottle surface can be measured. This control challenge is much like the concrete floor system focused around controlling a mass with a large heat capacity, where the temperature can only be measured at the actuating point. In both cases a temperature gradient can be observed within the large thermal. The proposed method utilizes the gradient to achieve fast control and obtain a temperature measurement in the off-cycle, where the gradient is close to zero.

The author believes that there are also other systems that have similar properties, where the method can be applied to solve the problems.

8.2.3 Future work

In this section, some suggestions for future work and research are stated concerning two aspects - academic and industrial.

8.2.3.1 Academic aspect

MPC was proposed to solve the problem for multiple heat source systems with different dynamics and energy costs. With well predicted disturbance, the method works well, however when prediction mismatch appears, the performance are unsatisfactory. Some ideas have been proposed but not investigated yet, e.g. to update prediction with the current condition, where the current situation is smoothly connected to the original prediction with a curve. Another method to solve this problem could be robust MPC with bounded disturbances.

8.2.3.2 Industrial aspect

The concrete temperature control method was developed based on one water circuit and the test results show that it performed well. However in most of the domestic houses, there are in some cases more than 10 circuits. The way of estimating concrete temperature by circulating the water without adding heat for a while in each circuit one by one is very time consuming. Therefore an important step is to find a faster way to approximate the temperature of the individual concrete subfloors. An idea could be to simply close the valve of a water circuit for a period corresponding to the period that the subfloor needs to equalize the temperature. After the idle period, the subfloor temperature is more even, and the water temperature inside the pipe (except close to the inlet and outlet) is approximately the same as the subfloor temperature. Then, when the valve is open, the water outlet temperature especially after a short while can be used to approximate the subfloor temperature. As an example, if it takes 5 minutes for the water to run through the water circuit in a floor, then following the procedure above, after the valve is open, the subfloor temperature could be estimated by the average outlet temperature from 2-4 minute. The water outlet temperature during the 1^{st} and the 5^{th} minute does not represent the subfloor temperature because they are too close to the inlet and outlet. The water outlet temperature after the 5^{th} minute is related to the temperature of the water that was sent to the pipe after the valve was open.

Another interesting direction is to study the possibility to store energy by utilizing the large thermal mass. The advantage of a heavy floor construction house is that this large thermal mass may be used as energy storage. This enables the system to store the energy when it is cheap to use or produce. An example is to combine floor heating system with a solar heater, which can only provide heat in day time. The idea would then be to store the energy in the floor heating system in day time and use it in night time to warm up the room.

Bibliography

[1] O. Fanger. Thermal comfort. *McGraw-Hill Book Co.,New York*, 1972.

[2] Lei Fang, Geo Clausen, and Ole Povl Fanger. Impact of temperature and humidity on the perception of indoor air quality. *Indoor Air*, 8:80–90, 19981.

[3] Riccardo Scattolini. Architectures for distributed and hierarchical model predictive control - a review. *Journal of Process Control*, 19:723 – 731, 2009.

[4] Wadysaw Findeisen, F.N. Bailey, M. Brdys, K. Malinowski, P. Tatjewski, and A. Wozniak. *Control and Coordination in Hierarchical Systems*. Wiley and Sons, 1980.

[5] Mihajlo D. Mesarovic and Y. Takahara. *Theory of hierarchical, multilevel, systems*. Academic press, 1970.

[6] T. Y. Chen. Application of adaptive predictive control to a floor heating system with a large thermal lag. *Energy and Buildings*, 34(1):45 – 51, 2002.

[7] Honglian Thybo, Lars Larsen, and Claus Thybo. Control challenge for domestic heating systems. *European Control Conference*, 2007.

[8] Honglian Thybo, Lars FS Larsen, and Claus Thybo. Control of a water based floor heating system. *Multi-conference on Systems and Control*, 2007.

[9] Honglian Thybo, Lars FS Larsen, and Claus Thybo. Disturbance rejection of a water-based floor heating system. *UKACC Control Conference*, 2006.

[10] C. Aprea, R. Mastrullo, and C. Renno. Fuzzy control of the compressor speed in a refrigeration plant. *International Journal of Refrigeration*, 27(6):639 – 648, 2004.

[11] T.Q. Qureshi and S.A. Tassou. Variable-speed capacity control in refrigeration systems. *Applied thermal engineering*, 16(2):103 – 113, 1996.

[12] D. Flieller, P. Riedinger, and J.P. Louis. Computation and stability of limit cycles in hybrid systems. *Nonlinear Analysis, Theory, Methods and Applications*, 64:352–367, 2006, January.

[13] S. Almér, H. Fujioka, U.T. Jönsson, C.-Y. Kao, D. Patino, P. Riedinger, A.G. Beccuti, G. Papafotiou, M. Morari, A. Wernrud, Anders Rantzer, and T. Geyer. Hybrid control techniques for switched-mode dc-dc converters part i: The step-down topology. *American Control Conference*, July 2007.

[14] Wilbert F. Stoecker. *Refrigeration and air conditioning*. McGraw Hill Higher Education, 1983.

[15] Jen-Jie Hsieh, Wen-Shing Lee, Wen-Fang Wu, and Sih-Li Chen. Effect of lubrication on the performance and dynamic loads of scroll compressors. *The Chinese Journal of Mechnics*, 17, 2001.

[16] Lars F. S. Larsen. *Model Based Control of Refrigeration Systems*. PhD thesis, Aalborg University, 2005.

[17] Jakobsen Arne and Rasmussen Bjarne. Energy-optimal speed control of fans and compressor in a refrigeration system. *Eurotherm Seminar no. 59*, 1998, July.

[18] Arne Jakobsen, Bjarne Dindler Rasmussen, Morten Juel Skovrup, and Morten Juel Skovrup Bjarne Dindler Rasmussen. Development of energy optimal capacity control in refrigeration systems. *Proceedings of 2000 International Refrigeration Conference*, pages 329–336, July 2000.

[19] L. Larsen and C. Thybo. Potential energy savings in refrigeration systems using optimal setpoints. *Proceedings of IEEE Conference on Control Applications*, 2004.

[20] Lars. Larsen, Tobias Geyer, and Manfred Morari. Hybrid model predictive control in supermarket refrigeration systems. *Proceedings of the 16th IFAC world congress*, 2005.

[21] Daniel Sarabia, Flavio Capraro, Lars F.S. Larsen, and César de Prada. Hybrid nmpc of supermarket display cases. *Control Engineering Practice*, 17(4):428 – 441, 2009.

[22] N. Lawrence Ricker. Predictive hybrid control of the supermarket refrigeration benchmark process. *Control Engineering Practice*, In Press, Corrected Proof:–, 2010.

[23] Christian Sonntag, Malte Kölling, and Sebastian Engell. Sensitivity-based predictive control of a large-scale supermarket refrigeration system. *International symposium on advanced control of chemical process*, 2009.

[24] D. Sarabia, F. Capraro, L. F. S. Larsen, and C. De Prada. Hybrid control of a supermarket refrigeration system. *Proceedings of American Control Conference*, pages 4178–4185, 2007.

[25] Jin-Long Lin, T.-J. Yeh, and Wei-Yang Hwang. A dynamic switching strategy for air-conditioning systems operated in light-thermal-load conditions. *Applied Thermal Engineering*, 29(14-15):2832 – 2842, 2009.

[26] Alberto Leva, Luigi Piroddi, Massimiliano Di Felice, Alessandro Boer, and Raffaele Paganini. Adaptive relay-based control of household freezers with on/off actuators. *Control engineering practice*, page doi:10.1016/j.conengprac.2009.09.008, 2009.

[27] A. Haj-Fraj and F. Pfeiffer. Optimal control of gear shift operations in automatic transmissions. *Journal of the Franklin Institute*, 338(2-3):371 – 390, 2001.

[28] Quan Zheng, Krishnaswamy Srinivasan, and Giorgio Rizzoni. Optimal engine-transmission control of neutral-idle clutch application. *JSAE Review*, 22(4):463 – 472, 2001.

[29] Manish Kulkarni, Taehyun Shim, and Yi Zhang. Shift dynamics and control of dual-clutch transmissions. *Mechanism and Machine Theory*, 42(2):168 – 182, 2007.

[30] M. Montanari, F. Ronchi, C. Rossi, A. Tilli, and A. Tonielli. Control and performance evaluation of a clutch servo system with hydraulic actuation. *Control Engineering Practice*, 12(11):1369 – 1379, 2004. Mechatronic Systems.

[31] John Y. Hung, Weibing Gao, and James C. Hung. Variable structure control: a survey. *IEEE Transactions on Industiral Electronics*, 40(1):2 – 22, 1993.

[32] R.B. van Varseveld and G.M. Bone. Accurate position control of a pneumatic actuator using on/off solenoid valves. *IEEE/ASME Transactions on Mechatronics*, 2(3):195–204, 1997.

[33] Alexandra Grancharova and Tor Arne Johansen. Explicit model predictive control of an electropneumatic clutch actuator using on/off valves and pulse-width modulation. *Proceedings of European Control Conference*, 2009.

[34] Hege Langjord and Tor Arne Johansen. Dual-mode switched control of an electropneumatic clutch actuator. *IEEE/ASME Transactions on Mechatronics*, PP(99):1–13, 2010.

[35] Piccoli B. Hybrid systems and optimal control. *Proceedings of the 37th IEEE conference on decision and control*, 1:13 – 18, 1998.

[36] Sussmann H.J. A maximum principle for hybrid optimal control problems. *Proceedings of the 38th IEEE conference on decision and control*, 1:425 – 430, 1999.

[37] Luus R. and YangQuan Chen. Optimal switching control via direct search optimization. *2003 IEEE International symposium on intelligent control.*, pages 371 – 376, 2003.

[38] F. Bernelli-Zazzera and P. Mantegazza. Linearization techniques for pulse width control of linear systems. In C.T. Leondes, editor, *Digital Control Systems Implementation Techniques*, volume 70 of *Control and Dynamic Systems*, pages 67 – 111. Academic Press, 1995.

[39] A. Bemporad and M. Morari. Control of systems integrating logic, dynamics, and constraints. *Automatica*, 35(3):407–427, March 1999.

[40] Manfred Morari and Miroslav Baric. Recent developments in the control of constrained hybrid systems. *Computers and Chemical Engineering*, 30(10-12):1619 – 1631, 2006. Papers form Chemical Process Control VII - CPC VII.

[41] Brian Solberg, Palle Andersen, Jan M. Maciejowski, and Jakob Stoustrup. Optimal switching controlo of burner setting for a compact marine boiler design. *Control engineering practice*, 2010, To appear.

[42] Xuping Xu and Panos J. ANTSAKLIS. Optimal control of switched systems based on parameterization of the switching instants. *Transactions on automatic control,*, 799:2–16, 2004.

[43] Sebastian Sager. Reformulations and algorithms for the optimization of switching decisions in nonlinear optimal control. *Journal of Process Control*, 19(8):1238 – 1247, 2009. Special Section on Hybrid Systems: Modeling, Simulation and Optimization.

[44] D Sarabia, C de Prada, S Cristea, and R Mazaeda. Hybrid model predictive control of a sugar end section. *Computer Aided Chemical Engineering*, 21:1269–1274, 2006.

[45] C de Prada, S Cristea D Sarabia, and W. Colmenares. Hybrid control of a mixed continuous-batch process. *Proc. European Symp. on Computer-Aided Process Engineering,*, pages 473–484, 2004.

[46] Chen Ying, Zhang Jia-fan, Yang Can-jun, and Niu Bin. Design and hybrid control of the pneumatic force-feedback systems for arm-exoskeleton by using on/off valve. *Mechatronics*, 17(6):325 – 335, 2007.

[47] Wei-Ling Jian and M. Zaheeruddin. Sub-optimal on-off switching control strategies for chilled water cooling systems with storage. *Applied Thermal Engineering*, 18(6):369 – 386, 1998.

[48] Timothy I. Salsbury. A new pulse modulation adaptive controller (pmac) applied to hvac systems. *Control Engineering Practice*, 10(12):1357–1370, december 2002.

[49] Alexandre Restrepo, Andres González, and Sergio Orduz. Cost effective control strategy for small applications and pilot plants: on-off valves with temporized pid controller. *Chemical Engineering Journal*, 89(1-3):101 – 107, 2002.

[50] Honglian Deng, L. F. S. Larsen, Jakob Stoustrup, and Henrik Rasmussen. Control of systems with costs related to switching: applications to air-condition systems. *Proceedings of Multi-conference on Systems and Control*, 2009.

[51] Julio E. Normey-Rico and Eduardo. F. Camacho. Dead-time compensators: A survey. *Control Engineering Practice*, 16(4):407 – 428, 2008. Special Section on Manoeuvering and Control of Marine Craft.

[52] O.J.M.Smith. A controller to overcome dead time. *ISA J.*, 6:28–33, 1957.

[53] K.J. Astrom, C.C. Hang, and B.C. Lim. A new smith predictor for controlling a process with an integrator and long dead-time. *Transactions on Automatic Control*, 39:343–345, 1994.

[54] T. Liu, Y.Z. Cai, D.Y. Gu, and W.D. Zhang. New modified smith predictor scheme for integrating and unstable processes with time delay. *Control Theory and Applications*, 152:238–246, 2005.

[55] M.R. Stojic, F.S. Matijevic, and L.S. Draganovic. A robust smith predictor modified by internal models forintegrating process with dead time. *IEEE Transactions on Automatic Control*, 46:1293–1298, 2001.

[56] Gang Liu, Alan Zinober, and Yuri B. Shtessel. Second-order sm approach to siso time-delay system output tracking. *IEEE Transactions on Industrial Electronics*, 56:3638–3645, 2009.

[57] B. del Muro-Cuellar, O. Jimenez-Ramirez, M. Velasco-Villa, G. Fernandez-Anaya, and J. Alvarez-Ramirez. Observer-based prediction scheme for time-lag processes. *American Control Conference*, pages 639–644, 2007.

[58] H. H. Niemann, J. Stoustrup, B. Shafai, and S. Beale. Ltr design of proportional-integral observers. *International Journal of Robust and Nonlinear Control*, 5:671–693, 1994.

[59] Bjarne W. Olesen. Control of floor heating and cooling system. *Clima 2000/ Napoli 2001 World Congress-Napoli(I)*, 2001.

[60] Bjarne W. Olesen. Radiant floor heating in theory and practice. *ASHRAE Journal*, 2002, July.

[61] ANSI/ASHRAE. Thernal environmental conditions for human occupancy. *ANSI/ASHRAE*, 2004.

[62] CEN. En iso 1264: Floor heating - systems and components. *European Committee for Standardization*, 1997.

[63] Abdelaziz Laouadi. Development of a radiant heating and cooling model for building energy simulation software. *Building and Environment*, 39(4):421 – 431, 2004.

[64] Peter Weitzmann. Modeling building integrated heating and cooling systems. *PhD thesis*, pages 201–245, 2004.

[65] S. Y. Ho, R. E. Hayes, and R. K. Wood. Simulation of the dynamic behaviour of a hydronic floor heating system. *Heat Recovery Systems and CHP*, 15(6):505 – 519, 1995.

[66] R.M.C: De Keyser, F.A. Dumortier, and A.R.van Cauwenberghe. Adaptive control for domestic floor heating. *Building research and information*, 1986.

[67] Feipeng Da. Sliding mode predictive control for long delay time systems. *Physics Letters A*, 348(3-6):228 – 232, 2006.

[68] Jean-Pierre Richard. Time-delay systems: an overview of some recent advances and open problems. *Automatica*, 39(10):1667 – 1694, 2003.

[69] S. H. Cho and M. Zaheer-uddin. Predictive control of intermittently operated radiant floor heating systems. *Energy Conversion and Management*, 44(8):1333 – 1342, 2003.

[70] J. Rekstad, M. Meir, and A. R. Kristoffersen. Control and energy metering in low temperature heating systems. *Energy and Buildings*, 35(3):281 – 291, 2003.

[71] S. H. Cho and M. Zaheer-uddin. An experimental study of multiple parameter switching control for radiant floor heating systems. *Energy*, 24(5):433 – 444, 1997.

[72] Andreas. K. Thienitis. A predictive control algorithm for massive buildings. *ASHRAE Trans.*, 94 part 2:45–51, 1988.

[73] Kristian Edlund, Jan Dimon Bendtsen, Simon Børresen, and Tommy Mølbak. Introducing model predictive control for improving power plant portfolio performance. *Proceedings of the 17th World Congress, The International Federation of Automatic Control*, 2008.

[74] Martin Kragelund, Rafael Wisniewski, Tommy Mølbak, Rene Just Nielsen, and Kristian Edlund. On propagating requirements and selecting fuels for a benson boiler. *Proceedings of the 17th World Congress, The International Federation of Automatic Control*, 2008.

[75] M. Kragelund, J. Leth, and R. Wisniewski. Optimal usage of coal, gas and oil in a power plant. *Control theory applications, IET*, 4(2):282 –293, february 2010.

[76] Martin Kragelund, Ulf Jönsson, John Leth, and Rafael Wisniewski. Optimal production planning of a power plant. *IEEE International Conference on Control and Automation*, 2009.

[77] Yunus A. Cengel and Robert H. Turner. Fundamentals of thermal-fluid sciences. *McGraw-Hill*, 2005.

[78] Junckers. E 4.0 solid hardwood flooring. general information. underfloor heating. *http://www.junckers.dk*, 2003.

[79] Eduardo Fernandez Camacho and Carlos Bordons Alba. Model predictive control. *Springer*, 2004.

[80] Jan Maciejowski. *Predictive Control with Constraints*. Prentice Hall, 2000.

Part IV

APPENDICES

Appendix A

Optimizing switch control: applications to air conditioning systems

(Submitted May 2010 for journal publication.)

Honglian Deng, Lars Larsen, Jakob Stroustrup, Henrik Rasmussen

Abstract

This paper presents a low complexity method for optimizing switch control of systems with binary inputs in the case where a cost is related to a switch. The method strives to minimize a quadratic tracking error plus a cost related to a switch of the control input. The method is developed for an open loop SISO (single input single output) stable system with monotonic step response and no non-minimum phase behavior and no time delays. It is shown, however, that systems with dominant time delays can be handled by utilizing a delay observer. The method has been tested in practice on a refrigeration plant. The results show that the derived method in fact drives the system towards the optimal limit cycle. A comparison to a baseline relay controller with fixed bounds shows that the optimizing switch control method outperforms the baseline.

A.1 Introduction and problem statement

In US commercial buildings, approximately 30% of total electrical energy use can be attributed to ON/OF and staged electrical devices [1]. Therefore potential savings in both

energy and economy costs with an improved control algorithm for this type of system is vast. An example of this type of system is domestic air conditioning system, which in most cases is equipped with an ON/OFF controlled compressor, that drives the refrigeration process. Turning on and off the compressor leads to as well an increased wear of the compressor as an efficiency loss during start/stop until nominal condition is reached. A high switching frequency provides output with small variations, but with excessive components' wear and low energy efficiency. On the other high, a very low switching frequency is not desirable as it results in large output variations far form the desired operation condition. Optimal control of switching systems is typically a trade-off between output variation (output deviation from reference) and switching cost. Moreover these systems are often installed with mass-produced low cost controllers where only limited computational power is available. Hence, the focus of this paper is on finding a low complexity optimal control method for systems with ON/OFF switched actuators, where switching the input has a related cost.

Further more in this paper, the term switching system will be used for systems with binary inputs and the control of such a system will be called switching control. The system wear, system low energy performance due to start and stop transients caused by switches is defined as switching cost. The contributions attempt to solve control problems for systems with binary inputs are reviewed in this section.

[2] proposes a framework for Mixed Logical Dynamical (MLD) systems, which enables finite horizon Model Predictive Control (MPC) to work with switching systems. More details of MPC can be found in [3]; [4]. This approach straight forward adding cost to a switch leads to rather suboptimal solutions. The problem is that the finite horizon prediction MPC controller pushes the discrete value changes as late as possible to reduce the cost for the current time instant, because it can not see the damage of the choice of such input sequence causes until it is too late. So if special care is not taken using finite horizon methods on systems with discrete inputs, it can lead to rather poor performance. To avoid the finite prediction horizon problem of MPC for switching systems, [5] suggests to calculate optimal steady state limit cycle trajectory, and then employ MPC to track the optimal trajectory. The method works fine for the specific application, but redesigning of the method is necessary for another system. Besides the method also requires high computational power.

Another idea to avoid finite prediction horizon problem of MPC is to formulate in terms of time instants of occurrence of events, which are real type of variables, instead of binary values in each sampling time as in [6]; [7]; [8]; [9]. The progress of this way of formulating the problem is surveyed in [10]. Suboptimal limit cycles caused by discrete inputs are avoided in this formulation, but solution to such a formulation often requires high computational demand solvers.

[11] tries to define a cost function with ON time and the time that the system should switch ahead of load changes as inputs. The results are good based on the assumption that the load profile is known a priori, which is not always easy to predict in reality. Another problem is also that a numerical search to find the inputs that minimize the cost

function requires high computation power.

The methods in the above literature all require large computational power, which makes them impossible to implement in domestic air conditioning systems. In the following, some low complexity methods from literature are reviewed.

[12] presents a temporized virtual PID controller for ON/OFF systems. The virtual PID is a function of the system output error, and the output from the PID varies according to this error. The opening time is therefore a function of the output error. The switching period is then calculated based on the opening time. The method works fine for the problem, but switching cost is not considered.

[13] proposes a continuous feedback controller to a system with low input limit. When the continuous control signal is lower than the low input limit, it switches OFF the systems if the signal is close to OFF than to low limit, otherwise run the system at the low input limit. A dynamic compensator implementing an observer structure is added to compensate the difference between the applied and the continuous input signal. The approach succeeds in avoiding an excessive compressor speed transient following an off period, but did not address the challenge with frequent compressor switching.

Some researchers have chosen to extend Pulse Width Modulation (PWM) for the switching systems. [14] proposes hybrid fuzzy control method for high-speed ON/OFF valve in pneumatic systems. The author tried to control the pressure in a chamber, which vibrates rapidly, by modifying the PWM signals. This method reduces valve switches caused by rapid vibrations in pressure, which is typical for pneumatic systems. However the challenge in switching controlled air conditioning systems is different. [15] proposes a pulse modulation adaptive controller, where a conventional feedback controller module is used to get the output feedback and calculates a continuous control signal, and then sends the signal to a pulse width and pulse frequency modulation module, which converts the continuous signal to a digital value suitable for input to the plant. The pulse width and pulse frequency are calculated based on the continuous signal, some constraints of shortest ON/OFF time and and the system time constant. The method reduces switches, but does not achieve the optimal solution since that was not the focus of the paper.

Another widely applied method to switching systems is relay control with fixed bounds on the output. Setting the output bounds to the maximal limit for the process, ensures a minimal switching frequency, however at the expense of large output variations. For relay controls disturbances on the system may cause many unnecessary switches. To reduce a faster wear-out of the components caused by these unnecessary switches, [16] describes an extended relay controller with an filter equipped with an adaption mechanism to tune the filter parameters to preserve the oscillation parameters facing the system dynamics change. The method achieves the result of less switches caused by disturbance, but finding the optimal tradeoff between switching frequency, duty cycle and output variations, by setting the bounds in a relay controller is difficult for different operating conditions, because the optimal bounds varies with the operating conditions, as it will be shown in Section A.4.

In this paper, a low complexity method is proposed for binary input systems that have costs associated with the switching. First an air conditioning system used for the study is presented in Section A.2. In Section A.3 a cost function is first defined and demonstrated to have only one minimum and no saddle points. The optimizing switch control method is then derived based on the cost function. Simulation results of the method are presented in Section A.4. At last validation of the method with experimental results are presented in Section A.5. Conclusions and discussions are included in Section A.6.

This paper is in part based on previous work of the same authors, see [17]; [18].

A.2 Model of a domestic air conditioning system

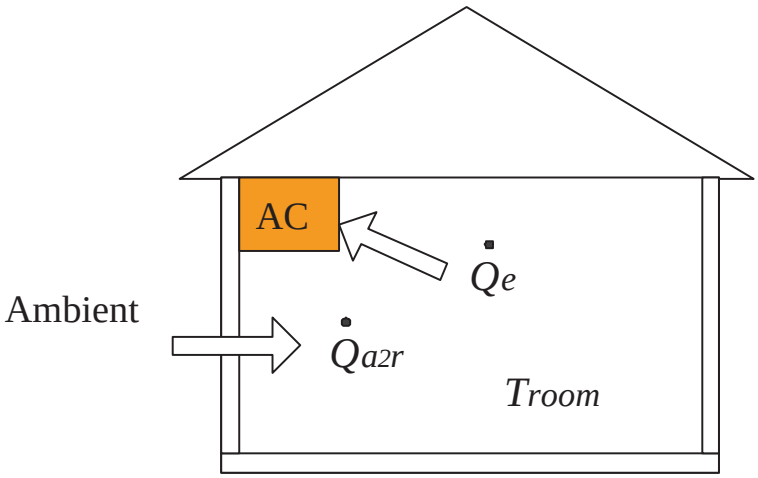

Figure A.1: A simplified air conditioned room

An simplified AC system used in this work is shown in Fig. A.1. The AC system is not modeled in detail, but represented by constant heat removal form the room model,

$$\begin{aligned} \frac{dT_{room}}{dt} &= \frac{\dot{Q}_{a2r} - \dot{Q}_e}{C_{p,air} M_{air}}, \\ \dot{Q}_{a2r} &= \frac{(T_{amb} - T_{room})}{R_{a2r}} \end{aligned} \tag{A.1}$$

where T_{room} is the temperature of the room air, $\dot{Q}_e$ is the heat flow absorbed by the AC system, $\dot{Q}_{a2r}$ is the heat flow from ambient to the room through wall, R_{a2r} is the thermal resistances from ambient to the room air, $C_{p,air}$ is the specific heat capacity

$C_{p,air}$	1005 $J/kg°C$
M_{air}	226 kg
R_{a2r}	0.022 $°C/W$
$\dot{Q}_e$	0 or 300 W

Table A.1: The parameters of the model.

of air, M_{air} is the mass of the room air, and T_{amb} is the ambient temperature. In this study, the AC system is ON/OFF switched, where $\dot{Q}_e = 300$ W when system is ON and $\dot{Q}_e = 0$ W when the AC system is OFF.

The model can be rewritten in the form of

$$\begin{aligned} \dot{x} &= ax + bu + d \\ y &= x, \end{aligned} \tag{A.2}$$

where $u \in \{\underline{u}, \overline{u}\}$ is the binary valued input and d is the term related to disturbance.

$$\begin{aligned} a &= \frac{-1}{R_{a2r} \cdot C_{p,air} \cdot M_{air}} = -2.00 \times 10^{-4} \quad s^{-1} \\ b &= \frac{-1}{C_{p,air} \cdot M_{air}} = -4.40 \times 10^{-6} \quad °C/J \\ d &= \frac{T_{amb}}{R_{a2r} \cdot C_{air} \cdot M_{air}} = 2 \times 10^{-4} \cdot T_{amb} \quad °C/s \\ u &\in \{\underline{u}, \overline{u}\} \\ \underline{u} &= 0 \quad W \\ \overline{u} &= \dot{Q}_e = 300 \quad W \end{aligned} \tag{A.3}$$

where T_{amb} is the ambient temperature. Throughout the paper a definition of load (in percentage) is used. This is defined as a percentage of the maximal capacity. For example 85% load means that the system has a load corresponding to 85% of $\underline{u}$. This model will later be used for method derivation and simulation study.

A.3 Derivation of the method

In this section first a cost function suitable for developing optimal switch control will be defined. Having defined this cost function, analysis of the properties with regards to various system dynamics will be carried out. At last an approach for optimizing switch control will be derived.

A.3.1 Cost function definition

An open loop stable system with a binary input, which is controlled by a relay controller, will typically converge to a first order limit cycle. Given such a system and a cost function, where making a switch is associated with a cost; it is assumed that the optimal steady state output trajectory follows a first order limit cycle. This is an assumption also made in [19]. The goal is to seek an optimizing switch control driving the output towards a stable limit cycle, meaning that the output is not converging to a fix-point. A standard summation of the squared control error does therefore not tend to a constant value and is thereby not a good measure of the performance. The system performance is consequently evaluated as the *average* squared control error over one switch period. For a first order limit cycle two switches are done in each cycle period. The total switch cost for one period therefore accounts to $2R$, where R is the cost of making one switch. The total average cost over one cycle period (T) can then be defined as follows

$$J = \frac{Q \int_{t_0}^{t_0+T} (y(t) - y_{\text{ref}})^2 dt + 2R}{T} \tag{A.4}$$

where t is the time, $y(t)$ is the measured output, y_{ref} is the output reference, Q is the cost associated with having a certain control error, and t_0 is the initial time for the cycle period. The control error and number of switches will then be balanced by the two weight factors Q and R. In the following, it is assumed that the cost R accounts for as well the costs of component wear as the efficiency loss at start/stops. This cost function represents the performance of the system over one cycle period, which will be used in the remainder of this paper.

A.3.2 Cost function analysis

Having defined the cost function, the next step will be to study whether the cost function has saddle points and more than one minimum point. In the following an analysis of this is based on general first order system model (A.2).

A stable first order limit cycle consists of an ON period and an OFF period as indicated in Fig. A.2. The output error accumulation can be divided into two parts: error from the ON period $t \in [t_0 \quad t_0 + \alpha T]$, and error from the OFF period $t \in [t_0 + \alpha T \quad t_0 + T]$, where α denotes the duty cycle which is the fraction of the cycle period T the input is ON ($0 \leq \alpha \leq 1$). The cost function (A.4) can therefore be written as

$$J = \frac{Q(\int_{t_0}^{t_0+\alpha T} (y_1(t) - y_{ref})^2 dt + \int_{t_0+\alpha T}^{t_0+T} (y_2(t) - y_{ref})^2 dt) + 2R}{T} \tag{A.5}$$

$y_1(t)$ and $y_2(t)$ refer to the output in respectively the ON and OFF period as indicated in Fig. (A.2).

In the following it is further assumed that the system given by (A.2) is stable, ($a \leq 0$). The convention that in ON periods $u = \overline{u}$ and the OFF periods $u = \underline{u}$ will be further

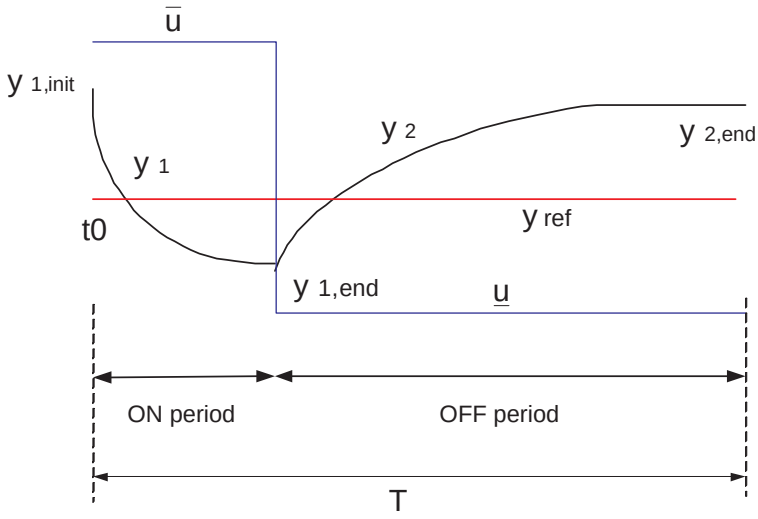

Figure A.2: One cycle period. In this example, $b < 0$

used. For the ON period , the explicit solution of (A.2) is given by (A.6), where $x_{1,\text{init}}$ is the initial value at the beginning of the ON period. For the OFF period, the explicit solution of (A.2) can be written as (A.7) where $x_{1,\text{end}}$ refers to the state value at the end of the ON period / beginning of the OFF period. (A.6) holds for $t \in [t_0 \quad t_0 + \alpha T]$. Remember that in this example, $y = x$.

$$y_1(t) = \frac{b \cdot \overline{u} + d}{-a} + \left(x_{1,\text{init}} + \frac{b \cdot \overline{u} + d}{a} \right) \cdot e^{at}, \qquad t \in [t_0, t_0 + \alpha T] \tag{A.6}$$

$$y_2(t) = \frac{b \cdot \underline{u} + d}{-a} + \left(x_{1,\text{end}} + \frac{b \cdot \underline{u} + d}{a} \right) \cdot e^{a(t-\alpha T)}, \quad t \in [t_0 + \alpha T, t_0 + \text{(A.7)}$$

By operating at steady limit cycles, the system output will be periodical under a constant disturbance. This means that the output at the end of one period equals the output at the beginning of the period, $y_{1,\text{init}} = y_{2,\text{end}}$. Applying this condition together with the continuous condition $y_{1,\text{end}} = y_{2,\text{init}}$ at $t = \alpha T$, to (A.6) and (A.7), the following can be derived,

$$x_{1,\text{init}} = \frac{\frac{b \cdot \underline{u} + d}{-a} + \frac{b \cdot \overline{u} - b \cdot \underline{u}}{-a} e^{a \cdot (1-\alpha) T} + \frac{b \cdot \overline{u} + d}{a} e^{a \cdot T}}{1 - e^{a \cdot T}} \tag{A.8}$$

$$x_{1,\text{end}} = \frac{\frac{b \cdot \overline{u} + d}{-a} + \frac{b \cdot \underline{u} + d}{a} \cdot e^{a \cdot T} + \frac{b \cdot \overline{u} - b \cdot \underline{u}}{a} \cdot e^{a \cdot \alpha T}}{1 - e^{a \cdot T}} \tag{A.9}$$

$y_{1,\text{init}}$ and $y_{1,\text{end}}$ can be obtained by applying $t = 0$ and $t = \alpha T$ to (A.6). $y_{2,\text{init}}$ and $y_{2,\text{end}}$

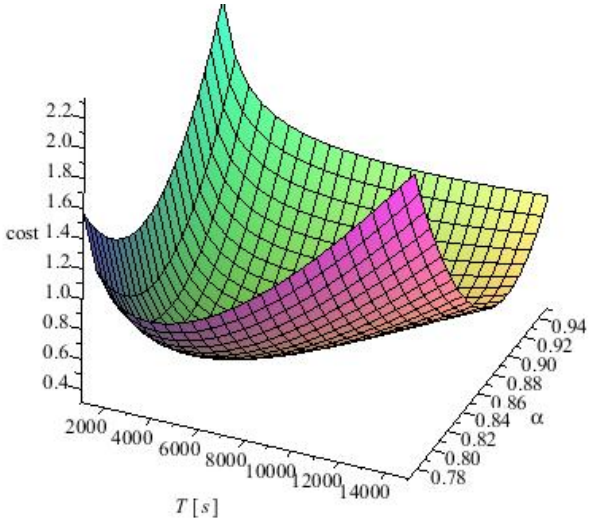

Figure A.3: Surface of cost function (A.4) for a first order system following a steady first order limit cycle, as function of the cycle period T and the duty cycle α.

can be obtained by applying $t = \alpha T$ and $t = T$ to (A.7).

In this set of equations $x_{1,\text{init}}$ and $x_{1,\text{end}}$ are functions of α and T, hence the cost according to (A.5) can be computed as a function of α and T. Even so it is not easy to prove directly that the cost function (A.5) is mathematically convex. The alternative is simply to calculate the cost with different value of α and T within a reasonable range of $\alpha \in [0, 1]$ and $T > 0$ to investigate the existence of an unique optimum by inspection. The result is shown in Fig. A.3, where the computed cost is plotted as a function of α and T. For the computations the parameter values given in (A.3) are used, where $T_{amb} = 28.61\ ^{\circ}C$, corresponding to 85% load.

In Fig. A.3, it clearly appears from the figure that the cost function for this system is indeed a smooth surface and has only one minimum close to T=4000 s and $\alpha = 85\%$, and no saddle points.

A.3.3 The optimizing switch control

In the previous section, it has been shown by inspection that the cost function for an stable first order without non-minimum phase behavior has one minimum only. In the following an approach for optimizing switch control based on this will be derived.

Consider the cost function (A.4). As the cost J is a continuous and smooth function of T, the minimum can be found among cycle periods T where $\frac{dJ}{dT} = 0$. Differentiating

(A.4) gives:

$$\frac{dJ}{dT} = \frac{Q(y(t0+T) - y_{ref})^2}{T} - \frac{Q\int_{t0}^{t0+T}(y(t) - y_{ref})^2 dt + 2R}{T^2} \tag{A.10}$$

A cycle period for a first order limit cycle includes two switches and hence two half periods: T_{old} which is the previous half cycle period and T_{new} which is the current half cycle period (either OFF or ON periods). By inserting T_{old} and T_{new} in (A.10) and setting equal to zero, the following is derived (note that $\frac{dJ}{dT} = \frac{dJ}{dT_{new}}$ as $T = T_{old}+T_{new}$, because T_{old} is assumed constant − a previous values.):

$$\begin{aligned}(y(t_0 + T_{old} + T_{new}) - y_{ref})^2(T_{old} + T_{new}) = \\ \int_{t_0}^{t_0+T_{old}} (y(t) - y_{ref})^2 dt + \int_{t_0+T_{old}}^{t_0+T_{old}+T_{new}} (y(t) - y_{ref})^2 dt + 2\frac{R}{Q}\end{aligned} \tag{A.11}$$

To keep the notation short, the left and right side of (A.11) are defined as follows:

$$\begin{aligned} ls(T_{new}) &= (y(t_0 + T_{old} + T_{new}) - y_{ref})^2(T_{old} + T_{new}) \\ rs(T_{new}) &= \int_{t_0}^{t_0+T_{old}} (y(t) - y_{ref})^2 dt \\ &+ \int_{t_0+T_{old}}^{t_0+T_{old}+T_{new}} (y(t) - y_{ref})^2 dt + 2\frac{R}{Q} \end{aligned} \tag{A.12}$$

Assuming the system follows the optimal steady limit cycle, then the following holds for T_{new} being in the neighborhood of T^*_{new} (optimal half period) :

$$ls(T_{new}) = rs(T_{new}) \Leftrightarrow \frac{dJ}{dT} = \frac{dJ}{dT_{new}} = 0 \Leftrightarrow T_{new} = T^*_{new} \tag{A.13}$$

Thus the idea is to use T_{new} as the adaptation variable for finding the switch time for the current half period and use a switching criterion, i.e. when $ls(T_{new}) = rs(T_{new}) \Leftrightarrow \frac{dJ}{dT_{new}} = 0$ at the time $t_0 + T_{old} + T_{new}$ the input will be switched. However to ensure that the switch in fact is done at a minimum cost, the second derivative should be positive $\frac{d^2J}{dT^2_{new}} > 0$.

$$\frac{d^2J}{dT^2_{new}}|_{T=T_{old}+T_{new}} = \frac{2\left(Q(y(t_0 + T) - y_{ref})\frac{dy(t_0+T)}{dT_{new}} - \frac{dJ}{dT_{new}}\right)}{T} \tag{A.14}$$

As $\frac{dJ}{dT_{new}} = 0$ when doing a switch (according to the switching criterion (A.12)), $\frac{d^2J}{dT^2_{new}} > 0$ requires that $(y - y_{ref})\frac{dy}{dT_{new}} > 0$. Note that y, $y(t_0 + T_{old} + T_{new})$, $y(t_0+T)$, $y(T_{new})$ all represent the current measured output. Given an open loop SISO stable system with monotonic step response and no non-minimum phase behaviors, the

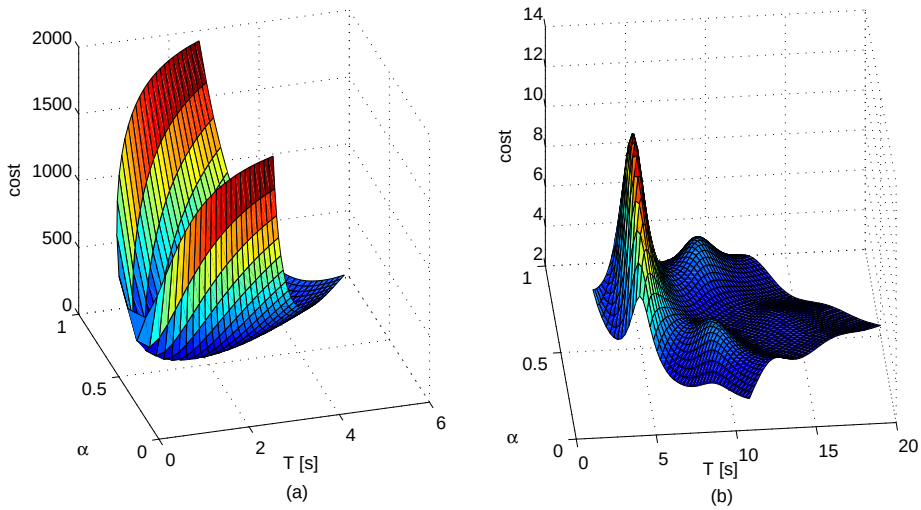

Figure A.4: Cost J as function of the period T and duty cycle α plotted for second order system $\frac{1}{(s-p_1)(s-p_2)}$ with: (a) poles $p_1 = -1, p_2 = -2$. $Q = 1, R = 50$. (b) poles $p_1 = -0.25 + 1.39i, p_2 = -0.25 - 1.39i, Q = 1, R = 5$.

output $y(t)$ monotonically increases/decreases depending on the direction of the input. Further assume, that the optimal switch time at the earliest will be after the output $y(t)$ has crossed the reference, thereby $(y(T) - y_{ref})\frac{dy(T)}{dT_{new}} > 0$. This ensures $\frac{d^2J}{dT_{new}^2} > 0$ for all values of T_{new} (being it in an ON as well as an OFF period) where $\frac{dJ}{dT_{new}} = 0$. Consequently there can be no maxima or saddle points with the convex domain $T > 0$ and $0 \leq \alpha \leq$, hence as J is continuous and smooth, there can be one minimum only.

The following conjecture is stated,
The cost function (A.5) has one minimum only (a global minimum) given an open loop SISO stable system with monotonic step response and no non-minimum phase behavior.

To illustrate the conjecture by examples, Fig. A.4a depicts a cost function for a SISO stable second order system with monotonic step response and no no-minimum phase behavior. In this case the cost function clearly has only one minimum and no saddle point. Fig. A.4b depicts the result for a second order system with complex poles, which clearly has many local minimum points. The maxima of the cost function, seen in Fig. A.4b, appears when the switching period corresponds to the harmonic frequencies of the system.

The optimizing switch control can be implemented in the following way, that at each time instance $t = t_0 + T_{old} + T_{new}$ it should be decided whether a switch should be made or not based on following criteria,

Switch the control input

if

$$\left((y(T_{new}) - y_{ref})\frac{dy(t)}{dt} > 0\right) \wedge (ls(T_{new}) \geq rs(T_{new})) \wedge (|y(T_{new}) - y(t_0)| \leq \Delta y) \tag{A.15a}$$

or

$$\left((y(T_{new}) - y_{ref})\frac{dy(t)}{dt} > 0\right) \wedge ((y(T_{new}) - y(t_0) > \Delta y) \wedge (y > y_{ref})) \tag{A.15b}$$

or

$$\left((y(T_{new}) - y_{ref})\frac{dy(t)}{dt} > 0\right) \wedge ((y(t_0) - y(T_{new}) > \Delta y) \wedge (y < y_{ref})) \tag{A.15c}$$

where Δy is adjustment parameter setting the maximal correction step, which is introduced to ensure that the output change should be maintained within the range of Δy. The last half cycle period T_{old} has been decided earlier, hence it should only be decided whether to do the switch for the current half cycle period T_{new} at the current time instance or not. The algorithm only strives at optimizing time for the current half cycle period T_{new}, based on the integrated error over the time elapsed of the total cycle period. It is worth of mentioning that, the control algorithm needs to measure only the output, and no disturbance information is needed.

In the following, a discrete version of the optimizing switch control algorithm based on (A.16) is applied, which is,

$$\begin{aligned} lsd(T_{new}) &= (y_{N_{t_0}+N_{T_{old}}+N_{T_{new}}} - y_{ref})^2 (N_{T_{old}} + N_{T_{new}}) \cdot T_{samp} \\ rsd(T_{new}) &= \sum_{N_{t_0}}^{N_{t_0}+N_{T_{old}}} (y_{N_{T_{new}}} - y_{ref})^2 \cdot T_{samp} \\ &\quad + \sum_{N_{t_0}+N_{T_{old}}}^{N_{t0}+N_{T_{old}}+N_{T_{new}}} (y_{N_{T_{new}}} - y_{ref})^2 \cdot T_{samp} + \frac{2R}{Q} \end{aligned} \tag{A.16}$$

where lsd, rsd are the discrete version of ls, rs. The integration term in (A.12) is expressed as a sum of the values, which is easy to implement in experiments. The sampling time is T_{samp}. N_{t_0} refers to the number of samples at the starting time of the total cycle

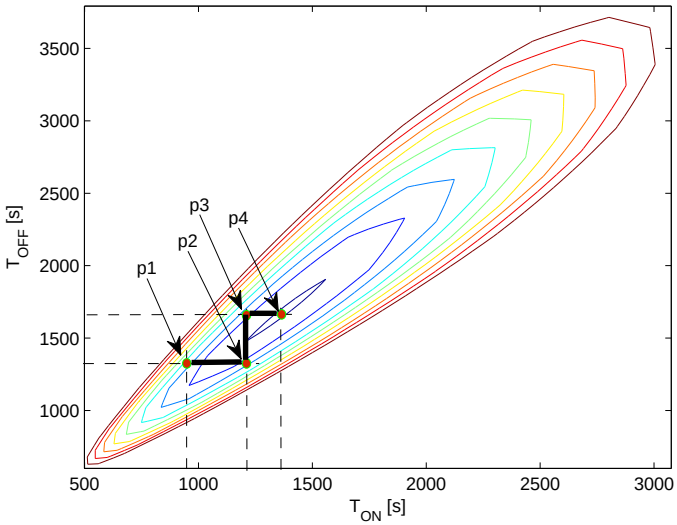

Figure A.5: Illustration of the periods update on a contour plot of the cost defined by (A.4) with a certain load. T_{ON} is the ON period and T_{OFF} is the OFF period.

period; $N_{T_{new}}$, $N_{T_{old}}$ represents the current half cycle period and the previous half cycle period respectively in samples.

According to the conjecture, the cost function (A.4) for a system fulfilling the requirements has one minimum only. Fig. A.5 shows how periods update take place on a contour plot of the cost defined by (A.5) for the first order system (A.2). In the example, at a certain time, the $T_{old} = T_{ON} = 950$ s, then $T_{new} = T_{OFF}$ found according to the T_{old} is $T_{OFF} = 1350$ s. Then update $T_{old} = T_{OFF} = 1350$ s, then $T_{new} = T_{ON}$ found based on the T_{old} is $T_{ON} = 1230$ s. Repeating the above procedures, at last the optimal solution $T_{ON} = 1374$ s, $T_{OFF} = 1685$ s is reached in this example.

The optimizing switch control algorithm deduced above optimizes the current half periods according to the previous period, i.e. T_{new} is optimized according to T_{old}. As an example, T_{new} is ON period, then T_{old} will be the OFF period. T_{new} will be different from the previous ON period $T_{new,previous}$. Therefore the duty cycle $T_{new}/(T_{new} + T_{old})$ will be different from $T_{new,previous}/(T_{new,pervious} + T_{old})$. This means that at each switch, both the period and duty cycle are updated. If the correction of the half periods is sufficiently small, the performance cost can be arbitrarily close to the steady limit cycle performance cost depicted in Fig. A.5. Hence if the maximal correction step is chosen sufficiently small the optimizing switch control will iteratively step towards the global minimum as indicated in Fig. A.5.

A.4 Simulation results

In this section, several simulations will be conducted to test the developed optimizing switch control method. The simulations are based on the simplified first order room model in in Section A.2. The room temperature reference for simulations is set to be 23 $^{\circ}C$. The sampling time is set to be 2 s.

A.4.1 Convergence

Simulations of the optimizing switch control method with different initial conditions but the same load sequences are conducted, and the results show that if the initial conditions are not too far away from the reference e.g. in this example with load 85%, when the initial temperature is within the range of 20 to 25 $^{\circ}C$, the results converge close to the optimal solution. The reason that the results do not converge to the optimal solution when initial condition is far from the reference is that the right side of (A.11), rs keeps integrating, which becomes large with this initial condition, but the left side of (A.11), ls will not be able to catch up rs due to the first order system behavior. The result would converge for an integrative system due to that the time constant is infinite. Under the condition that the initial values are far from the reference, the system should be kept on until the indoor air temperature gets down close to the reference and then change to the optimizing switch controller.

As an example, experiments of the optimizing switch control of room temperature T_{room} for system (A.2) under load 85% is carried out. The cost function surface for this example is shown in Fig. A.3. Two different initial conditions $x_0 = 22.8\ ^{\circ}C$ and $x_0 = 25\ ^{\circ}C$ for the same load 85% are tested and the results are shown in Fig. A.6, where both outputs converge to a result very close to the optimal solution. The optimal solution in Fig. A.6 is achieved by applying a pulse input with the optimal duty cycle and cycle period calculated directly from the cost function J, to the system given by (A.2). The resulting period, duty cycle and cost are presented in Table A.2, where the initial conditions are not too far away from the reference.

Notice in Table A.2, that the duty cycles are 85.69% which is different from the load. According to the definition of the load, if the system runs with the duty cycle equal to the load, the average temperature will be maintained at the reference. Therefore the results with the optimal duty cycle actually do not maintain the average output at the reference. The reason why the duty cycle is different from the load is explained in Subsection A.4.4.

To demonstrate the optimizing switch method functionality, the left and the right side of (A.11) and the input switches are plotted in Fig. A.7. The figure shows that during each half of the cycle period, the right side (rsd) of the equation is accumulating, and is re-initialized at each switch; the left side (lsd) of equation after a switch first decreases, and later increases again. This is due to that the half cycle period T_{new} is initialized to 0 at each switch, and the output moves from one limit towards the reference, crosses the reference and at last move towards the other output limit on the other side of the

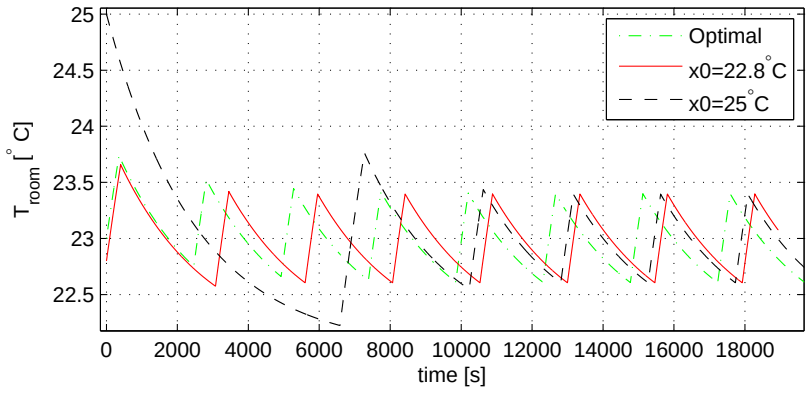

Figure A.6: Comparison of the optimizing switch controller outputs with the optimal solution. 'Optimal': the optimal solution. $x_0 = 22.8\ ^\circ C$: optimizing switch control method with initial state $22.8\ ^\circ C$. $x_0 = 25\ ^\circ C$: optimizing switch control method with initial state $25\ ^\circ C$. The results in this figure are all from load 85%. Q/R=2/500.

	period [s]	duty cycle	cost
opt.	4919	85.69%	0.31115
$x_0 = 22.8^\circ C$	4925	85.69%	0.31117
$x_0 = 25^\circ C$	4925	85.69%	0.31117

Table A.2: Comparison of the results from different initial conditions with the optimal solution. The load is 85%, and Q/R=2/500.

reference. The switches only take place when the left (lsd) and the right side (rsd) equal.

Simulations are made to study whether the optimizing switch control algorithm drives the output towards the optimal solution under different Q/R ratios and different loads. The results are shown in Fig. A.8. It can be seen that the optimizing switch control method indeed converges close to the optimal solution under different Q/R ratio and different loads at the specified initial condition.

A.4.2 Benchmark with a relay control

Since the output of the system (as shown in Fig. A.6) seems to be very similar to a traditional relay control result, the following question arises: What is the difference between the proposed method and a traditional relay control method when applied to the considered system? A comparison between the two controllers is made based on

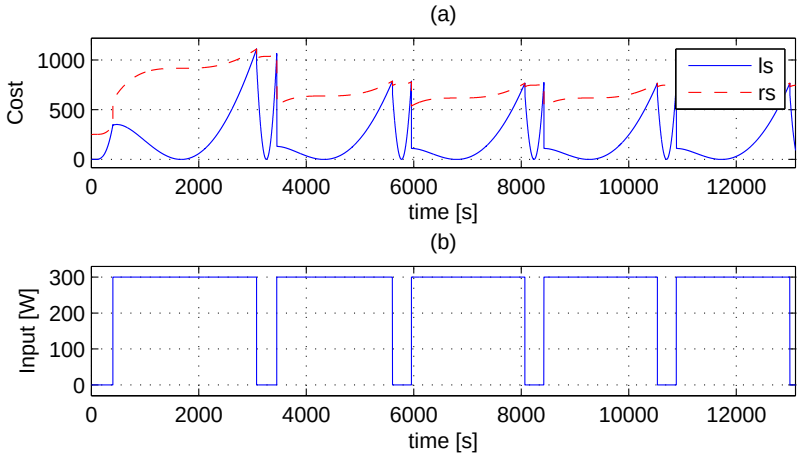

Figure A.7: lsd, rsd from the simulations with initial state $x_0 = 22.8\ ^\circ C$, and load 85%

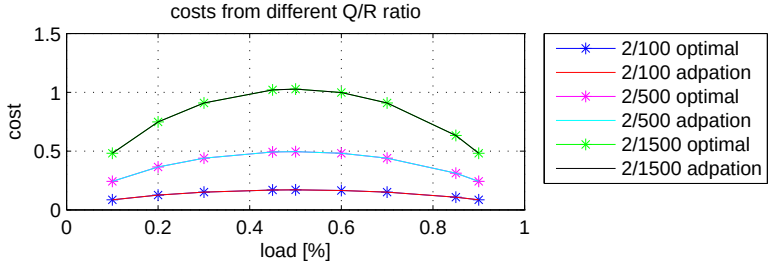

Figure A.8: Simulation results of the optimizing switch control method with different Q/R ratio compared with the optimal solution. The initial state $x_0 = 22.8^\circ C$

simulations and the results are presented in Fig. A.9 with respect to cost, period and duty cycle deviation (The duty cycle deviation is defined as the difference between the duty cycle from the controller and the optimal duty cycle under the same load.).

The relay controller is tuned at 50% load, where input limits reference$\pm 0.5\ ^\circ C$, gives the same duty cycle and period as the optimal solution. Applying the tuned relay controller and the optimizing switch controller on system (A.2) under different loads, yields the results shown in Fig. A.9. It is clear to see that at 50% load, the relay controller and the optimizing switching controller has same good performance - very close to the optimum, but away from 50% load, the relay results deviates from the optimal solution, for example at 90% load, the performance cost defined by (A.4) for the relay controller is about 20% higher than the optimal solution, while the optimizing switch controller achieves results close to the optimum with different loads. Therefore it can be concluded that the proposed optimizing switch control method attains close to the optimal solution as stated previously.

A.4.3 Performance during load change

A simulation test of the optimizing switch control method with load change has been performed, and the result can be seen in Fig. A.10. The load at the beginning is 85% corresponding to $T_{amb} = 28.61\ ^\circ C$, and at time 30000 s it is reduced to 10% corresponding to $T_{amb} = 23.66\ ^\circ C$. The result shows that the optimizing switch control method drives the system to another limit cycle corresponding the changed load. It should be noted that the load should be below 100% corresponding to $T_{amb} = 29.6\ ^\circ C$, otherwise, saturation problem has to be considered.

A.4.4 Notes regarding the load and duty cycle

It is worth mentioning that the optimal duty cycle and load might be different for a first order switching system. This can be seen in Table A.2, where the load is 85% while the optimal duty cycle is 85.69%. In other words, the optimal duty cycle actually results in an average different from the reference, which can be clearly seen in Fig. A.10 from time 30000 to 80000 s, where the average is higher than the reference. This is caused by the first order system behavior. The reason is that, when the load is not at 50%, the system output has a smaller gradient at the end of longer half cycle period than at the end of the short half cycle period, which means that prolonging the longer half cycle period will not result in much output deviation, but a much longer period and smaller cost. Therefore the optimal duty cycle is different from the load as long as the load is not 50%.

Two further studies were carried out to demonstrate the effect of the load and Q/R ratio on the differences between the load and duty cycle.

The first investigation concerned the influence of the load and was carried out by calculating the optimal solution under different loads. The results are presented in Table A.3 which show that if the load α is not equal to 50%, the optimal duty cycle and the

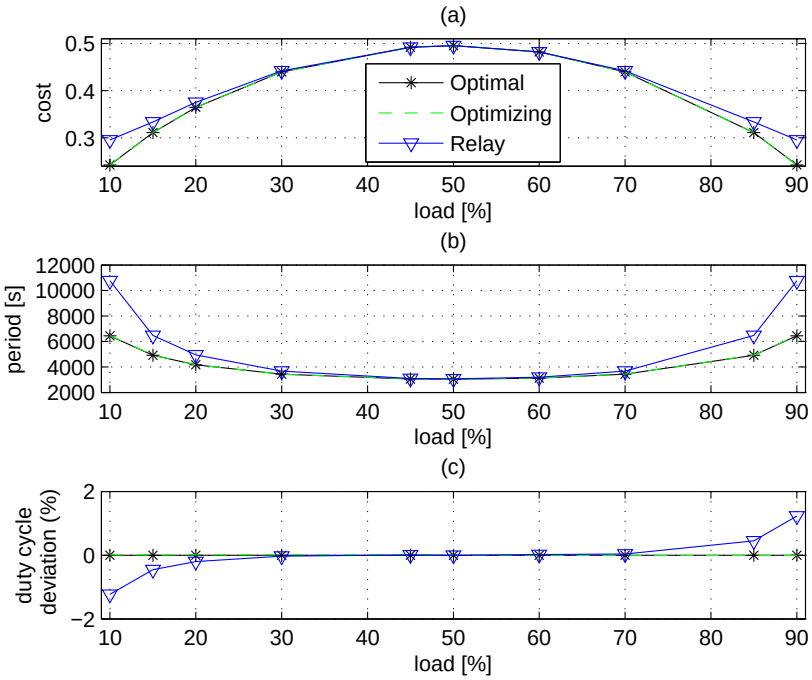

Figure A.9: Comparison of solutions from the different methods. 'Optimal': the optimal solution. 'Optimizing': the developed optimizing switch control method. 'Relay': relay control. The initial state is $x_0 = 22.8\,^{\circ}C$.

load are always different.The closer the load to 1 (or 0), the larger difference is between the optimal duty cycle and the load, as explained at the beginning of this subsection.

The second investigation concerned the impact of the choice of the Q/R ratio on the obtained solution. It was carried out by evaluating the obtained optimal solutions with different Q and R but under the same load condition. The results are presented in Table A.3 which shows that the value of the difference depends also on the Q/R ratio. With increase of R, the difference becomes bigger because the penalty of switching is increasing, therefor, the long half cycle period will be prolonged even longer. For 50% load, the error accumulation in both the ON and the OFF period has the same gradient over the corresponding period, therefore, the optimal duty cycle is the same as the load. More details can be found in [17]. A note here is that when the system is under load α, the optimal periods are the same as under load $1 - \alpha$.

Until now an optimizing switch control method has been developed, which controls

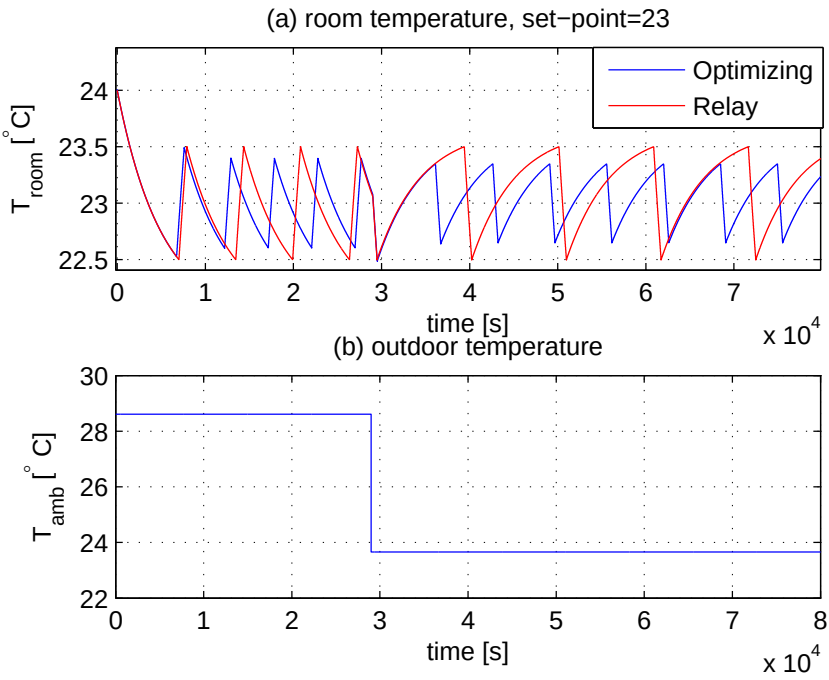

Figure A.10: The performance of optimizing switch control and relay control method under load change. The disturbance $T_{amb} = 28.61\ ^{\circ}C$ and $T_{amb} = 23.66\ ^{\circ}C$ is corresponding to load=85% and 10%. Penalty ratio Q/R=2/500.

stable first order systems towards the optimal limit cycle, has low complexity, and outperforms relay controllers in simulation tests. Next step is to experiment the optimizing switch control method with a real plant.

A.5 Experiments with a refrigeration plant

In this section, validation of the optimizing switch method with a refrigeration plant is carried out. First a description of the refrigeration plant is given. Then extension of the method to work with systems with delays is briefly described. At last, experimental results are presented.

Q/R	results from	load							
		90%		60%		50%		10%	
		period [s]	duty cycle	period [s]	duty cycle	period [s]	duty cycle	period [s]	duty cycle
2/500	opt.	6447	90.91%	3125	60.12%	3037	50.00%	6447	9.09%
	cont.	6460	90.89%	3130	60.16%	3042	50.00%	6460	9.10%
2/2500	opt.	13947	93.12%	5421	60.48 %	5257	50.00%	13947	6.88%
	cont.	13955	93.11%	5427	60.48 %	5262	50.00%	13956	6.89%

Table A.3: The solutions for different load and different penalty ratio. 'opt.' is the optimal solution is calculated from the cost function. 'cont.' are the solutions from the optimizing switch controller.

A.5.1 Test system description

The refrigeration plant in Aalborg University Denmark as shown in Fig. A.11 is used for the experiments. The detailed information of the refrigeration plant can be found in [20]. The schematic view of the plant is presented in Fig. A.12. The system emulates an air conditioning system, where the tank simulates the room, and the refrigeration system works as the air conditioning unit. The heat load on the system is provided by an electrical heater with an adjustable power supply for the heat element in the water tank. The overall control goal is to maintain the tank water temperature at the reference by switching the compressor in the refrigeration system ON/OFF under a heating load.

Since the tank is well insulated, the heat loss to the ambient is so little that it can be neglected, which means that the tank behaves like an integrative system. A mixer is installed to keep the water in the tank well mixed so that the water temperature can be considered even. The compressor is operated with a variable speed drive from 35 to 60 Hz. Temperature sensors and a mass flow sensor are installed on the water pipe passing the heat exchanger.

In the experiments, the refrigeration system evaporation and condensation pressure are set to be 1×10^6 Pa and 3.5×10^5 Pa. The accuracy of the temperature sensors is $\pm 0.3 \circ C$ at $0 \circ C$ within the operating range. There are two temperature measurements used in this experiment: the inlet water temperature to the tank $T_{w,in}$ and the outlet water temperature of the tank $T_{w,out}$.

A.5.1.1 Modeling of the test system

The refrigeration system is considered as a whole unit with discrete input control signal in this paper. When the refrigeration system is switched on, the compressor runs with 35 Hz, which in steady state can remove approximately 3200 W from the water through the heat exchanger under the specified working condition for the experiments. When the refrigeration system switches off, it removes 0 W from the water, which is expressed as $\dot{Q}_e$ =3200 or 0 W. More details of the refrigeration system can be found in [20].

Figure A.11: Refrigeration test plant in Aalborg University

The water tank is roughly modeled as

$$\begin{aligned} \dot{T}_{water} &= \frac{\dot{Q}_{load} - \dot{Q}_e}{c_{p,water} \cdot m_{water}} \\ T_{w,out} &= T_{water}(t-\theta) \end{aligned} \tag{A.17}$$

where $\dot{T}_{water}$ is the time derivative of water temperature in the tank . $T_{w,out}$ is the measured temperatures of the water coming out of the tank. $c_{p,water}$ is the specific heat capacity. m_{water} is the mass of the water in the tank. T_{water} is the water temperature in the tank.

$\dot{Q}_{load}$ is the heating load from the electrical heater. $\dot{Q}_e$ is the estimation of the power removed from the water tank by the refrigeration system, and it can be modeled from the water side of the refrigeration system,

$$\dot{Q}_e = c_{p,water} \cdot \dot{m}_{water}(T_{w,out} - T_{w,in}) \tag{A.18}$$

$T_{w,in}$ is the measured temperature of the water coming into the tank as shown in Fig. A.12. $\dot{m}_{water}$ is the mass flow of water into the tank. The disturbance from the ambient to the water tank is ignored due to the very good insulation of the tank.

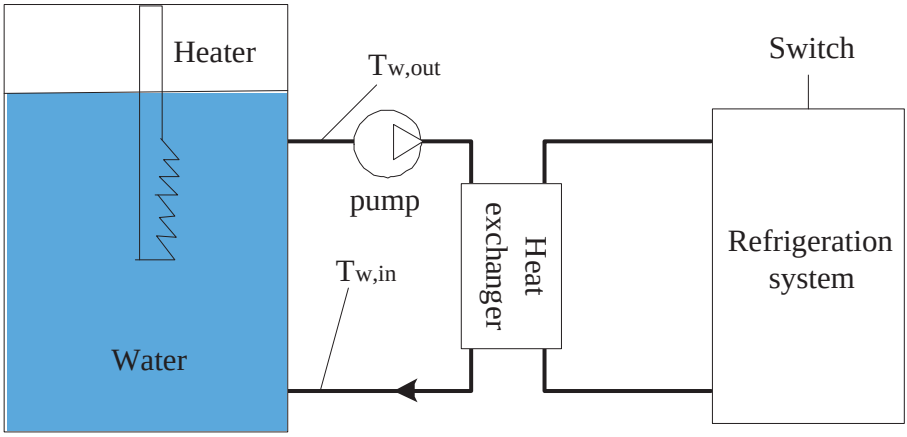

Figure A.12: Schematic view of the test system: the refrigeration plant

The water temperature coming into and out of the tank are $T_{w,in}$ $T_{w,out}$ which are corresponding to the water temperatures after and before passing the evaporator. Although a mixer is installed to keep the water in the tank well mixed so that the water temperature is even and therefore the water coming out of the tank $T_{w,out}$ can be approximated as the water temperature inside the tank. However, there is a delay from when the refrigeration system removes the power until $T_{w,out}$ reacts. This is caused by the flow transportation in the pipe, among other factors. In this case the delay is approximately θ =90 s.

The parameter for the models are $c_{p,water} = 4180$ J/(kg·°C), $m_{water} = 65$ kg, θ =90 s, $\dot{Q}_e \in \{0, 3200 \quad W\}$.

It should be noted that the optimizing switch control method was developed based on a first order model, but it works on an integrative system as well, which is a special first order system with infinite time constant.

A.5.1.2 Validation of the model

Validation of the model with the experimental results are carried out, and the results are shown in Fig. A.13. The model output is obtained by applying the measured $\dot{Q}_e$ and $\dot{Q}_{load}$ into to model (A.17). It can be seen that at before time 10000 s s the output from the model matches the measured output very well, but after that there is some mismatch. The mismatch is mainly caused by the approximation of a higher order system as a integrative system.

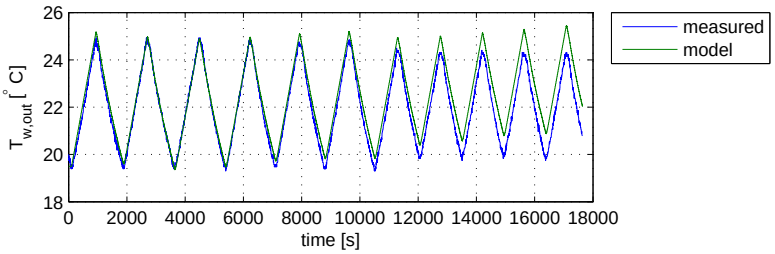

Figure A.13: Validation of the refrigeration system model (A.17). $measured$ represents $T_{w,out}$ from experiment and $model$ refers to $T_{w,out}$ from the model.

A.5.2 System with delays

In the real world, systems can very seldom be modeled as first order systems, which the optimizing switch control method is designed based on. Under some operating conditions, some of these plants can be modeled as high order linear systems. In many applications, these high order linear systems can be approximated as a first order system with a delay. Therefore extension of the method to system with delays is necessary in order to implement it in industrial systems.

Applying the optimizing switch method directly to a first order system with a delay leads to suboptimal solution because the information that is fed back to the controller is 'old'. The optimal solution for a first order switching system is independent of whether the system has a delay or not, meaning that if the delay-free output is fed back to the controller, the system should perform exactly the same as for the systems without delay under no disturbances. The question is how the delay-free output information can be achieved.

Extensive research has been carried out on controlling systems with delays, see the survey [21]. One classical method is based on the Smith Predictor [22]. To extend Smith Predictor to work with unstable systems as for example systems with an integrator, [23], [24], [25] have proposed modified Smith Predictor methods. A common prerequisite for successful employment of Smith Predictor is the accurate knowledge of the model and delay. For most industrial cases this knowledge is not easily available.

Another approach is based on the idea of representing the delay with a Pade approximation, see e.g.[26]. A systematical approach of designing observer based on Pade approximation is introduced in [27], which is used in this work. An integration term is added to the observer to remove input offset. The procedure of observer implementation on a first order system with delay is as follows:

- Get 1^{st} order Pade approximation of the delay.
- Find the state space model for the whole system including delay using (A.2) and the Pade approximation (A.19).

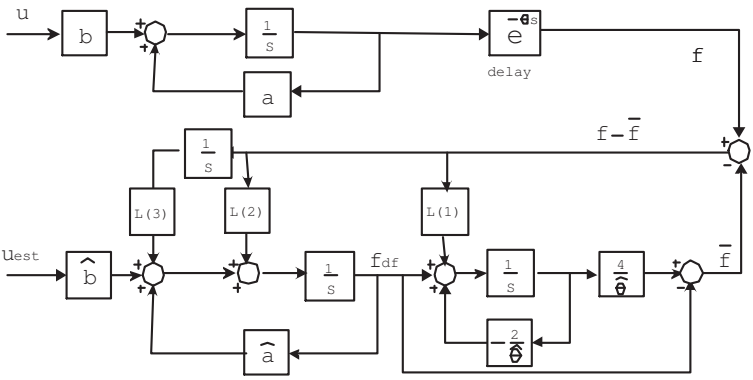

Figure A.14: Pade PI observer, where the delay is based on Pade approximation. θ is the delay time. u is the actual input energy to the system. u_{est} is the input to the observer which is estimation of u. f is the measured output. $\overline{f}$ is the estimated output. f_{df} is the delay-free output.

- Reformulate the system state space model following the instructions for designing a PI observer in [28].
- Place the poles of the observer left to the reformulated system poles and calculate the corresponding gains.

$$e^{-\theta S} \approx \frac{1 - \frac{\theta}{2}S}{1 + \frac{\theta}{2}S} \tag{A.19}$$

The structure of such an observer is shown in Fig. A.14. The advantage of this observer over Smith Predictor is that the inaccurate delay information in the observer is compensated, and the offset in the input to the observer is also taken care in this formulation.

Therefore the optimizing switch method is extended to work with systems with delay by including such an observer and using the predicted delay-free output for control signal calculation.

A.5.3 Experimental results

Two groups of experiments with the refrigeration plant described in Section A.5.1 are conducted to answer the following questions: (1) does the optimizing switch control method drive the system towards the optimal solution? (2) Does the optimizing switch

control method outperform the relay control method? For the experiments, the test plant water tank set-point temperature is 22 $^{\circ}C$. The ambient temperature is also controlled around 22 $^{\circ}C$ so that there is no significant heating disturbance from the ambient.

The observer applied in the experiments is based on model (A.17), and the parameters found following the procedure in Section A.5.2 are $\mathbf{L} = [1.23 \times 10^{1}, 6.75 \times 10^{-2}, 1.25 \times 10^{-4}]$.

A.5.3.1 Optimizing switch control method vs. optimal solutions

In this part, experiments have been conducted to investigate whether the developed optimizing switch control method including the observer drives the refrigeration plant towards the optimal solution defined by (A.5).

The first question is what is the optimal solution for the refrigeration plant. The optimal solution for the refrigeration plant is different from the calculated optimal solution based on the model (A.17), because the model (A.17) (integration and delay) is a rough approximation of a high order system. The only way to achieve the optimal solution for the test system is to run pulse experiments with different periods and duty cycles until it reaches the stable limit cycle, then calculate the cost using (A.5) to find the period and duty cycle combination corresponding to the smallest cost. Due to that the refrigeration plant is very close to an integrative system, the duty cycle and the load are very close to each other, which can be calculated directly by the heating to cooling ratio, while for a first order system, the optimal duty cycle will be different from the load when the load is different from 50%.

The above procedure of finding the real optimal solutions is illustrated by Fig. A.15. where the penalty is $Q = 20$, $R = 500$ and heating load is 1000 W. A polynomial fit of the test points has minimal cost at around 350 s. The benefit of the polynomial fit is that with discrete test points, a continuous expression of the cost as a function of the period can be achieved.

To investigate the ability of the optimizing switch control method to achieve the optimal solution at different penalty ratios, another two optimal solutions for the penalty $Q = 2$, $R = 500$ and $Q = 80$, $R = 500$ are also demonstrated with pulse experiments. The resulting three optimal solutions at three different Q (R is kept at 500 for all the experiments) are shown in Fig. A.16. For comparison, the optimizing switch control resulting costs at different Q/R ratio and heating disturbance 1000 W are also plotted Fig. A.16.

Fig. A.16 demonstrates that the solutions from the optimizing switch control (legend 'optimizing') are very close to the optimal solution (legend 'real'). The error defined by (A.20) at the three $Q = 2, 20, 80$ are $2.30\%, 4.85\%, 3.00\%$.

$$error = \frac{|cost_{optimizing} - cost_{real}|}{cost_{real}} \tag{A.20}$$

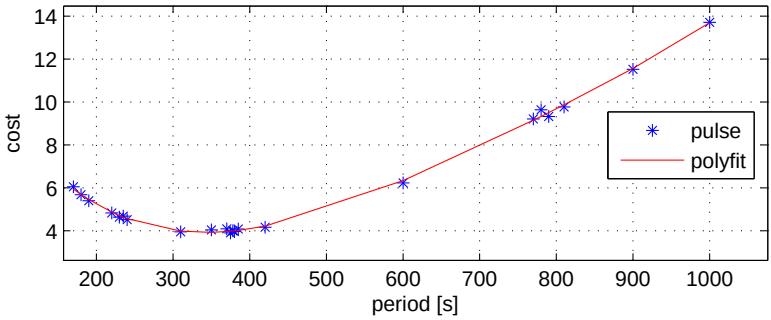

Figure A.15: Cost vs. periods. $Q = 20$. $R = 500$. Heating load 1000 W. 'pulse' refers to the cost results from the pulse input experiments. 'polyfit' is the polynomial fit of the discrete test points of the pulse experimental results.

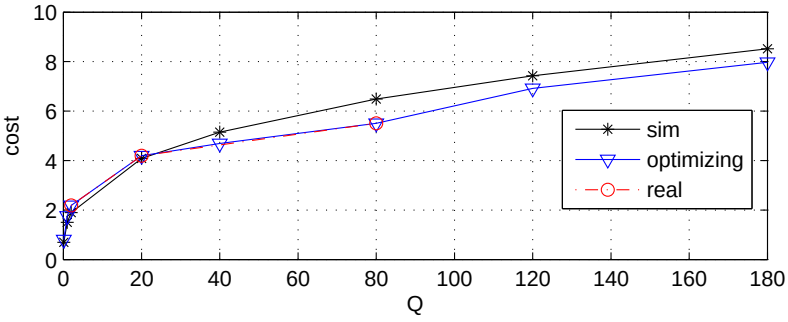

Figure A.16: Comparison of optimizing switch controller and real optimal solution at heating load 1000 W. R is kept at 500. 'sim' is the optimal solution for the model (A.17). 'optimizing' is the optimal solutions by applying the optimizing switch control on the refrigeration system. 'real' is the optimal solution from the pulse experiments with the refrigeration system.

A.5.3.2 Optimizing switch control method vs. relay control

In Subsection A.4.2, simulation results from the optimizing switch control and relay controller for a first order system have been compared, and they show that the optimizing switch control method outperforms the relay control when the systems are not at the nominal working condition for the relay.

Several experiments have been carried out to investigate the performance of the optimizing switch control method and the relay controller with and without observers at different heating loads.
(1) Optimizing switch control method. Run the optimizing switch control method including the Pade PI observer at different heating loads with parameter $Q = 2$, $R = 500$. The observer gains are $L = [1.23 \times 10^1, 6.75 \times 10^{-2}, 1.25 \times 10^{-4}]$.
(2) Standard relay controller. Tune the relay controller at about 50% corresponding to about 1500 W heating load, which reaches results very close to the optimizing switch control. The resulting relay band is 0.36 $^\circ C$, which means that the refrigeration system switches on when $T_{w,out}$ is higher than 22+0.36 $^\circ C$ and switches off when $T_{w,out}$ is lower than 22-0.36 $^\circ C$. Then run the experiments with this relay controller at different heating loads.
(3) Relay controller with observer. An improvement for the relay controller could be to include the Pade PI observer. Apply the Pade PI observer and feed the non-delayed information to the relay controller. Repeat the procedure of tuning the standard relay controller. The resulting relay band is 1 $^\circ C$. which means that the refrigeration system switches on when $T_{w,out}$ is higher than $22 + 1^\circ C$ and switches off when $T_{w,out}$ is lower than 22-1 $^\circ C$. Then run the experiments with this controller at different heating loads.

The results from the above three experiments are shown in Fig. A.17, where it can be seen that close to the nominal condition 50% load, the relay controller with and without an observer produces fine results, but when the heating load moves away from 50%, for example at heating load 500 W, the standard controller cost deviation from the optimizing switch controller is very large, while the relay controller including the observer improves the result, but still the cost is much larger than the optimizing switch control result.

The temperature outputs from these three controllers at heating load 500 W are plotted in Fig. A.18. It can be easily seen that when the system reaches a stable limit cycle, the standard relay control output has an offset, which results in an increased cost. The reason for this offset is that during the delay time, the heating power $\dot{Q}_{load}$ to raise the temperature (when refrigeration system is switched OFF) and the heating power minus the cooling power $\dot{Q}_e - \dot{Q}_{load}$ (when refrigeration system is switched ON) to remove heat is different. The offset in the standard relay is removed by applying the delay observer to the relay controller and it performs better than the standard relay controller. The difference in the controlled temperature between the relay controller plus the observer and the optimizing switch controller including the observer is not that obvious. However the difference in performance cost defined by (A.4) between the two controllers can easily be seen with the switching cost in Fig. A.17, where the switching cost for

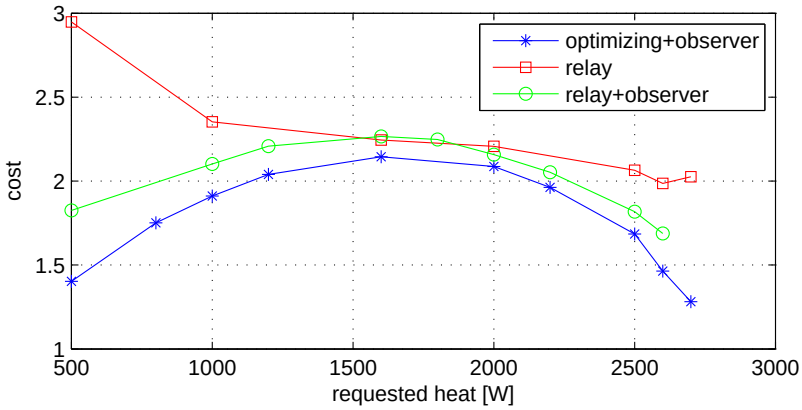

Figure A.17: Comparison: optimizing switch controller with Pade PI observer, standard relay controller and relay controller with observer. The relay controller is tuned under 50% load

the optimizing switch method including the observer is smaller than the relay controller with the observer. From these results it can be concluded that the optimizing switch controller outperforms the traditional relay and relay with Pade PI observer.

Despite that the optimizing switch controller performs well during stable limit cycles, the result from the optimizing switch controller converges much slower to the stable limit cycle, and consequently a much larger temperature variation at the beginning is resulted. This is caused by the initial states of the observer, mainly due to the Pade approximation state. The problem can be solved by a better assignment of the initial states in the observer.

From all the experimental results in this section it can be concluded that the optimizing switch controller drive the plant towards to the optimal solution and outperforms the traditional relay and relay with Pade PI observer.

A.6 Discussion and conclusions

A.6.1 Discussion

The optimizing switch control method is designed to solve a class of problems related to balancing output deviations and switching frequency. The method is of a low complexity and therefor can be easily implemented to mass produced low level controllers. It is worth noticing that the method itself does not even require a system and disturbance model. In case of presence of delay, a model is needed for observer design. It only needs the measurement of the controlled variable. Tuning of the control, for instance weight factors, demands certain knowledge about the system. These can be the economical

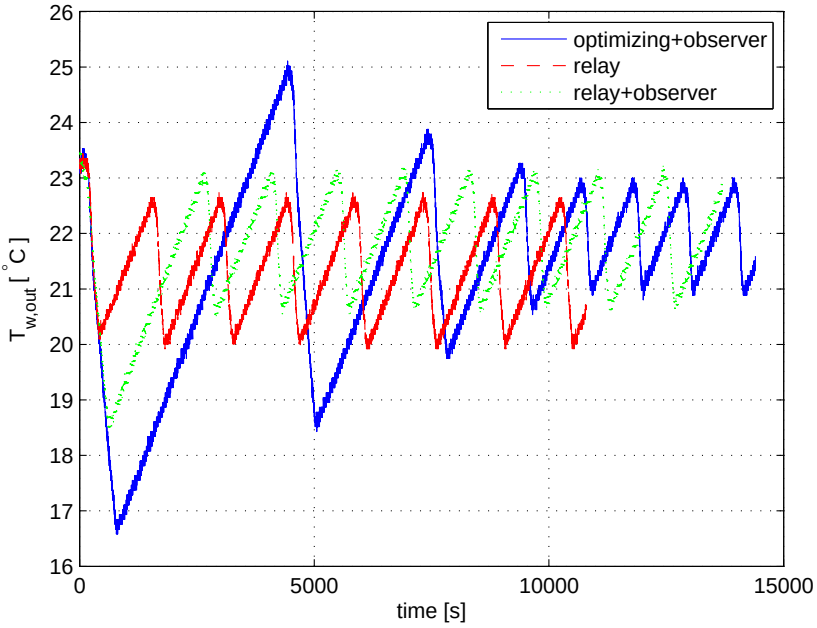

Figure A.18: Comparison: the temperature output from the optimizing switch controller with Pade PI observer, standard relay controller and relay controller with observer at heating load 500 W.

cost of each switch for wear of components, output variation band, time constants of the system etc. The method controls the system towards optimal limit cycle.

Comparing with a standard relay method, the optimizing switch control method requires little more computational power, for example an extra state for integration term etc. In case delay presents, an observer can be included to estimate the delay free information. The proposed method improves the system performance over the relay controller under non-nominal conditions. This means that systems with serious problems related to high switching frequency, e.g. wear, low performance, can improve with the optimizing switch control method is applied instead of the relay method. When delays appear, both the relay and the optimizing switch control method takes the delay-free information, which can be achieved by introducing an observer.

In the form presented, the method is limited to only first order (including delay) and stable high order SISO system with real poles and monotonic step response. For both cases the system is confined to systems with binary inputs. The current version of the algorithm can not solve multi input problems, and high order SISO linear system with complex poles is also a challenge.

A.6.2 Conclusions

An optimizing switch control method for optimal control of systems with binary inputs that have costs related to switching has been developed, and the method has been extended to incorporate first order systems with delays and SISO high order systems with real poles. The method has a low complexity and at the same time avoids the fundamental problem of finite horizon prediction methods as mentioned in Section A.1. The test with a refrigeration plant verifies that the method is applicable to real systems. Experimental results also show that the optimizing switch control method outperforms relay controller at non-nominal condition.

Bibliography

[1] USA Energy Information Administration. Energy information administration. 1998.

[2] A. Bemporad and M. Morari. Control of systems integrating logic, dynamics, and constraints. *Automatica*, 35(3):407–427, March 1999.

[3] Jan Maciejowski. *Predictive Control with Constraints*. Prentice Hall, 2000.

[4] Eduardo Fernandez Camacho and Carlos Bordons Alba. Model predictive control. *Springer*, 2004.

[5] Brian Solberg, Palle Andersen, Jan M. Maciejowski, and Jakob Stoustrup. Optimal switching controlo of burner setting for a compact marine boiler design. *Control Engineering Practice*, 18(6):665–675, 2010. doi:10.1016/j.conengprac.2010.03.009.

[6] Daniel Sarabia, Flavio Capraro, Lars F.S. Larsen, and César de Prada. Hybrid nmpc of supermarket display cases. *Control Engineering Practice*, 17(4):428–441, 2009.

[7] Xuping Xu and Panos J. Antsaklis. Optimal control of switched systems based on parameterization of the switching instants. *Transactions on Automatic Control,*, 799:2–16, 2004.

[8] D Sarabia, C de Prada, S Cristea, and R Mazaeda. Hybrid model predictive control of a sugar end section. *Computer Aided Chemical Engineering*, 21:1269–1274, 2006.

[9] C de Prada, S Cristea D Sarabia, and W. Colmenares. Hybrid control of a mixed continuous-batch process. *Proceedings European Symposium on Computer-Aided Process Engineering*, pages 473–484, 2004.

[10] Sebastian Sager. Reformulations and algorithms for the optimization of switching decisions in nonlinear optimal control. *Journal of Process Control*, 19(8):1238–1247, 2009.

[11] Wei-Ling Jian and M. Zaheeruddin. Sub-optimal on-off switching control strategies for chilled water cooling systems with storage. *Applied Thermal Engineering*, 18(6):369 – 386, 1998.

[12] Alexandre Restrepo, Andres González, and Sergio Orduz. Cost effective control strategy for small applications and pilot plants: on-off valves with temporized pid controller. *Chemical Engineering Journal*, 89(1-3):101 – 107, 2002.

[13] Jin-Long Lin, T.-J. Yeh, and Wei-Yang Hwang. A dynamic switching strategy for air-conditioning systems operated in light-thermal-load conditions. *Applied Thermal Engineering*, 29(14-15):2832 – 2842, 2009.

[14] Chen Ying, Zhang Jia-fan, Yang Can-jun, and Niu Bin. Design and hybrid control of the pneumatic force-feedback systems for arm-exoskeleton by using on/off valve. *Mechatronics*, 17(6):325–335, 2007.

[15] Timothy I. Salsbury. A new pulse modulation adaptive controller (pmac) applied to hvac systems. *Control Engineering Practice*, 10(12):1357–1370, december 2002.

[16] Alberto Leva, Luigi Piroddi, Massimiliano Di Felice, Alessandro Boer, and Raffaele Paganini. Adaptive relay-based control of household freezers with on/off actuators. *Control Engineering Practice*, page doi:10.1016/j.conengprac.2009.09.008, 2009.

[17] Honglian Deng, L. F. S. Larsen, Jakob Stoustrup, and Henrik Rasmussen. Control of systems with costs related to switching: applications to air-condition systems. *Proceedings of Multi-conference on Systems and Control*, 2009.

[18] Honglian Deng, L. F. S. Larsen, Jakob Stoustrup, and Henrik Rasmussen. A new method for control of systems with costs related to switching: applications to air-conditioning systems. *Proceedings of European Control Conference*, 2009.

[19] D. Flieller, P. Riedinger, and J.P. Louis. Computation and stability of limit cycles in hybrid systems. *Nonlinear Analysis, Theory, Methods and Applications*, 64:352–367, 2006.

[20] Lars F. S. Larsen. *Model Based Control of Refrigeration Systems*. PhD thesis, Aalborg University, 2005.

[21] Julio E. Normey-Rico and Eduardo. F. Camacho. Dead-time compensators: A survey. *Control Engineering Practice*, 16(4):407–428, 2008.

[22] O.J.M Smith. Closer control of loops with dead time. *Chemical Engineer Progress*, 53:217–219, 1957.

[23] K.J. Aström, C.C. Hang, and B.C. Lim. A new smith predictor for controlling a process with an integrator and long dead-time. *Transactions on Automatic Control,*, 39:343–345, 1994.

[24] T. Liu, Y.Z. Cai, D.Y. Gu, and W.D. Zhang. New modified smith predictor scheme for integrating and unstable processes with time delay. *Control Theory and Applications*, 152:238–246, 2005.

[25] M.R. Stojic, F.S. Matijevic, and L.S. Draganovic. A robust smith predictor modified by internal models forintegrating process with dead time. *IEEE Transactions on Automatic Control*, 46:1293–1298, 2001.

[26] Gang Liu, Alan Zinober, and Yuri B. Shtessel. Second-order sm approach to siso time-delay system output tracking. *IEEE Transactions on Industrial Electronics*, 56:3638–3645, 2009.

[27] B. del Muro-Cuellar, O. Jimenez-Ramirez, M. Velasco-Villa, G. Fernandez-Anaya, and J. Alvarez-Ramirez. Observer-based prediction scheme for time-lag processes. *American Control Conference*, pages 639–644, 2007.

[28] Hans Henrik Niemann, Jakob Stoustrup, Bahram Shafai, and S. Beale. Ltr design of proportional-integral observers. *International Journal of Robust and Nonlinear Control*, 5:671–693, 1994.

Appendix B

Control of systems with costs related to switching: applications to air-condition systems

(Proceedings of the IEEE Multi-conference on Systems and Control, 2009, St. Petersburg, Russia.)

Honglian Deng, Lars Larsen, Jakob Stroustrup, Henrik Rasmussen

Abstract

The objective of this paper is to investigate a low complexity method for controlling systems with binary inputs that have costs related to switching. The control objective for this type of systems is often a trade off between the deviation from the reference and the number of switches (weariness energy efficiency etc.). For such systems a steady state solution might never be attained, but rather the optimal behavior might be constituted by a limit cycle. In this paper we consider the problem of finding and controlling the system towards an optimal limit cycle. A low complexity approach giving a suboptimal solution, and avoiding the above problems will be proposed.

B.1 Introduction

In this paper we aim at developing a low complexity method for optimal control of system with binary inputs that have costs related to switching. The method is exemplified by a motivating example based on developing energy optimal control for Air-condition (AC) system.

The basic objective of an AC system is to remove heat from a room to keep the room temperature close to the reference. The AC system is composed of a compressor, an evaporator, a condenser, and an expansion valve, where the compressor determines the cooling capacity. In a typical AC system, the room temperature will vary around the reference level, due to the fact that the compressor only can be switched on/off. Hence determining the optimal switch frequency and duty cycle is a trade-off between comfort, energy consumption (which is measured by COP, coefficient of performance) and compressor weariness due to switching. It should be noted that the compressor weariness here refers to the compressor component weariness caused by a poor lubrication at a low speed. The reason the weariness is important in the AC system in our case study is that the compressor components wear in every startup due to the poor lubrication condition.

From the comfort point of view, a small temperature variation is preferred, hence the switch frequency should be very fast. With such a fast switching frequency, the compressor has problem with lubrication, but a high efficiency (COP) is achieved[1]. The reason for the high COP is that the evaporator will not get empty during the short off period, therefore the effect of low COP from filling the refrigerant into the evaporator is avoided. However the conclusion in [1] is based only on the criterion of energy consumption. Therefore in this paper, we will focus on the switch frequency range which is much slower than above.

With a slower switching frequency, the weariness of compressor due to the poor lubrication condition in the startup phase is obvious and it gets worse with the increase of switch frequency. The temperature variation with the slower switching frequency is much bigger. COP varies with the switch frequency too. Therefore the 3 parameters of temperature variation, compressor weariness, and energy efficiency should all be used for evaluating the system performance. For simplicity, in this paper, we will use comfort and compressor weariness for the performance measure.

Several methods exists that can handle systems with binary inputs that have costs related to switching. They can be divided into two categories: low complexity and advanced methods. In the low complexity category, pulse width modulation (PWM) and hysteresis controllers are the two popular controller types. In the advanced methods category, methods related to model predictive control (MPC) is one example.

PWM has to have very fast switching frequency, which has been proven not suitable in the AC system control case.

Hysteresis controller are widely used today. The problem with hysteresis controller is that the system always work on the same constraint (usually temperature). The hysteresis controller are usually tuned under a certain working condition, which performs

not so good when working condition changes, therefore the optimality is destroyed.

One of the standard methods for hybrid switched systems is MPC using the mixed logical dynamical framework (MLD)[2]. An experiment with simulation model has been done to investigate how the prediction horizon affects the resulted switch period (Fig.B.1). The cost function of the MPC composes of quadratic error (deviation from reference) and switches numbers and both terms are penalized. The results are presented in Fig.B.1). It has shown the problem of finite horizon prediction - the controller postpones the switches because of the penalty on switching, until at last a short switch period has to be used in order not to violate the constraint. One way to improve it is to use longer prediction horizon. It seems that with increasing prediction horizon, the resulting switch period converges to 16 minutes. It can be concluded from the results that an extremely long prediction horizon is needed in order to get a good result. However MPC with very long prediction horizon requires a high computational power, which is not feasible in an AC application.

A different way of using MPC is proposed in [3], where the first step is to find the optimal limit cycle and then use MPC to bring the system to an optimal limit cycle. The author has shown that this method can avoid the problem of finite horizon method for optimal limit cycles and this method provides good results for the particular application. However the method has to be modified for the AC system and the computational power is not affordable for the AC application.

Other MPC methods based on solving finite horizon optimization problems also exists such as [4] and [5]. Common for these methods based on finite horizon prediction is that they typically produce rather complex controllers requiring large computational power which is not feasible for mass production application and special care is not taken using finite horizon methods on systems with discrete inputs, it can lead to rather poor performance.

Our objective in this paper is to develop a method which has low complexity as PWM and hysteresis, but at the same time achieves close to the optimal solution for controlling systems with binary inputs.

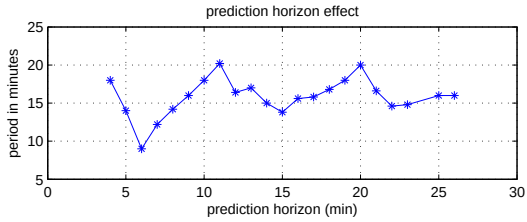

Figure B.1: Prediction horizon and periods. With increase of the prediction horizon, the compressor switch period moves towards 16 minutes.

The paper is organized in the following way. Modeling of the system is briefly presented in Section B.2. An analysis of performance function nature for discrete input

system are carried out in section B.3. A new method is presented in Section B.4. The conclusion is given in Section B.5.

B.2 System description and modelling

The AC system is a unit which composes of compressor, evaporator, condenser, and evaporation valve. The refrigeration cycle works in this way: The compressor compresses the refrigerant gas into high pressure at a high temperature, and then gas is sent to condenser, where high pressure low temperature liquid comes out. Then expansion valve releases the liquid into low pressure liquid (or gas liquid mix), and the liquid flows into evaporator and evaporates there. During the evaporation, the refrigerant absorbs heat from outside of the evaporator, which produces coldness for the room. The switch on/off is referred to the compressor switches. The detailed explanation can be found in [6]

Whenever the compressor is switched on (assume that it is switched off long enough that the evaporator is empty), the evaporator has to be filled in first. This leads to low COP during the start up. Another reason for low COP during startup is also that the compressor is lubricated well enough, which then results in low energy efficiency.

For simplification, the air condition system is considered as a unit, which removes energy from the room. In order to illustrate the method, for simplicity, the air-conditioned room is modelled as a first order system, which is shown in Fig.B.2. In this paper the AC system is not modeled in detail, but presented as an energy input to the room model.

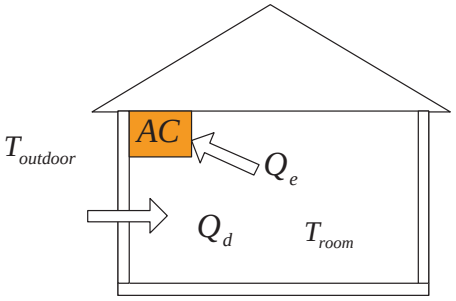

Figure B.2: First order room model

$$\frac{dT_{room}}{dt} = \frac{\dot{Q}_d - \dot{Q}_e}{C_p m} \tag{B.1}$$

$$\dot{Q}_d = \frac{(T_{outdoor} - T_{room})}{R} \tag{B.2}$$

Insert (B.2) into (B.1), the model can be formulated as (B.3),

$$\frac{dT_{room}}{dt} = \frac{-1}{C_p m R} T_{room} + \frac{-1}{C_p m} \dot{Q}_e + \frac{1}{C_p m R} T_{outdoor} \tag{B.3}$$

where T_{room} is the temperature of room air.
$\dot{Q}_d$ is the heat flow from ambient to the room.
$\dot{Q}_e$ is the energy removed by the AC system when it is switched on.
R is the thermal resistance from ambient to the room.
$m$is the mass of room air.
C_p, is the specific heat capacities of room air.

Equation (B.3) can be expressed by state space equation (B.5), where T_{room} is the state, $\dot{Q}_e$ is the input u, and the last term in (B.3) is disturbance E. In this paper, the following parameters are used for simulation.

$A = -2.00123 \times 10^{-4}$;
$B = -4.4028 \times 10^{-6}$;
$E = 5.73 \times 10^{-3}$;
$u = 0$ or $300w$

B.3 Cost function analysis

For the type of system described above, the existing methods have proved to be very unreasonably computationally demanding and some have fundamental problems with finite horizon prediction, therefor a new method has to be developed. We know that the optimal solution for the AC system with discrete input will be a stable limit cycle, where the compressor switches on and off with a certain frequency and duty cycle. The optimal solution will achieve the smallest deviation from the reference with the least number of the switches. Inspired by MPC, a cost function can be formulated in the similar way where both the comfort and cost of getting the comfort (switches in this problem) appear. Since the system is running periodically, the system performance can be measured by only one period, which leads to (B.4). The widely accepted definition for comfort is Predicted Mean Vote (PMV) and Predicted Percentage Dissatisfied (PPD), (details see [7]), where temperature, humidity, draught, occupant activity level, cloth level etc. are all taken into account. For our case study, the PMV and PPD are both too complicated as a start point. Therefore a quadratic error is used. It might not represent the best comfort, but it gives an indication of the AC system performance. On the numerator of (B.4), the squared error of the output is accumulated through the whole period, and two switches in one period are used. On the denominator, period T_s is used to express that the cost J here is the cost per time unit. This makes it possible to calculate the performance for a system by observing only one period. The corresponding figure is presented in Fig.B.3.

Before we start developing new method which can be measured by this cost function,

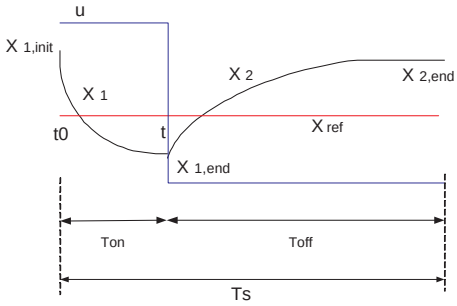

Figure B.3: one period

a thorough study on the cost function (B.4) is necessary.

$$J(T_{\mathrm{s}}) = \frac{Q \cdot \int_{t0}^{t0+T_s} (y - y_{ref})^2 dt + R \cdot J_{sw}}{T_s} \tag{B.4}$$

T_{s} is the total period. Q is the penalty on temperature deviation from the reference and R is the penalty on 2 switches in one period.

Since a period includes on and off parts, the cost J actually is a function of T_{on} and T_{off}. This function is not convex and it is not easy to determine when its gradient is zero. Our interest here is to find out if the cost J has only one optimum in T_{on} and T_{off} and if so, whether we can find the optimum explicitly. This type of generic cost function is relevant for a huge number of systems with discrete inputs.

Since in the discrete system, T_{on} and T_{off} have the equal meaning for the system as period T_s and duty cycle α. A question here might come up: 'is the optimal duty cycle the same as the load?'. (in this context: the load is defined as a percentage and it means that a system running with this percentage of the high limit power (300W in this example) will be controlled at the reference. In this example, 50% load means that running with 150W (50%x300) will make the system stay at the reference.)

The solution to the state space model (B.5) is (B.6) and (B.7), where (B.6) is for the on period and (B.7) is for the off period. $x_{1,\text{init}}$ refers to the state when the system switches from off to on, and $x_{1,\text{end}}$ refers to the state when the system switches from on to off. When the input u is 0, which means that AC is switched off, the system becomes (B.7), where $x_{1,\text{end}}$ is the state when the system switches from on to off.

$$\dot{x} = Ax + Bu + E \tag{B.5}$$

$$x_1 = \frac{Bu + E}{-A} + (x_{1,\text{init}} + \frac{Bu + E}{A}) \cdot e^{At} \tag{B.6}$$

$$x_2 = \frac{E}{-A} + (x_{1,\text{end}} + \frac{E}{A}) \cdot e^{A(t - T_{on})} \tag{B.7}$$

The cost J depending on T_{on} and T_{off} should be evaluated under the steady state conditions, otherwise it does not make sense to compare. Under steady state conditions, the system is periodical, which means that the states at the start of a cycle is same as the end of the cycle, which is described in equation (B.8). $x_{2,\text{end}}$ denotes the state when the system switches from off to on. From equation (B.6), (B.7) and (B.8), $x_{1,\text{init}}$ and $x_{1,\text{end}}$ can be achieved and they are equation (B.9) and(B.10). Therefor equation (B.6), (B.7) are function of only T_{on} and T_{off}

$$x_{1,\text{init}} = x_{2,\text{end}} \tag{B.8}$$

$$x_{1,\text{init}} = \frac{\frac{E}{-A} + \frac{Bu}{-A}e^{A\cdot T_{off}} + \frac{Bu+E}{A}e^{A(T_{on}+T_{off})}}{1 - e^{A(T_{on}+T_{off})}} \tag{B.9}$$

$$x_{1,\text{end}} = \frac{\frac{Bu+E}{-A} + \frac{E}{A}\cdot e^{A(T_{on}+T_{off})} + \frac{Bu}{A}\cdot e^{A\cdot T_{on}}}{1 - e^{A(T_{on}+T_{off})}} \tag{B.10}$$

The output of the system is

$$\begin{aligned} y_1 &= c\cdot x_1 \\ y_2 &= c\cdot x_2 \end{aligned}$$

The cost function now becomes

$$\begin{aligned} J(T_{on}, T_{off}) = &\frac{Q\cdot\int_0^{T_{on}}(x_1 - x_{ref})^2 dt}{T_{on}+T_{off}} \\ +&\frac{Q\cdot\int_{T_{on}}^{T_{on}+T_{off}}(x_2 - x_{ref})^2 dt + R\cdot J_{sw}}{T_{on}+T_{off}} \end{aligned} \tag{B.11}$$

Inserting B.9 and B.10 into B.11, the corresponding plot (cost J) can be seen in Fig. B.4, where T_1 is the on period, and T_2 is the off period. From the figure it can be seen that there is only one optimum. Using Newton's method with (B.11), the optimal period can be found easily. However, the initial guess for the Newton search is actually critical for this problem, which is due to the irregularity of cost surface J.

An adjustment of (B.11) has been done to check if it could help to get surface for which is easier to find the optimal solution. What we did is to parameterize the cost J with period T_{s} and duty cycle α. This can be simply done by replacing T_{on} by $T_{\text{s}}\cdot\alpha$, and T_{off} by $T_{\text{s}}\cdot(1-\alpha)$. The result is plotted in Fig.B.5. The surface J is much more regular, which means that the initial guess for the Newton search is not that strict anymore. Form several tests, it seems like that the initial guess is much less strict than parameterizing the system over T_{on} and T_{off}.

Applying the above idea on the system with 90% load, we found that the optimal period is 6447s, and the duty cycle is 91%. The optimal solution (duty cycle 91%) is different from the load (90%), which answers the question in beginning of this section.

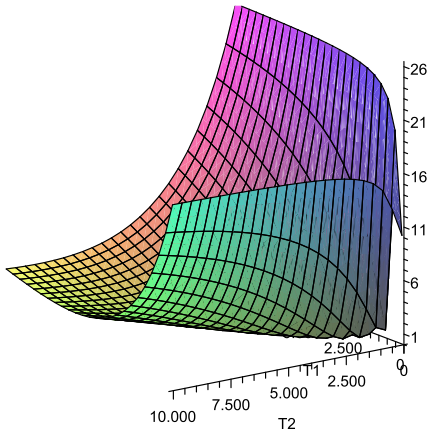

Figure B.4: Cost J in T_1 (T_{on}) and T_2 (T_{off})

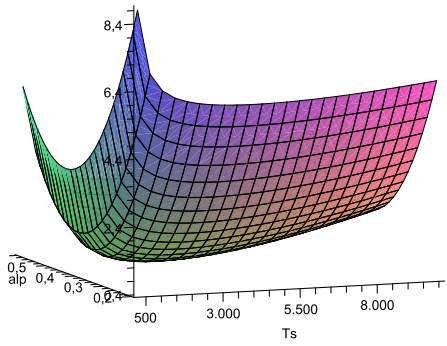

Figure B.5: Cost J in period T_s and duty cycle α

weight factor Q/R	load			
	90%		10%	
	period (S)	duty cycle	period (S)	duty cycle
2/500	6447	90.91%	6447	9.09%
2/2500	13947	93.12%	13947	6.88%

Table B.1: Experimental result - the difference between load and duty cycle.

A further investigation was carried out to learn if this is a special case or holds in general, what factors affect the difference between the load and optimal duty cycle and what are the reasons that that cause the difference between the load and optimal duty cycle.

To answer these questions, two experiments were designed. One is to run with different load to check if the load has influence on the difference between the load and optimal duty cycle. The other is to change penalty ratio Q and R. As an example the results from 90% and 10% load with different penalty ratio is presented in Tab. B.1.

The results show that for duty cycle α (or $1 - \alpha$) close to 1, there is a difference between optimal duty cycle and load. When the load is close to 1, the optimal duty cycle is always bigger than the load, but when the load is close to 0, the optimal duty cycle is always smaller than the load. The reason is that, the error accumulation of the longer half period (either on or off period) has smaller gradient in the longer period than the short half period error accumulation in the short half period, which is shown in Fig.B.3. Therefor the optimal will always prolong the longer half period which results in a duty cycle different than load. The value of the difference depends on the ratio of Q and R. With the increase of switch penalty R, the difference will become bigger. For 50% load, both on and off period has the same gradient over the corresponding period, therefor, the optimal duty cycle is the same as the load.

The computational load of finding the optimum grows fast with increase of the system size.

B.4 A simple method

In previous section, we have demonstrated that there is a unique optimum for the cost function J at least for this example. A method of finding the optimum has been presented, and following that the system will be controlled to the optimal period and duty cycle. This is a way of doing it, but it is very computationally demanding, especially for higher order system. What we are really looking for here is a simple method which requires little computation power and at the same time overcomes the fundamental problem of the finite prediction horizon. An idea for such a simple method is presented below.

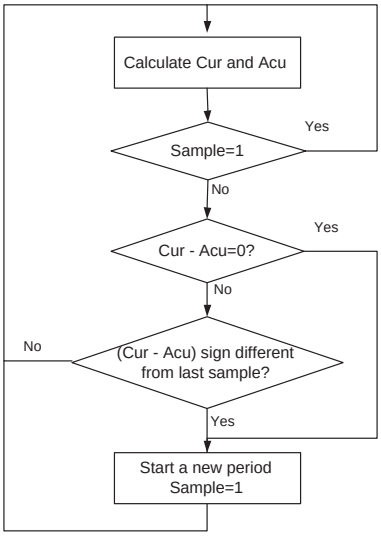

Figure B.6: Flow chart of the proposed method. Cur is the current cost and Acu is the accumulated error and switch cost.

We have known that cost function J has only one optimum, and it should make the derivative of (B.4) over T_s give 0 which is (B.12), but it is not easy to find the analytical solution. (B.12) can be rewritten as (B.13) and it has 3 terms, the cost of current output, the integration of error in a period, and the switch. If we rearrange the three terms as in (B.13), it can be understood in this way: the left side involves only the current output, while the right side involves the accumulated comfort error and a fixed switch cost. The two sides can only become equal when the period is optimal, since the cost function J has no local optimum. Hence, it can be used to find the optimum. For simplicity, we rename both sides of (B.13) as in (B.14) and (B.15). The controller always compare Acu (which is the error accumulation from the beginning of a period) and Cur with the value from last sample at each time sample to check if the switch should happen at the current time sample. We have the knowledge that if $T_s < T_{optimal}$, $\frac{\partial J}{\partial T_s} < 0$ and that if $T_s > T_{optimal}$, $\frac{\partial J}{\partial T_s} > 0$. Therefore we can use the switch criterion of Acu-Cur=0 (in reality if the sign of Acu-Cur is different from last sample, then a switch should happen, although care should be taken that measurement noise do not cause undesirable switches) for switch. The system should switch when this condition fulfills. Otherwise, the system should just wait for next sample. The flow chart of the algorithm is shown in Fig.B.6, from which it can be seen that the algorithm is very simple and requires very little computation power.

$$\frac{\partial J}{\partial T_s} = 0 \tag{B.12}$$

$$Q \cdot (y_{t0+T_s} - y_{ref})^2 T_s = Q \cdot \int_{t0}^{t0+Ts} (y - y_{ref})^2 dt + R \cdot J_{sw} \tag{B.13}$$

$$Cur = Q \cdot (y_{t0+T_s} - y_{ref})^2 T_s \tag{B.14}$$

$$Acu = Q \cdot \int_{t0}^{t0+Ts} (y - y_{ref})^2 dt + R \cdot J_{sw} \tag{B.15}$$

The basic idea of the method has been explained, but some adjustments have to be made in order to apply it in applications. The reason is that with this method, a decision of switch can only be made for the current sample, but in one period, there are two switches. The following two adjustments have been made without introducing prediction for the next half period, and they are named Method 1 and Method 2 and explained in details below.

B.4.1 Method 1

For this method, the idea is to use the past period decided just before the current period. This past period and the current period together composes a whole period with both on and off. By doing this, prediction for the next half period is avoided. So the system will only use the information from the past. Equation (B.13) is modified to (B.16) according to the adjustments.

The switch criteria will be

$$Q \cdot (y_{t0+T_s+T_{last}} - y_{ref})^2 (T_s + T_{last}) =$$

$$Q \cdot \int_{t0}^{t0+T_s+T_{last}} (y - y_{ref})^2 dt + R \cdot J_{sw} \tag{B.16}$$

It should be noted that when we calculate for the first switch, the error accumulated from earlier period is 0, therefor the switch cost should be only half of the later calculation.

Two experiments using this method have been carried out with the on/off AC-system example. One experiment is to apply this controller for the same system with different load and the result is shown in Fig.B.2, in the 'on/off together' block. Compared with the optimal solution from cost analysis result, the results from this method are close to the optimal (in period, duty cycle and cost).

The other experiment is to use the same load, but apply different initial conditions. The results indicate that different initial conditions lead to different results. For example,

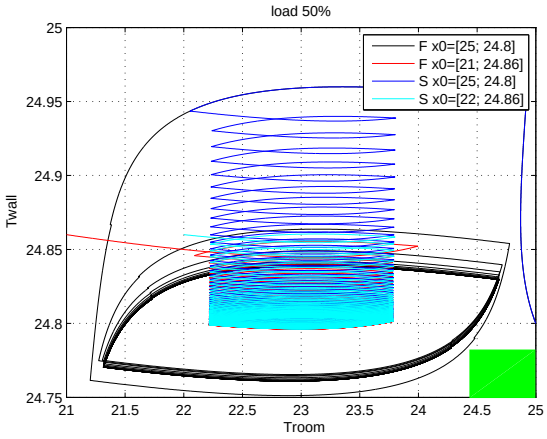

Figure B.7: Phase trajectory 2^{end} order system. F means Method 1, and S means Method 2. x_0 is initial temperature

with the same load, initial conditions 22.8°C and 24°C lead to different results. Some more experiments have been carried with different initial conditions. The conclusions is that, for the first order system, if the initial guess is bigger than the reference, then the result will not reach the optimal, but when the initial is smaller than the reference, the system reaches optimal.

Since it is difficult to visualize the result from first order system, a second order system example is chosen here. The experiment is to run the system with 50% load from different initial conditions and the resulting state trajectories are plotted in Figure B.7. The initial conditions located in the lower part of the right half plane out outside of the larger limit circle converges to the big limit circle, but others converge to the small one. The experimental results lead to the same conclusion that Method 1 is sensitive to the initial conditions. The reason is that the controller carries the influence of the initial condition because it always takes the last half period into account.

B.4.2 Method 2

Method 2 aims at changing (B.16) to look at the two half periods (T_{on},T_{off}) separately.

The same experiments with the conditions as in subsection B.4.1 have been conducted using the method 2.

The experimental results with different loads for the same first order system are shown in Fig.B.2, on/off separately block. Compared with the solution from Method 1, the solutions from Method 2 are further away from the optimal (in period, duty cycle and cost).

load (%)	optimal from cost analysis			on/off period separately (initial: 22.8)			on/off period together together (initial: 22.8)		
	period (S)	cost	duty cycle (%)	period	cost	duty cycle (%)	period	cost	duty cycle (%)
90	6447	0.242	90.91	7796	0.290	89.20	6460	0.242	90.90
45	3059	0.492	44.92	3072	0.493	45.18	3062	0.492	44.94
85	4919	0.311	85.69	5630	0.347	84.05	4930	0.311	85.68
15	4919	0.311	14.31	5630	0.347	15.95	4930	0.311	14.32
50	3037	0.495	50.00	3044	0.495	50.00	3044	0.495	50.00

Table B.2: Comparison of the results from the 2 methods and the optimal solution from the cost analysis.

The experimental results with different initial conditions are also conducted, and the results show that Method 2 is insensitive to the initial condition. For visualization, the results for 50% load from second order system with two different initial conditions are plotted in Fig.B.7. It is obvious that taking the on and off periods separately, the system converges to the same limit cycle here.

More initial conditions in different part of the plane have been tested, and they all converge to the same limit cycle. Trajectories for the two initial conditions, that can be used for comparing with the results from method 1, are illustrated in Fig.B.7.

An idea is to combine Method 1 an Method 2, where Method 2 will be used first to take the states to the right track, and then Method 1 can be used to get the solution closer to the optimal. Due to space limitations, these will not be presented here.

B.4.3 Stability problem.

The focus of this paper is to demonstrate the feasibility of a computationally simple approach to optimization. Analyzing and proving stability is omitted due to space limitations.

B.5 Conclusion

A low complexity method of controlling discrete input systems has been developed. With this method, problem of the inherited finite prediction horizon and heavy computation demand has been avoided. It was shown that for a class of systems it is capable of achieving close to optimal solutions. The computational power required for the developed method is very low which is only several memories. This can be applied for the mass produced controllers. The methods proposed are empirical, and it is not claimed that they hold in all generality. The authors, however, are convinced that the methods can be applied to a wide class of systems, including many arising from practical problems.

Bibliography

[1] Arne Jakobsen. Energy optimisation of refrigeration systems. *PhD thesis*, 1995.

[2] Alberto Bemporad and Manfred Morari. Control of systems integrating logic, dynamics and constraints. *Automatica*, 35:407–427, 1999.

[3] Brian Solberg, Palle Andersen, Jan M. Maciejowski, and Jakob Stoustrup. Hybrid model predictive control applied to switching control of burner load for a compact marine boiler design. *Proceedings of the 17th IFAC World Congress*, 2008, June.

[4] D. Sarabia, F. Capraro, L. F. S. Larsen, , and C. De Prada. Hybrid control of a supermarket refrigeration system. *Proceedings of American Control Conference*, pages 4178–4185, 2007.

[5] C. Sonntag, A. Devanathan, and S. Engell. Hybrid nmpc of a supermarket refrigeration system using sequential optimization. *IFAC World Congress*, 2008.

[6] L. Larsen and C. Thybo. Potential energy savings in refrigeration systems using optimal setpoints. *Proceedings of IEEE Conference on Control Applications*, 2004.

[7] O. Fanger. Thermal comfort. *McGraw-Hill Book Co.,New York*, 1972.

Appendix C

A new method for control of systems with costs related to switching: applications to air-conditioning systems

(Proceedings of the European Control Conference, 2009, Budapest, Hungary.)

Honglian Deng, Lars Larsen, Jakob Stroustrup, Henrik Rasmussen

Abstract

The objective of this paper is to investigate a control method for systems with discrete inputs that have switch related cost. For such systems, the control objective often is a trade off between the deviation from the reference (performance) and the number of switches (weariness, energy efficiency etc.). For such systems a steady state might never be attained, but rather the optimal behavior might be constituted by a limit cycle. In this paper we consider the problem of finding and controlling the system towards an optimal limit cycle. A low complexity approach will be proposed.

C.1 Introduction

Within the recent years optimal control of hybrid systems has attained a lot of focus. Among the recent results can be mentioned [1], [2], [3], [4], [5], [6], [7]. One reason is that numerous industrial applications have the features of a hybrid system. In this paper

we will however only consider systems with discrete inputs, which can be categorized as a subclass of hybrid systems. Examples of such systems in the industry are numerous. Here we will focus on air conditioning system (AC-system) with a discrete compressor capacity, for motivating the analysis and demonstrate the proposed method.

A method for synthesizing optimal control for hybrid systems is hybrid model prediction control using the mixed logical dynamical framework (MLD)[4], but also other MPC methods based on solving finite horizon optimization problems exists such as [8] and [9]. Common for these methods is that they typically produce rather complex controllers requiring large computational power. Furthermore, if special care is not taken using finite horizon methods on systems with discrete inputs, it can lead to rather poor performance,[6],[10]. There exist also other methods based on steady state optimization of limit cycles, for instance [7] on page 253. Some of these methods give good results for particular applications, but are complex and difficult to apply especially in the lower levels of the control hierarchy where sufficient computational power is not available. This motivates the development of much less complex methods overcoming the potentially poor performance that finite horizon methods leads to. This is the focus of this paper.

The paper is organized in the following way. Modeling of the system is briefly presented in Section C.2. An analysis of performance function nature for discrete input system are carried out in Section C.3. A novel method is presented in Section C.4. Some tests of the method on a second order system system is explained. Comparison of the developed method and hysteresis control are made in Section C.5. The conclusion is given in Section C.7.

C.2 System modeling

A simplified first order room model with an air conditioning system (AC-system) is shown below. In this paper the AC-system is not modeled in detail, but presented as an energy input to a simple room model.

$$\frac{dT_{room}}{dt} = \frac{\dot{Q}_{a2r} - \dot{Q}_e}{Cp_{air} m_{air}},$$

$$\dot{Q}_{a2r} = \frac{(T_{amb} - T_{room})}{Res}$$

where T_{room}, is the temperature of room air.
$\dot{Q}_{a2r}$, is the heat flow from ambient to the room through wall.
$\dot{Q}_e$, is the cooling energy.
Res is the thermal resistances from ambient to the room air.

C.3 Cost function analysis

In AC-systems, the objective is usually to control the indoor temperature sufficient close to the reference. At a certain load, where the system can not run continuously, a discrete input has to be used, and the result will be a limit cycle instead of a steady state solution. Let us assume that the AC-system with lowest possible speed can remove 300W. Hence, in case 150W needs to be removed, the system can only run between on (300W) and off (0W) to achieve an average close to the reference temperature. In this paper a definition of load is used. It is a percentage and it means that a system running with this percentage of the high limit power (300W in this example) will be controlled at the reference. In this example, 50% load means that running with 150W (50%·300) will make the system stay at the reference.

For a small temperature variation, a fast switch is needed which is at the cost of AC-system components wearing out fast and a low efficiency due to frequent starts and stops often, and vice versa. Hence the optimal control of AC-system is in fact a trade-off between comfort (small temperature deviation from reference) and economic cost (number of switches) and can be formulated as Equation (C.1), which is the comfort and economic cost per time unit under a stable limit cycle. This formulation represents a control objective of a discrete input system for which switch costs have to be taken into consideration.

The comfort error accumulation is divided into on $(0-\alpha T)$ and off $(\alpha T - T)$ periods (C.1), where α is the duty cycle and T is the cycle period. x_{ref} is the room set-point temperature. Through the user specification, the comfort and economic objectives can be balanced by assigning the two weight factors (Q and R in (C.1)).

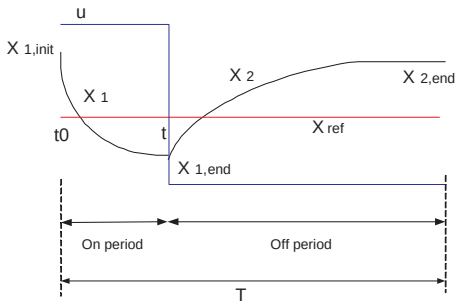

Figure C.1: one period

$$J = \frac{Q \cdot (\int_0^{\alpha T}(x_1 - x_{ref})^2 dt + \int_{\alpha T}^{T}(x_2 - x_{ref})^2 dt) + R \cdot J_{sw}}{T} \tag{C.1}$$

T is the total period. Q and R are the weight factors which balances the comfort and the

switch terms.

The AC-system state space model is as Equation (C.2) where E is a disturbance, and u is a power input. For the on period, the model becomes Equation (C.3), and for the off period where u is 0, the model becomes Equation (C.4). $x_{1,\text{init}}$ is the state when the system switches from off to on.

$$\dot{x} = Ax + Bu + E \tag{C.2}$$

$$x_1 = \frac{Bu+E}{-A} + (x_{1,\text{init}} + \frac{Bu+E}{A}) \cdot e^{At} \tag{C.3}$$

$$x_2 = \frac{E}{-A} + (x_{1,\text{end}} + \frac{E}{A}) \cdot e^{A(t-\alpha T)} \tag{C.4}$$

Under steady state conditions, the system is periodical, which means that the states at the start of a cycle is the same as the end of the cycle, which is described in Equation (C.5). $x_{2,\text{end}}$ denotes the state at the end of the off period, and can be got by applying $t = T$ to Equation (C.4). $x_{1,\text{end}}$ in Equation (C.4) can be got by applying $t = \alpha T$ to Equation (C.3). The result can be seen in Equation (C.6)and(C.7). So now x_1 and x_2 are functions of α, T, t. Therefore Equation (C.1) becomes a function of only α, T.

$$x_{1,\text{init}} = x_{2,\text{end}} \tag{C.5}$$

$$x_{1,\text{init}} = \frac{\frac{E}{-A} + \frac{Bu}{-A}e^{A\cdot(1-\alpha)T} + \frac{Bu+E}{A}e^{A\cdot T}}{1 - e^{A\cdot T}} \tag{C.6}$$

$$x_{1,\text{end}} = \frac{\frac{Bu+E}{-A} + \frac{E}{A} \cdot e^{A\cdot T} + \frac{Bu}{A} \cdot e^{A\cdot \alpha T}}{1 - e^{A\cdot T}} \tag{C.7}$$

For simplicity, the above idea is tested with a first order system example, which is a simplification of the AC-system model. The parameters are:

$$\begin{aligned} A &= -2.00 \times 10^{-4} \\ B &= -4.40 \times 10^{-6} \\ D &= 5.73 \times 10^{-3} \end{aligned}$$

The corresponding plot of (C.1) (function J) can be seen in Fig.C.2. From the figure it can be seen that there is only one optimum.

For a system with 90% load, the optimal period is 6447 seconds, and the duty cycle is 91%, which is different from the load (90%). The cost J for running with the optimal solution is 0.242. If the system runs with 90% duty cycle, which gives the smallest cost for 90% duty cycle is 6082 seconds, and the cost is 0.249. There it shows that

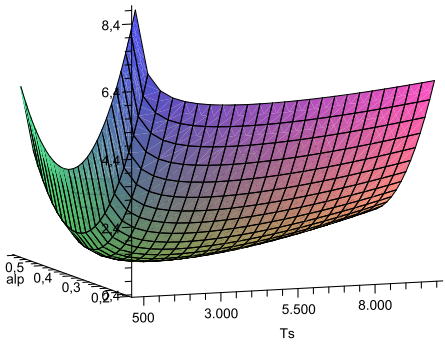

Figure C.2: Cost J in period T_s and duty cycle α, load 45$\%$

the optimal solution actually runs with longer period ((6447-6082)/6082=6$\%$) but at the same time gives smaller cost.

Two experiments were designed to study the above phenomena. One is to run with different load to check if the load has influence on the different between the load and optimal duty cycle. The other is to change penalty ratio Q and R. The results show that for duty cycles α or $1-\alpha$ close 1, there is a difference between optimal duty cycle and load. When the load is close to 1, the optimal duty cycle is always bigger than the load, but when the load is close to 0, the optimal duty cycle is always smaller than the load. The reason is that, the longer half period error accumulation (either on or off period) has smaller gradient in the longer period than the short half period error accumulation in the short half period. Therefor the optimal will always prolong the longer half period which results in a duty cycle bigger than load. The value of the difference depends on the ratio of Q and R. With the increase of R, the difference will become bigger. For 50$\%$ load, both on and off period has the same gradient over the corresponding period, therefor, the optimal duty cycle is the same as the load. (More details can be found in [10])

The computational load of finding the optimum grows fast with increase of the system size.

C.4 A novel method

In last section, we have mentioned that there is only one optimum for the cost function J assuming the first order limit cycle. The challenge is to find a method that automatically drives the system towards the optimal limit cycle. In the following we make the assumption that the optimal limit cycle can be found in the set of first order limit cycles. An analysis of finding the optimum of cost function (C.1) has been presented, and following

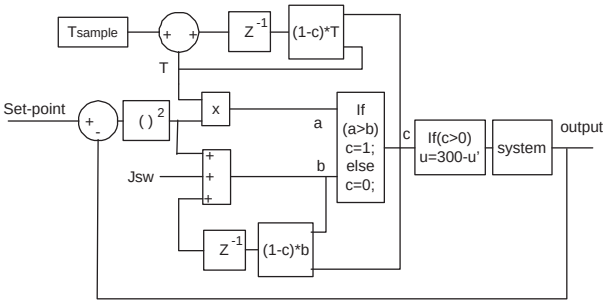

Figure C.3: Illustration of the control method. T_{sample} is the sampling time. T is the current adapting period

that the system will be controlled to the optimal period and duty cycle. Computing the optima explicitly is difficult for higher order systems due to the heavy computational load. What we are really looking for here is a simple method which requires little computational power and at the same time overcomes the fundamental problem of the finite prediction horizon. An idea for such a simple method is presented below.

We have known that cost function J has only one optimum, which should fulfill Equation (C.8). The analytical solution is difficult to find, but (C.8) can be rewritten as (C.9) and it has 3 terms, the cost of current output, the integration of error in a period, and the switch. If we rearrange the three terms as in (C.9), it can be understand in this way: the left side involves only the current output, while the right side involves the accumulated comfort error and a fixed switch cost. The two sides can only become equal when the period and duty cycle are optimal, since the cost function J has no local optimum. Hence, it can be used to find the optimum. For simplicity, we rename both sides of (C.9) as in (C.10) and (C.11). The controller always compare b (which is the error accumulation from the beginning of a period) and a with the value from last sample at each time sample to check if the switch should happen at the current time sample. If a-b=0 (in reality if the sign of a-b is different from last sample, then a switch should happen.), the system should switch now and start a new period (T is reset to 0). Otherwise, the system should update T ($T = T + T_{sample}$) and then wait for next sample time and repeat the above procedure. The control diagram of this idea is shown in Fig.C.3 where u is the control input to the system u' is the control input from last sampling time. From Fig.C.3 it can be seen that the algorithm is very simple and requires very little computational power.

$$\frac{\partial J}{\partial T} = 0 \tag{C.8}$$

$$Q \cdot (x_{t0+T} - x_{ref})^2 T = Q \cdot \int_{t0}^{t0+T} (x_{t0+T} - x_{ref})^2 dt + R \cdot J_{sw} \tag{C.9}$$

$$a = Q \cdot (x_{t0+T} - x_{ref})^2 T \tag{C.10}$$

$$b = Q \cdot \int_{t0}^{t0+T} (x_{t0+T} - x_{ref})^2 dt + R \cdot J_{sw} \tag{C.11}$$

The basic idea of the method above has been explained, but some adjustments have to be made in order to apply it in this application, because, with this method, only one decision of switch can be made for the current time sample, but in a period, there are two switches. A straight forward way to apply it is to just take **half period** into consideration (we name it 'half period adaptation') and using (C.10) directly. The equations become (C.12) and (C.13, where T_{now} means half period (either on or off). By doing this, the correlation between on/off periods are not taken into account by the controller, and therefore we expects to see solutions that are suboptimal.

$$a = Q \cdot (x_{t0+T_{now}} - x_{ref})^2 T_{now} \tag{C.12}$$

$$b = Q \cdot \int_{t0}^{t0+T_{now}} (x_{t0+T_{now}} - x_{ref})^2 dt + R \cdot J_{sw} \tag{C.13}$$

Some experiments with different loads have been done with the half period adaptation, and the results can be seen in Fig.C.4. Comparing the period cost and duty cycle from the half period adaptation (the curve marked with 'Half') with the optimal solution (the curve marked with 'Optimal'), it can be seen that close to 50% load, the results are very close to the real optimal, but when the load is away from 50%, this method gives a deviation. For instance, with 90% load, the period from this method is about 7796 seconds, but real optimal is 6447 seconds, which is about 20% error. It demonstrates that our prediction of a method based on considering only a half period will not be able to make the system reach the real optimal solution.

An idea now is to extend the method to take both on and off periods into account (we name it full period adaptation). There could be two ways of doing it. One is to introduce a prediction for the next period (either on or off). Since the method is very simple, which only uses the accumulated square error information form the past and the current output, we would like to keep the simplicity of the method therefore a prediction based approach which requires a fairly accurate model is not preferred. An easy way of avoiding taking in models but still using the full period adaptation is to use the last period (either on or off)which has just been found, together with the current period to compose a full period, which can be expressed as Equation (C.14). The algorithm of (C.14) can seen in Fig. C.5, where after a switch, the accumulated error is set to the accumulated square error for the last period, while with half period adaptation it is reset to zero. Another

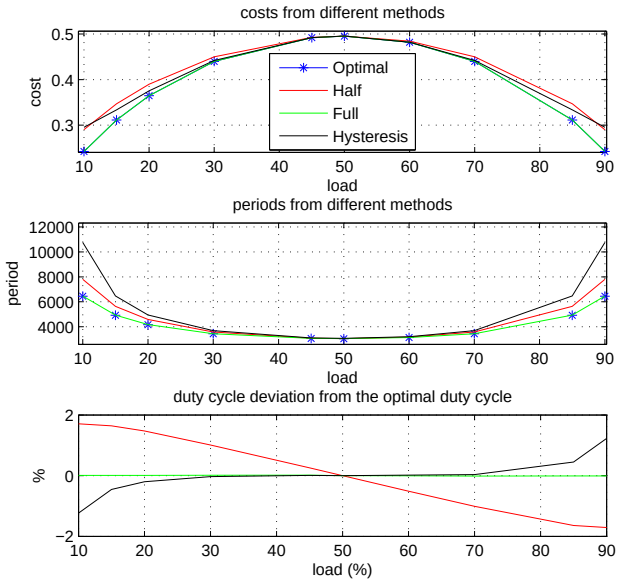

Figure C.4: Comparison of solutions from the different methods. The initial room temperature $x_0 = 22.8°C$ 'Optimal': the optimal solution. 'Half': half period adaptation. 'Full': full period adaptation. 'Hysteresis': hysteresis control.

difference is that T_{last} is added to the a term. It should be noted that when we calculate for the first switch with the full period adaptation, the error accumulated from earlier period is 0, and the switch cost should be only half of the later calculation because the calculation is only for a half period for the first switch. The switch cost in (C.9) and (C.14) are different and their relations are, for the first switch $J_{sw}^{'} = \frac{1}{2}J_{sw}$, otherwise $J_{sw}^{'} = J_{sw}$.

Since the algorithm takes the information from past, it might be sensitive to the initial conditions because the adaptation will carry the error(between the initial condition and the reference) all the way. An analysis of the significance of this sensitivity is given below

The same experiments with the same initial condition as for half period adaptation has been carried out with the full period adaptation, and the results are shown in Fig.C.4(green curve). it can be seen that the full period adaptation results reach the optimal solution at different loads, but the half period adaptation gives only good results when the load is close to 50%. Therefore we would like to have the full period adaptation.

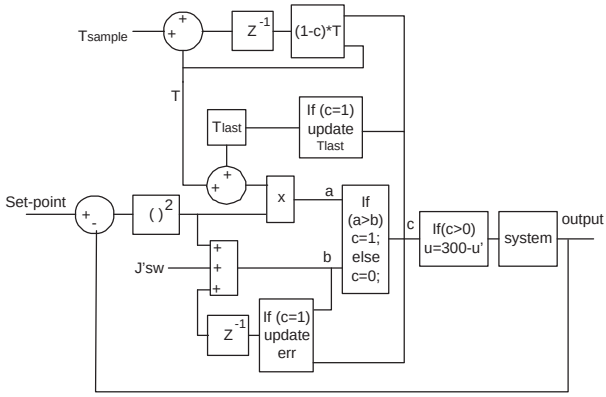

Figure C.5: Illustration of the full period control method. T_{sample} is the sampling time. T is the current adapting period

$$(x_{t0+T} - x_{ref})^2(T_{now} + T_{last})$$
$$= \int_{t0}^{t0+T_{now}} (x_{t0+Tnow} - x_{ref})^2 dt + err + J'_{sw} \tag{C.14}$$

Unfortunately, it has been proved that the full period adaptation is sensitive to the initial conditions, while the half period adaptation is insensitive to the initial conditions in [10]. It means that the full period adaptation can lead to some unsatisfactory results under some of initial conditions. Some experimental results show that if the initial conditions is on the track of or close to the real optimal room temperature, the temperature converges to the optimal limit cycle, otherwise it converges to a larger one. This can been seen in Fig.C.6 (the curve marked with Full, $x_0 = 22.8°C$ and $x_0 = 25°C$. The experiments condition is: 85% load. It is obvious that the full period adaptation with initial $22.8°C$ gives optimal results (the temperature variation is between 22.6 and $23.4°C$, the red curve), but the full period method with initial $25°C$ (the blue curve) results in a much larger limit cycle (between 22.2 and $24.4°C$). This means that $25°C$ is a 'bad' initial condition for the full adaptation method. Therefore our concern about the full period adaptation on initial conditions is not unnecessary.

The full period adaptation results are very promising when the initial conditions are good, but the problem of depending on the initial conditions really degrades the method. It is natural to ask a question: is it possible to get rid of the problem with initial conditions for the full period adaptation? or to combine the two methods - first start with the half period method to get rid of the bad initial condition and then switch to the full period method to get to the real optimal solution?

A new method

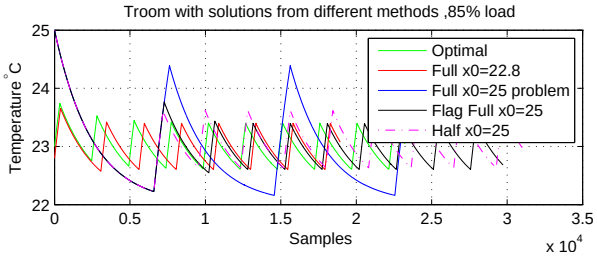

Figure C.6: Comparison of room temperature from the different methods. 'Optimal': the optimal solution. 'Half': half period adaptation. 'Full': full period adaptation. 'Flag Full': full period adaptation method with a fix. 'x0': the initial room temperature

The problem and good properties of the full period adaptation with initial conditions has been shown in last subsection. The interest here is to find out what is the reason that causes the problem and how it can be fixed.

The full period adaptation is based on (C.14), and the switch criteria is that the left side of the equation (a) equals to the right side (b). Before a switch, the left side is smaller than the right side. For comparison, results from full period adaptation with two initial conditions are plotted. One of them converges to the real optimal cycle and the other converges to a larger limit cycle. The left and right side of (C.14) are plotted for each initial condition in Fig.C.7. The inputs for the two initial conditions are also plotted in Fig.C.7.

The a and b curves from 22.8C initial condition are very much different from $25°C$ initial condition and so are the input curves. It looks strange with the input from $25°C$ initial condition - there are some peaks. The period of the cycle (disregarding the peaks) is too long compared with the input from $22.8°C$, which of course result in large temperature variation as shown in Fig.C.6.

Amplification of the input switch with initial $25°C$ around the peak at 16000 sample is shown in Fig.C.8. At sample 16003, the system switches from off to on, but at sample 16004, the system switches from on to off again. This short switch will not cause much difference in temperature, but constitute a heavy cost in switching. This is going away from the control purpose of reducing switches - this switch is unnecessary, but what is the reason it happened?

According to the original idea, the switch should only happen when a becomes equal to or larger (discrete) than b, and after the switch, a should become smaller than b again and a new period adaptation starts again. Amplification of a and b plot for initial $25°C$ at around 16003 and 16004 are shown as Fig.C.9 and Fig.C.10. The system switches on at sample 16003, where the cost a is larger than b as shown in Fig.C.9 but the strange thing is that at sample 16004, the cost a is still larger than b, which is the reason why the system switch again. After the switch at sample 16004, a becomes smaller than b.

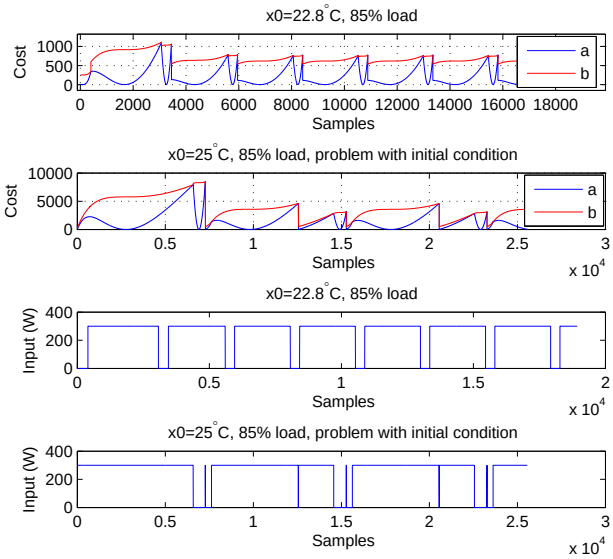

Figure C.7: Problem of full period method

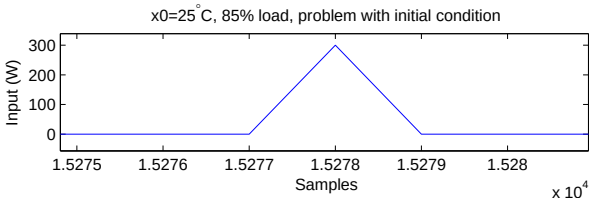

Figure C.8: Amplification of u at problem area

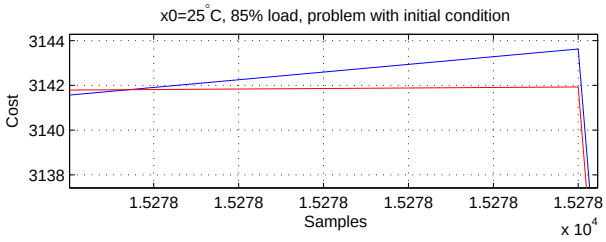

Figure C.9: Amplification of cost

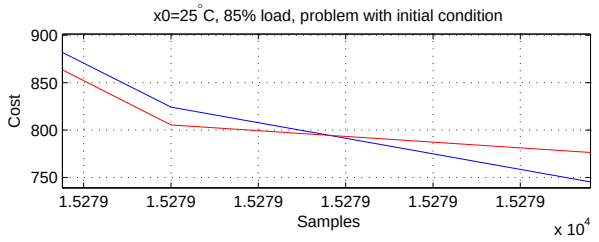

Figure C.10: Amplification of cost

The reason here is that, the room temperature change after the switch at sample 16003 is very little (it might be caused by quantization error), which was not able to make a smaller than b.

One easy way to solve the problem is to use a larger sampling time, this has been tried with 20 seconds in stead of 2 seconds. The problem can be solved, but it is not preferred because we do not exactly know what is the limit of the sampling time that will cause this problem.

A better way to solve it is to add an extra condition for the switch criterion. The extended switch criterion is at the last sample $a-b<0$ and at current sample $a-b\geq 0$, which earlier was only $a-b\geq 0$ at the current sample. This extra condition helps to avoid the switch right after another switch due to the slow change of the room temperature or the quantization error. The result of the full period adaptation algorithm with such a correction (we call the full period adaptation with adaptation 'the new adaptation method' later in this paper.) is shown in Fig.C.6 the black curve, where the 'bad' initial $25°C$ the room temperature converges to the optimal solution (with legend 'flag full x0=25'). Now we have found a method, which gives results very close to the optimal solution and which is not sensitive to the initial condition. For the initial condition $22.8°C$, the full period result with or without this correction is the same, because $a-b\geq 0$ happens only at the switch sample, otherwise $a-b<0$.

From the example shown in Fig.C.6, it can be seen that with good initial condition

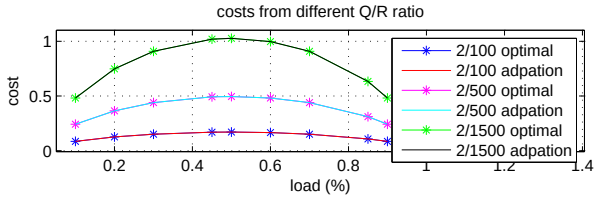

Figure C.11: Experiment result of the new method with different Q/R ratio compared with the optimal solution.

($22.8°C$), the results converges to the optimal solution after one optimal period length and with a 'bad' initial condition ($25°C$), the room temperature converges to the optimal solution after three optimal period length.

Different Q/R ratio has also been tested with this new adaptation method, and the costs are compared with the optimal solution for different load. The results can be seen in Fig.C.11. It can be seen that the new adaptation method gives optimal solution under different Q/R and different load.

We have suggested also another idea using half and full period together to solve the problem, but it will not be studied here because the fixed full period method works very good, and that if we first use half period and then switch, we will not get a faster converging rate.

A note has to be made here that, with simple modification the algorithm can be made to work even under the conditions corresponding to infinitely long cycle times. An example is to start with a room temperature that is far from the reference for example $28°C$ (assume that the outdoor is also $28°C$). The adaptation method does not work, because the error accumulation is very big at the beginning due to the difference between initial and reference and therefore the term a can not catch up with the term b. In this case, much higher power (>300w) will be continuously (corresponding to infinitely long cycle times) used to bring the room temperature down close to the reference at the beginning, and later when the load is is less than 100%, (300W) running continuous later, then the system will switch to this control algorithm.

C.5 Experiments with 2^{nd} order system

In last section, a method of controlling switch system has been developed based on a 1^{st} order system, but the AC-system behavior is more like a second order system. Therefore we would like to see how this method work with a 2^{nd} order system. Some investigations have been done and they show that this method only works with 2^{nd} order system with real poles. Therefore here we focus only on 2^{nd} system with real poles. The reason we toyed with the first order example was that it has much less computational load, and that the results are easy to visualize graphically.

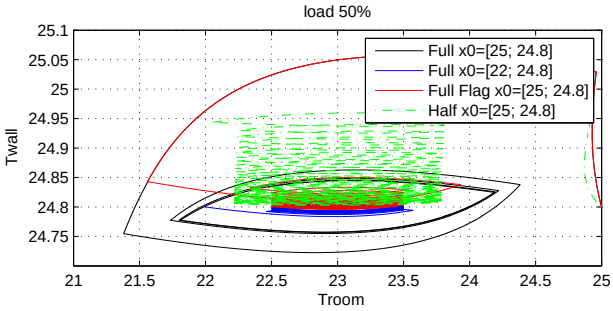

Figure C.12: Phase plot of second order example.

By experiments, we have found out that for a second order system using the full period adaptation gives better solution than the half period, and that the full period adaptation method is sensitive to the initial conditions without the extra switch condition. These are the same results as for the first order systems. The problem with initial condition for the full period adaptation is the same as for first order systems - it results in a second order limit cycle with some initial conditions, and it has the same problem in the a and b values where after a switch, the sign of $a - b$ is not changed because of the reaction on temperature is slow or the quantization error. The result of applying the new adaptation method (full period with the extra switch condition) is experimented and it gives a solution which seems to be the optimal. The results from different methods are shown in Fig.C.12. The initial condition x_0 here is the temperature of room and wall.

Among the green (half period method), blue (full period x0=[22$^\circ C$ 24.8$^\circ C$]) and black (full period, x0=[25$^\circ C$ 24.8$^\circ C$]), the blue curve represents the smallest limit cycle. The black curve converges to a much larger one, which is caused by the 'bad' initial condition. The red curve uses the new adaptation method (full period method with the extra switch condition), and it proceeds very close to the limit cycle illustrated by the blue curve. This example shows that the new adaptation method adapts to a limit cycle like the optimal solution.

C.6 Comparison between the novel method and hysteresis control

A comparison of the adaptation method and a traditional hysteresis controller is carried out to find out how much we can gain by using the new developed adaptation method.

First step is to tune the hysteresis controller at 50% load, such that the best possible hysteresis bounds can be found, i.e which gives the same cost as the optimal solution. The results are shown in Fig.C.13. It is obvious that 0.5$^\circ C$ deviation (i.e. hysteresis

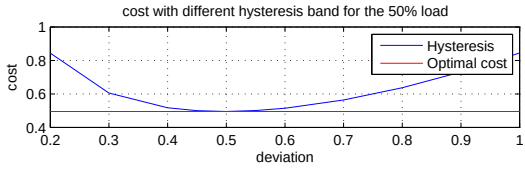

Figure C.13: Tuning of the hysteresis controller.

bounds equals the reference$\pm 0.5^{\circ}C$) gives the cost closest to the real optimal solution at 50% load.

The next step is to run the tuned hysteresis controller with the AC-system under different loads. The results can be seen in Fig.C.4 (black curve), where the cost, period, duty cycle from different loads are plotted. Obviously the hysteresis controller tuned at 50% load has results very close to the optimum at this load. Away from 50% load, the results are deviating from the optimal solution, for example at 90% load, the cost of hysteresis control has 20% higher cost than the optimal solution. It can be seen that the new adaptation method attains the optimal solution as stated previously. Further more the adaptation method converges quite fast which has been discussed in last section.

C.7 Conclusion

The paper has proposed a novel low complexity adaptation method for systems with discrete inputs that have costs related to switching. It should also be noted that the method currently works only for single input and single output systems. The method has been tested with first order systems which achieves the optimal solution and second order systems which in general also seems to attain the optimal solution reasonably fast. A comparison between the developed adaptation method and traditional hysteresis control was made. It showed that the performance of the hysteresis controller tuned at a nominal working condition gives suboptimal results when the working condition changes. In this example, the cost from the hysteresis controller is 20% higher than the optimal solution. The new adaptation method gives the optimal solution regardless at different load and different initial conditions. The complexity of the adaptation method is not increasing dramatically compared to the hysteresis control. In fact it requires only three states more than the hysteresis controller, the period for the last half period, the comfort error accumulation for the last half period, and the current period comfort error accumulation.

Further studies on this method will be focused on first order system with delay. In reality systems are often delayed or high order. The complexity of the presented method increases dramatically with system size, but often higher order system can be approximated as first order system and delay. Experiment will be carried to validate the

method.

J	cost per time unit
J_{sw}	cost for two switches in one period
J'_{sw}	J'_{sw}=$\frac{1}{2}J_{sw}$ before the first switch.J'_{sw}=J_{sw} after the first switch.
Q	penalty on temperature deviation
R	penalty on switch
a	current error
b	accumulated error and switch cost
T	cycle period
α	duty cycle
T_{last}	last half period
T_{now}	the current half period
x_1	temperature when AC-system is on
$x_{1,init}$	temperature at the beginning of on period under stable limit cycle
$x_{1,end}$	temperature at the end of on period under stable limit cycle
x_2	temperature when AC-system is off
$x_{2,end}$	temperature at the end of the off period under stable limit cycle
$x_{t0+T_{now}}$	current measured temperature
T_{sample}	sampling time
T_{room}	room temperature
T_{amb}	ambient temperature
$\dot{Q}_{a2r}$	energy from ambient to the room
$\dot{Q}_e$	cooling energy from AC-system
Res	thermal resistance from ambient to the room

Table C.1: Nomenclature.

Bibliography

[1] E. Verriest, M. Egerstedt, Y. Wardi, and M. Boccadoro. Optimal control of switching surfaces in hybrid dynamical systems. *Discrete Event Dynamic Systems*, 14:433–448, 2005.

[2] P. Riedinger, C. Zanne, and F. Kratz. Time optimal control of hybrid systems. *Proceedings of the American Control Conference*, 4:2466–2470, 1999.

[3] S. Hedlund and A. Rantzer. Optimal control of hybrid systems. *Conference on Decision and Control*, 4:3972–3977, 1999.

[4] Alberto Bemporad and Manfred Morari. Control of systems integrating logic, dynamics and constraints. *Automatica*, 35:407–427, 1999.

[5] P. Lohnberg and B.A.Mulder. Adaptive simple predictive control for a high-efficiency domestic heater. *Benelux quarterly journal on automatic control*, 40,N 3:25–30, 1999.

[6] Brian Solberg, Palle Andersen, Jan M. Maciejowski, and Jakob Stoustrup. Hybrid model predictive control applied to switching control of burner load for a compact marine boiler design. *Proceedings of the 17th IFAC World Congress*, 2008, June.

[7] Brian Solberg. Optimisation of marine boilers using model-based multivariable control. *PhD thesis*, 2008.

[8] D. Sarabia, F. Capraro, L. F. S. Larsen, and C. De Prada. Hybrid control of a supermarket refrigeration system. *Proceedings of American Control Conference*, pages 4178–4185, 2007.

[9] C. Sonntag, A. Devanathan, and S. Engell. Hybrid nmpc of a supermarket refrigeration system using sequential optimization. *IFAC World Congress*, 2008.

[10] Honglian Deng, L. F. S. Larsen, Jakob Stoustrup, and Henrik Rasmussen. control of systems with costs related to switching: applications to air-condition systems. *Proceedings of Multi-conference on Systems and Control*, 2009.

Appendix D

Control of delay dominant systems with costs related to switching

(Proceedings of Multi-conference on Systems and Control, 2010, Yokohoma, Japan.)

Honglian Deng, Lars Larsen, Jakob Stroustrup, Henrik Rasmussen

Abstract

The objective of this paper is to extend a novel low complexity method for optimizing switch control developed by the authors earlier to work with delay dominant systems and demonstrate that the method works in practice with a refrigeration test system. The extended method solves switching problems for high order systems which can be approximated as a first order with a delay as well. The extension of the method is realized with an observer to retrieve the delay-free information. Experimental validation of the extended method is carried out with a test system. A comparison to a baseline relay controller with fixed bounds shows that the optimizing switch control outperforms the baseline.

D.1 Introduction

Within the recent years optimal control of hybrid switching systems has attained a lot of focus. Among the recent results can be mentioned [1], [2], [3]. In this paper we will focus on systems with discrete inputs, which can be categorized as a subclass of hybrid

switching systems. Examples of such systems in the industry are numerous. In this paper, we will extend the method proposed by the authors in [4] and [5] to include delay dominant systems. The method is analyzed using a generic delay dominant model and the applicability is tested using an air conditioning system (AC-system) with a ON/OFF compressor capacity as case study.

A method for synthesizing optimal control for hybrid systems is hybrid model prediction control (MPC) using the mixed logical dynamical framework (MLD)[1], but also other MPC methods based on solving finite horizon optimization problems exist such as [6] and [7]. Common for these methods is that they typically produce rather complex controllers requiring large computational power. Furthermore, if special care is not taken using finite horizon methods on systems with discrete inputs, it can lead to rather poor performance,[2],[4]. There exist also other methods based on steady state optimization of limit cycles, for instance [3] on page 253. Some of these methods give good results for particular applications, but are complex and difficult to apply especially in the lower levels of the control hierarchy where sufficient computational power is not available. This motivates the authors to develop a much less complex optimizing switch control method [4] and [5] overcoming the potentially poor performance that finite horizon methods leads to. The focus of this paper is on extending the developed method to systems with delay and multi-order systems, and demonstrating that the method is applicable in practice.

The paper is organized in the following way. The development of the optimizing switch control method is briefly introduced in Section D.2. Observer design to retrieve delay-free information is presented in Section D.3. Experimental validation of the optimizing switch control method and a comparison to a baseline relay controller is presented in Section D.4. Finally conclusions are drawn in Section D.6.

D.2 Brief review of the method

The process of deriving optimizing switch control method will be briefly presented in this section. More details can be found in [4] and [5]. The process can be divided into three steps: defining a cost function, cost function convexity study and deriving the method.

D.2.1 Cost function definition

For an open loop stable system with a binary input, we assume that the optimal steady state output trajectory follows a stable first order limit cycle (which is defined as a period including two switches and a constant duty cycle) instead of a fixed point. The system performance is therefore evaluated as the *average* squared control error over one switch period. For a first order limit cycle two switches are done in each period. The total switch cost for one period therefore accounts to $2R$, where R is the cost of making a

switch. The total average cost over one cycle period (T) can then defined as follows

$$J = \frac{Q \int_{t_0}^{t_0+T} (y(t) - y_{ref})^2 dt + 2R}{T}, \tag{D.1}$$

where t is the time, $y(t)$ is the measured output, y_{ref} is the output reference, Q is the cost associated with having a certain control error, and t_0 is the initial time for the period in question. In the following we assume that the cost R accounts for as well the costs of component wear as the efficiency loss at start/stops. This cost function represents the performance of the system over one cycle period. This cost function will be applied in the remainder of this paper.

D.2.2 Convexity

Having defined the cost function we will now study convexity based on first order (SISO) system, i.e.

$$\begin{aligned} \dot{x} &= ax + bu + d \\ y &= cx, \end{aligned} \tag{D.2}$$

where $u \in \{\underline{u}, \overline{u}\}$ is the binary valued input and d is a disturbance. Further more (D.2) is stable, $a \leq 0$, and $c = 1$.

A first order limit cycle consists of an ON-period and an OFF-period as indicated in Fig.D.1. The output error accumulation can be divided into two parts: error from the ON-period $t \in [t_0, t_0 + \alpha T]$, and error from the OFF-period $t \in [t_0 + \alpha T, t_0 + T]$, where α denotes the duty cycle. The cost function (D.1) can therefor also be written as

$$\begin{aligned} J(T) &= \frac{Q \cdot \int_{t_0}^{t_0+\alpha T} (y_1(t) - y_{ref})^2 dt}{T} \\ &\quad + \frac{Q \int_{t_0+\alpha T}^{t_0+T} (y_2(t) - y_{ref})^2 dt + 2R}{T} \end{aligned} \tag{D.3}$$

y_1 and y_2 refer to the output in respectively the ON and OFF period as indicated in Fig.D.1.

Operating at steady state limit cycles, the system output is periodical, meaning that the output at the end of one period equals the output at the beginning of the next, $y_{1,\text{init}} = y_{2,\text{end}}$, and $y_{1,\text{end}} = y_{2,\text{init}}$. Therefore y_1 and y_2 can be solved explicitly with the above conditions and become only functions of T and α. Hence the cost according to (D.3) can be computed as a function of α and T. Even so it is not easy to prove that the cost function (D.3) is mathematically convex. The alternative is simply to calculate the cost (D.3) within a reasonable range of $\alpha \in [0, 1]$ and $T > 0$ and investigate the existence of a unique optimum.

The cost function calculation with first order system (D.2) is carried out the following parameters,

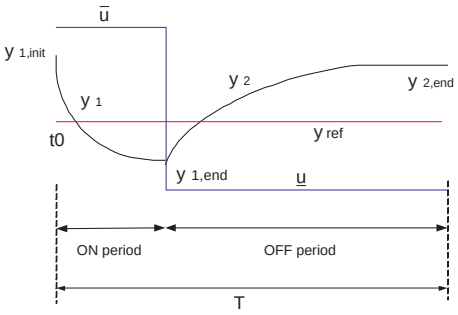

Figure D.1: One cycle period

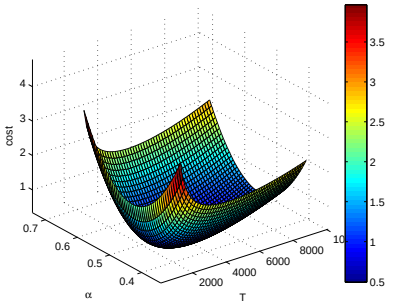

Figure D.2: The computed cost, for a 1^{st}. order system following a steady 1^{st}. order limit cycle, as function of the period time T and the duty cycle α.

$a = -2.00 \times 10^{-4}$
$b = -4.40 \times 10^{-6}$
$c = 1$
$\underline{u} = 0$
$\overline{u} = 300$
which are from a first order air conditioned room model (presented in [4] and [5]) where the air conditioning unit is not modeled in detail but as energy input. The output set-point is $y_{ref} = 23$. d is corresponding to different outdoor temperature disturbance.

In Fig.D.2 the computed cost with $d = 5.19 \times 10^{-3}$ is plotted as function of α and T. It clearly appears from the figure the cost function for this system indeed is convex.

Following this way, it can be demonstrated that the cost function (D.3) is convex for SISO high order systems with real poles.

D.2.3 The optimizing switch control method

From the study of the cost function (D.3) above, we know that (D.3) is convex, therefore

$$\frac{\partial J}{\partial T} = 0 \tag{D.4}$$

is true for the optimal solution.

Insert (D.1) into (D.4), we derive (D.5), which can be written as (D.6) by applying $T = T_{now} + T_{last}$. T_{now} is the current half cycle period (either ON or OFF half cycle period) and T_{last} is the last half cycle period (either OFF or ON). It can be understood in this way: the left side of (D.6) is the current output deviation from the reference and the right side is the accumulated output error from the beginning of last switch and switch related cost.

So an optimizing switch method using (D.6) is derived, and the simulation results show that it drives the system towards the optimal solution both in duty cycle and period. More details regarding derivation of the optimizing switch control method and simulation results is referred to [4] and [5]

$$\cdot(y_{t0+T} - y_{ref})^2 T = \cdot \int_{t0}^{t0+T} (y_t - y_{ref})^2 dt + \frac{2R}{Q} \tag{D.5}$$

$$\begin{aligned} &(y_{t0+T} - y_{ref})^2 (T_{now} + T_{last}) \\ &= \int_{t0}^{t0+T_{now}} (y_t - y_{ref})^2 dt + err + \frac{2R}{Q} \end{aligned} \tag{D.6}$$

The new method is developed based on a first order single input single output model. However, the method works as well for integration systems, because the cost function (D.1) for integration system is also convex. The proof of the convexity of the cost function for integration switching system is straightforward therefore it is not included in the paper.

Delay dominant systems pose challenges for the optimizing switch method. The reason is that, when the controller gets the delayed output information, it is already too late to react. To extend the method to delay dominant systems, the method can solve a set of multi-order system problems as well. The reason is that multi-order systems in many applications can be approximated by a first order system and a delay. So the next section will focusing on delay dominant systems.

D.3 System with delays

The reason why it is important to extend the optimizing switch control method to work with delay dominant systems has been explained. Applying the optimizing method directly to a first order system with a delay leads to suboptimal solution due to that the

feedback to the controller is 'old'. The optimal solution for a first order switching system is independent of whether the system has a delay or not, meaning that if the delay-free output is fed back to the controller, the system should perform exactly the same as for the system without delay under same disturbances. The question is how the delay-free output information can be achieved.

Extensive research has been carried out on controlling systems with delays [8]. One traditional method is based on the Smith Predictor (SP) [9]. Due to the problem that SP does not work with unstable systems for example systems with an integrator, [10], [11], have proposed modified SP methods. A common prerequisite for successful employment of SP (both the original as well as the modified ones) is the accurate knowledge of the model and delay. However, for most industrial cases this knowledge is not easily available.

Another approach is based on the idea of representing the delay with Pade approximation, e.g. [12]. A systematical approach of designing observer based on Pade approximation is introduced in [13], which will be explained briefly here.

D.3.1 Observer based on Pade approximation

The proposed observer design approach in [13] is to first partition the delay θ into p non-overlapping delays as (D.7), then introduce Pade approximation (D.8) to each partition of the delay and formulate a state space model of the Pade approximated delay together with the system model (D.2). This approach facilitates using well-established design techniques to construct an observer that provides the delay-free output.

$$e^{-\theta s} = (e^{-\frac{\theta}{p}s})^p \tag{D.7}$$

$$e^{-\frac{\theta}{p}s} \approx \frac{1 - \frac{\theta}{2p}s}{1 + \frac{\theta}{2p}s} \tag{D.8}$$

D.3.2 A new approach of designing observer for systems with delay

Our proposal of designing observer for delay system can be explained in the following steps:
(1) Discretize the system including delay with a large sampling time $\frac{\theta}{m}$, so that the delay can be partitioned into m partitions, and each of the delay partition can be modeled as one sampling time delay, and therefor the whole system becomes discrete.
(2) Design an observer for this discrete time system - find the gain L_d.
(3) Check whether the observer is stable if the discrete observer gain is directly applied into the continuous system (or a system with a much faster sampling time). If it is stable, then the observer is found, otherwise, increase m, and repeat the above procedure. It is preferred to have a minimal m because it ensures that the observer has a minimal number of states.

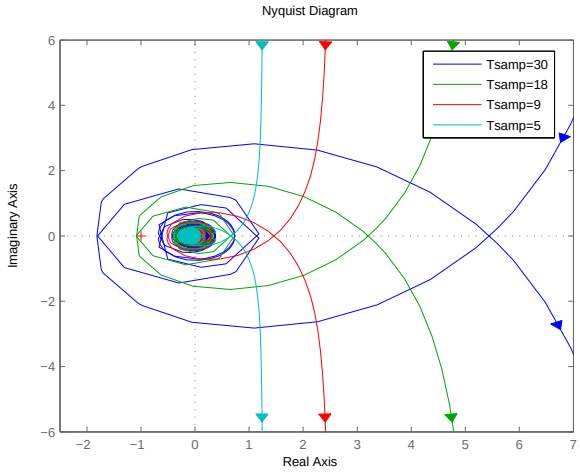

Figure D.3: Nyquist diagram of the continuous observer transfer function. The observer gain is designed in discrete time based on different sampling times.

In continuous time, the delay in the observer is divided into m number of delays $e^{\frac{\theta}{m}s}$, and the corresponding terms in gain L_d to compensate each term of $e^{\theta s}$. The observer stability can be checked in this way: find the observer transfer function from the error (between the measured and estimated output) to the estimated output, and check the stability based on e.g. a Nyquist diagram. Such a observer stability Nyquist diagram is shown in Fig.D.3, where the observer gains are designed based on different sampling times. From the figure, it can be seen that the observer stability increases with decreasing sampling time.

The proposed observer design approach is systematical. Comparing with the observer based on Pade approximation, the advantage is, that the observer stability is ensured. However, in the experiments the observer based on Pade observer $p = 1$ turns out to be stable. Thus, the more general method described above is given for completeness, but in the experimental testing, the simpler design with Pade observer p=1 has been applied, since that the focus of the paper is on the optimizing switch control method.

D.4 Test system description

To verify the optimizing switch control method, experiments are carried out with a refrigeration plant in Aalborg University in Denmark [14]. The schematic view of the refrigeration plant is shown in Fig.D.4. The system emulates an air conditioning system, where the tank simulates a room, and the refrigeration system works as an air

conditioning unit installed in the room. The overall control goal is to maintain the tank water temperature close to the reference by switching the refrigeration system ON/OFF.

The heat load on the system is maintained by an electrical heater with a adjustable power supply for the heat element in the water tank. Since the tank is well insulated, the heat loss to the ambient is so little that it can be neglected, which means that the tank behaves like a integration system. The compressor is with a variable speed drive from $35Hz - 60Hz$. Temperature sensors and mass flow sensor are installed on the water pipe passing the heat exchanger.

D.4.1 Modeling of the test system

The refrigeration system is considered as a whole unit with discrete input control signal 1 or 0 to the compressor. When 1 is sent to the compressor, the compressor starts and therefore the refrigeration system switches on. In the experiments, when the compressor is on, it runs with $35Hz$, which in steady state can remove approximately $3200W$ from the water through the heat exchanger. When 0 is sent to the compressor, the refrigeration system switches off, which means no power is removed. The power removed by the refrigeration system is expressed as $\dot{Q}_e = 3200,0W$. More details of the refrigeration system can be found in [14].

The water tank is roughly modeled as

$$\dot{T}_{water} = \frac{\dot{Q}_{load} - \dot{Q}_e}{c_{p,water} \cdot m_{water}} \tag{D.9}$$

whereT_{water} is the delay-free average tank water temperature, $T_{w,out}$ is the measured outlet water temperature, $\dot{Q}_e$ is the estimated power removed from the water tank, which can be modeled from the water side,

$$\dot{Q}_e = c_{p,water} \cdot \dot{m}_{water}(T_{w,out} - T_{w,in}) \tag{D.10}$$

$\dot{T}_{water}$ is the average tank water temperature. $c_{p,water}$ and m_{water} is the specific heat capacity and mass of water in the tank. $\dot{Q}_e$ is the cooling capacity from the refrigeration system. $\dot{Q}_{load}$ is the heating load from the electrical heater. The disturbance from the ambient to the water tank is ignored due to the very good insulation of the tank.

The water temperature coming into and out of the tank is $T_{w,in}$ $T_{w,out}$ which is corresponding to the water temperature after and before passing the evaporator. A mixer is installed to keep the water in the tank well mixed so that the water temperature is even and therefore the temperature of the water coming out of the tank $T_{w,out}$ can be approximated as the water temperature inside the tank. However, there is a delay from when the refrigeration system removes the power until $T_{w,out}$ reacts. This could be caused by the flow transportation in the pipe etc. In this case the delay is approximately $\theta = 90s$, and it is modeled as

$$T_{w,out} = T_{water(t-\theta)} \tag{D.11}$$

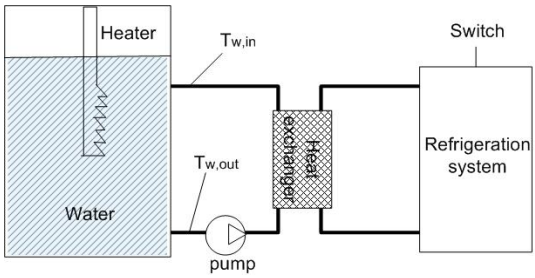

Figure D.4: Schematic view of the test system: the refrigeration plant

The parameter for the models are $c_{p,water} = 4180J/(kg \cdot^{\circ} C)$, $m_{water} = 65kg$, $\theta = 90s$, $\dot{Q}_e = 0$ or $3200W$.

In all of our experiments, the reference for the tank ($T_{w,out}$) is $22^{\circ}C$, and the ambient temperature is controlled around $22^{\circ}C$ so that there is no significant heating disturbance from the ambient. The disturbance from the electrical heating element is $1000W$.

It should be noted that the optimizing switch control method was developed based on a first order model, but it works on an integration system as well, which can be seen as a special first order system with infinite time constant. The proof of convexity of the cost function (D.3) for an integration system is not hard, therefore is not included here.

D.5 Experimental results

In this part, two group of experiments are carried out. The first group of experiments are designed to validate the developed optimizing switch control method. The second group is to compare the optimizing switch control method with a basedline relay control. An observer is needed to retrieve the delay-free output.

The observer applied in the experiments is based on a first order Pade approximation as described in D.3.1. The model of the refrigeration plant used for the observer is (D.9). Due to the difference between the input energy to the refrigeration plant and the estimation of the input to the observer, an offset appears on the estimated delay-free output. To remove the offset, an extra integration term is introduced, which at last becomes a proportional and integral (PI) observer. Design of such a PI observer can be found in [15], and the procedure will not be repeated here. The resulting observer is shown as in Fig.D.5, which is referred to as Pade PI observer in this paper. The following observer gains $L = [1.23 \times 10^{1}, 6.75 \times 10^{-2}, 1.25 \times 10^{-4}]$ which are obtained from off-line simulations with some recorded data from one experiment are applied in the experiments in this section.

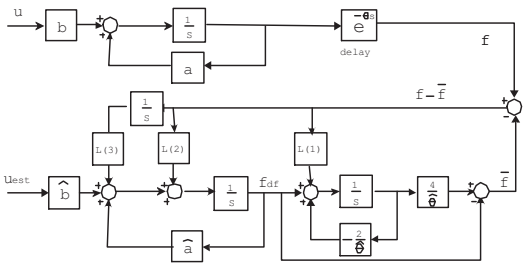

Figure D.5: PI observer, where the delay is based on Pade approximation. $L = [L_{(1)}, L_{(2)}, L_{(3)}] = [1.23 \times 10^{1}, 6.75 \times 10^{-2}\, 1.25 \times 10^{-4}]$. θ is the delay time. u is the actual input energy to the system. u_{est} is the input to the observer which is estimation of u. f_{df} is the delay-free output

D.5.1 Validation of the optimizing switch control method

Validation of the optimizing switch control method is carried out by comparing the control result with the optimal solutions.

The first question is what the optimal solution for the ON/OFF switching refrigeration plant with respect to the water outlet temperature is. The optimal solution for the refrigeration plant is different from the calculated optimal solution based on the model (D.9), because the model (D.9) (integration and delay) is a crude approximation of a high order system. The only way to achieve the optimal solution for the test system is to run pulse experiments with different periods until it reaches steady states, then calculate the cost using (D.3) to find the period corresponding to the smallest cost. Due to that the refrigeration plant is very close to an integration system, therefore duty cycle and the load percentage are very close to each other, which can be calculated directly by the heating to cooling ratio, while for a first order system, the optimal duty cycle will be significantly different from the load percentage when the load is different from 50%.

The above procedure of finding the real optimal solutions is illustrated by Fig.D.6. where the penalty is $Q = 20, R = 500$ and heating load is $1000W$. A polynomial fit of the test points has minimal cost at around 350s. The benefit of the polynomial fit is that with discrete test points, a continuous expression of the cost as a function of the period can be achieved.

To investigate the ability of the optimizing switch control method to drive a system towards the optimal solution at different penalty ratios, another two optimal solutions for the real penalty $Q = 2, R = 500$ and $Q = 80, R = 500$ are also demonstrated with pulse experiments. The resulting three optimal solutions at three different Q (R is kept at 500 for all the experiments) are shown in Fig.D.7. For comparison, the optimizing switch control resulting costs at different Q/R ratio and heating disturbance $1000W$ are also plotted Fig.D.7.

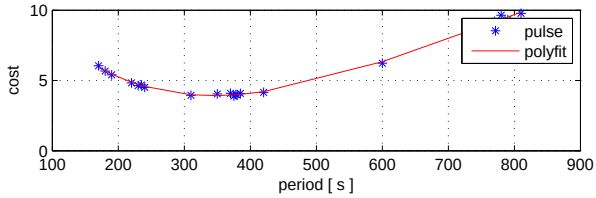

Figure D.6: Cost vs. periods. Q=20, R=500. Heating load 1000w. 'pulse' refers to the cost results from the pulse input experiments. 'polyfit' is the polynomial fit of the discrete test points of the pulse results.

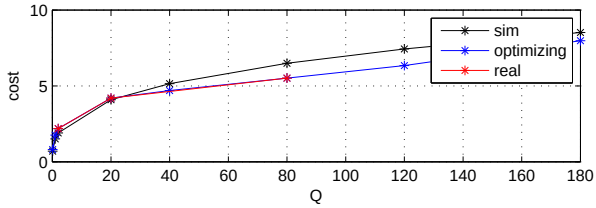

Figure D.7: Comparison of optimizing controller and real optimal solution at heating load $1000W$. R is kept at 500. 'sim' is the optimal solution for the model. 'optimizing' is the solutions from applying the optimizing switch control on the test system. 'real' is the optimal solution from the pulse experiments with the test system.

Fig.D.7 demonstrates that the solutions from the optimizing switch control (legend 'optimizing') are very close to the optimal (legend 'real'). The error defined by (D.12) at the three $Q = 2, 20, 80$ are $2.30\%, 4.85\%, 3.00\%$. These results prove that, the optimizing controller achieves results very close to the optimal solutions.

$$error = \frac{|cost_{adaptive} - cost_{real}|}{cost_{real}} \tag{D.12}$$

D.5.2 Optimizing switch method vs. relay control

In [5], simulation results from the optimizing and relay controller for a first order system has been compared, and they show that the optimizing switch control method outperforms relay control when the systems are not at the nominal working condition for the relay.

Several experiments have been carried out to investigate the performances of the optimizing switch control method and relay controller with and without observer at different heating load.

(1) Optimizing switch control method. Run the optimizing switch control method including the Pade PI observer at different heating loads with parameter $Q = 2, R = 500$. The observer gains are $L = [1.23 \times 10^{1}, 6.75 \times 10^{-2}, 1.25 \times 10^{-4}]$.
(2) Standard relay controller. Tune the relay controller at about 50% corresponding to about $1500W$ heating disturbance, which reaches results very close to the optimizing switch control. The resulting relay band is $0.36°C$, which means that the refrigeration system switches on when $T_{w,out}$ is higher than $22 + 0.36°C$ and switches off when $T_{w,out}$ is lower than $22 - 0.36°C$. Then run the experiments with this controller at different heating loads.
(3) Relay controller with observer. An improvement for the relay controller could be to include the PI observer. Apply the Pade PI observer and feed the non-delayed information to the relay controller. Repeat the procedure of tuning the standard relay controller. The resulting relay band is $1°C$. which means that the refrigeration system switches on when $T_{w,out}$ is higher than $22 + 1°C$ and switches off when $T_{w,out}$ is lower than $22 - 1°C$. Then run the experiments with this controller at different heating loads.

The results from the above three experiments are shown in Fig.D.8, where it can be seen that close to the nominal condition 50% load, the relay controller with and without produces fine results, but when the heating load moves away from 50%, for example at heating load $500W$, the standard controller cost deviation from the optimizing controller is very large, while the relay controller including observer improves, but still the cost is much larger than optimizing switch control result.

The temperature outputs from these three controllers at heating load $500W$ are plotted in Fig.D.9. Comparing Fig.D.9a,b,c, it can be easily seen that the standard relay control output has an offset, which results in a large cost. The reason for the offset is that during the delay time, the heating power $\dot{Q}_{load}$ to raise the temperature (when refrigeration system is switched ON) and the heating power minus the cooling power $\dot{Q}_{load} - \dot{Q}_e$ (when refrigeration system is switched OFF) to remove heat is different. The offset in the standard relay has been removed and it performs more close to the optimizing switch control result. The optimizing switch control output is offset free.

D.6 Conclusions

A newly developed optimizing switch control method for optimal control of system with binary inputs that have costs related to switching has been tested with a refrigeration test systems. An observer design has been made to attack the delay problems for the optimizing switch control method. The method including the observer drives the system to the optimal limit cycle solution and it performs better than relay controllers with/without observer at non-nominal condition. The optimizing switch control method has only been tested with SISO first order systems and integration, but it has been proven to work also with SIMO first order and integration systems as long as the cost function has no local optima. For multi-order single input systems, the phase shift problem can also be solved with this method by approximating the system with a first order system with a delay in a

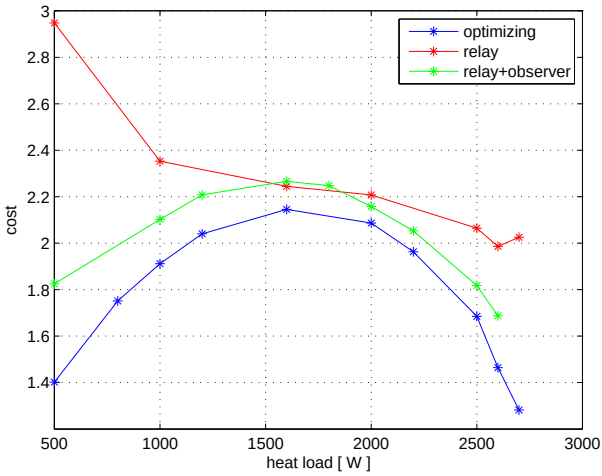

Figure D.8: Comparison: optimizing switch controller, standard relay controller and relay controller with observer. The relay controller is tuned under heating load 1600W. 'optimizing' is the results from the optimizing switch controller. 'relay' refers to experimental results. 'relay+observer' refers to experimental results from a relay controller and observer.

proper frequency range. The method has low complexity which at the same time avoids the fundamental problem of finite horizon prediction methods.

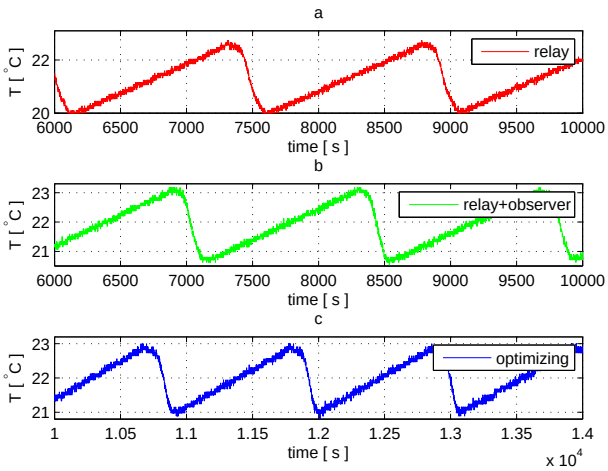

Figure D.9: Comparison: the temperature output from optimizing controller, standard relay controller and relay controller with observer at heating load $500W$. 'optimizing' is the results from the optimizing switch controller. 'relay' refers to experimental results. 'relay+observer' refers to experimental results from a relay controller and observer.

Bibliography

[1] A. Bemporad and M. Morari. Control of systems integrating logic, dynamics, and constraints. *Automatica*, 35(3):407–427, March 1999.

[2] Brian Solberg, Palle Andersen, Jan M. Maciejowski, and Jakob Stoustrup. Hybrid model predictive control applied to switching control of burner load for a compact marine boiler design. *Proceedings of the 17th IFAC World Congress*, 2008, June.

[3] Brian Solberg. Optimisation of marine boilers using model-based multivariable control. *PhD thesis*, 2008.

[4] Honglian Deng, L. F. S. Larsen, Jakob Stoustrup, and Henrik Rasmussen. Control of systems with costs related to switching: applications to air-condition systems. *Proceedings of Multi-conference on Systems and Control*, 2009.

[5] Honglian Deng, L. F. S. Larsen, Jakob Stoustrup, and Henrik Rasmussen. A new method for control of systems with costs related to switching: applications to air-conditioning systems. *Proceedings of European Control Conference*, 2009.

[6] D. Sarabia, F. Capraro, L. F. S. Larsen, and C. De Prada. Hybrid control of a supermarket refrigeration system. *Proceedings of American Control Conference*, pages 4178–4185, 2007.

[7] C. Sonntag, A. Devanathan, and S. Engell. Hybrid nmpc of a supermarket refrigeration system using sequential optimization. *IFAC World Congress*, 2008.

[8] Julio E. Normey-Rico and Eduardo. F. Camacho. Dead-time compensators: A survey. *Control Engineering Practice*, 16(4):407 – 428, 2008. Special Section on Manoeuvering and Control of Marine Craft.

[9] O.J.M.Smith. A controller to overcome dead time. *ISA J.*, 6:28–33, 1957.

[10] K.J. Astrom, C.C. Hang, and B.C. Lim. A new smith predictor for controlling a process with an integrator and long dead-time. *Transactions on Automatic Control,*, 39:343–345, 1994.

[11] T. Liu, Y.Z. Cai, D.Y. Gu, and W.D. Zhang. New modified smith predictor scheme for integrating and unstable processes with time delay. *Control Theory and Applications*, 152:238–246, 2005.

[12] Gang Liu, Alan Zinober, and Yuri B. Shtessel. Second-order sm approach to siso time-delay system output tracking. *IEEE Transactions on Industrial Electronics*, 56:3638–3645, 2009.

[13] B. del Muro-Cuellar, O. Jimenez-Ramirez, M. Velasco-Villa, G. Fernandez-Anaya, and J. Alvarez-Ramirez. Observer-based prediction scheme for time-lag processes. *American Control Conference*, pages 639–644, 2007.

[14] Lars F. S. Larsen. *Model Based Control of Refrigeration Systems*. PhD thesis, Aalborg University, 2005.

[15] H. H. Niemann, J. Stoustrup, B. Shafai, and S. Beale. Ltr design of proportional-integral observers. *International Journal of Robust and Nonlinear Control*, 5:671–693, 1994.

Appendix E

Control of a water-based floor heating system

(Proceedings of the IEEE Multi-conference on Systems and Control, 2007, Singapore.)

Honglian Thybo, Lars Larsen and Claus Thybo

Abstract

The objective of this study is to propose a control scheme that aims at increasing the control performance of a water-based floor heating system with a large thermal capacity. Experience shows that although floor heating is preferred due to the comfort of the warm floor, the slow control dynamics decreases the overall customer satisfaction. This paper analyzes the control problem and proposes a control scheme with increased dynamic performance. The proposed control scheme is validated using simulation and experimental results.

E.1 Introduction

Water-based floor heating systems have during the recent years been increasingly used. The reason why floor heating systems are preferred is mainly due to the increased comfort of having a warm floor (e.g. in bathrooms) and a more uniform temperature distribution in the heated room (due to the large heat transmitting surface i.e. the floor).

A typical water-based floor heating system consists of a circulation pump that maintains the required flow of heated water to casted-in water pipes in the floors of the heated rooms. In particular, each floor can be divided into a top-floor, made of e.g. wood or tiles, and a sub-floor, where the water pipes are casted into concrete. Each of the heated

floors has a control valve for hot water, that needs to be opened and closed such that the air temperature in room is kept close to the desired reference to ensure the indoor comfort.

For many years, the control of water-based floor heating systems has been based on relay controllers, which are flexible and simple. Typically each room is equipped with an independent relay controller that regulates the air temperature in the room by manipulating the control valve. Furthermore the inlet temperature of the hot water to the floor is regulated by a thermostat, thus indirectly assuring that the temperature in the top-floor does not exceed the material limitation (e.g. wooden floors can be destroyed) and the comfort criteria (that the floor does not get too hot). The major drawback, however, is that the control due to the large heat capacity of the concrete sub-floor and the limited upper inlet temperature of the water exhibits a very slow response and an extensive overshoot in the air temperature. Some studies have been done on rejecting passive sun heating by changing set-point temperature [1] and outdoor temperature change by adjusting the water inlet temperature [2], but they didn't solve the time delay problem caused by large heat capacity of the concrete sub-floor and the slow response by limited upper inlet water temperature. A numerical study on the effects of thermostat profiles for radiant floor heating and effect of concrete mass is presented by [3]. One of the conclusions is that a larger thermal mass effectively can function as a thermal storage for auxiliary supplied heat while keeping the comfort limits. It is also found that a large thermal mass can contribute to an increased temperature swings with high solar gains. General predictive control is applied to a high thermal mass floor heating system with good results by [4]. The heat is here emitted by electrical panels, where the power is directly controlled. This points to benefits of a more sophisticated control, when the emitted power can be controlled directly. Study [5] points out that it would be beneficial to control both the temperature of the storage and the room temperature. However attempts to use temperature measurements have failed mainly because it is difficult to represent a distributed temperature profile by using a single temperature measurement.

Motivated by these difficulties, an approach for estimating and controlling the estimated sub-floor temperature is presented and we propose a cascaded control structure with an inner loop that controls the estimated temperature of the sub-floor (concrete) and an outer loop that controls the air temperature in the room which increases the dynamic performance. The direct control of the estimated concrete temperature enables a more precise outer loop room temperature control, when the large thermal capacity of the concrete is controlled. This strategy removes overshoot and allows a higher inlet temperature of the hot water hence decreasing the air temperature response time.

The paper is structured in the following way. Section E.2 describes the basic layout of a typical water-based floor heating system and the used test system. Section E.3 provides an overview of the traditional control setup and the control objectives. Section E.4 summarizes the simplified model of the floor heating system and in Section E.5 the model is validated against experimental data. In Section E.6, the control strategy is formulated and an approach for controlling and estimating the sub-floor (concrete)

temperature is proposed. In Section E.7 the proposed control scheme is implemented on the test system. Conclusions are drawn in Section E.8.

E.2 System description

A typically water-based floor heating system can be divided into two parts; a water circuit and the heated floor and room. In the following we describe each of these parts.

E.2.1 Water circuit

The water circuit supplies warm water to the heated floors by mixing the return water from the heated floors with an external supply of hot water, see Figure E.1. The redundant amount of cold water in the water circuit is released at the outlet of the return manifold.

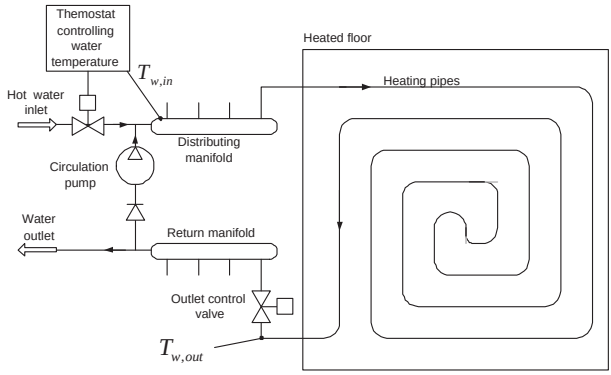

Figure E.1: Sketch of the water based floor heating system

The inlet temperature to the distributing manifold and hence to the heated floors ($T_{w,in}$) is controlled by a thermostatic valve that adjusts the amount of hot water mixed in the water circuit as shown in Figure E.1.
The inlet temperature to the floor is measured at the distributing manifold. The outlet temperature is measured just before the outlet valve.

E.2.2 Heated floor and room

The heated floor can be divided into a top-floor and a sub-floor. The sub-floor is typically made of concrete where the heating pipes are casted into. By supplying heated water ($\dot{Q}_w$) to the heating pipes the sub-floor is heated. The heat from the sub-floor is transmitted to the room through the top-floor ($\dot{Q}_f$), i.e. the top-floor can be regarded as

a resistance in the heat transmission, see Figure E.2. The top-floor, which is placed on top of the sub-floor is made of e.g. wood or tiles etc.

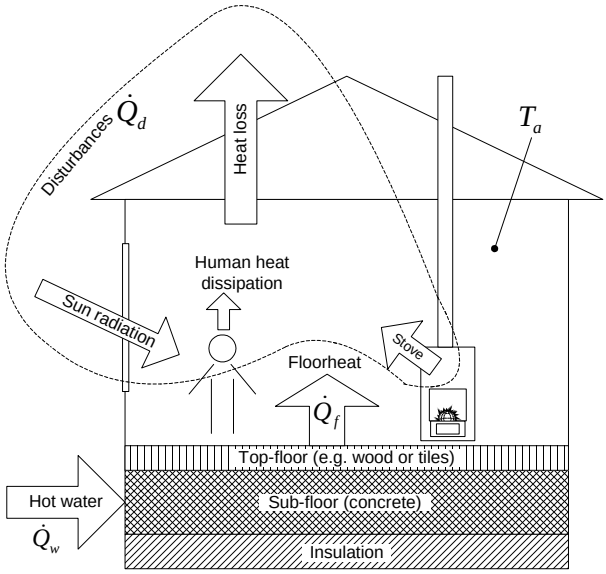

Figure E.2: Sketch of the floor heated room and the affecting disturbances

The room temperature (T_a) is measured by a temperature sensor mounted, typically on the wall of the room in question. This temperature measurement is used in the room temperature control. Figure E.2 furthermore depicts a number of possible disturbances to the temperature control.

The experimental results are obtained on a test system having the features described above.

E.3 Control problem description

The control challenges of a water-based floor heating system can be divided into two objectives, rejecting disturbances and following set-point. In most domestic houses the temperature set-point is fairly constant and only changed in relation to away periods, such as holidays. The objective after a set-point increase is as quickly as possible to get up to the new set-point without overshoot. Rejecting disturbances is the main day to day challenge. The outdoor climate is often treated as the sole disturbance, but additional heat sources and also water inlet temperature and pressure variations contribute. Climate disturbances are primarily outdoor temperature variations, but also wind and radiation play a role. Other disturbances can be in form of sun radiation through the window, a

wood burning stove or human heat dissipation etc. (see Figure E.2).

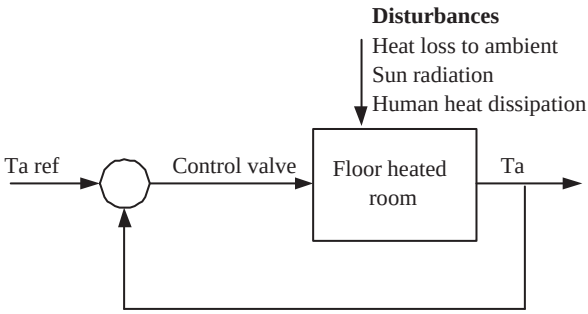

Figure E.3: A sketch of the current control approach

Figure E.3 shows the floor heating system as it is viewed from typical control system perspective, where the outlet valve is used as actuator, using the air temperature of the room directly as feedback for a relay type control. The main problem with this approach is in regards to disturbances, where the large uncontrolled thermal capacity of the concrete floor makes it difficult to compensate for outdoor climate variations and other heat-sources. The current relay approach waits for the inside temperature to fall below the set-point before the control valve is opened. The concrete subfloor then has to increase the temperature to a level, where it can accommodate the increased heat load. This gives an undesired undershoot in temperature until the concrete temperature catches up. The same type of problem can appear in the early hours of the day, where the outdoor temperature increases fast. Sun radiation through the windows may even further decrease the heating demand very fast. Even when the control system closes the inlet valve when the inside temperature exceeds the set-point, the thermal capacity of the warm under-floor will still contribute to an increase of the room temperature. The severity of these problems greatly depends on the thermal resistance of the top floor. A high thermal resistance floor type, such as a wooden floor requires a much higher subfloor temperature to provide the needed heating compared to a low thermal resistance type (e.g. tiles). A wood floor also needs to respect a maximum temperature to ensure that the floor is not damaged. The wood floor producer Junckers Ltd. [6] recommends a maximum concrete temperature of $37.5°C$, which in the current control structure limits the inlet temperature, and as a result of that also limits ability to change the concrete temperature fast.

E.4 Modelling

The model focuses on the heated floor and the room. This part contains the slowest dynamic which poses the limitations to the dynamic performance of the control system.

The dynamics of the water circuit is much faster than the heated floor and is therefore considered static.

The model of the floor and the heated room can be divided into 3 parts; the sub-floor, the top-floor and the room. These 3 parts are connected as depicted in Figure E.4.

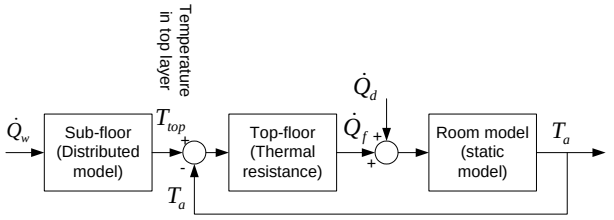

Figure E.4: Schematic view of the room and floor model.

The concrete sub-floor is heated by circulating hot water through the floor, i.e. by transmitting the heat $\dot{Q}_w$ from the water to the concrete. The temperature difference between the top-layer in sub-floor T_{top} and the room temperature T_a drives the heat transmission $\dot{Q}_f$ from the sub-floor through the top-floor to the room. The room temperature is then determined by the heat received from the floor $\dot{Q}_f$ and the disturbances $\dot{Q}_d$.

In the following we will present the modelling of each of the 3 parts, depicted in Figure E.4.

E.4.1 The sub-floor

The relatively thick concrete layer, the low heat transfer from the concrete to the room and the low heat conduction in the concrete results in a a high Biot number $>> 1$, i.e. the concrete temperature can not be considered to be lumped, hence a distributed temperature model has to be used [7]. To simplify the modelling, the concrete sub-floor is divided in to a number of volumes with a uniform temperature. As the temperature gradient changes in a radial direction from the heating pipes into the concrete, the concrete is divided into $n+1$ ring-shaped volumes with identical thicknesses L (see Figure E.5). The last "top layer" (number $n+1$) is not ring-shaped but still considered to have a uniform temperature. When the heat is transmitted from the water to the concrete, the water and concrete temperature drops along the pipe. This feature can be modelled by slicing the concrete subfloor into m slices along the pipe, as depicted in Figure E.6. However the transversal heat conduction between slices is neglected. Furthermore the "top concrete layer" in all of the slices are assumed to have the same temperature, i.e. it can be considered as one big piece. All in all this results in a 2 dimensional model as depicted in Figure E.5 and E.6.

In the following we will use the description $E_{i,j}$ for the element located at j^{th} layer in i^{th} slice. This means that $T_{i,j}$ is the temperature of the cylindrical concrete element

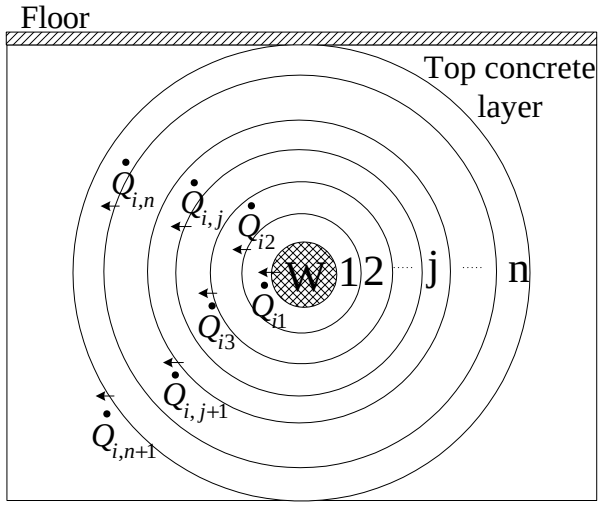

Figure E.5: Finite elements-layers around water pipe

(i,j) and $\dot{Q}_{i,j}$ is heat flow from the cylindrical element $(i,(j-1))$ to (i,j), note that $\dot{Q}_{i,1}$ is the heat flow from water pipe slice i to concrete layer $(i,1)$. $T_{w,in,i}$ is the water inlet temperature of the i^{th} pipe slice. $T_{w,out,i}$ is the water outlet temperature of the i^{th} pipe slice. The mean temperature of the water in a slice is approximated by the inlet temperature of the slice.
Using this notation the heat flow $\dot{Q}_{i,j}$ can be written as,

$$\dot{Q}_{i,j} = \begin{cases} \frac{(T_{w,in,i}-T_{i,j})}{Rwc} & i=1,2\cdots m, j=1, \\ \frac{(T_{i,j-1}-T_{i,j})\cdot K\cdot A_{i,j}}{L} & i=1,2\cdots m, j=2,3\cdots n, \\ \frac{(T_{i,j-1}-T_{top})\cdot K\cdot A_{i,j}}{L} & i=1,2\cdots m, j=n+1, \end{cases} \tag{E.1}$$

where $R_{wc}$is the thermal resistance from water to the concrete, $A_{i,j}$ is the surface area between element $(i,j-1)$ and (i,j) and, K is heat conductivity of concrete. The total heat transmitted from water is given by $\dot{Q}_w = \sum_{i=1}^{m} \dot{Q}_{i,1}$

The temperature $T_{i,j}$ can be determined as:

$$\frac{dT_{i,j}}{dt} = \frac{\dot{Q}_{i,j} - \dot{Q}_{i,j+1}}{C_{pc}\cdot m_{i,j}} \quad \text{where } i=1,2\cdots m, j=1,2\cdots n \tag{E.2}$$

Where C_{pc} is the specific heat capacity of concrete and m_{ij} is the mass of the element (i,j).

Since the top concrete layer is considered as a whole piece the temperature of this

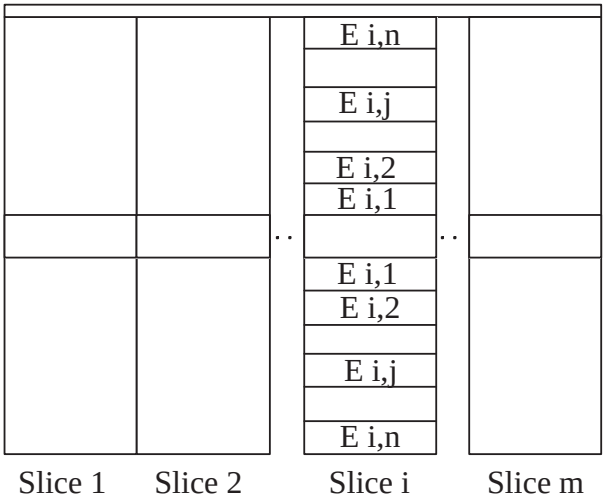

Figure E.6: Finite elements-slices along water pipe

layer is assumed to be uniform, and hence it can be computed as,

$$\frac{dT_{top}}{dt} = \frac{\sum_{i=1}^{m} \dot{Q}_{i,n+1} - \dot{Q}_f}{C_{pc} \cdot m_{top}} \tag{E.3}$$

The temperature of the water out of slice i is

$$T_{w,out,i} = T_{w,in,i} - \frac{\dot{Q}_{i,1}}{C_{pw} \cdot \dot{m}} \quad \text{where } i = 1, 2 \cdots m, \tag{E.4}$$

where C_{pw} is specific heat capacity of water, $\dot{m}$ is water mass flow and the inlet temperature of water to the i^{th} slice $T_{w,in,i}$ is given by,

$$T_{w,in,i} = \begin{cases} T_{w,out,i-1} & i = 2, 3 \cdots m \\ T_{w,in} & i = 1 \end{cases} \tag{E.5}$$

where $T_{w,in}$ is the inlet temperature of water to the floor and $T_{w,out} = T_{w,out,m}$ is the outlet temperature from the floor.

E.4.2 The top-floor and the room

The heat capacity of the top-floor is neglected as it is much smaller than that of the sub-floor. The energy flow from the concrete to the room through the top-floor is simply computed considering the top-floor as a heat resistance, i.e.

$$\dot{Q}_f = \frac{(T_{top} - T_a)}{R_{ca}}, \tag{E.6}$$

where R_{ca} is the thermal resistance between the top concrete layer and the room air. T_a is the room temperature.
Finally the room temperature is computed, assuming a uniform temperature of the room (i.e. perfect mixing of the air) as follows,

$$\frac{dT_a}{dt} = \frac{\dot{Q}_f - \dot{Q}_d}{C_{pa} m_a}, \tag{E.7}$$

where $\dot{Q}_d$ is the net heat loss from room to the ambient environment, C_{p_a} is the specific heat capacity of air and, m_a is the mass of the air inside the room.

Connecting the models as depicted in Figure E.4 gives the total model.

E.5 Model validation

The model validation is carried out by comparing experimental data from the test floor heating system with the data from the mathematic model. The experiment is done in a test room of 16 m^2, which has 10cm thick concrete sub-floor with a cast in water pipe $4m$ per m^2.

An experiment is conducted, where an 1 hour burst of hot water is led into the floor. Hereafter, the heating valve is switched off, and the water circulates through the floor without adding heat. In this way the outlet water temperature $T_{w,out}$ (test floor) in Figure E.7, can be seen. $T_{w,in}$ is the water inlet temperature. By applying the same water inlet temperature and the same initial conditions to the model, the outlet water temperature from the model $T_{w,out}$ (model) is computed. By studying Figure E.7 it can be seen that the outlet water temperature from test system and the model are very close to each other. This shows that the model gives a very good description of the temperature propagation in the real floor system, as the outlet temperature of the water equals the warmest layer in the concrete.

Figure E.8 shows how the outlet water temperature reacts when the floor design parameters of the same house is changed in the model, when conducting the same experiment as described above. This is in an effort to investigate what will happen to the characteristics of the floor heating system, when the thickness of the sub-floor and the length of the heating pipes are changed. For a house of $16m^2$ with concrete sub-floor and wooded top-floor, in theory, the water outlet temperature from a 5cm and 10cm concrete sub-floor should be the same in the first period of the experiment, when bursting hot water into the floor. When the heat "wave" in the 5 cm sub-floor reaches the surface of the concrete, after approximately 0.5 hours, the overall concrete temperature starts to increase faster than in the 10 cm sub-floor. This is because the large thermal resistance of the wooden top-floor largely prevents heat transmission to the room. When heat burst stops, the outlet temperatures from both systems drop down, however after approximately 4 hour the outlet temperature form 5cm sub-floor will be lower than the temperature from 10cm sub-floor because of the smaller heat capacity.

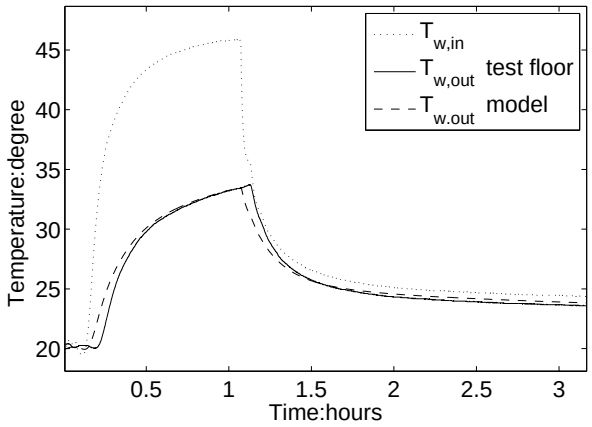

Figure E.7: Water outlet temperatures from test system and model, when applying the same inlet temperature

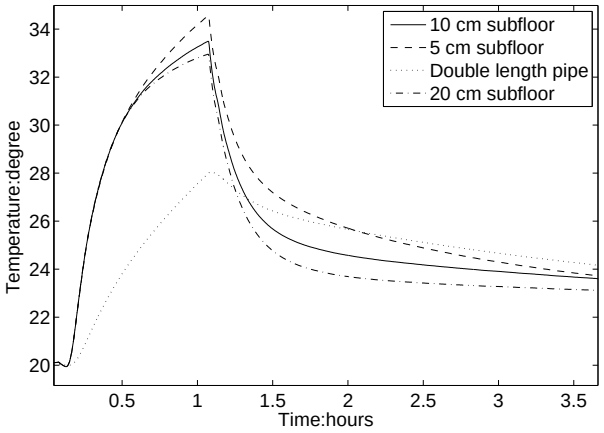

Figure E.8: Outlet water temperature from the models with different design parameters

For the same house, if there is a double length water pipe casted into the sub-floor ($8m$ per m^2), the water outlet temperature should be lower comparing to the house with $4m$ per m^2. This is because the heat transfer from the water to the concrete is twice as good, and hence more heat is transmitted to the sub-floor. When the heat burst stops, the outlet water temperature decreases slower than the $4m$ per m^2, because the distance between the pipes is smaller and the temperature therefore equalizes faster in the concrete.

The results from the mathematic model, shown in Figure E.8, give a good insight on how the various design parameter of the sub-floors alters the behavior of the temperature propagation in the floor. This information is useful later on when the generality of the proposed control strategy is discussed.

E.6 Control approach

The proposed control strategy depicted in Figure E.9 aims at dividing the control problem into two parts, an inner loop that maintains a desired concrete temperature, and an outer loop that controls the room temperature. The overall strategy can be formulated

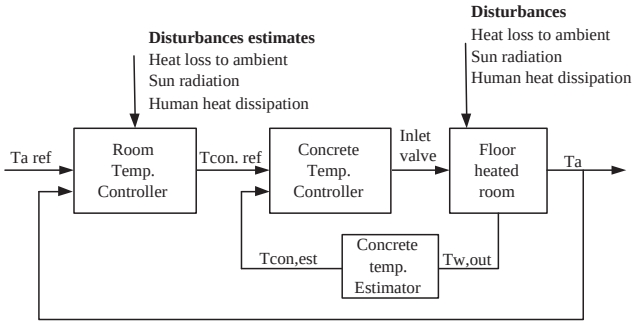

Figure E.9: A sketch of the proposed control design with an inner loop controlling the concrete temperature and an outer loop controlling the room temperature

by the repeated three steps

1 Estimate the current concrete temperature $\widehat{T}_{concrete}(t)$

2 Calculate heat burst Q_{burst} that will bring the concrete temperature up to set-point

3 Apply the needed heat

E.6.1 Estimating the concrete temperature

To install a temperature sensor in the concrete layer has proven impractical for a number of reasons. Firstly, a sensor placed in the concrete layer is hard to service and replace,

especially with a wooden floor on top. Secondly, the placement of the sensor is very important. If it is placed close to the water pipes it will react very fast to the heating. If it is placed in the middle between two heat pipes, it would not react until the heat gradients reach the place furthest away from the water pipe.

We propose to use the water temperature to estimate the concrete temperature. After an idle period without heating, the water and the concrete equalize temperature. If we measure the water temperature after such an idle period, the measurement will reflect the warmest place of the concrete that is closest to the water pipes. With an increased idle period the temperature gradients in the concrete becomes smaller and we will obtain a lower temperature measurement as illustrated with the temperature curve after the heating burst in Figure E.7.

E.6.2 Estimating the concrete heat capacity

We propose an experimental based approach that gives a "dynamic" heat capacity of the concrete. The main idea is to perform an experiment where we add a know amount of heat in a burst Q_{burst} and measure the temperature increase $\Delta T_{concrete}$. The heat capacity $Cp_{concrete}$ can the be calculated as

$$Cp_{concrete} = \frac{Q_{burst}}{\Delta T_{concrete}}. \tag{E.8}$$

Figure E.10 illustrates such an experiment performed on our test setup. In the initial phase after the heating burst (from t=68min) the water temperature drops fast. After the initial phase, the temperature decay becomes much smaller, which reflects that the temperature gradients goes from a radial phase to a transversal phase. We can extend Equation E.8 to give a dynamic heat capacity

$$\widehat{Cp}(t) = \frac{Q_{burst}}{\Delta T_{water}(t)}, \tag{E.9}$$

which is illustrated in the second axis of Figure E.10. Hence the dynamic heat capacity $\widehat{Cp}(t)$ value describes the level of equalization and not the actual heat capacity of the concrete floor. The temperature distribution in the concrete, where the layers closest to the water pipes are the warmest, ensures that the estimate of the dynamic heat capacity always is smaller than the real heat capacity.

E.7 Results

The inner control loop, i.e. the concrete temperature estimation and temperature controller, has been tested on the test system. As it is the inner control loop that poses the limitations in the obtainable performance as previously mentioned, we have focused our experiments on testing that. In order to test the dynamic performance of the proposed concrete temperature controller a heating up scenario has been conducted.

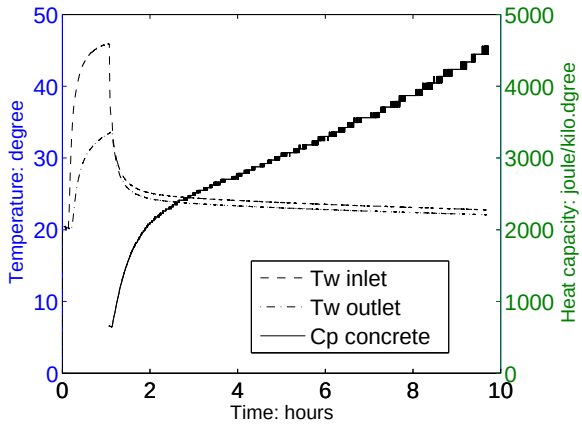

Figure E.10: A heat burst and the corresponding concrete heat capacity

An experiment was started from the following initial conditions; floor temperature of (23.5 ^oC) an outdoor temperature about 17 ^oC. The reference to the inner loop ($T_{con,ref}$) was the output from an outer room temperature controller, which had a reference $T_{a,ref}$=23.5 ^oC for the duration of the experiment.

We start by investigating how the concrete temperature reacts in an experiment using the proposed controller. Figure E.11 depicts the water outlet temperature ($T_{w,out}$), the estimated concrete temperature ($T_{con,est}$) and a "measured" concrete (sub-floor) temperature ($T_{con,mes}$). The measured concrete temperature is obtained by placing an isolated temperature sensor on the top floor, hereby an approximate temperature of the concrete top layer can be obtained. The concrete temperature is obtained by using the proposed method in Section E.6, i.e. by measuring the water outlet temperature a certain period (20 min) after a burst. In Figure E.11, at the beginning, the difference between the estimated concrete temperature and the measured top layer temperature is large. Recall that the estimated concrete temperature reflects the warmest place in the concrete (close to the pipe). Just after a burst (the spikes in $T_{w,out}$) the (radial) temperature gradient in the concrete is high meaning the temperature difference between the top layer and the inner layer close to the pipe is large. As time goes by after a burst the temperature in the concrete equalizes, meaning that the concrete temperature estimate ($T_{con,est}$) closes in on the measured top layer temperature. Because of the heat transmission to the room, the inner temperature of the concrete ($T_{con,est}$) will always be higher than the top layer temperature.

Figure E.12 depicts the reference for the inner control loop ($T_{con,ref}$) along with the estimated concrete temperature ($T_{con,est} = \hat{T}_{concrete}$). Furthermore the inlet temperature of the water ($T_{w,in}$) and the maximal allowed temperature of the bottom part of the wooden top-floor (37.5 ^oC) are depicted. At the beginning, when the reference is much

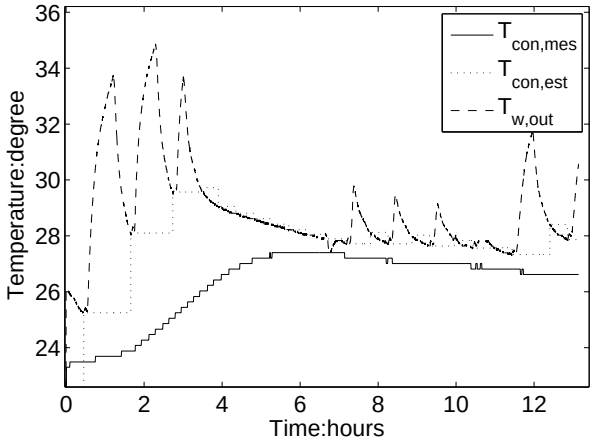

Figure E.11: Temperature of water outlet, estimated concrete temperature and measured top layer temperature from experiment of concrete temperature control

higher than estimated temperature, the concrete temperature increases fast. The concrete temperature control is limited to give the amount of heat that increases concrete temperature in maximum steps of 3K. Later when the reference temperature is lower than the estimated temperature, the heating stops and the concrete temperature drops until it is lower than reference temperature and heating is started again. In this state, the reference and the estimated temperature are very close to each other which shows that the concrete temperature can be controlled.

From Figure E.12 it can furthermore be seen that although the inlet water temperature exceeds the recommended maximum temperature $37.5°C$[6] of the concrete subfloor (which it would not in the current control schemes) the concrete temperature never exceeds the limitation. The estimated concrete temperature describes, as previously mentioned, the temperature in the warmest place of the concrete. By controlling the estimated concrete temperature to be lower than the limit of the floor, it can therefore be ensured with a good margin that the top layer temperature never exceeds the temperature limitation. As the test shows it is therefore possible to have a much higher inlet temperature and hence increase the response time considerably.

Figure E.13 shows the simulated temperature distribution in the concrete floor using the same concrete temperature controller and initial conditions as in the experiment above. The reference to the concrete controller was set to 30 ^oC. By conducting this experiment on the model we are able to study temperature distribution in the different layers. Concrete layer 1 (5mm) is the closest to the water pipe and layer 2 (3cm) is further away from the water pipe. The top layer is adjacent to the top floor which can be see in Figure E.5. We can see that the concrete close to the pipe get a higher temperature than the outer layers. The applied principle of estimating the concrete temperature

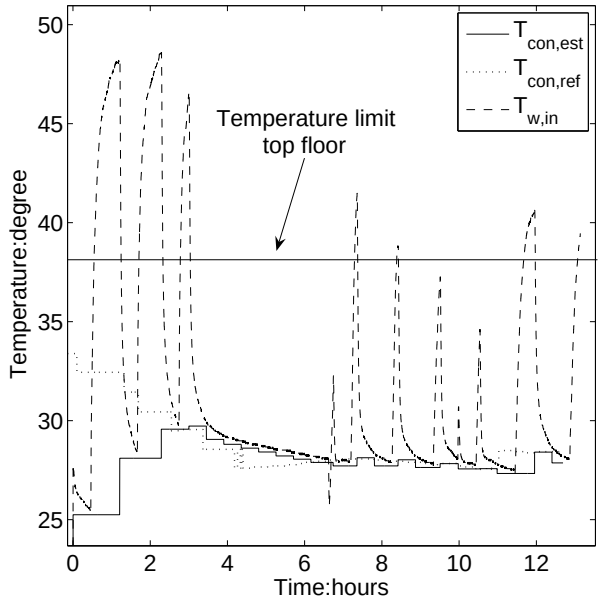

Figure E.12: Concrete temperature reference and estimate from experiment of concrete temperature control

is also illustrated, where the concrete estimate is assigned to the water temperature 20 min. after a heating burst.

E.8 Concluding remarks

The objective of this paper was to present and evaluate a proposed control strategy for controlling the temperature in a water-based floor heating system. The inherited problems with the current strategy was discussed and a finite element type of model of the concrete floor was defined and validated with experimental data. The proposed strategy - a cascaded setup - was presented and validated by applying it to a real application. Simulation results elaborates the experimental results by demonstrating how the different layers of the concrete respond to the control approach. The main conclusion is that the control scheme is capable of controlling the concrete temperature in a fast and precise way without overshoot and without exceeding the temperature limit of the floor. Furthermore, it is possible to estimate the concrete temperature using the return water temperature.

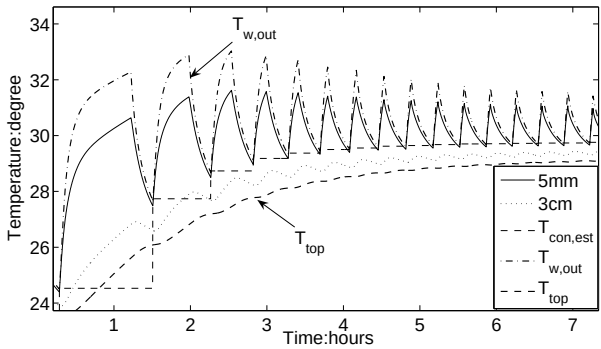

Figure E.13: Concrete temperature distribution from mathematic model test

Bibliography

[1] A.K. Athienitis and T.Y. Chen. Experimental and theoretical investigation of floor heating with thermal storage. *ASHRAE Transactions*, 99, 1049-1057.

[2] Bjarne W. Olesen. Control of floor heating and cooling system. *Clima 2000/ Napoli 2001 World Congress-Napoli, Italy*, 2001.

[3] A. K. Thienitis and T. Chen. Numerical study of thermostat setpoint profiles for floor radiant heating and the effect of thermal mass. *ASHRAE Transactions*, 103, 1997.

[4] T.Y. Chen. Application of adaptive predictive control to a floor heating system with a large thermal lag. *energi building*, 34, 2002.

[5] A. K. Thienitis. A predictive control algorithm for massive buildings. *ASHRAE Transactions*, 94, 1998.

[6] The QR Transformation I Junckers Ltd. E 4.0 solid hardwood flooring. general information. underfloor heating. *junckers.techinfo.wp.dk/PDF/E40uk.pdf*, 2006.

[7] Yunus A. Cengel and Robert H. Turner. Fundamentals of thermal-fluid sciences. *McGraw-Hill*, 2005.

Appendix F

Disturbance rejection of a water-based floor heating system

(Proceedings of International Control Conference , 2006, Glasgow, Scotland, United Kingdom.)

Honglian Thybo, Lars Larsen and Claus Thybo

Abstract

The objective of this study is to propose a control scheme that aims at increasing the control performance of a water-based floor heating system with a large thermal capacity. Experience shows that although floor heating is preferred due to the comfort of the warm floor, the slow control dynamics decreases the overall customer satisfaction. This paper analyzes the disturbance rejection problem and proposes a dynamic feed-forward scheme, aimed at rejecting the outdoor temperature disturbance. The proposed control scheme is validated using simulation and experimental results.

F.1 Introduction

Water-based floor heating systems have during the recent years been increasingly used. The reason why floor heating systems are preferred is mainly due to the increased comfort of having a warm floor (e.g. in bathrooms) and a more uniform temperature distribution in the heated room (due to the large heat transmitting surface i.e. the floor)[1].
A typical water-based floor heating system consists of a circulation pump that maintains the required flow of heated water to casted-in water pipes in the floors of the heated rooms. In particular, each floor can be divided into a top-floor, made of e.g. wood or

tiles, and a sub-floor, where the water pipes are casted into concrete. Each of the heated floors has a control valve for hot water, that needs to be opened and closed such that the air temperature in room is kept close to the desired reference to ensure a high comfort.
For many years, the control of water-based floor heating systems has been based on relay controllers, which are flexible and simple. Typically each room is equipped with an independent relay controller that regulates the air temperature in the room by manipulating the control valve [2] and [3]. Furthermore the inlet temperature of the hot water to the floor is regulated by a thermostat, thus indirectly assuring that the temperature in the top-floor does not exceed the material limitation (e.g. wooden floors can be destroyed) and the comfort criteria (that the floor does not get too hot). The major drawback, however, is that the control due to the large heat capacity of the concrete sub-floor and the limited upper inlet temperature of the water exhibits a very slow response and an extensive overshoot in the air temperature.
Motivated by these difficulties, we presents a novel control for increasing the dynamic performance. We propose a cascaded control structure with an inner loop that controls the temperature of the sub-floor (concrete) and an outer loop that controls the air temperature in the room. The control problem is however significantly complicated by the fact that the temperature in the sub-floor is distributed and hard to measure, and the control valves are restricted to discrete values (open/closed). To accommodate these difficulties a novel approach for estimating and controlling the sub-floor temperature was introduced in a earlier paper [4]. This paper treats the other problem of rejecting the disturbances, here especially the effects of outdoor temperature changes is considered.
The paper is structured in the following way.
Section F.2 describes the basic layout of a typical water-based floor heating system and the used test system. Section F.3 provides an overview of the traditional control setup and the control objectives. Section F.4 summarizes the simplified model of the floor heating system with emphasis on the room modelling and in Section F.5, the control strategy is formulated and a dynamic feed-forward scheme is proposed. The results with disturbance rejection is discussed in Section F.6. Conclusions are drawn in Section F.7.

F.2 System description

A typically water-based floor heating system can be divided into two parts; a water circuit and the heated floor and room. In the following we describe each of these parts.
Water Circuit
The water circuit supplies warm water to the heated floors by mixing the return water from the heated floors with an external supply of hot water, see Figure F.1. The redundant amount of cold water in the water circuit is released at the outlet of the return manifold. The inlet temperature to the distributing manifold and hence to the heated floors ($T_{w,in}$) is controlled by a thermostatic valve that adjusts the amount of hot water mixed in the water circuit as shown in Figure F.1.
The inlet temperature to the floor is measured at the distributing manifold. The outlet

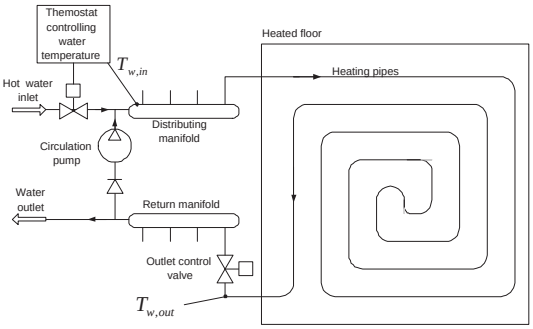

Figure F.1: Sketch of the water based floor heating system

temperature is measured just before the outlet valve.

Heated Floor and Room

The heated floor can be divided into a top-floor and a sub-floor. The sub-floor is typically made of concrete where the heating pipes are casted into. By supplying heated water ($\dot{Q}_w$) to the heating pipes the sub-floor is heated. The heat from the sub-floor is transmitted to the room through the top-floor ($\dot{Q}_f$), i.e. the top-floor can be regarded as a resistance in the heat transmission, see Figure F.2. The top-floor, which is placed on top of the sub-floor, is made of e.g. wood or tiles etc. The walls of the room is typically made of bricks and is insolated with a layer of insolation to prevent heat loss to the outdoor surroundings.

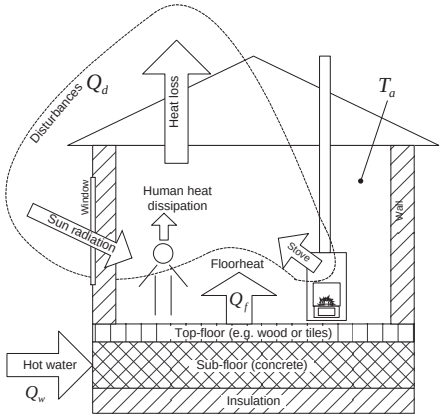

Figure F.2: Sketch of the floor heated room and the affecting disturbances

The room temperature (T_a) is measured by a temperature sensor mounted, typically on the wall of the room in question. This temperature measurement is used in the room

temperature control. Figure F.2 furthermore depicts a number of possible disturbances to the temperature control.

The experimental results are obtained on a test system having the features described above.

F.3 Control problem description

The control challenges of a water-based floor heating system can be divided into two objectives, rejecting disturbances and following set-point. In most domestic houses the temperature set-point is fairly constant and only changed in relation to away periods, such as holidays. The objective after a set-point increase is as quickly as possible to get up to the new set-point without overshoot. Rejecting disturbances is the main day to day challenge. The outdoor climate is often treated as the sole disturbance, but additional heat sources and also water inlet temperature and pressure variations contributes. Climate disturbances are primarily outdoor temperature variations, but also wind and radiation play a role. Other disturbances can be in form of sun radiation through the window, a wood burning stove or human heat dissipation etc. (see Figure F.2).

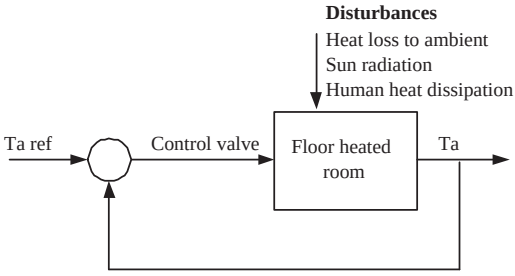

Figure F.3: A sketch of the current control approach

Figure F.3 shows the floor heating system as it is viewed from typical control systems, where the outlet valve is used as actuator, using the air temperature of the room directly as feedback for a relay type control. The main problem with this approach is in regards to disturbances, where the large uncontrolled thermal capacity of the concrete floor makes it difficult to compensate for outdoor climate variations and other heat-sources. The current relay approach wait for the inside temperature to fall below the set-point before the control valve is opened. The concrete subfloor then has to increase the temperature to a level, where it can accommodate the increased heat load. This gives an undesired undershoot in temperature until the concrete temperature catches up. The same type of problem can appear in the early hours of the day, where the outdoor temperature increases fast. Sun radiation through the windows may even further decrease the heating demand very fast. Even when the control system closes the inlet valve when the inside

temperature exceeds the set-point, the thermal capacity of the warm under-floor will still contribute to an increase of the room temperature. The severity of these problems greatly depends on the thermal resistance of the floor. A high thermal resistance floor type, such as a wooden floor requires a much higher sub-floor temperature to provide the needed heating compared to a low thermal resistance type (e.g. tiles). A wood floor also needs to respect a maximum temperature to ensure that the floor is not damaged. The wood floor producer Junckers Ltd. [5] recommends a maximum concrete temperature of $37.5°C$, which in the current control structure limits the inlet temperature, and as a result of that also limits ability to change the concrete temperature fast.

F.4 Modelling

The model of the floor heating system can be divided into three parts, the sub-floor, the top-floor and room, which are connected as depicted in Figure F.4. In this section, we will first briefly state the floor model (top-floor and sub-floor) for a detailed description the reader is referred to [4]. Secondly, a model of the room that takes the walls in to account is derived.
The floor contains the slowest dynamic in the control system and hence poses the limitations to the obtainable dynamic performance. The dynamics of the water circuit is much faster than the heated floor and therefor is not discussed in detail here. The concrete

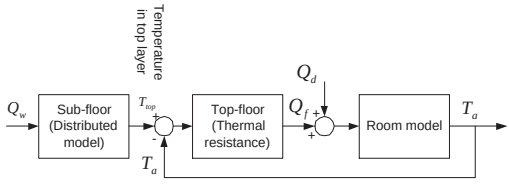

Figure F.4: Schematic view of the room and floor model.

sub-floor is heated by circulating hot water trough the floor, i.e. by transmitting the heat $\dot{Q}_w$ from the water to the concrete. The temperature difference between the top-layer in sub-floor T_{top} and the room temperature T_a drives the heat transmission $\dot{Q}_f$ from the sub-floor through the top-floor to the room. The room temperature is then determined by the heat received from the floor $\dot{Q}_f$ and the disturbances $\dot{Q}_d$ from the heat loss through the walls.
In the following we will present the modeling of each of the 3 parts, depicted in Figure F.4.
The Sub-Floor
The relatively thick concrete layer, the low heat transfer from the concrete to the room and the low heat conduction in the concrete results in a a high biot number $>> 1$, i.e.

the concrete temperature can not be considered to be lumped, hence a distributed temperature model has to be used [6]. The detailed model of the subfloor can be in [4].

The Top-Floor

The heat capacity of the top-floor is neglected as it is much smaller than that of the subfloor. The energy flow from the concrete to the room through the top-floor is simply computed considering the top-floor as a heat resistance, i.e.

$$\dot{Q}_f = \frac{(T_{top} - T_a)}{R_{ca}}, \tag{F.1}$$

where R_{ca} is the thermal resistance between the top concrete layer and the room air. T_a is the room temperature.

Room Model

In the modelling of the heated room, we will consider the air inside the room and the walls (we assume that the roof is well insulated and no heat is transmitted through the windows).

The room temperature T_a can be simply computed using equation F.1, with the assumption of a uniform temperature distribution in the room (i.e. perfect mixing of the air).

$$\frac{dT_a}{dt} = \frac{\dot{Q}_f - \dot{Q}_d}{C_{pa} m_a}, \tag{F.2}$$

C_{p_a} is the specific heat capacity of air and, m_a is the mass of the air inside the room. The main disturbance $\dot{Q}_d$ is the climate disturbances, i.e. day to day temperature change, sun radiation etc. Among these disturbances the outdoor temperature variations is one causing the largest heat losses. In this paper we will only consider the heat loss through the wall due to the outdoor temperature variation. The amount of the heat loss through the wall is mainly determined by the wall construction. There are many different ways to construct a wall. In this paper we will consider a wall type with an insulation layer placed between an inner and outer wall layer as depicted in Figure F.5. The insulation

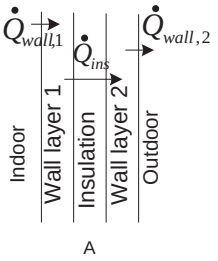

Figure F.5: wall construction

layer is place between an inner and outer wall, i.e. the heat loss from indoor air $\dot{Q}_d$ is

the heat transferring from indoor air to wall layer 1. By assuming each layer (insolation and walls) are lumped following model can be derived:

$$\dot{Q}_d = \dot{Q}_{wall,1}, \tag{F.3}$$

$$\dot{Q}_{wall,1} = \frac{(T_a - T_{wall,1})}{R_{aw}}, \tag{F.4}$$

where R_{aw} is the thermal resistance from indoor air to wall layer 1. The temperature of the wall layer 1 can be calculated as,

$$\frac{dT_{wall,1}}{dt} = \frac{\dot{Q}_d - \dot{Q}_{ins}}{C_{pw,1} \cdot m_{wall,1}}, \tag{F.5}$$

where $C_{pw,1}$ is the specific heat capacity of wall layer 1, $m_{wall,1}$ is the mass of the wall layer 1. The heat transmission through insulation layer is,

$$\dot{Q}_{ins} = \frac{(T_{wall,1} - T_{wall,2})}{R_{ins}} \tag{F.6}$$

where R_{ins} is the thermal resistance of the insulation layer. The temperature of wall layer 2 is,

$$\frac{dT_{wall,2}}{dt} = \frac{\dot{Q}_{ins} - \dot{Q}_{wall,2}}{C_{pw,2} \cdot m_{wall,2}}, \tag{F.7}$$

$C_{pw,2}$ is the specific heat capacity of wall layer 2. The heat loss from wall layer 2 to ambient environment is,

$$\dot{Q}_{wall,2} = \frac{(T_{wall,2} - T_o)}{R_{wa}}, \tag{F.8}$$

where R_{wa} is the thermal resistance from wall layer 2 to ambient environment. Connecting the models as depicted in Figure F.4 gives the total model.

F.5 Control strategy

In this section, the overall disturbance strategy is introduced and the disturbance rejection will be discussed in detail.

The overall control strategy

The proposed control strategy depicted in Figure F.6 aims at dividing the control problem into two parts, an inner loop that maintains a desired concrete temperature, and an outer loop that controls the room temperature. The overall strategy can be formulated by the repeated three steps

1 Estimate the current concrete temperature $\widehat{T}_{concrete}(t)$

2 Calculate heat burst Q_{burst} that will bring the concrete temperature up to set-point

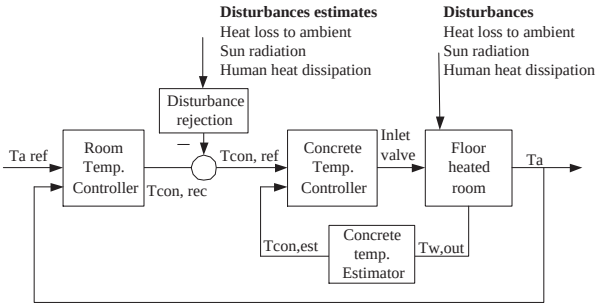

Figure F.6: A sketch of the proposed control design with an inner loop controlling the concrete temperature and an outer loop controlling the room temperature

3 Apply the needed heat

The details of the approach can be found in [4].
The disturbance rejection
There are several kinds of disturbances as previously mentioned. In order to perfectly compensate a given disturbance, the heating source must have faster dynamics than the disturbance coming into the heating system. The disturbance caused by the heat loss through the wall due to the outside temperature variations is quite slow, and thus we can use the water based floor heating system to reject it. For the faster disturbances like e.g. sun radiation, other faster heat sources like a radiator would be required.
In the following we will propose a feed forward compensation for rejecting the outdoor temperature disturbance. For the dynamic disturbance compensation shown in Figure F.6, the key idea is to compensate the concrete temperature reference by feeding the outdoor temperature To forward through a transfer function containing a disturbance model (the wall model) an inverse system model (the controlled floor temperature). The models are both approximated to first order models. The reason for using such a low order approximation is that the disturbance can be assumed to be sinusoidal with a 24 hour period. The modelling problem can therefore be reduced to identifying a transfer function with the same gain and phase-shift as the real system at this particular frequency, hence a first order functions will be sufficient.
Transfer Function of Wall
An experiment to get the parameters for the wall transfer function was conducted, where we gave a constant reference to the concrete temperature controller. For the model, an outdoor temperature change was simulated as a sinusoid wave, which had a mean value of 2 $^{\circ}C$, amplitude of 4$^{\circ}C$, and a 24 hour period. The results can be seen in Figure F.10. The phase shift and the gain of the room air temperature to the outdoor temperature change can be calculated in Figure F.10, by finding the phase-shift between the two curves and the amplitude ratio of the two curves. The information is then used to

calculate the time constant and gain for the estimation of wall transfer function.
A real house experiment was carried out to test this method, and the results are shown in Figure F.9(in this paper, all the experiments with real house were conducted in May 2006 in Denmark.). In reality, it is difficult to get a sinusoidal indoor temperature. The affecting factors are outdoor temperature which is not ideal sinusoidal, sun radiation, which was treated by closing the curtain in the real house test, but still some affects from sunshine, wind etc. The temperature results from outdoor and indoor were filtered with same low pass filter (but not shown in FigureF.9) for calculation , so that they could have same phase shift and same gain from the filter, which would not affect phase shift and amplitude ratio between indoor temperature and outdoor temperature. Then we can calculate the time constant and gain for the estimation of transfer function.
For the experiments, the ideal condition should be that there is only heat transferring between indoor and outdoor, no heat coming into the room from floor. In the experiments with both the model and the test house, it would be ideal that the concrete temperature is same as the indoor temperature all the time, so that no heat transfers into the room from floor, but in reality we can not control the floor temperature so precisely. We used a constant concrete floor temperature instead in the experiments.
Approximating the System Transfer Function
This experiment was done in the same way as transfer function of wall estimation experiment, by applying sinusoid signal into the concrete temperature controller, which had a mean value 25 $^{\circ}C$ and an amplitude of $2^{\circ}C$. So we get Figure F.7, from which the phase shift and gain can be calculate for the transfer function of controller+the heated floor.
An experiment with test house was also conducted, the result can be seen in Figure F.8. The temperature signals from both the concrete set-point and the room were filtered through same filter (but not shown in Figure F.8), so that we could get better temperature curves and easy to find the phase shift and amplitude ratio between concrete temperature and room air temperature.

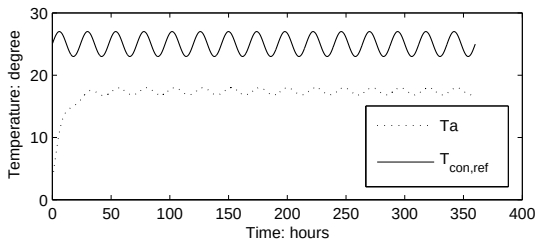

Figure F.7: Experiment of transfer function estimation for concrete temperature controller and floor heated room-model

Obtaining the transfer function form the wall (G_d) and for the controlled concrete floor (G_c) the dynamic compensation term is simply given by $\frac{G_d}{G_c}$.

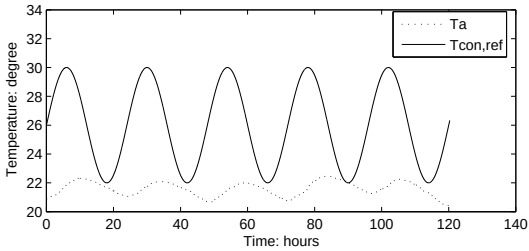

Figure F.8: Experiment of transfer function estimation for concrete temperature controller and floor heated room-test house

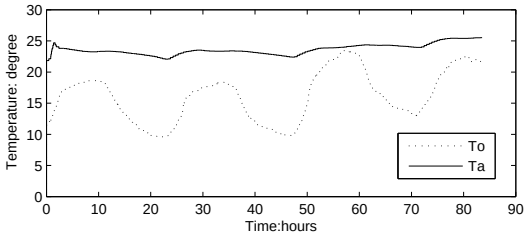

Figure F.9: Experiment of transfer function estimation for wall transfer function-test house

F.6 Results

The inner control loop, i.e. the concrete temperature estimation and temperature controller, has been tested previously on the test system, for details see paper [4]. In this section we will therefore only focus on the affects of disturbance rejection. Following 3 experiments are conducted for the floor heating system.(For all the experiments the reference concrete temperature $T_{con,ref}$ has been kept a constant see Figure F.6)

F.6.1 The system without disturbance compensation

The aim of this experiment is to see how the disturbance affects the indoor temperature. For the experiment with model, at the beginning of the experiment, a constant 2 was applied to outdoor temperature, and later sinusoid temperature disturbance was applied. The results are shown in Figure F.10. we can see that when there is no outdoor temperature change (constant 2 $^{\circ}C$), the room temperature keeps at a constant value when the heating system reaches a steady state. When disturbance comes the room temperature changes between 16.5 to 17.5 $^{\circ}C$, i.e. a temperature variation of $\pm 0.5^{\circ}C$. For a test house the outdoor temperature disturbance can be seen in Figure F.9. The indoor temperature changes with the outdoor temperature variations.

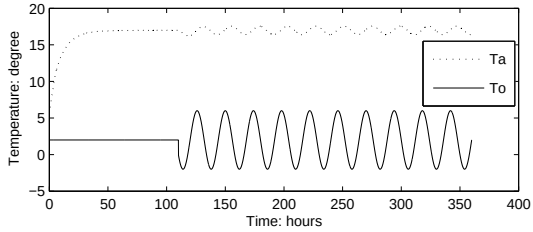

Figure F.10: Outdoor disturbance affects on indoor temperature-model

F.6.2 The system with static disturbance compensation

Static disturbance rejection experiment is carried out by applying a constant value to the disturbance compensation term, which is a result of wall static gain divided by gain of concrete temperature controller + floor heated room. The static gains can be obtained from a step response for the wall with outdoor temperature change from 2 to 6$^{\circ}C$, and for the concrete temperature controller+floor with concrete set-point temperature change from 28 to 32$^{\circ}C$. The function of static disturbance rejection is shown in Figure F.11 when a sinusoid wave is adopted as a outdoor temperature and a constant controller reference temperature 28 $^{\circ}C$ is applied. Comparing with Figure F.10, the indoor temperature change is from 16.7 to 17.35$^{\circ}C$ ($\pm 0.33^{\circ}C$), so a static gain is not very effective for the disturbance rejection. This is of course due to the fact that phase is not taken in to account.

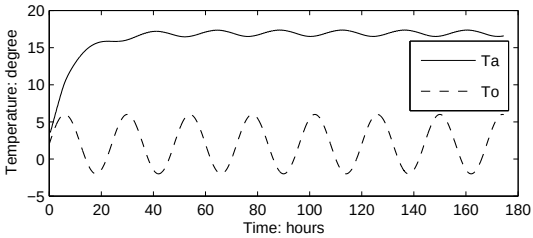

Figure F.11: Disturbance rejection using a static feed forward scheme-model

F.6.3 The system with dynamic disturbance compensation

This experiment aims at investigating the effect of dynamic disturbance rejection. First an experiment was carried out with a mathematical model. A sinusoid wave with bias 2 $^{\circ}C$ and amplitude 4 $^{\circ}C$ was applied to outdoor temperature. A dynamic disturbance compensation term was added to the control system as shown in Figure F.6. Figure F.12 shows the results. We can see that the indoor temperature change has been limited to

16.86 to 17 $^{\circ}C$, i.e. the temperature variations are reduced to $\pm 0.07^{\circ}C$. This is much better than the system without disturbance compensation term, comparing to the system with static disturbance rejection, this system can almost eliminate the influence from disturbance.
An experiment with real house was also conducted. The result can be see in Figure F.13. From hour 0 to 32, it was cloudy outside, and the room temperature was kept at a stable level with a outdoor temperature change from 8 to 16 $^{\circ}C$. From hour 32, the indoor temperature T_a increased as a result of sun radiation. The room was facing east. Hence, the main sun radiation was in the early hours of the day.

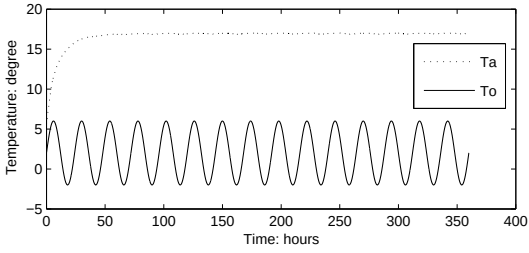

Figure F.12: Disturbance rejection using a dynamic feed forward scheme-model

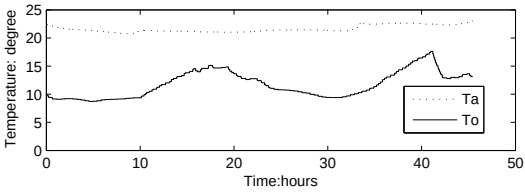

Figure F.13: Disturbance rejection using a dynamic feed forward scheme-test house

F.7 Concluding remarks

The objective of this paper was to present and evaluate a proposed disturbance compensation scheme for a water-based floor heating system. The inherited problems with the current strategy was discussed. The proposed rejection strategy - a dynamic feed forward compensator - was presented and validated by simulation and applying it to a real application. The main conclusion is that the disturbance rejection scheme is capable of rejecting the outdoor temperature variations almost totally and hence improve the indoor climate. This assumes however that the disturbances are sinusoidal, which is a crude simplification. Hence, disturbances with higher frequencies are not rejected

totally. The paper also points out that the problem of obtaining the wall and concrete transfer function is not trivial in practice.

Bibliography

[1] Bjarne W. Olesen. Radiant floor heating in theory and practice. *ASHRAE Journal*, July 2002.

[2] Bjarne W. Olesen. Control of floor heating and cooling system. *Clima 2000/ Napoli 2001 World Congress-Napoli(I)*, 2001.

[3] Weitzmann P. and Svendsen S. Numerical investigation of floor heating system in low energy house. *Paper for 6th symposium on Building Physics in the Nordic Countries,*, pages 905–912, 2002.

[4] Honglian Thybo, Lars FS Larsen, and Claus Thybo. Control of a water based floor heating system. *CCA*, 2007.

[5] Junckers. E 4.0 solid hardwood flooring. general information. underfloor heating. *http://www.junckers.dk*, 2003.

[6] Yunus A. Cengel and Robert H. Turner. Fundamentals of thermal-fluid sciences. *McGraw-Hill*, 2005.

Appendix G

Control challenges in domestic heating systems

(Proceedings of the European Control Conference, 2007, Kos , Greece.)

Honglian Thybo, Lars Larsen and Peter Weitzmann

Abstract

The objective of this paper is to analyze domestic heating applications and identify unfavorable building constructions and control challenges to be addressed by high performance heating control systems. Heating of domestic houses use a large amount of the total energy consumption in Scandinavia. Hence the potential of reducing energy consumption by applying high performance control is vast. Indoor climate issues are becoming more in focus, which also leads to a demand for high performance heating systems. The paper presents an analysis of how the building elements of today's domestic houses with water based floor heating affect the control challenge. The analysis is documented with simulation results.

G.1 Introduction

Heating control in domestic houses is not a new application. Thermostatic control valves has for years been applied in order make heat emitters deliver the amount of heat. This has proven to be a huge step in energy efficiency and still is today.
The control objectives domestic heating systems control can essentially be divided two i.e. following a desired temperature set-point, and rejecting disturbances. The desired temperature is normally fairly constant. People might want to lower the temperature a

little at night or when they are away from the house in longer periods. The argument here is mainly to save energy. Disturbances comes in form of sun radiation (especially through windows), changing outdoor temperature or wind, but also in form of changing indoor heat dissipation. The sensitivity to disturbances and the response time in set-point changes factors greatly depends on the house construction type as it will be shown later on.
The two current driving forces in the future trends of building style are; 1) the increasing price of energy and 2) environmental issues. They both drives the customer of new houses to demand low energy house constructions. Furthermore legislation, such as [1] has an impact on the construction types. Nevertheless a large part the market for heating controls is for retrofit, meaning that it is important to analyze the control challenge of the retrofit type as well. More and more domestic houses in Scandinavia are equipped with floor heating. An approach to design of a high-performance is discussed in [2]. Active disturbance rejection using adaptive wall and floor models are treated in [3] The objectives in this paper is analyze how the construction type influences the control challenge. This results can be used two ways, to design high performance control systems that meet the specific control challenge and by increasing the awareness of how the construction type affects the control challenge. Hence, it is the objective of this paper to identify what challenges a high performance control system faces in the different domestic houses.
The paper is organized in the following way. Section G.2 gives an overview of house design standards. Modeling of the key parts of the application is presented in Section G.3. Section G.4 analyzes the system and gives discusses the simulation results. The conclusion is given in Section G.5.

G.2 How are houses designed

G.2.1 House design

The effectiveness of controlling floor heating systems is, as described in the introduction, affected by the floor heating system type as well as the building type. This means that constructions, thermal mass, insulation and the placement in the wall, the amount of insulation and as a consequence of this also the age of the building plays an important part for the building dynamics.

G.2.2 Floor heating types

In Denmark hydronic - or water borne - floor heating is today by far the most used type of heating in newly built houses. This is the case especially for detached single-family houses, but the system is also used in apartments. Concerning retrofit of existing buildings, it is also common to change the heating system from a conventional radiator heating system or direct electrical heating into floor heating.

Two main types of floor heating systems are used in today's buildings. These two are heavy and lightweight systems. In the heavy system, the floor heating pipe is casted into a concrete floor. The floor construction can be concluded with tiles, linoleum, carpet or wooden floor towards the room. In the lightweight system, the floor heating pipes are placed in a heat distributing plate, which is typically a thin aluminum sheet with tracks for the pipe. This type of floor construction is typically used in connection with wooden floors, since tiles, linoleum and carpet requires a plywood plate or similar load bearing material between the heat distribution plate and the actual floor covering. Below the floor construction towards the ground or another room, a layer of insulation is inserted to reduced unwanted heat flows. In house with floor heating a thicker subfloor insulation layer is required [4]. The design and dimensioning of heavy floor heating systems can be done using EN1264 [5], while Nordtest VVS 127 [6] applies for lightweight floor heating systems. There are other types available for instance capillary systems which uses very small pipe diameters but very small pipe distance. These other types are not regarded here.

The two types are very different seen from a control point of view, which is indicated by the name of the types. The heavy system has a slow reaction to changes in the room temperature. The time constant of the heavy floor is typically between 2-6 hours depending on the floor covering, where the lowest heat transfer resistance leads to the lowest time constant. On the other hand, the lightweight system has a time constant around 30 minutes when equipped with a wooden floor, again depending on the thermal resistance of the floor covering.

G.2.3 Building types

Just as the floor heating systems can be divided into heavy and light, so can the building. If the building is generally made of heavy building materials such as concrete or brick, the building can be referred to as 'heavy', while it is considered 'light' if the building is made of a timber frame construction. Other building materials are also used such as lightweight concrete. In the same way as the floor heating type influences the reaction time to changes in the heating system, so does the weight of the building when it comes to temperature changes due to disturbances such as solar heat gains, people and equipment.

The 'weight' of the building is as influenced by the position of the insulation, in the same way the weight of the building components does. If for instance the insulation of the walls is placed on the inside of the walls, an otherwise heavy building can act as a light building, because the insulation then is blocking for the storing capacity of the walls.

In this work three building types are considered. The first is a heavy brick building with little or no insulation, which is a typical old Danish building. In this building the brick wall is only separated from the room by a layer of paint and/or wallpaper. The second and third types are both well insulated new buildings which are heavy respec-

tively light. Both fulfill the Danish building code. The last two building types can also represent retrofitted buildings, which have been improved with new windows and/or insulation. Examples of how buildings can be designed to meet the future energy demands can for instance be found in [7] and [8]. The conclusion in both is, that regardless of stricter building codes, buildings with low energy consumption can still be designed and still be visually attractive.

G.3 Modeling

The domestic heating system can be divided up into 3 main parts, the floor, the walls and the room. In this section, we will describe and model these 3 parts. The focus here is laid on describing different floor and wall types and their influence on the dynamic behavior on the room.

G.3.1 Floor modeling

The floor construction types influences dynamic of the room temperature. As we briefly mentioned earlier is the difference between a heavy floor and a light floor mainly that the heavy floor has a sub concrete floor which has a large heat capacity and casted-in water pipes, while the light floor has the water pipes attached to a heat distribution plate placed directly in contact with the surface floor. In the heavy floor the heat ($\dot{Q}_w$) is transported from water pipes through the concrete mass and to surface whereas for the light floor the heat is transported more or less directly to the surface floor. This means that the heavy floor type has much slower dynamic compared to the light floor type.

For heavy floors, the relatively thick concrete layer, the low heat transfer from the concrete to the room, and the low heat conduction in the concrete results in a a high biot number $>> 1$, i.e. the concrete temperature can not be considered to be lumped. Hence a distributed temperature model has to be used [9] for concrete sub floor. The surface floor can be considered as heat resistance because the heat capacity of the surface floor is much smaller than that of the concrete sub floor. This is not the case for the light construction floor. Here the heat capacity of surface floor can not be neglected because it represents the largest heat capacity in light floor.

G.3.1.1 Heavy Floor

To simplify the modeling, the concrete sub-floor is divided in to a number of volumes with a uniform temperature. As the temperature gradient changes in a radial direction from the heating pipes into the concrete, the concrete is divided into $n + 1$ cylindric volumes with identical thicknesses L (see Figure G.1). The last "top layer" (number $n + 1$) is not cylindric but still considered to have a uniform temperature. When the heat is transmitted from the water to the concrete, the water and concrete temperature drops along the pipe. This feature can be modeled by slicing the concrete subfloor into

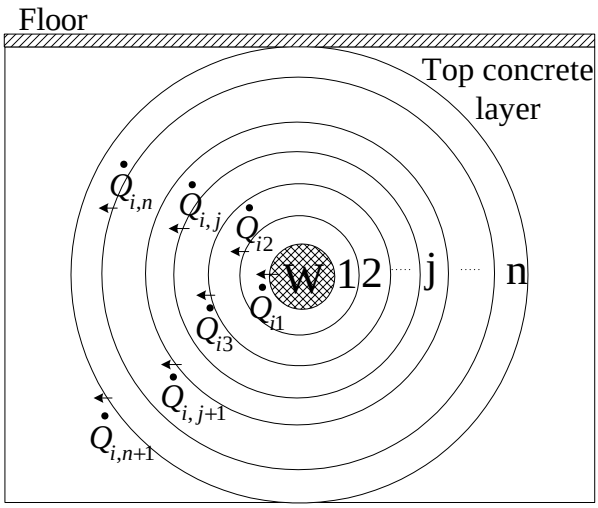

Figure G.1: Finite elements-layers around water pipe

m slices along the pipe, as depicted in Figure G.2. Here the transversal heat conduction between slices is neglected. Furthermore the "top concrete layer" in all of the slices are assumed to be one big lumped mass with uniform temperature. All in all this result in a

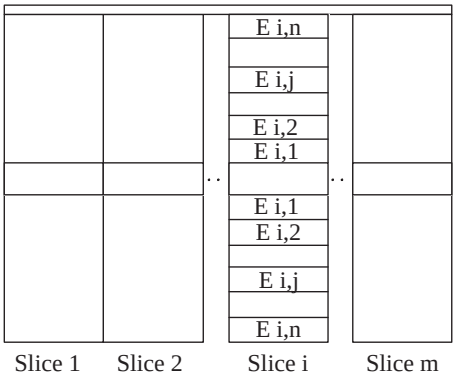

Figure G.2: Finite elements-slices along water pipe

2 dimensional model as depicted in Figure G.1 and G.2.

In the following we will use the description $E_{i,j}$ for the element located at j^{th} layer in i^{th} slice. This means that $T_{i,j}$ is the temperature of the cylindrical concrete element (i, j) and $\dot{Q}_{i,j}$ is heat flow from the cylindrical element $(i, (j-1))$ to (i, j), note that $\dot{Q}_{i,1}$ is the heat flow from water pipe slice i to concrete layer $(i, 1)$. $T_{w,in,i}$ is the water

inlet temperature of the i^{th} pipe slice. $T_{w,out,i}$ is the water outlet temperature of the i^{th} pipe slice. The mean temperature of the water in a slice is approximated by the inlet temperature of the slice.

Using this notation the heat flow $\dot{Q}_{i,j}$ can be written as,

$$\dot{Q}_{i,j} = \begin{cases} \frac{(T_{w,in,i} - T_{i,j})}{Rwc} & i = 1, 2 \cdots m, j = 1, \\ \frac{(T_{i,j-1} - T_{i,j}) \cdot K \cdot A_{i,j}}{L} & i = 1, 2 \cdots m, j = 2, 3 \cdots n, \\ \frac{(T_{i,j-1} - T_{top}) \cdot K \cdot A_{i,j}}{L} & i = 1, 2 \cdots m, j = n + 1, \end{cases} \tag{G.1}$$

where $R_{wc}$is the thermal resistance from water to the concrete, $A_{i,j}$ is the surface area between element $(i, j-1)$ and (i, j) and, K is heat conductivity of concrete. The total heat transmitted from water is given by $\dot{Q}_w = \sum_{i=1}^{m} \dot{Q}_{i,1}$

The temperature $T_{i,j}$ can be determined as:

$$\frac{dT_{i,j}}{dt} = \frac{\dot{Q}_{i,j} - \dot{Q}_{i,j+1}}{C_{pc} \cdot m_{i,j}} \quad \text{where } i = 1, 2 \cdots m, j = 1, 2 \cdots n \tag{G.2}$$

Where C_{pc} is the specific heat capacity of concrete and m_{ij} is the mass of the element (i, j).

Since the top concrete layer is considered as a whole piece the temperature of this layer is assumed to be uniform, and hence it can be computed as,

$$\frac{dT_{top}}{dt} = \frac{\sum_{i=1}^{m} \dot{Q}_{i,n+1} - \dot{Q}_f}{C_{pc} \cdot m_{top}} \tag{G.3}$$

The temperature of the water out of slice i is

$$\frac{dT_{w,out,i}}{dt} = T_{w,in,i} - \frac{\dot{Q}_{i,1}}{C_{pw} \cdot \dot{m}} \quad \text{where } i = 1, 2 \cdots m, \tag{G.4}$$

where C_{pw} is specific heat capacity of water, $\dot{m}$ is water mass flow and the inlet temperature of water to the i^{th} slice $T_{w,in,i}$ is given by,

$$T_{w,in,i} = \begin{cases} T_{w,out,i-1} & i = 2, 3 \cdots m \\ T_{w,in} & i = 1 \end{cases} \tag{G.5}$$

where $T_{w,in}$ is the inlet temperature of water to the floor and $T_{w,out} = T_{w,out,m}$ is the outlet temperature from the floor.

The heat capacity of the top-floor is neglected as it is much smaller than that of the sub-floor. The energy flow from the concrete to the room through the top-floor is simply computed considering the top-floor as a heat resistance, i.e.

$$\dot{Q}_f = \frac{(T_{top} - T_a)}{R_{ca}}, \tag{G.6}$$

where R_{ca} is the thermal resistance between the top concrete layer and the room air. T_a is the room temperature.

G.3.1.2 Light floor

The modeling of light floor is much simpler comparing to heavy floor, as the distributed model of concrete sub floor is removed. Similar to the heavy floor; when the heat is transmitted from the water to the surface floor, the water temperature drops along the pipe. Hence, the water pipe can be modeled the same way into m slices along the pipe. Here we can consider the surface floor as one big lumped mass with a heat capacity.

G.3.2 Room model

In the modeling of the heated room, we will consider the air inside the room and the walls (we assume no heat loss through the roof nor the windows). The room temperature T_a can be computed using equation G.7, under the assumption of a uniform temperature distribution in the room (i.e. perfect mixing of the air).

$$\frac{dT_a}{dt} = \frac{\dot{Q}_f - \dot{Q}_d}{C_{pa} m_a}, \tag{G.7}$$

C_{p_a} is the specific heat capacity of air and, m_a is the mass of the air inside the room. The main disturbance $\dot{Q}_d$ is the climate disturbances, i.e. day to day temperature change, sun radiation etc. Among these disturbances the outdoor temperature variations is one causing the largest heat losses. In this paper we will only consider the heat loss through the wall due to the outdoor temperature variation. The amount of the heat loss through the wall is mainly determined by the wall construction.

G.3.3 Wall model

There are many different ways to construct a wall, in this paper we will consider the 3 different types (a, b and c) depicted in Figure G.3. Despite the many ways to construct walls, these 3 wall-types covers large specter of what can be found.

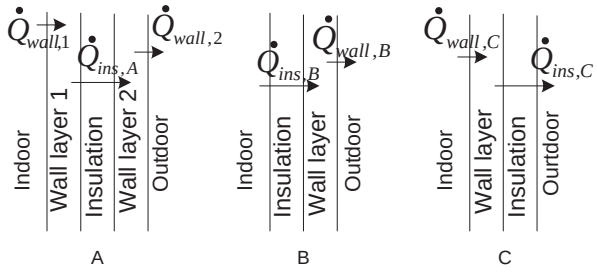

Figure G.3: Different types of wall construction

G.3.3.1 Wall type A

The insulation layer is place between an inner and outer wall, i.e. the heat loss from indoor air $\dot{Q}_d$ is the heat transferring from indoor air to wall layer 1. By assuming each layer (insolation and walls) are lumped following model can be derived:

$$\dot{Q}_d = \dot{Q}_{wall,1}, \tag{G.8}$$

$$\dot{Q}_{wall,1} = \frac{(T_a - T_{wall,1})}{R_{aw,A}}, \tag{G.9}$$

where $R_{aw,A}$ is the thermal resistance from indoor air to wall.

The temperature of the wall 1 can be calculated as,

$$\frac{dT_{wall,1}}{dt} = \frac{\dot{Q}_d - \dot{Q}_{ins}}{C_{pw,1} \cdot m_{wall,1}}, \tag{G.10}$$

where $C_{pw,1}$ is the specific heat capacity of wall 1, $m_{wall,1}$ is the mass of the wall 1.

The heat transmission through insulation layer is,

$$\dot{Q}_{ins,A} = \frac{(T_{wall,1} - T_{wall,2})}{R_{ins,A}} \tag{G.11}$$

where $R_{ins,A}$ is the thermal resistance of the insulation layer.
The temperature of wall 2 is,

$$\frac{dT_{wall,2}}{dt} = \frac{\dot{Q}_{ins,A} - \dot{Q}_{wall,2}}{C_{pw,2} \cdot m_{wall,2}}, \tag{G.12}$$

$C_{pw,2}$ is the specific heat capacity of wall 2 The heat loss from wall 2 to ambient environment is,

$$\dot{Q}_{wall,2} = \frac{(T_{wall,2} - T_o)}{R_{wa,A}}, \tag{G.13}$$

where $R_{wa,A}$ is the thermal resistance from wall 2 to ambient environment in type A.

G.3.3.2 Wall type B

For type B, the insulation layer is placed on the inside. The heat loss from indoor air $\dot{Q}_d$ is the heat loss through the insulation layer, which can be calculated as,

$$\dot{Q}_d = \dot{Q}_{ins,B}, \tag{G.14}$$

$$\dot{Q}_{ins,B} = \frac{(T_a - T_{wall,B})}{R_{aw,B}}, \tag{G.15}$$

where $R_{aw,B}$ is the thermal resistance from indoor air to wall, which includes the insulation layer.

The temperature of the wall B can be calculated,

$$\frac{dT_{wall,B}}{dt} = \frac{\dot{Q}_{ins,B} - \dot{Q}_{wall,B}}{C_{pw,B} \cdot m_{wall,B}}, \tag{G.16}$$

where $C_{pw,B}$ is the specific heat capacity of wall in type B, $m_{wall,B}$ is the mass of the wall in type B.

The heat transmission through insulation layer is,

$$\dot{Q}_{wall,B} = \frac{(T_{wall,B} - T_o)}{R_{wa,B}}, \tag{G.17}$$

where $R_{wa,B}$ is the thermal resistance from wall to ambient environment in type B.

G.3.3.3 Wall type C

The insulation layer is placed on the outside of the wall. The heat loss from indoor air $\dot{Q}_d$ is the heat transferring from indoor air into wall, which can be expressed as,

$$\dot{Q}_d = \dot{Q}_{wall,C}, \tag{G.18}$$

$$\dot{Q}_{wall,C} = \frac{(T_a - T_{wall,C})}{R_{wa,C}}, \tag{G.19}$$

where $R_{aw,C}$ is the thermal resistance from indoor air to wall.

The temperature of the wall B can be calculated as,

$$\frac{dT_{wall,C}}{dt} = \frac{\dot{Q}_{wall,C} - \dot{Q}_{ins,C}}{C_{pw,C} \cdot m_{wall,B}}, \tag{G.20}$$

where $C_{pw,C}$ is the specific heat capacity of wall in type C, $m_{wall,C}$ is the mass of the wall in type C.

The heat transmission through insulation layer is,

$$\dot{Q}_{ins,C} = \frac{(T_{wall,C} - T_o)}{R_{wa,C}}, \tag{G.21}$$

where $R_{wa,C}$ is the thermal resistance from wall to ambient environment in type C.

G.4 System analysis and results

The dynamics of the indoor temperature is expected to depend on house design-floor and wall construction types as described in section G.2. The reason is that houses with different construction types also have different heat capacities. In the following, the scenarios has been constructed such that even though the houses have different construction

types they have the same heat resistance to ambient, in order to get the same steady state solution. The different house construction types here refers to the floor and wall construction types. The influence of the different construction types on the dynamic of the indoor temperature is discussed below and simulation results are presented to demonstrated the influences.

G.4.1 Construction type influence on indoor temperature

G.4.1.1 Floor construction impact

As described in section G.2, there are mainly two types of floor construction- heavy and light floor. Seen from construction, the main difference between them is that the heavy floor has a concrete sub floor while the light floor has the water pipe attached to a heat distributing plate placed close to surface floor.

Heavy floor: A room with heavy floor, modeled in Eq. G.1-G.6 has a slow dynamic of indoor temperature. With a water based floor heating system, the water first needs to heat the concrete sub floor. Then the temperature different between the top layer of the concrete and room air drives heat to transfer to room, as described in Eq. G.6. Due to the large heat capacity of the concrete subfloor, it takes long time to heat up. Vice versa, it takes long time to release the large amount of energy stored in the concrete to the room. This means that the heavy floor heating requires a longer time to increase the temperature as well as for decreasing the temperature (when heating is turned off).

There are other 2 factors that influences the dynamics of the floor. One is the supply water temperature, the other is the heat resistance of the top floor. We know that wood has much higher heat resistance than tiles. In order to transfer heat to the room through a wood floor, a much higher temperature of concrete sub floor is needed compared to tiles.

Light floor: For a light floor, the heat goes through the surface floor directly to the room. There is no large heat capacity in floor construction which determines that the room temperature reacts much faster to an opening or closing of the loop valve.

G.4.1.2 Wall construction impact

The 3 basic wall construction types has been described in section G.2. The difference between these 3 wall types is that the insulation layer is placed in different places, in the middle of the two brick layers, at the inside layer or at the outside layer. All the 3 types of wall have same heat resistance because the total brick wall thickness is same, and they have same amount of insulation. The different effects on the indoor temperature dynamic from this 3 types wall are explained in the following.

Wall type A: With wall type A, modeled in Eq. G.8-G.13, the insulation layer is placed in between the two brick layers, so there is only half of the brick heat capacity in the room and it absorbs/releases a large amount of heat energy when room needs to be heated up/cooled down. This contributes to a slow temperature dynamic of the room.

Wall type B: The insulation is installed inside the room, which means that there is very little heat capacity from the inner wall. The outdoor brick wall affects not so much on the indoor temperature dynamic because the energy transmission from indoor to outdoor is blocked by the insulation layer. The room with such kind of wall has very fast temperature dynamic comparing to type A.

Wall type C: The insulation layer is installed as outer layer, so all the brick heat capacity is inside the room. A room with this kind of wall construction has very slow dynamic due to the large heat capacity of the inner wall. Among this 3 types, this is with the slowest indoor temperature dynamic.

The heat capacity of the inner wall affects the indoor temperature dynamics. So when we need to heat up/cool down a room, a wall with large heat capacity results in slow temperature dynamic. When it come to disturbances, for instance outdoor temperature, sun radiation, human dissipation etc. this room itself has better rejection ability due to the large inner heat capacity.

The influence on indoor temperature from different floor and wall construction types is further illustrated with some simulation results.

G.4.2 Simulation results

The simulation results are from models with same room dimension but different floor and wall construction types. The temperature dynamic behavior and disturbance sensitivity of different house constructions can be easily seen from the simulation result. There are 6 room models: heavy floor with 3 different wall types and light floor with 3 different wall types. The concrete sub floor is 10 cm thick. The water supply is 30°C for heavy floor and 29°C for light floor.

G.4.2.1 Simulation of dynamic behavior

The simulation is conducted to simulate a room temperature step response for rooms with different construction types. The initial room temperature is 5°C, the outdoor temperature is 1°C and the hot water is applied at time 0. The temperature curves from different floor and wall types are shown in figure G.4.

From the figure we can see that for rooms with heavy floor construction, wall C reacts slowest and with wall B fastest. The reason is that the room with wall C has largest heat capacity, while the room with wall B has smallest heat capacity. The result is similar for the rooms with light floor construction. We can also observe that the heavy floor room is slower than light floor as we expected. An important and perhaps bit surprising thing that should be noticed is that the for wall type A and C the wall is actually is the main factor determining the dynamic, where as for floor type B it is the floor type that determines the main dynamic.

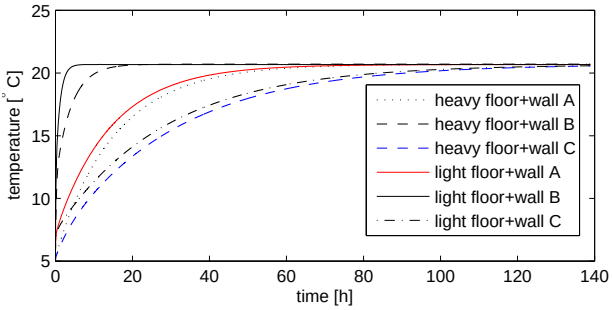

Figure G.4: Temperature dynamics when heating a cold room up.

G.4.2.2 Disturbance sensitivity simulation

The disturbance here refers to outdoor temperature change, sun radiation, human heat dissipation, electrical equipment etc. which all contributes to the heat dissipation. The disturbance sensitivity describes how sensitive the indoor temperature of a house is to those disturbances. The disturbances can be divided into 3 groups according to how they influence the air temperature of the room. Simulations illustrate how the disturbances affect the room temperature of a house with different construction types.

1. Outdoor temperature, wind etc.: This type of disturbance affects the temperature of the room through the wall. Equation G.9-G.13 models the dynamic heat loss through the wall. In steady state, this can be reduced to equation G.22, which means that house with three types of wall construction types have the same amount of heat loss through the wall at steady state when they are under same indoor and outdoor temperature condition.

$$\dot{Q}_{in,out} = \frac{T_a - T_o}{R_{ins,A} + R_{aw,A} + R_{aw,A}} \tag{G.22}$$

Because the three kind of wall constructions have same heat resistance, the disturbance sensitivity affecting factor depends on the heat capacity in the room. The room is heated and the room temperature is at steady state at time 0 when outdoor temperature is at 1°C. At time 0, the outdoor temperature disturbance (figure G.5) is simulated as a sinusoidal. Figure G.6 shows how a heavy floor room with different wall types reacts and Figure G.7 shows how a light floor room with different wall types reacts.

From Figure G.6 and G.7 we can see that, for both heavy floor and light floor rooms, indoor temperature with wall type B is the most sensitive. It has the largest amplitude and smallest phase shift. Second most sensitive is the room with wall type A, and the least sensitive is the room with wall type C. Comparing the temperature from the room with same wall type different floor type, for example, a room with heavy floor and wall type A with a room with light floor and wall type A, in Figure G.6 and G.7, we can not see much difference. The reason is that the floor is much warmer than the room air, so

the floor heat capacity can not absorb heat from the air. Hence, we can say that the floor type does not affect the disturbance sensitivity in heating season when the room subjects to daily outdoor temperature change, but if the house subjects to a sudden outdoor temperature drop, then the heavy floor construction contributes to a lower disturbance sensitivity. In warm season, the surface floor type and the heat capacity of floor affect the room disturbance sensitivity. A heavy floor with tile surface floor would act as an inner wall, which leads to a low disturbance sensitivity. while a heavy floor with wood surface floor would not work in the same way, because the wood floor has very good heat resistance, which slows down the energy transmission between the concrete sub floor and room.

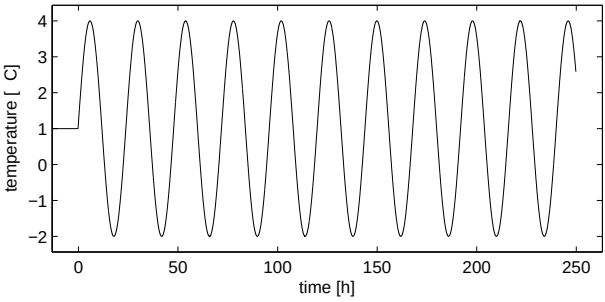

Figure G.5: Outdoor temperature

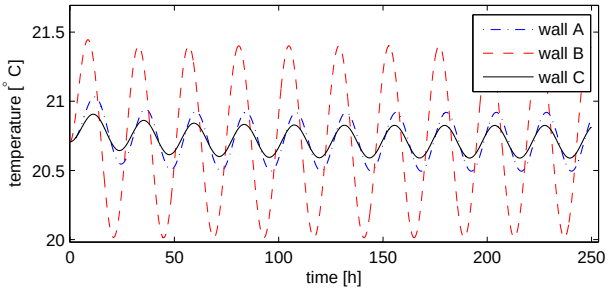

Figure G.6: Outdoor temperature disturbance effects on heavy floor room temperature

2. Human dissipation, electrical equipment etc.: This kind of disturbances transfer energy directly to the room air and heats up the room.

Simulations illustrates how the room temperature is affected when people (300W heating) come into rooms with different floor and wall construction types. The room is equipped with an On/Off controller which uses room temperature as feedback and the room set-point temperature is 20.5°C, and the outdoor temperature is 1°C. Figure

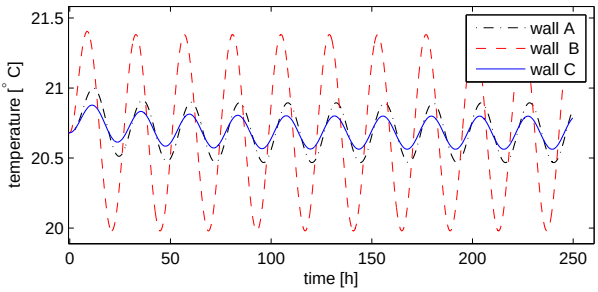

Figure G.7: Outdoor temperature disturbance effects on light floor room temperature

G.8 and G.9 shows the indoor temperature response of a room with different floor and wall construction types. At time 0, the room is at steady state, and the people enters the room. The human heat dissipation causes an increased of the room temperature, which then causes the heating controller to switch off.

Figure G.8 shows the simulation results from heavy floor room with different wall types. When the floor heating is shut off, there is a large amount of energy stored in the concrete sub floor. The release of this energy contributes to an temperature overshoot. During the 20 hours with human heat dissipation the temperature of the concrete floor drops. Hence, after the 20 hours the concrete is cold, and reacts slow to the increased heating demand. This causes the large undershoot. In Figure G.8, the temperature curve of wall B has largest overshoot and undershoot. The reason is that the room with wall B has lowest heat capacity. The simulation results also indicates that a larger inner wall heat capacity gives a lower disturbance sensitivity.

For light floor room, the results are different. The indoor temperature overshoot for light floor and light wall is much smaller than for the heavy floor room and light wall when the people comes into the room. This is mainly due to the light floor has much faster dynamic compared to the heavy floor. We can see that with the same wall type, the light floor room temperature is closer to the set-pointed temperature.

3. Sun radiation: Sun radiation doesn't not transfer heat directly to the indoor room air. It first heats up the objects, for example, the surface of the wall, floor and furniture etc., then these objects transfers heat into the inner layer of the wall, floor and room air. So if there is a large heat capacity in the wall, most of the sun radiation energy is absorbed by the wall and the room temperature will not increase much. As we discussed above about the floor construction type and surface floor material affects the room air temperature.

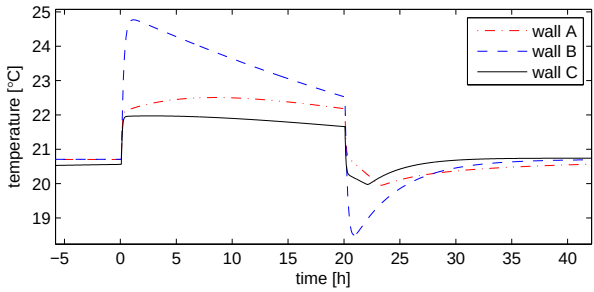

Figure G.8: Human dissipation effects on heavy floor room temperature

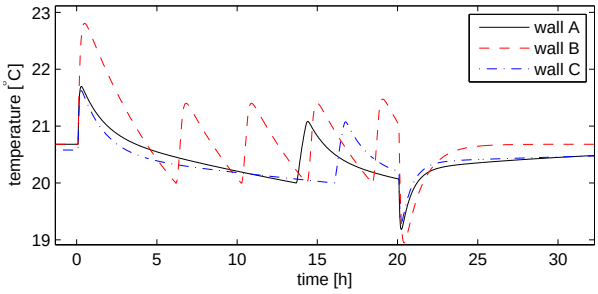

Figure G.9: Human dissipation disturbance effects on light floor room temperature

G.5 Conclusion

First of all it can be concluded that the building style has a major impact on building dynamic i.e. with respect to the room temperature. It was shown that for heavy wall types (i.e. wall types with a large indoor thermal mass), the walls actually was the most important factor determining the dynamic behavior, whereas for light wall types it is mainly the floor type that determines the dynamics. Furthermore the results points out that a lightweight inner wall is very sensitive to disturbances, but because of the little thermal mass the set-point can be changed fast. A heavy inner wall will help reducing the disturbance sensitivity, but with the cost of a much slower response to set-point changes. This means that a light wall in combination with a heavy floor is not recommendable as this brings together the worst of two worlds namely high sensitivity to disturbances and a slow dynamic.

Bibliography

[1] Boligstyrelsen. Bygningsreglement (in danish) (danish building code). *København*, 2006.

[2] Honglian Thybo, Lars FS Larsen, and Claus Thybo. Control of a water based floor heating system. *ACC*, 2007.

[3] Honglian Thybo, Lars FS Larsen, and Claus Thybo. Disturbance rejection of a water-based floor heating system. *UKACC Control Conference*, 2006.

[4] P Weitzmann, J Kragh, P Roots, and S Svendsen. Modelling floor heating systems using a validated two-dimensional ground-coupled numerical model. *Building and Environment*, 40:153–163, 2005.

[5] CEN. En iso 1264: Floor heating - systems and components. *European Committee for Standardization*, 1997.

[6] CEN. Nt vvs127. floor heating systems: Design and type testing of waterborne heat systems for lightweight structures. *Nordtest*, 2001.

[7] J Munch-Andersen, S Svendsen, and HM Tommerup. Exterior walls to meet future danish requirements. *Proceedings of the Third international conference on Detail Design in Architecture*, 2001.

[8] J Rose and S Svendsen. Single-family houses that meet the future energy demand. *Proceedings of the 6th Symposium on Building Physics in the Nordic Countries*, pages 269–276, 2001.

[9] Yunus A. Cengel and Robert H. Turner. Fundamentals of thermal-fluid sciences. *McGraw-Hill*, 2005.

Appendix H

Model predictive control of domestic heating systems

(Technical report, August 2007)

Honglian Deng

Supervisor: Lars Larsen, Jakob Stroustrup, Henrik Rasmussen

Abstract

The objective of this report is to investigate model predictive control (MPC) on domestic heating systems. Due to the slow dynamic of heavy construction floor heating systems, fast heaters are usually installed in domestic houses to compensate the fast disturbances. The two heating systems have different dynamics and different cost of using electrical or water heating. To make them working together providing good comfort and at the same keep a low economic cost can be a challenge. In this report, control of such a domestic heating system is introduced.

H.1 Introduction

Floor heating systems have been widely used during recent years. The reason is that it provides increased comfort with a warm floor (e.g. in bathrooms) and a more uniform temperature distribution in the heated room[1]. Heavy water-based floor heating is the most popular type in newly built single family houses in Denmark because it is easy to construct when building new houses. However the disadvantage of such a floor heating system is that the room temperature dynamic with such a floor heating system is very

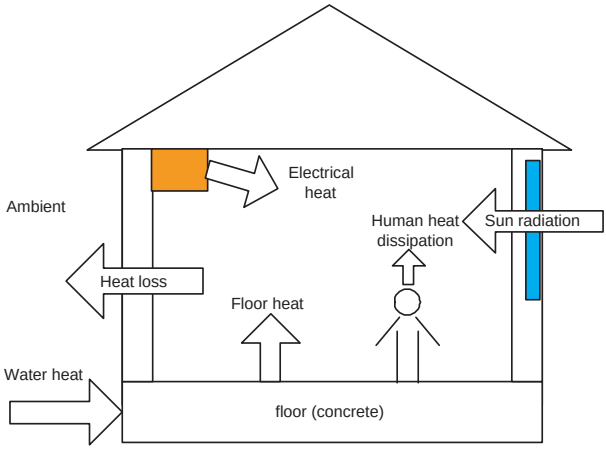

Figure H.1: Heating and disturbances of a domestic house.

slow due to the large heat capacity of the concrete subfloor. Houses with this type of floor heating system often have to install a fast heater to compensate the slow dynamic of the floor heating system, such as an electrical heater. Control of such a multiple heat source system poses challenges due to that the two heating systems are characterized with different dynamics and different cost of using electrical or water heating.

The focus of this report is on control of a multiple heat source system in a domestic house. The challenge is how to make the different heating systems work together to provide a good comfort using as little money for heating as possible. MPC is proposed to solve this type of problems.

In this report, MPC application on a multiple heat source system is demonstrated with a domestic house installed with a heavy construction water-based floor heating system and an electrical heater. The report is organized this way: modeling of the house with a floor heating and an electrical heater is presented in Section H.2. MPC formulation is briefly reviewed in Section H.3. Section H.4 presents the simulation results of the proposed controllers. At last conclusions are given in Section H.5.

H.2 System and modeling

A simplified domestic house with one room is illustrated in Fig. H.1 and the wall is shown in H.2. The house is equipped with a heavy construction water-based floor heating system where the water pipes are cast in the concrete subfloor and an electrical heater. The disturbances to such a house are usually the changing outdoor temperature, sun radiation through window and human dissipation etc. In this paper, we use outdoor temperature as a disturbance example.

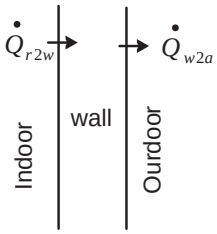

Figure H.2: The wall of a domestic house.

The temperature distribution in the subfloor of the floor heating system is not uniform when heating is applied. The concrete temperature is higher close to water pipe, and it drops along the water pipe. A detailed model of such a floor heating system can be seen in [2]. However a simplified model of the house is used here for MPC with the assumption that the temperature is even distributed in floor, room and wall. Using of a even distributed floor temperature is consistent with the floor temperature estimation method introduced in [3], where an even floor temperature is assumed after an idle period. The reason is for the even wall temperature assumption is that we should use the least states for MPC due to the computational power limitations in such a application.

H.2.1 Modeling of the house with the two heating systems

The model of the simplified house with two heaters is presented as,

$$\begin{aligned}
\frac{dT_{con}}{dt} &= \frac{\dot{Q}_{wf} - \dot{Q}_{c2r}}{Cp_{con}m_{con}}, \\
\frac{dT_{room}}{dt} &= \frac{\dot{Q}_{c2a} - \dot{Q}_{r2w} + \dot{Q}_{el}}{Cp_{air}m_{air}}, \\
\frac{dT_{wall}}{dt} &= \frac{\dot{Q}_{r2w} - \dot{Q}_{w2a}}{Cp_{wall}m_{wall}}, \\
\dot{Q}_{c2r} &= \frac{(T_{con} - T_{room})}{R_{c2r}}, \\
\dot{Q}_{r2w} &= \frac{(T_{room} - T_{wall})}{R_{r2w}}, \\
\dot{Q}_{w2a} &= \frac{(T_{wall} - T_{amb})}{R_{w2a}}
\end{aligned} \tag{H.1}$$

Where T_{con}, T_{room}, T_{wall} are the temperature of the concrete floor, the room air, and the wall.
$\dot{Q}_{wf}$,$\dot{Q}_{el}$ are the heating power from the floor heating system and the electrical heater.
$\dot{Q}_{c2r}$, $\dot{Q}_{r2w}$, $\dot{Q}_{w2a}$ are the heat flow from the concrete to the room air, the room air to

the wall and the wall to the ambient.
R_{c2r}, R_{r2w}, R_{w2a} are the thermal resistance from the concrete floor to the room air, the room air to the wall and the wall to the ambient.
m_{con}, m_{air}, m_{wall} are the mass of the concrete floor, the room air and the wall.
Cp_{con}, Cp_{air}, Cp_{wall} are specific heat capacity of the concrete floor, the room air and the wall.

Usually in such a floor heating system, the heating is controlled by switching the water inlet valve ON and OFF. The heating power delivered from the water to the floor is not controlled directly. The heat from the water to the floor is modeled as an input power, which in fact is not easy to control. An energy based control method of such a floor heating is proposed in Appendix E, which enables us to use power as the control input to the floor heating system.

H.2.2 State space model

In the MPC controller, state space model is used as the internal model. (H.1) can be formulated in state space form as:

$$\begin{aligned} \dot{x} &= A_c x + B_c u + E_c d \\ y &= Cx \end{aligned} \tag{H.2}$$

Where $x = [T_{con}, T_{room}, T_{wall}]^T$, $u = [\dot{Q}_w, \dot{Q}_{el}]^T$, $d = T_{amb}$, $y = [T_{con}, T_{room}, T_{wall}]^T$, i.e. $C_z = I$.

$$A_c = \begin{bmatrix} A_{11} & A_{12} & 0 \\ A_{21} & A_{22} & A_{23} \\ 0 & A_{32} & A_{33} \end{bmatrix}, B_c = \begin{bmatrix} B_{11} & 0 \\ 0 & B_{22} \\ 0 & 0 \end{bmatrix}, E_c = \begin{bmatrix} 0 \\ 0 \\ E_3 \end{bmatrix}$$

$$\begin{aligned} B_{11} &= \tfrac{1}{Cp_{con}} & B_{22} &= \tfrac{1}{Cp_{air} m_{air}} \\ E3 &= \tfrac{1}{Cp_{wall} m_{wall} R_{w2a}} & A_{11} &= -\tfrac{1}{Cp_{con} m_{con} R_{c2r}} \\ A_{12} &= \tfrac{1}{Cp_{con} m_{con} R_{c2r}} & A_{22} &= \tfrac{1}{Cp_{air} m_{air} R_{c2r}} - \tfrac{1}{Cp_{air} m_{air} R_{r2w}} \\ A_{23} &= \tfrac{1}{Cp_{air} m_{air} R_{r2w}} & A_{33} &= -\tfrac{1}{Cp_{wall} m_{wall} R_{r2w}} - \tfrac{1}{Cp_{wall} m_{wall} R_{w2a}} \end{aligned}$$

Convert the (H.2) to discrete time, we have

$$\begin{aligned} x_{k+1} &= Ax_k + Bu_k + Ed_k, k = 0, 1, \cdots N-1 \\ y_k &= C_k x_k \end{aligned} \tag{H.3}$$

Where A, B, E, C_z are the discrete version of A_c, B_c, E_c, C. (H.3) will be used for the MPC internal model.

H.3 Control design

H.3.1 Control structure

In this report, MPC is proposed for control of multiple heating systems. The control is divided into two layers, where the upper-layer is a central controller, MPC in this case, which governs the overall system performance. The lower layer controllers locate in the floor heating and the electrical heating systems and are only responsible for the individual subsystems. The central controller gets the signals from temperature sensors equipped in the rooms, calculates the the power that the floor heating system and the electrical system need to delivery and send out the signals to local controllers. The local controllers execute the commands received from the central controller.

The reason why the control is divided into hierarchy is that such a structure provides flexibility of changing, adding or removing subsystems without reconfiguring the whole system. For the domestic house, it means that the power that the heating systems delivery will have to be used as the communication signals between the central and local controllers. The floor temperature controller proposed in [3] suits this control structure where the amount of energy from the water to the floor is controlled. The focus of this report is on the cental controller of the multiple heating systems.

H.3.2 Objective function

The following objective function is formulated for the MPC control of the multiple heat source systems.

$$\phi = \sum_{k=1}^{N} \frac{1}{2}\|y_k - r_k\|_{Q_z}^2 + \frac{1}{2}\sum_{k=0}^{N-1} \|\triangle u_k\|_S^2 + \frac{1}{2}\|u_k\|_G^2 \tag{H.4}$$

$$\tag{H.5}$$

N is the prediction horizon. Q_z weighs the output deviation from the reference r. S weighs the rate of change of the control input and G weighs the control signal. Assignment of the elements in G will be based on energy price of using water heating vs. electrical heating here. A balance should be set up in weight matrix G($G = \begin{bmatrix} G_w & 0 \\ 0 & G_{el} \end{bmatrix}$ G_w is penalty on using of water-based floor heating and G_{el} is is penalty on using of electrical heater). In the multiple heating system example, electrical energy is much more expensive than water heating, so the penalty on using electricity is penalized more.

The objective function represents a balance between comfort and economic cost. By adjusting the ratio between Q_z and G, the comfort and energy expenses can be balanced e.g. increasing Q_z results in better output reference tracking by using more electrical heating or fast output rate change and vice versa. The price of getting more comfort is at high energy cost, and vice versa.

The physical limitations on the heaters' capacity, and the concrete floor temperature etc. imposed by the comfort and material limitations, have to be taken in to consideration. Usually there are also limits on how fast the actuator can change. For example, the floor heating system can not get a step of $500W$ increase in one time instance. An input movement rate constraint should also be considered. Therefore we need to solve a constraint optimization problem. Violation of the limitations may result in discomfort, destroying the floor surface floor or heating system saturation.

There are two ways of dealing with constraints-hard constraints and soft constraints. Hard constraints refer to the constraints that are not allowed to be violated. Examples in such a multiple heating systems are the heating power of the floor heating system and the electrical heater - input capacity, and the rate of change of the heating power from the heating systems. The soft constraints means that the constraints can be violated, but the violation will be penalized, e.g. the temperature of the floor, the room and the wall. One way of formulating the problem with both hard and soft constraints is presented below.

Objective formulation with soft constraints

$$\phi = \sum_{k=1}^{N} \frac{1}{2}\|y_k - r_k\|^2_{Q_z} + \frac{1}{2}\|\eta_k\|^2_{Sn} + sn^{'}\eta_k + \frac{1}{2}\sum_{k=0}^{N-1}\|\triangle u_k\|^2_S + \frac{1}{2}\|u_k\|^2_G \quad \text{(H.6)}$$

$$\begin{aligned} s.t. \quad & x_{k+1} = Ax_k + Bu_k && k = 0, 1, \cdots, N-1 \\ & z_k = c_z x_k \\ & u_{min} \leq u_k \leq u_{max} && k = 0, 1, \cdots, N \\ & \Delta u_{min} \leq \Delta u \leq \Delta u_{max} && k = 0, 1, \cdots, N-1 \\ & y_k - \eta_k \leq y_{max,k} && k = 1, 2, \cdots, N \\ & y_k + \eta_k \leq y_{min,k} && k = 1, 2, \cdots, N \\ & \eta_k \geq 0 && k = 1, 2, \cdots, N \end{aligned}$$

u_{max}, u_{min}: the maximum and minimum power of the heating systems.
Δu_{min} Δu_{max}: the maximum and minimum change rate of the heating systems.
$y_{max,k}, y_{min,k}$: the soft output constraints at time k. In this report they are set to be 90% of maximum and minimum power of the heating systems.
η_k: the output value amount above the constraints.
Sn, sn: penalty on exceeding the soft constraints. These values are set to be very large comparing to Q_z, S, which means that exceeding soft constraints will be penalized heavily.

H.4 Simulation results

Simulations of the MPC controller on a system using a floor heating and an electrical heating source have been carried out to investigate whether MPC can make the two heat

sources cooperate and thereby achieve a better comfort and disturbance rejection. Two scenarios are simulated, a predicted reference change and a predicted ambient temperature change. The reference change could be applied in a house that is empty during day time and occupied in the night. During the day time a low room temperature reference is set to save energy, but in the evening a higher room temperature is required for comfort. The outdoor temperature change scenario simulates when cold air comes, and a large outdoor temperature drop is expected. The results are presented in Fig. H.3. For the simulations, the house model used for simulation is the same as the MPC internal model (H.3).

The controller has a sampling time of 0.5 hour, and the prediction horizon $N = 20$; the weight matrices used in the simulations are

$$Q_z = 5000 \begin{bmatrix} 0 & 0 & 0 \\ 0 & 1 & 0 \\ 0 & 0 & 0 \end{bmatrix}, S = 0.1 \begin{bmatrix} 1 & 0 \\ 0 & 1 \end{bmatrix}, G = 0.001 \begin{bmatrix} 0 & 0 \\ 0 & 1 \end{bmatrix}$$

Q_z indicates that there is no penalty on the subfloor and wall temperature deviation from their reference. The matrix S shows that on the input change rate is equal for the two heat sources. G indicates that only using of the energy from electrical heating system is penalized according to the fact that water district heating is much cheaper than electricity in the test house area.

Hard constraints are applied on the floor heating system input power(working range $0 - 1000w$) and the power of the electrical heater (working range $0 - 500w$).

At the beginning of the simulation, the electrical heater starts to drive the room temperature to the reference fast instead of only using the floor heating system. However when the room temperature reaches steady state, the electrical heater is switched off. This follows the weight matrix G where using the electrical heating system is penalized. This is seen in period 0-150 hours.

At hour 150, the ambient temperature drops from $0°C$ to $-5°C$ and back to $0°C$ again at hour 350. It can be seen in Fig. H.3 that when the system is in steady state between hour 150 to 350, the electrical heater is activated although the floor heating is not saturated (max. power delivery of the floor heating system is $1000W$, here it deliveries only about $780W$). This is because the concrete subfloor temperature already reaches the limit ($29°C$), which means that no more heat can be transmitted through the concrete subfloor floor. Therefore electrical heating has to be applied heat to maintain the room temperature close to the reference.

At hour 550, the room temperature reference is set down from $21°C$ to $19°C$ and back to $21°C$ again at hour 750. It can be seen that both floor heating and electrical heater starts to react before the time of reference change. For instance the electrical heater starts to heat at hour 530, and the floor heating system decrease the heat delivery at the same time. The amplification of Fig. H.3 around hour 550 is shown in Fig. H.4. It might seems strange that the floor heating power drops much lower than the steady state value $600W$ between hour 550-750, and the electrical heating power increases and decreases two times. The reason is that with the prediction of reference decrease

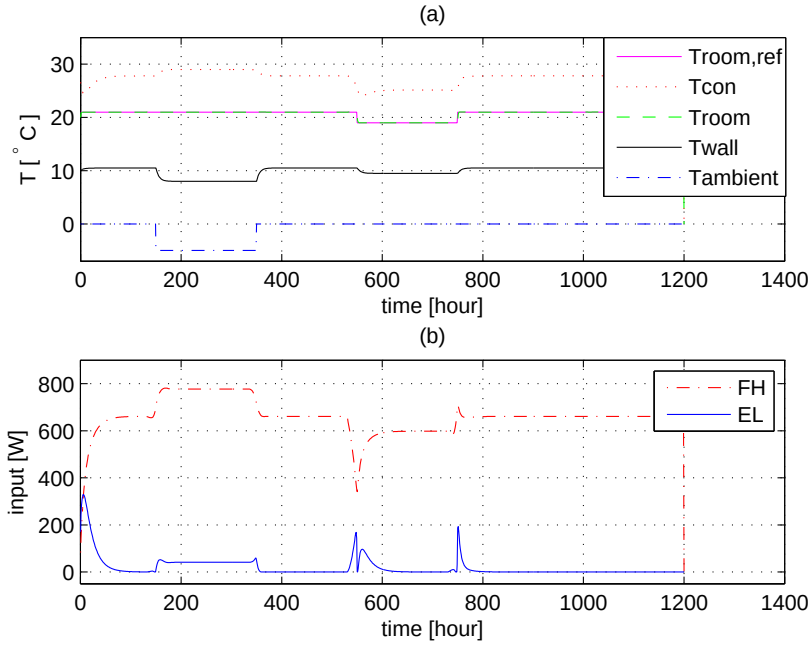

Figure H.3: MPC simulation results. The ambient temperature drops from $0°C$ to $-15°C$ during hour 150-350. The reference changes from $21°C$ to $19°C$ during hour 550-750. 'FH' refers to the energy delivered by the floor heating system. 'EL' refers to the energy delivered by the electrical heater.

at hour 550, to get the room room temperature very close to the reference when the reference happens, the electrical heater has to be activated in advance, and switch off to achieve a fast temperature before hour 550. The floor heating system also decreases at the same time to make the temperature much closer to the reference when the reference changes happens. After this, due to the power to applied to concrete subfloor is too low, the electrical heating power has to be used until the floor heating power again is high enough. After that, during the steady state between hour 550 to 750 only the floor heating system is activated and the reference can be reached with only floor heating which is corresponding to the weight matrix G. Similar happens at hour 750 when the reference is set back.

It should be noted that the wall temperature shown in the figure is within the constraints but the value is rather low. The reason is that the wall in the model is considered a lumped mass, therefore the wall temperature here is the average wall temperature. In fact, the wall surface towards indoor has higher temperature than the average and on the other hand, the outside layer of the wall has a lower temperature close to the ambient

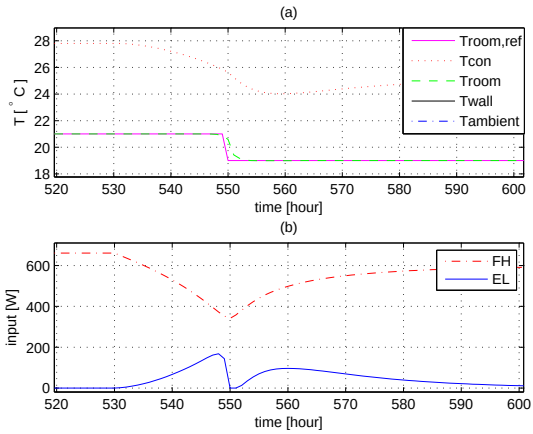

Figure H.4: Amplification of Fig. 6.11 around hour 550.

temperature.

H.5 Conclusion

From the results it can be seen that MPC can handle control of multiple heat source with very different characteristics assuming well predicted disturbance information. The floor heating system which is cheap in energy price is utilized most. The electrical heater which is expensive to use is only activated when the floor heating system reaches saturation, constraints, disturbances that the floor heating system can not reject alone and during reference changes.

Although the MPC scheme shows potential on controlling multiple heat source systems, there are some issues that have to be investigated before implementing the MPC scheme in commercial products. One of the challenge is prediction mismatch for MPC. For instance, when the weather forecast predicted sunshine for the whole day, but in reality the sun disappears for three hours. The MPC control will not be able to control the room temperature very close to the reference due to the prediction mismatch. A suggestion could be to update the prediction with the current condition, where the current situation is connected to the original prediction with a smooth curve.

Bibliography

[1] Bjarne W. Olesen. Radiant floor heating in theory and practice. *ASHRAE Journal*, 2002, July.

[2] Honglian Thybo, Lars Larsen, and Claus Thybo. Control challenge for domestic heating systems. *European Control Conference*, 2007.

[3] Honglian Thybo, Lars FS Larsen, and Claus Thybo. Control of a water based floor heating system. *Multi-conference on Systems and Control*, 2007.